

The Borneol Cycle of Cytochrome P450_{cam} and Evolution of the Enzyme for New Applications

by

Brinda Prasad

M.Sc., University of Pune, 2006
B.Sc., Osmania University, 2004

Thesis Submitted in Partial Fulfillment
of the Requirements for the Degree of
Doctor of Philosophy

in the

Department of Chemistry
Faculty of Science

© **Brinda Prasad 2013**

SIMON FRASER UNIVERSITY

Summer 2013

All rights reserved.

However, in accordance with the *Copyright Act of Canada*, this work may be reproduced, without authorization, under the conditions for "Fair Dealing." Therefore, limited reproduction of this work for the purposes of private study, research, criticism, review and news reporting is likely to be in accordance with the law, particularly if cited appropriately.

Approval

Name: Brinda Prasad
Degree: Doctor of Philosophy (Chemistry)
Title of Thesis: *The Borneol Cycle of Cytochrome P450_{cam} and Evolution of the enzyme for new applications*

Examining Committee:

Chair: Dr. Michael H. Eikerling, Position

Dr. Erika Plettner
Senior Supervisor
Professor

Dr. David Vocadlo
Supervisor
Professor

Dr. Dipankar Sen
Supervisor
Professor

Dr. Daniel B. Leznoff
Internal Examiner
Professor
Department of Chemistry

Lindsay Eltis
External Examiner
Professor
Department of Chemistry
University of British Columbia

Date Defended/Approved: April 10, 2013

Partial Copyright Licence



The author, whose copyright is declared on the title page of this work, has granted to Simon Fraser University the right to lend this thesis, project or extended essay to users of the Simon Fraser University Library, and to make partial or single copies only for such users or in response to a request from the library of any other university, or other educational institution, on its own behalf or for one of its users.

The author has further granted permission to Simon Fraser University to keep or make a digital copy for use in its circulating collection (currently available to the public at the "Institutional Repository" link of the SFU Library website (www.lib.sfu.ca) at <http://summit/sfu.ca> and, without changing the content, to translate the thesis/project or extended essays, if technically possible, to any medium or format for the purpose of preservation of the digital work.

The author has further agreed that permission for multiple copying of this work for scholarly purposes may be granted by either the author or the Dean of Graduate Studies.

It is understood that copying or publication of this work for financial gain shall not be allowed without the author's written permission.

Permission for public performance, or limited permission for private scholarly use, of any multimedia materials forming part of this work, may have been granted by the author. This information may be found on the separately catalogued multimedia material and in the signed Partial Copyright Licence.

While licensing SFU to permit the above uses, the author retains copyright in the thesis, project or extended essays, including the right to change the work for subsequent purposes, including editing and publishing the work in whole or in part, and licensing other parties, as the author may desire.

The original Partial Copyright Licence attesting to these terms, and signed by this author, may be found in the original bound copy of this work, retained in the Simon Fraser University Archive.

Simon Fraser University Library
Burnaby, British Columbia, Canada

revised Fall 2011

Abstract

Cytochrome P450_{cam} isolated from the soil bacterium *Pseudomonas putida* catalyses the hydroxylation of camphor to 5-exo-hydroxy camphor and further to 5-ketocamphor. Unexpectedly, we have also observed the formation of the reduction product, borneol in our enzymatic assays performed under shunt conditions using meta-chloro perbenzoic acid (*m*-CPBA) or with the complete P450 system under low O₂ conditions. Under shunt conditions using *m*-CPBA, borneol was the major product. To further demonstrate the origin of H_{exo} in borneol, we monitored the bioconversion of camphor in deuterated buffer (pD = 7.4) under shunt conditions using *m*-CPBA as the oxidant and mono-deuterated borneol at C-2 was detected. We demonstrate that the source of electrons for this reduction reaction is water and not the nicotinamide cofactor. When ¹⁷O labeled buffer was used in the reaction mixture, labeled hydrogen peroxide (H₂¹⁷O₂) formed. We propose a novel reduction mechanism for P450_{cam}, discuss its generality and also the ecological implications of this reaction for *P. putida* and *E. coli*.

To accommodate unnatural substrates in the active site, a mutant library of P450_{cam} was constructed by Sequence Saturation Mutagenesis (SeSaM). With an objective to identify mutants from SeSaM library that would dehalogenate the chlorinated pesticide endosulfan, the library was screened with 3-chloroindole as a substrate and the active clone(s) were identified by isatin/indigo formation. The mutant (E156G/V247F/V253G/F256S) was the most active in the conversion of 3-chloroindole to isatin, ($K_M = 250 \mu\text{M}$) compared to the WT enzyme (which did not accept 3-chloroindole). The mutant also degrades endosulfan and endosulfan diol to phthalaldialdehyde under shunt conditions using *m*-CPBA. We propose a mechanism for the dechlorination of endosulfan and the formation of phthalaldialdehyde with mutant (E156G/V247F/V253G/F256S) of P450_{cam}.

Keywords: peroxide shunt; camphor; borneol; SeSaM; endosulfan; phthalaldialdehyde

Dedication

*To my parents and my husband
for their love and encouragement*

Acknowledgements

I am grateful to my senior supervisor, Dr. Erika Plettner for the support and encouragement in my research. I am thankful to her for trusting me and giving enormous opportunities to learn the novel techniques. I would like to thank my supervisors, Dr. David Vocadlo and Dr. Dipankar Sen for their ideas and valuable suggestions. I also thank Dr. Daniel B. Leznoff and Dr. Lindsay Eltis for being my thesis examiners.

I am grateful to Dr. Andrew Lewis for teaching me to run my NMR samples and for all the support and encouragement with my research projects. Many thanks to Dr. Ulrich Schwaneberg at RWTH University, Aachen, Germany for allowing me to work in his laboratory and learn the SeSaM technique.

I am thankful to Dr. Carlos Castillo for teaching me the basic microbiological techniques during the start of my research. Mr. Jason Nardella and Ms. Parisa Ebrahimi are thanked for their valuable support and friendly conversations. In addition, I would like to thank all the past and present group members: Dr. Yongmei Gong, Dr. Anoma Mudalige, Dr. Hao Chen, Dr. Yang Yu, Mr. Derrick J. Mah, Ms. Linda Cameron, Ms. Yulia Rozen, Mr. Govardhana reddy Pinneli, Mr. Abdul Rehman and the lovely co-op students for their support. I am indebted to thank all my friends, especially Swati Vartak, Saswati Chakladar, Sankar Mohan, Cynthia Gershome, Tirtadipa Pradhan, Ketaki Athani, Manku Rana, Aarati Sriram and Vidhya Ramanathan for their timely help. I would like to thank Dr. A. Parameswaran's family for being so supportive to me in the tough times of my research.

I am grateful to my parents, Amrutha Prasad and Nagaraja R. Prasad for their continued encouragement which helped me to finish my thesis. My heartfelt thanks to my husband, Mr. Magesh Rao for his understanding and patience with my completion without which I could not have accomplished so far.

Table of Contents

Approval.....	ii
Partial Copyright Licence	iii
Abstract.....	iv
Dedication.....	v
Acknowledgements.....	vi
Table of Contents.....	vii
List of Tables.....	xi
List of Schemes and Figures.....	xiii
List of Acronyms and Abbreviations	xxi

1. Introduction	1
1.1. Cytochrome P450s: Importance and Classification.....	1
1.2. Catalytic cycle of P450s	3
1.2.1. Peroxide shunt.....	5
1.2.2. Other reactions	6
1.2.2.1. Alkene epoxidation	7
1.2.2.2. Dealkylation reactions.....	8
1.2.2.3. Dehydrogenation reactions.....	8
1.2.2.4. Baeyer Villiger oxidation	9
1.2.2.5. P450 as an aromatase.....	10
1.2.2.6. Dehalogenation reactions	11
1.2.2.7. Oxidative decarbonylation	11
1.2.2.8. Biosynthesis of cyanogenic glucosides.....	12
1.3. Structural aspects.....	12
1.4. Protein Engineering with P450 _{cam}	17
1.4.1. Alkanes.....	17
1.4.2. Polychlorinated and aromatic pollutants.....	18
1.5. Other P450s.....	19
1.6. Recent advances in the use of P450s:	22
1.7. Reactivity of P450 _{cam}	24
1.8. Objectives of my thesis.....	26
1.9. Thesis layout	26

2. Identification of Camphor Oxidation and Reduction Products in Pseudomonas Putida. New Activity of the Cytochrome P450_{cam} System.....	27
2.1. Abstract.....	28
2.2. Introduction	29
2.3. Materials and Methods	30
2.3.1. General methods and chemicals.....	30
2.3.2. D(+) camphor purification.....	31
2.3.3. NMR	32
2.3.4. Protein production (from <i>P. putida</i>) ^{160, 177} and the purification steps.....	32
2.3.5. In vivo Assays with <i>P. putida</i>	33

2.3.6.	In vitro Assays with Isolated P450 _{cam} , PdR, and PdX Complex	33
2.3.7.	Toxicity Assays of Tetracycline, DMSO, Camphor, and Borneol against <i>P. putida</i> and <i>E. coli</i>	34
2.3.8.	IC ₅₀ Experiments with Camphor and Borneol against <i>E. coli</i>	35
2.4.	Results	36
2.4.1.	Analysis of Products Formed in <i>P. putida</i> Culture with (1R)-(+)- Camphor During in vivo Assays with Purified P450 _{cam} System	36
2.4.2.	In vitro assays with the partially purified P450 _{cam} , PdR and PdX system:	38
2.4.3.	Enzymatic assays involving borneol as the substrate.....	41
2.4.4.	Toxicity Assays for Camphor and Borneol.....	41
2.5.	Discussion.....	42
2.6.	Summary.....	44
2.7.	Supplementary information.....	45
3.	The Borneol Cycle of Cytochrome P450_{cam}: Mechanism and Advantages to <i>Pseudomonas Putida</i>.....	46
3.1.	Abstract.....	47
3.2.	Introduction	48
3.3.	Materials and Methods	49
3.3.1.	General.....	49
3.3.1.1.	Materials.....	49
3.3.1.2.	Methods.....	50
3.3.1.3.	Protein expression and purification	51
3.3.1.4.	Determination of new P450 _{cam} extinction coefficient.....	52
3.3.2.	Description of Enzymatic Assays	53
3.3.2.1.	Assays with recombinant proteins.....	53
3.3.2.2.	Steady-state kinetics.....	53
3.3.2.3.	Assays in D ₂ O buffer	54
3.3.2.4.	Assays with human P450 (CYP3A4).....	55
3.3.2.5.	Assays with dithionite	55
3.3.2.6.	Alignment of cytochromes P450 and superposition of CYP101A1 (P450 _{cam}) and CYP3A4	55
3.3.2.7.	The effect of camphor, borneol and DMSO on the expression of P450 _{cam} , PdX, and PdR	56
3.4.	Results and Discussion	57
3.4.1.	Reaction conditions leading to formation of borneol	57
3.4.2.	Source of the 2-H in borneol.	59
3.4.2.1.	Assays with other shunting agents.....	61
3.4.2.2.	¹⁷ O NMR of H ₂ O ₂	62
3.4.3.	Dependence of the H ₂ O ₂ (¹⁷ O) chemical shift on pH.....	64
3.4.4.	Kinetic Isotope Effects (KIE).....	65
3.4.5.	Determination of <i>K_M</i> and <i>k_{cat}</i> for borneol formation.....	66
3.4.6.	Reduction Mechanism.....	69
3.4.7.	Thermodynamic calculations in hydroxylation and the borneol cycle.....	71
3.4.8.	Control experiments with reactive O ₂ species/quenchers:	79
3.4.9.	Role of oxygen in the borneol cycle.....	82

3.4.10. Toxicity assays of borneol, hydrogen peroxide with <i>E. coli</i> and <i>P. putida</i>	84
3.4.11. Adaptive advantage of the borneol cycle to <i>P. putida</i>	86
3.5. Conclusions of this chapter.....	90
4. Screening of Cytochrome P450_{cam} SeSaM library with 3-chloroindole as the substrate to identify the dehalogenated metabolites of Endosulfan.....	92
4.1. Introduction	92
4.2. Materials and Methods	95
4.2.1. Experimental	95
4.2.2. SeSaM methodology.....	96
4.2.3. Cloning of SeSaM libraries.....	97
4.2.4. Preparation of 3-chloroindole	97
4.2.5. IC ₅₀ experiments with 3-chloroindole and endosulfan.....	98
4.2.6. Screening of 3-chloroindole with the SeSaM library using additives	98
4.2.7. Protein expression with the selected clone(s):.....	99
4.2.8. In vitro assays with the mutated and the wild type P450 _{cam} proteins.....	99
4.2.9. Determination of Cl ⁻ and H ₂ O ₂ in the enzymatic assays by ³⁵ Cl and ¹⁷ O NMR:	100
4.2.10. Steady-state kinetic assays for indole and 3-chloroindole hydroxylation with the P450 _{cam} mutant(s):.....	100
4.2.11. Determination of Fe-CO absorbance at 450 nm	100
4.2.12. MOE simulations.....	100
4.2.13. Screening of the SeSaM library with endosulfan as the substrate	101
4.2.14. Transformation of the selected mutant in <i>P. putida</i> (ATCC 17453) ²⁶²	101
4.2.15. Biodegradation of endosulfan using P450 _{cam} SeSaM library.....	102
4.2.16. In vitro assays with endosulfan as the substrate	103
4.2.17. Biodegradation of endosulfan diol using P450 _{cam} mutant (E156G/V247F/V253G/F256S)	103
4.2.18. In vitro assays with endosulfan diol as the substrate	104
4.3. Results.....	104
4.3.1. Identification of active mutants for the hydroxylation of 3-chloroindole	104
4.3.2. Steady-state kinetic analysis of the isolated mutants:.....	107
4.3.3. Proposed hypothesis for the formation of isatin:.....	108
4.3.4. Screening of SeSaM library with endosulfan as the substrate:	109
4.3.5. Biodegradation of endosulfan diol using the P450 _{cam} mutant (IND1) isolated from 3-chloroindole screen:.....	109
4.3.6. Biodegradation of endosulfan using the P450 _{cam} mutant V247F/D297N/K314E (E7) isolated from endosulfan screen:.....	111
4.3.7. Isolation and identification of metabolites obtained from the in vivo and in vitro assays of endosulfan diol biodegradation:	112
4.3.8. Proposed mechanism in the biodegradation of endosulfan and the formation of phthalaldehyde:	114
4.3.9. Docking of 3-chloroindole in the active site of P450 _{cam} :	118
4.3.10. Docking of endosulfan diol in the active site of P450 _{cam} :	120
4.3.11. Docking of endosulfan dialdehyde in the active site of P450 _{cam} :	122

4.4.	Discussion.....	125
4.5.	Conclusions:.....	126
4.6.	Supplementary information.....	128
4.6.1.	Sequence Saturation Mutagenesis (SeSaM).....	128
4.6.1.1.	Step 1 of SeSaM:	128
4.6.1.2.	Step 2 of SeSaM: Universal base addition.....	130
4.6.1.3.	Step 3 of SeSaM: Full length gene synthesis.....	130
4.6.1.4.	Step 4: Replacement of degenerate base.....	130
4.7.	Supplementary Tables and Figures	132
5.	Future work.....	148
6.	References	153

List of Tables

Table 1.1.	Classic reactions reported for P450s	3
Table 1.2.	Selected reactions of P450s to explain the versatility of the enzyme.....	9
Table 1.3.	P450 _{cam} mutants and their corresponding substrates (camphor analogues, alkanes)	18
Table 1.4.	P450 _{cam} mutants that accept halogenated and polycyclic aromatic mutants	19
Table 2.1.	Assays with P450:PdR:PdX complex isolated from <i>Pseudomonas putida</i>	40
Table 3.1	Calculated and literature values of P450 _{cam} extinction coefficients at selected wavelengths.	53
Table 3.2.	Assays with recombinant proteins. Formation of borneol, 5-exo-hydroxy camphor and 5-ketocamphor under various conditions.	59
Table 3.3.	Formation of 2-D-borneol and 5-ketocamphor in D ₂ O buffer, with the full P450 _{cam} system and with the shunted P450 _{cam}	61
Table 3.4.	Formation of borneol and hydrogen peroxide from the P450 catalytic cycle using other shunt agents.....	62
Table 3.5.	Assays with recombinant P450 _{cam} under selected temperatures. Formation of borneol and D-borneol under shunt conditions with the addition of m-CPBA.	66
Table 3.6.	Assays with recombinant P450 _{cam} , shunted with m-CPBA in H ₂ O and D ₂ O at selected temperatures. Formation of H ₂ O ₂ or D ₂ O ₂	66
Table 3.7.	Tests for involvement of free reactive oxygen species: formation of borneol, 5-ketocamphor and H ₂ O ₂	81
Table 4.1.	Active mutants isolated by screening the P450 _{cam} SeSaM library with 3-chloroindole.....	105
Table 4.2.	Active mutants isolated by screening the P450 _{cam} SeSaM library with 3-chloroindole.....	107
Table 4.3.	Steady-state kinetic assays with the three most active mutants towards 3-chloroindole oxidation.	108
Table 4.S1.	The results from SeSaM library validation	147

Table 4.S2. List of mutants obtained from the endosulfan screen with their sequences 147

List of Schemes and Figures

Scheme 1:	The incorporation of oxygen in a non-activated hydrocarbon to form an alcohol.....	1
Figure 1.1.	Catalytic cycle of cytochrome P450. The cycle, from species 1 to 8, shows the accepted pathway by which P450s couple the reduction of O ₂ to the oxidation of an organic substrate, represented here by RH. The bold horizontal lines on either side of Fe represent the porphyrin moiety. Path “a” shows the direct formation of the high-valent Fe ^{IV} -oxo-porphyrin radical cation species (Compound I, Cpd I) by oxidants such as m-CPBA. Paths “b”-“c” represent uncoupling of O ₂ reduction from the oxidation of organic substrate. Intermediates 5, 6 and 7 participate in the substrate oxidation reactions shown.....	5
Figure 1.2	The possible mechanisms of formation of Compounds I, II and ES from compound 0 by homolytic and heterolytic cleavage of the peroxy complex 6. When R=H in 6, the complex is known as Compound 0.....	6
Figure 1.3.	Two possible mechanisms by which (A) Compound 0 or (B) Compound I can epoxidise an alkene.....	7
Figure 1.4.	The desaturation of valproic acid catalysed by P4502B1 and its mechanism.....	8
Figure 1.5	A)The general Baeyer-Villiger mechanism for the formation of lactone from a ketone as catalysed by ferric hydroperoxy species. B) CYP85A2 catalyses the rate determining Baeyer-Villiger reaction in the brassinolide biosynthesis from castasterone.	10
Figure 1.6.	The 19-methyl hydroxylation of androst-4-ene-3, 17-dione, formation of diol and the aromatisation of the ring as catalysed by human placenta aromatase.	11
Figure 1.7.	P450 _{cam} (CYP101) catalyses the reductive dehalogenation of hexachloroethane.....	11
Figure 1.8.	Biosynthesis of linomarin and lotanstralin in cassava.	12
Figure 1.9	Structure of P450 _{cam} (PDB code: 2ZUW ⁸⁷)with the important helices coloured. Sheets shown in yellow and turns by green. The sequence comprising of 415 amino acids is listed below the structure. Camphor (the natural substrate of P450 _{cam}) shown in cyan, heme in beige and Cys357 shown in purple (and by an asterick in the sequence).....	14

Figure 1.10.	The hydrogen bond co-ordination between Y96 (present on B' helix) and camphor (shown in cyan). PDB code 2ZWU ⁸⁷ taken for studies.....	15
Figure 1.11.	T252 present in the I-helix (coloured by blue) of P450 _{cam} (A) helps in the proton shuttle mechanism and is substituted by N242 in P450 _{cin} (B). PDB code 2ZWU ⁸⁷ taken for studies.	16
Figure 1.12	The hydrophobic residues present in the substrate binding pocket of P450 _{cam} . PDB code 2ZWU ⁸⁷ taken for studies.	17
Figure 1.13.	The biosynthesis of plant hormones, secondary metabolites (8'-hydroxyabscisic acid, glycyrrhizin) in plants by P450s	20
Figure 1.14.	The synthesis of 20-hydroxyecdysone from cholesterol.....	21
Figure 1.15.	Conversion of chlorzoxazone by an engineered CYP102 variant.....	21
Figure 2.1.	The hydroxylation reaction of camphor: Formation of 5-exo-hydroxycamphor and 5-ketocamphor.....	29
Figure 2.2.	Borneol (12), the reduction product of camphor and isoborneol. Borneol is formed in <i>P. putida</i> but not isoborneol.....	30
Figure 2.3.	Time course quantities of 5-ketocamphor and borneol from an induced culture of <i>Pseudomonas putida</i> under aerated and non-aerated conditions.	38
Figure 2.4.	Toxicity assays for camphor and borneol in two strains of bacteria: ATCC 17453 of <i>P. putida</i> (a) and <i>E. coli</i> (b).....	42
Figure 2.5.	IC ₅₀ experiments on <i>Escherichia coli</i> with varying concentrations of camphor and borneol.....	42
Supplementary figure 2.S1.	The SDS-PAGE gel analysis of the proteins (P450 _{cam} , PdR and PdX) obtained after purification from anion-exchange (DE-52) column. Lanes 1, and 5 are molecular markers; Lane 2 is the BSA standard. Lanes 3, 4, 6, and 7 are the fractions collected from the DE-52 column. The arrows show the approximate positions where we expect P450 _{cam} (47 kDa), PdR (46 kDa) and PdX (12 kDa) to appear.....	45
Figure 3.1	Under highly oxygenated conditions, P450 _{cam} hydroxylates camphor (9) to 5-exo-hydroxy camphor (10) and further to 5-ketocamphor (11), whereas under low oxygen conditions, P450 _{cam} reduces camphor to borneol (12). Details of the high O ₂ cycle are shown in Fig. 1.1 and the details of the low O ₂ cycle are shown in Fig. 3.6.	49

Figure 3.2.	^2H NMR of the 2-D-borneol obtained from the recombinant proteins incubated in 50 mM deuterated phosphate buffer (pD = 7.4) with camphor and m-CPBA. The extracted product was backwashed with H_2O	60
Figure 3.3.	^{17}O NMR spectrum of the incubation mixture in ^{17}O phosphate buffer (pH 6.3) containing: a) camphor, recombinant P450_{cam} and m-CPBA, b) camphor and recombinant P450_{cam} (m-CPBA absent), c) camphor and m-CPBA (enzyme absent), and d) m-CPBA and recombinant P450_{cam} (substrate absent). The peaks at 0 ppm and 178 ppm correspond to H_2^{17}O and $\text{H}_2^{17}\text{O}_2$, respectively.	63
Figure 3.4.	^{17}O NMR spectra of the incubation mixture under shunt conditions using 1 mM m-CPBA in ^{17}O phosphate buffer (final pH 6.3) containing 1 mM substrate camphor and recombinant P450_{cam} : a) before and b) after addition of catalase (1 unit). The peak at 178 ppm corresponds to $\text{H}_2^{17}\text{O}_2$ and that at 0 ppm is due to H_2^{17}O	64
Figure 3.5.	^{17}O NMR spectra of $\text{H}_2^{17}\text{O}_2$ (obtained by electrolysis of H_2^{17}O) buffered at a) pH 10, b) pH 3, and c) pH 9.	65
Figure 3.6	a) Michaelis-Menten kinetics for borneol and b) 5-ketocamphor formation, under shunt conditions (with m-CPBA). To ensure a constant high O_2 concentration for the 5-ketocamphor formation kinetics, reactions were run in vials fitted with septa and pressurized with pure O_2	68
Figure 3.7	The proposed reduction mechanism and the Born-Haber estimates. a) Proposed reduction mechanism of P450_{cam} that accounts for the simultaneous formation of borneol (12) and H_2O_2 in a 1:1 stoichiometry. b) Born-Haber estimates of the reduction mechanism.	70
Figure 3.8	a) Summary of the borneol cycle steps and of the net reaction b) Possible routes by which the borneol cycle could end.	74

Figure 3.9. Alignment of microbial cytochromes P450 against P450_{cam} (upper portion) and of vertebrate class II P450s, also against P450_{cam} (lower portion). Microbial sequences used: gamma prot 1 = marine gamma proteobacterium HTCC2207 (ZP_01225512), Novo ar CYP = *Novosphingobium aromaticivorans* CYP 101D2 (PDB 3NV6), Sphingo echi = *Sphingomonas echinoides* ATCC14820 (ZP_10341012), Novo CYP 101D1 = a camphor hydroxylase from *Novosphingobium aromaticivorans* DSM 12444 (PDB 3LXI), Sphing chlor = *Sphingomonas chlorophenicum* camphor hydroxylase (ZP_10341012), Azospir B510 = *Azospirillum* sp. B510 (YP_003451823), Azospir = (BAI74843), P450 Burk H160 = *Burkholderia* sp. H160 (ZP_03264429), P450 Burk MCO-3 *Burkholderia cenocepacia* MC0-3= (YP_001774494), Sping Witt R = *Sphingomonas wittichii* RW1 (YP_001262244), Citromicrobi = *Citromicrobium bathyomarimum* JL354 (ZP_06860768), Novo CYP 101 = *Novosphingobium aromaticivorans* DSM12444 CYP 101C1 (PDB 3OFT_C), Sping E 14820 = *Sphingomonas echinoides* ATCC 14820 (ZP_10339023), gamma prot 2 = marine gamma proteobacterium NOR51-B (ZP_04956740), Sphingomonas = *Sphingomonas* sp. KC8 (ZP_09138048), Sphing chl L = *Sphingobium chlorophenicum* L-1 (YP_004553185), P450 nor = Cytochrome P450nor from *Fusarium oxysporum* (BAA03390). Vertebrate P450s: Cyp lan deme = lanosterol 14- α demethylase isoform 1 precursor *Homo sapiens* (NP_000777), CYP 2C9 = human liver limonene hydroxylase (P11712), CYP 4A11 *Homo sapiens* (NP_000769), CYP 4F12 = fatty acyl Ω -hydroxylase *Homo sapiens* (NP_076433), CYP 4F2 = leukotriene-B(4) omega-hydroxylase 1 precursor *Homo sapiens* (NP_001073), CYP 3A5 form 1 = CYP 3A5 isoform 1 *Homo sapiens* (NP_000768), CYP 3A4 = CYP 3A4 isoform 1 *Homo sapiens* (NP_059488), CYP26B1 = retinoic acid hydroxylase *Homo sapiens* (NP_063938)..... 77

Figure 3.10 Superposition of P450_{cam} and P450 3A4. a) Top row: superimposed ribbon diagrams of P450_{cam} (1DZ4) and CYP3A4 (1TQN). P450_{cam} is shown with red helices and yellow sheets, whereas CYP3A4 is shown all in pink. The porphyrin for P450_{cam} is shown in gray and the one for CYP3A4, in brown. The two views are orthogonal to each other. The substrate access channel (SAC) is marked, as is Helix I, the central pillar of the fold. b) Lower row: superimposed active sites of P450_{cam} and CYP3A4. The porphyrin of P450_{cam} is shown in gray, the one for CYP3A4 in brown. The camphor ligand of P450_{cam} is shown in green. Residues from the two proteins are red (P450_{cam}) and pink (CYP3A4). The two views are orthogonal to each other..... 78

Figure 3.11.	Sites in P450 _{cam} and in CYP3A4 with camphor docked. A) Oxygen binding site in P450 _{cam} (residues shown in red), with superimposed residues in CYP3A4 shown in pink. The porphyrin of P450 _{cam} is gray, and the one for CYP3A4 is brown. B) Water channel in P450 _{cam} (residues shown in red), with superimposed residues in CYP 3A4 shown in pink. The view in a) and b) are from a similar angle, to emphasize the closeness of the O ₂ binding site and the water channel in P450 _{cam} . C) and D) Camphor docked into the active site of CYP3A4 (orthogonal views). The H-bond from Arg 105 to the camphor ketone can be seen in the lower right portion of D).	83
Figure 3.12.	IC ₅₀ determination of a) H ₂ O ₂ and b) of a 1:1 (molar) mixture of borneol and H ₂ O ₂ against <i>E. coli</i> , a species of bacterium that lacks cytochrome P450.....	85
Figure 3.13.	Effect of 16 h incubation of stationary <i>E. coli</i> (a) and <i>P. putida</i> (b) cultures with borneol: H ₂ O ₂ (1:1), borneol, or H ₂ O ₂ (1 mM).....	86
Figure 3.14.	a) Outline of the experiment used to determine the effect of camphor and borneol on P450 _{cam} , PdX and PdR expression. b) The effect of camphor, borneol and DMSO on the P450 expression by <i>P. putida</i> (ATCC 17453). The concentration of P450 _{cam} was obtained from the Soret peak absorbances and was normalized against the number of colony forming units/mL. The absorbances at 392 nm and 410 nm correspond to the substrate containing and free P450 _{cam} Soret band. Points represent the average ± S. E. of three replicates.....	87
Figure 3.15.	The effect of camphor, borneol and DMSO on the PdX expression by <i>Pseudomonas putida</i> (ATCC 17453). The concentration of PdX was obtained from the absorbance at 325 nm that corresponds to the Fe ₂ S ₂ cluster of PdX and was normalized against the number of colony forming units/mL. Points represent the average ± S. E. of three replicates.....	88
Figure 3.16.	The effect of camphor, borneol and DMSO on the PdR expression by <i>Pseudomonas putida</i> (ATCC 17453). The concentration of PdR was obtained from the absorbance at 454 nm that corresponds to the flavin moiety of PdR and was normalized against the number of colony forming units/mL. Points represent the average ± S. E. of three replicates.....	89
Figure 4.1.	Endosulfan and its metabolites reported in the literature.....	95
Figure 4.2.	A) HPLC of isatin produced in the in vitro assays with P450 _{cam} mutant IND1 (Table 4.2), 3-chloroindole under shunt conditions B) Gas chromatogram and C) Mass spectrum of enzyme-produced isatin purified by HPLC	106

Figure 4.3.	Proposed mechanism for the formation of isatin from 3-chloroindole, catalysed by P450 compound I.....	109
Figure 4.4.	Biodegradation of endosulfan diol by the P450 _{cam} mutant IND1 and the formation of metabolites endosulfan dialdehyde and the M+1 = 135 compound in the treatments. Treatment: P450 _{cam} mutant IND1 in plasmid pALXtreme-1a transformed in <i>P. putida</i> ATCC 17453. Control: Wild-type P450 _{cam} in plasmid pALXtreme-1a transformed in <i>P. putida</i> ATCC 17453.	111
Figure 4.5.	Biodegradation of endosulfan by the isolated mutant ES7 and the formation of metabolites endosulfan diol and the M+1 = 135 compound in the treatments. Treatment: P450 _{cam} mutant ES7 in plasmid pALXtreme-1a transformed in <i>P. putida</i> ATCC 17453. Control: Wild-type P450 _{cam} in plasmid pALXtreme-1a transformed in <i>P. putida</i> ATCC 17453.	112
Figure 4.6.	Gas chromatogram and mass spectrum of phthaldialdehyde isolated from the in vitro and in vivo assays with P450 _{cam} mutants (see above) and endosulfan diol as the substrate.....	113
Figure 4.7	Gas chromatogram and mass spectrum of silylated 3-hydroxy phthaldialdehyde isolated from the in vitro and in vivo assays with P450 _{cam} mutants (see above) and endosulfan diol as the substrate.....	114
Figure 4.8.	Stage 1 in the metabolism of endosulfan. Formation of metabolites 3-9.....	115
Figure 4.9.	Stage 2 in endosulfan metabolism: Biodegradation of endosulfan dialdehyde.....	116
Figure 4.10.	Stage 3 in endosulfan metabolism. Formation of phthaldialdehyde.	117
Figure 4.11.	A) The ³⁵ Cl NMR spectrum of the incubation mixture containing i) endosulfan diol, mutant IND1, and m-CPBA. ii) mutant IND1 and m-CPBA (diol absent). iii) diol and m-CPBA (mutant IND1 absent). iv) diol and IND1 (m-CPBA absent). The peak at 0 ppm corresponds to aq. Cl ⁻ , and the peak at -10 ppm is a synthetic peak (ERETIC2) with an area equal to that observed for an external sample of 10 mM NaCl in D ₂ O. B) ¹⁷ O NMR spectrum of the incubation mixture in ¹⁷ O phosphate buffer containing: i) endosulfan diol, mutant IND1, and m-CPBA. li) mutant IND1 and m-CPBA (diol absent). lii) diol and m-CPBA (mutant IND1 absent). lvi) diol and IND1 (m-CPBA absent). The peak at 175 ppm corresponds to H ₂ ¹⁷ O ₂	118

Figure 4.12.	A) Graphical representation of the distances from C-2 and C-3 to Fe in the poses of 3-chloroindole obtained after docking 3-chloroindole in the active site of IND1. B) Graphical representation of the distances from C-2 and C-3 to Fe and the poses of 3-chloroindole obtained after docking 3-chloroindole in the active site of WT P450 _{cam} .	119
Figure 4.13	A) 3-chloroindole docked in the wild-type P450 _{cam} (pose 3 from the Fig. 4.10 B selected). B) 3-chloroindole docked in the mutant IND1 (pose 5 from the Fig. 4.10 A selected). The porphyrin is shown in black, 3-chloroindole in green and the amino acid residues in yellow.	120
Figure 4.14.	A) Graphical representation of the distances of C-2, C-3, C-8 and C-9 to Fe in the poses of endosulfan diol obtained after docking it in the active site of IND1. B) Graphical representation of the distances of C-2, C-3, C-8 and C-9 to Fe in the poses of endosulfan diol obtained after docking it in the active site of WT P450 _{cam} .	121
Figure 4.15	A) Endosulfan diol docked in the wild-type P450 _{cam} . B) Endosulfan diol docked in the mutant IND 1 (pose 19 selected from 4.11 B). The porphyrin is shown in black, 3-chloroindole in green and the amino acid residues in yellow.	122
Figure 4.16	A) Graphical representation of the distances of C-2, C-3, C-8 and C-9 to Fe in the poses of endosulfan dialdehyde obtained after docking it in the active site of IND1. B) Graphical representation of the distances of C-2, C-3, C-8 and C-9 to Fe in the poses of endosulfan dialdehyde obtained after docking it in the active site of WT P450 _{cam} .	124
Supplementary figure 4.S1.	Steps involved in SeSaM library preparation.	132
Supplementary figure 4.S2.	The vector map of pALXtreme-1a, an inhouse pET(+28a) vector	133
Supplementary figure 4.S3.	0.8% agarose gel analysis of culture PCR for the randomly picked clones from MEGAWHOP step 2 reaction. The positive clones are shown by circles. Lanes 11, 19 and 25 represent the DNA marker with molecular weights ranging from 0.25-6 kbp.	134
Supplementary figure 4.S4.	Determination of Fe-CO absorbance at 450 nm a) The Soret peak of P450 _{cam} was detected at 410 nm b) P450 _{cam} was reduced by Na ₂ S ₂ O ₄ and the intensity of Soret peak was reduced. c) CO was bubbled in the reduced protein for ~ 2 min and the absorption of Fe(II)-CO was recorded.	135

Supplementary figure 4.S5.	Transformation of SeSaM P450 _{cam} mutant library in BL21(DE3) cells and further screening with 3-chloroindole.	136
Supplementary figure 4.S6.	IC ₅₀ experiments on Escherichia coli using varying concentrations of 3-chloroindole and endosulfan.....	137
Supplementary figure 4.S7.	¹ H NMR of isatin.....	138
Supplementary figure 4.S8.	¹³ C NMR of isatin.....	139
Supplementary figure 4.S9.	Steady state kinetic analysis for 3-chloroindole oxidation and formation of isatin	140
Supplementary figure 4.S10.	In vitro assay results with endosulfan diol as the substrate under shunt conditions using m-CPBA and detection of metabolites by GC-MS. Endosulfan dialdehyde was detected as a major product.	141
Supplementary figure 4.S11.	Transformation of the mutant P450 _{CAM} plasmid isolated from 3-chloroindole screen in P. putida. The cytochrome P450 _{cam} hydroxylase operon present on the CAM plasmid of P. putida is responsible for the camphor degradation pathway	142
Supplementary figure 4.S12.	Experimental design and apparatus for the endosulfan biodegradation experiment with mutant-transformed P. putida.	143
Supplementary figure 4.S13.	¹ H NMR of pure phthalaldialdehyde obtained from in vitro assays and the biodegradation studies.	144
Supplementary figure 4.S14.	¹³ C NMR of pure phthalaldialdehyde obtained from in vitro assays and the biodegradation studies.	145
Supplementary figure 4.S15.	¹ H NMR of 3-hydroxy phthalaldialdehyde obtained from in vitro assays and the biodegradation studies.	146

List of Acronyms and Abbreviations

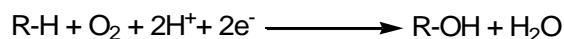
ABA	Abscicic acid
ANOVA	Analysis of variance
ATCC	American Type Culture Collection
BHT	butylated hydroxytoluene
BLAST	Basic Local Alignment Search Tool
BL	Brassinolide
BSTFA	N,O-Bis(trimethylsilyl)trifluoroacetamide
BVMOs	Baeyer-Villiger Monooxygenases
Cpd I	Compound I or iron-oxo species
Cpd II	Compound II
CFU	Colony forming units
CHP	Cumene hydro-peroxide
CYPs	Cytochrome P450s
CS	Castasterone
7-dc	7-dehydrocholesterol
DE	Diethylaminoethyl cellulose
DMSO	Dimethyl sulphoxide
DTT	Dithiothreitol
<i>E. coli</i>	<i>Escherichia coli</i>
EDTA	Ethylene diamine tetraacetic acid
EI	Electron impact
FAD	Flavine adenine dinucleotide
Fld	FMN-containing flavodoxin
FMN	Flavin mononucleotide
FMOs	FAD-dependent Monooxygenases
GC-MS	Gas-Chromatography Mass spectrometry
KIE	Kinetic isotope effect
IPTG	Isopropyl- β -D-1-thiogalactopyranoside
LB	Luria Broth
<i>m</i> -CPBA	meta-chloro perbenzoic acid

MOE	Molecular Operating Environment
MOPS	3-(N-morpholino)-propane sulfonic acid
NADH	Nicotinamide adenine dinucleotide
NBP	γ -(4-Nitro benzyl) pyridine
NIH	National Institute of Health
PCR	Polymerase Chain Reaction
PdR	Putidaredoxin reductase
PdX	Putidaredoxin
PeCB	Pentachloro benzene
ppm	parts per million
<i>P. putida</i>	<i>Pseudomonas putida</i>
PTFE	Polytetra fluoroethylene
rP450	Recombinant P450
SDS-PAGE	Sodium dodecyl sulphate-polyacrylamide gel electrophoresis
SeSaM	Sequence Saturation Mutagenesis
SOD	Superoxide Dismutase
TdT	Deoxynucleotidyl terminal transferase
Tris	Tris(hydroxymethyl)aminomethane
TLC	Thin Layer Chromatography
Tyr	Tyrosine
Y96	Tyrosine 96
WT	Wild-type

1. Introduction

1.1. Cytochrome P450s: Importance and Classification

Cytochromes P450 are heme-thiolate proteins that catalyze numerous reactions. All cytochromes P450 (CYPs) have the iron protoporphyrin IX (heme) coordinated to the thiolate of a conserved cysteine residue.¹ In prokaryotes and eukaryotes, more than 400 P450's have been identified and studied for their unique mechanism of inserting oxygen into a non-activated C-H bond of aliphatic or alicyclic substrates²⁻⁴ (Table 1.1). While breaking of carbon and hydrogen bonds requires high temperature and pressure, the enzyme successfully drives this uphill reaction (~350 kJ/mol)⁵ by reducing oxygen from air to water and subsequently oxidizing the hydrocarbon (Scheme 1).



Scheme 1: *The incorporation of oxygen in a non-activated hydrocarbon to form an alcohol*

Recent studies have been extended to other reactions, such as aromatic⁶ (Table 1.2, entry 1) and aliphatic hydroxylation,⁷ epoxidation⁸ (Table 1.2, entry 2),⁹ NIH shift (which occurs when aromatic substrates are hydroxylated via an epoxy intermediate) (Table 1.2, entry 1),¹⁰ sulfur oxidation,¹¹ aromatization,¹² oxidative demethylation^{13, 14} N- and O-dealkylations¹⁵ (Table 1.2). The active sites of these enzymes are hydrophobic^{16,17} and have a Fe-protoporphyrin IX as the prosthetic group, with Fe axially coordinated to the -SH of a conserved cysteine residue.¹⁸

There are two classifications of the cytochromes P450. One classifies the enzymes according to their electron transfer partners and/or the need for dioxygen.¹⁹ The other classification groups the cytochromes P450 (CYPs) according to their degree of sequence identity (<http://drnelson.uthsc.edu/CytochromeP450.html>).²⁰ Based on the electron transfer partners, P450s are divided into three classes: I, II and III.²¹

Class I P450s: The class I P450s are primarily found in cytosol of bacteria and in mitochondria, use NAD(P)H as the source of electrons and two electron transfer partners: an iron sulfur protein (such as putidaredoxin (*PdX*) or adrenodoxin) and, a FAD-containing reductase of the iron sulfur protein (such as putidaredoxin reductase (*PdR*) or adrenodoxin reductase).^{22,23} The iron sulfur protein in these cases interacts with P450 for the transfer of electrons from NAD(P)H.²⁴ Examples include the P450_{cam} isolated from *Pseudomonas putida* (CYP101A1),²⁵ P450_{terp} (CYP108A1),²⁶ P450_{scc} (CYP 11A1)²⁷ (Table 1.1, entries 1-3).

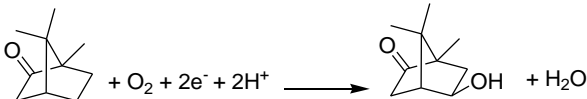
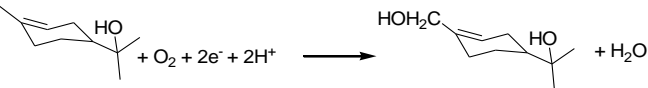
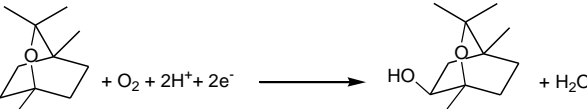
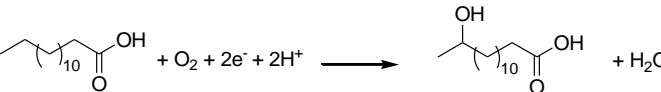
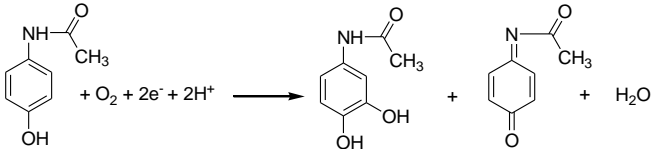
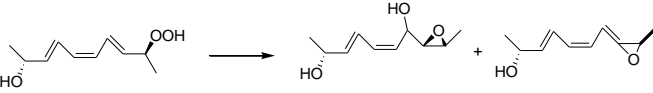
Class II P450s (microsomal P450s): The class II P450s have a reductase (a FAD/FMN dependent electron-transfer partners), and they use NADPH as the cofactor. Class II P450s are found primarily in the endoplasmic reticulum (Table 1.1, entries 4-5) with the exception of cytochrome P450_{BM3} (CYP102A2), isolated from *Bacillus megaterium*.²⁸ P450_{BM3} occurs as a fusion protein with the P450 and reductase domains on the same polypeptide chain, making it the most active hydroxylation catalyst known to date (Table 1.1, entry 4).²⁹

Class III P450's: The class III P450s do not catalyse monooxygenation reactions and do not require the electron transfer partners.¹⁹ Instead, these enzymes accept hydroperoxides as substrates. Allene oxide synthase (CYP74A),³⁰ thromboxane synthase (CYP5A1),³¹ and prostacyclin synthase³² belong to this category (Table 1.1, entry 6).

Nebert et.al.³³ classified the CYPs based on their amino acid sequence similarity. This classification suggests that any two CYPs with a sequence identity greater than 40% belong to a single CYP family, and CYPs with a sequence identity greater than 55% belong to a subfamily.³³ The clan system approach, introduced by Nelson et. al.³⁴ was then used to classify CYPs based on their sequence similarity. Based on the hypothesis that CYPs are of monophyletic origin, the CYP families are placed into a single clan and new CYPs with same sequence similarity are placed in the same clan. As of 2011, there are 16000 CYP genes that are partially classified into classes B and E.³⁵ CYP101A1 (P450_{cam}), isolated from *Pseudomonas putida* belongs to class B, which includes some of the cytochromes P450 from prokaryotes and fungi.³⁵ In CYP101A1, CYP represents the abbreviation of P450 gene, the number 101 represents the family, the letter 'A' denotes the subfamily and the last numeral denotes the number of the gene that

encodes the protein. As another example, class E is sub-divided into 10 groups that includes vertebrates, plants, arthropods, some fungi and some prokaryotes.³⁵

Table 1.1. Classic reactions reported for P450s

Entry	Class	CYP	Reported reaction
1	I	P450 _{cam} (CYP101A1)	
2	I	P450 _{terp} (CYP108A1)	
3	I	P450 _{cin} (CYP176A)	
4	II	P450 _{BM3} (CYP102A1)	
5	II	P450 (CYP2E1/1A2/3A4)	
6	III	CYP74A	

1.2. Catalytic cycle of P450s

The resting state of the enzyme (1) contains hexacoordinated heme, with a water molecule bound to the axial position opposite to the cysteine thiolate. The substrate (in the case of P450_{cam}, camphor) displaces the coordinated water molecule to form a pentacoordinated ferric-substrate complex (2).³⁶ This causes a change in the spin state

from low spin ($S=1/2$) to high spin ($S=5/2$)³⁷ and increases the heme-iron reduction potential by 130 mV,³⁶ which makes the first step in the catalytic cycle (electron transfer to the heme), more favourable than in the absence of bound substrate. In the class I P450s, the substrate-bound ferric complex accepts electrons from the pyridine nucleotide cofactor NAD(P)H, via its redox partner(s) to form the ferrous species (**3**).³⁸ (**3**) binds to oxygen to form the superoxo species (**4**) which accepts a second electron and a proton, to form the hydroperoxo species (also known as Compound 0) (**6**).³⁹ Following proton transfer, compound 0 (**6**) loses a water molecule to form the high valent iron-oxoporphyrin moiety (Fe(IV)=O Por^+), known as compound I (**7**).⁴⁰⁻⁴³ Hydroxylation occurs when compound I abstracts a hydrogen atom from the substrate, forming a carbon radical and Fe(IV)-OH (**8**) and an alcohol then forms by a rebound mechanism (Fig. 1.1).⁴⁴ There has been a long search to identify and characterize the most reactive species in the catalytic cycle⁴⁵ and recently, Rittle and Green have provided strong evidence for the existence of compound I (Cpd I) by EPR experiments.⁴⁶ Though Cpd I was reported as the reactive species responsible for the insertion of oxygen in a substrate, the ferric hydroperoxo species (Cpd 0) (**6**) has also been determined to be reactive in hydroxylation and epoxidation reactions.^{47,48} The peroxo species (**5**) has been reported to be active in Baeyer-Villiger reactions.⁴⁹

Newcomb *et.al.*^{50,51} reported that one electron oxidation of the resting enzyme by peroxynitrite or shunting by peroxyacids forms Compound II (Fig. 1.2) (characterised by a Soret band of ~420 nm in its unprotonated form ($\text{Fe}^{1V}=\text{O}$). Cpd II is proposed to act as an alternative oxidant in the C-H hydroxylations and epoxidations (Fig. 1.1 and Fig. 1.2).

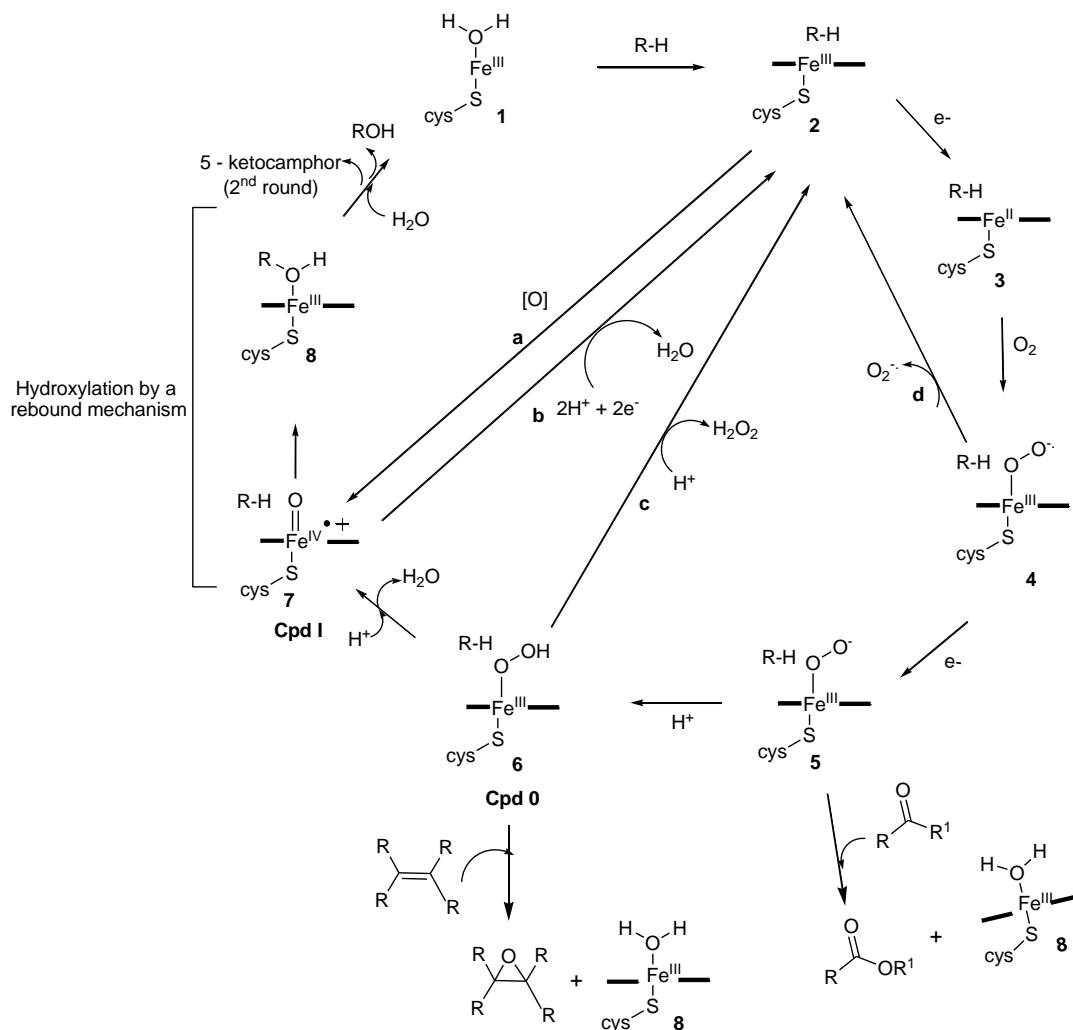


Figure 1.1. Catalytic cycle of cytochrome P450. The cycle, from species 1 to 8, shows the accepted pathway by which P450s couple the reduction of O₂ to the oxidation of an organic substrate, represented here by RH. The bold horizontal lines on either side of Fe represent the porphyrin moiety. Path “a” shows the direct formation of the high-valent Fe^{IV}-oxo-porphyrin radical cation species (Compound I, Cpd I) by oxidants such as *m*-CPBA. Paths “b”-“c” represent uncoupling of O₂ reduction from the oxidation of organic substrate. Intermediates 5, 6 and 7 participate in the substrate oxidation reactions shown.

1.2.1. Peroxide shunt

Recent reports show that Cpd I (7, Fig. 1.1) can also be generated in a shunt pathway of the catalytic cycle using artificial oxidants like alkyl hydroperoxides,⁵² iodosobenzene,⁵³ H₂O₂⁵⁴ or *m*-CPBA.⁵⁵ This eliminates the need to transfer electrons from NAD(P)H for

the reduction of O₂ in the catalytic cycle. The reaction between the resting ferric state of P450 with alkyl/acyl hydroperoxide forms alkyl/acyl hydroperoxo species (Fe^{III}-OOR or Cpd 0) which splits either heterolytically to form Cpd I (path a, Fig. 1.2) and alcohol/acid or homolytically (path b, Fig. 1.2) to Compound II (Cpd II) and a neutral organic hydroxyl/acid radical depending on the pH or the heme environments.⁵⁶ (Fig. 1.2)

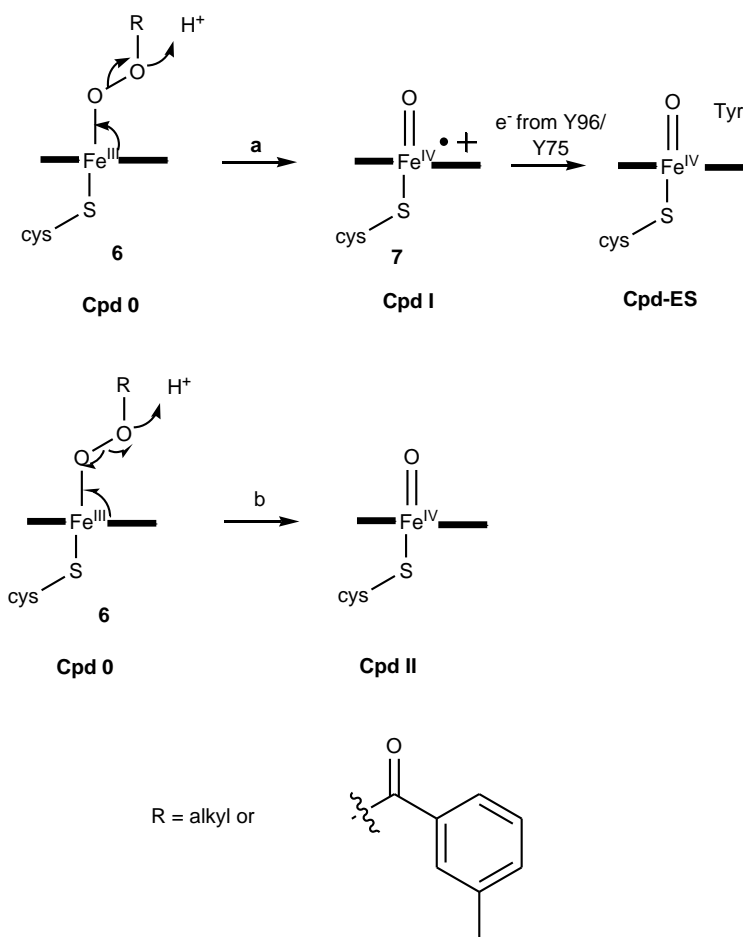


Figure 1.2 The possible mechanisms of formation of Compounds I, II and ES from compound 0 by homolytic and heterolytic cleavage of the peroxo complex 6. When R=H in 6, the complex is known as Compound 0.

1.2.2. Other reactions

Cytochrome P450s have been reported to catalyse reactions other than C-H hydroxylations. A few examples are listed below and also in Table 1.2.

1.2.2.1. Alkene epoxidation

There are two intermediates in the P450 catalytic cycle that can epoxidise an alkene: compound 0 (**6**) or compound I (**7**). A) The epoxidation of an alkene by a hydroperoxo species in a concerted mechanism is shown in Fig. 1.3 (A). B) The oxidation of trichloroethylene to trichloroethylene epoxide (Fig. 1.3 (B)) can open and rearrange to trichloroacetaldehyde.⁵⁷

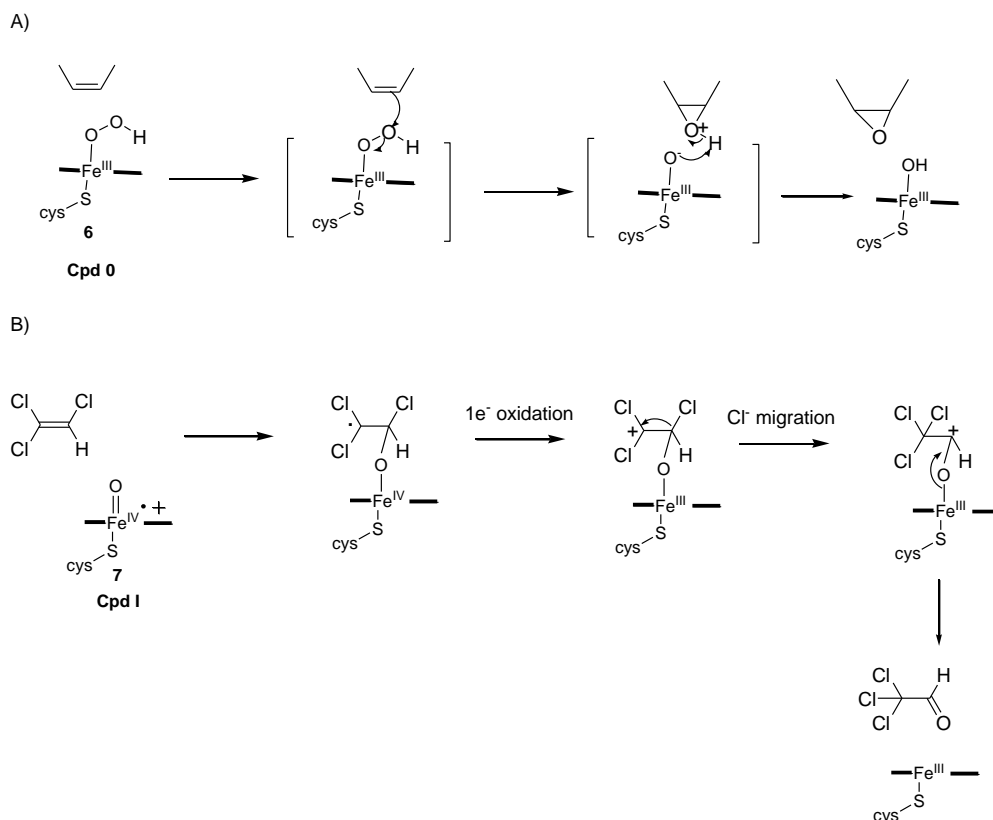


Figure 1.3. Two possible mechanisms by which (A) Compound 0 or (B) Compound I can epoxidise an alkene.

The epoxidation of *p*-cymene is catalysed by three different P450s (CYP1A2, 2D6 and 2A6), and the resulting intermediate undergoes an NIH shift to yield thymol⁵⁸ (Table 1.2, entry 1). CYP2D6 epoxidises linalool to linalool 6,7-epoxide which then rearranges within the enzyme's active site to yield tetrahydropyran product (a) or tetrahydrofuran product (b) (Table 1.2, entry 2).⁴²

1.2.2.2. Dealkylation reactions

CYP2A6 catalyzes the dealkylation of N,N-dimethyl nitrosamine by hydroxylating one of the pendant methyl groups. This hemiaminal hydrolyses to formaldehyde which is further oxidized to formic acid (Table 1.2, entry 3).⁵⁹ Similarly, CYP2D6 demethylates anisole (entry 4) to form phenol.⁶⁰

1.2.2.3. Dehydrogenation reactions

The oxidation of alcohols to ketones and the conversion of saturated to unsaturated hydrocarbons come under this category of reactions. The conversion of 2-*n*-propyl-pentanoic acid (valproic acid) to 2-*n*-propyl-2(*E*)-pentenoic acid is catalysed by P4502B1 in human liver microsomes⁶¹ (Fig. 1.4). Further reported desaturation reactions include the conversion of lindane (1,2,3,4,5,6-hexachlorocyclohexane) to 1,2,3,4,5,6-hexachlorocyclohexene by P450,⁶² desaturation of ergosterol by yeast microsomes⁶³ and oxidation of dihydronaphthalene to naphthalene.⁶⁴ Desaturation reactions are also reported in non-heme iron enzymes,⁶⁵ fatty acid desaturases⁶⁶ and CYPs probably use a similar mechanism.

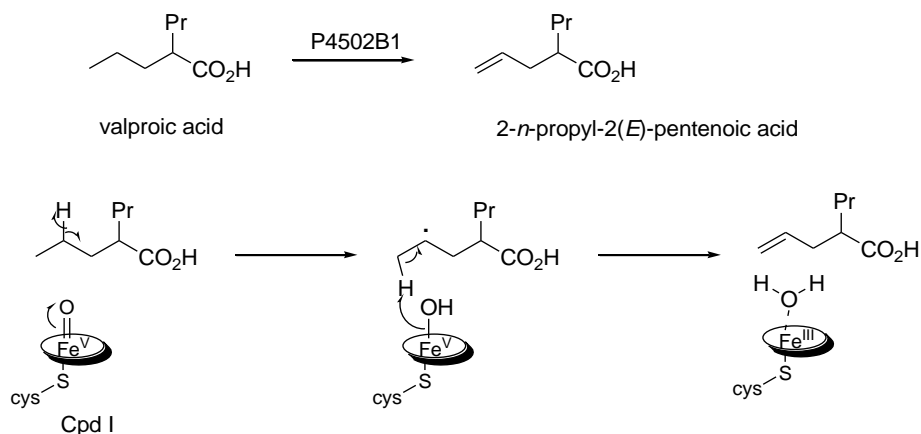
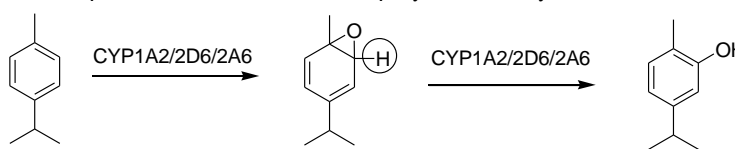
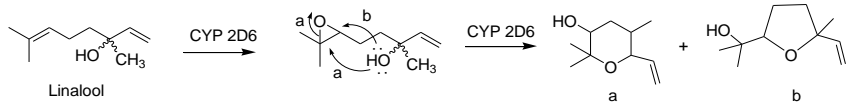
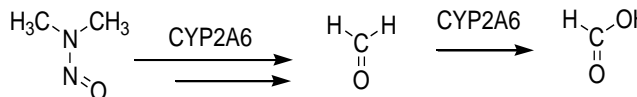
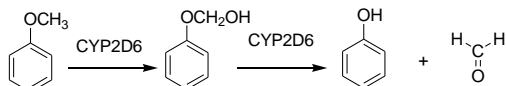


Figure 1.4. The desaturation of valproic acid catalysed by P4502B1 and its mechanism.

Table 1.2. Selected reactions of P450s to explain the versatility of the enzyme

Entry	Type of reaction	Reference
1	<p>Arene epoxidation and NIH shift of p-cymene to thymol</p> 	58
2	<p>Epoxidation of linalool and the formation of rearranged products</p> 	42
3	<p>Nitrosamine dealkylation to formaldehyde</p> 	59
4	<p>Oxidative demethylation of anisole</p> 	60

1.2.2.4. Baeyer Villiger oxidation

The conversion of castasterone (CS) to brassinolide (BL) in plants is catalysed by CYP85A2, ⁶⁷ a P450 that mediates the introduction of an oxygen atom in a C-C bond, a reaction typically known as a Baeyer-Villiger Oxidation (Fig. 1.5). This reaction is mediated in Baeyer-Villiger Monooxygenases (BVMOs) in some plants and fungi which are typically FAD-dependent monooxygenases (FMOs). ⁶⁸ The presence of 26 FMOs in plants suggested that they act as enzymes catalyzing Baeyer-Villiger reactions but recently, Kim *et.al.* ⁶⁷ by their biochemical studies have indicated that P450 mediates this reaction in plants. A generalized mechanism for the formation of lactone from ketone by the ferric hydroperoxo species (6, Fig. 1.1) is shown in Fig. 1.5 A. The Baeyer-Villiger rearrangements in the progesterone oxidation, lanosterol 14 α -demethylation reactions have shown to be catalysed by CYP17 and CYP51 respectively. ⁶⁹

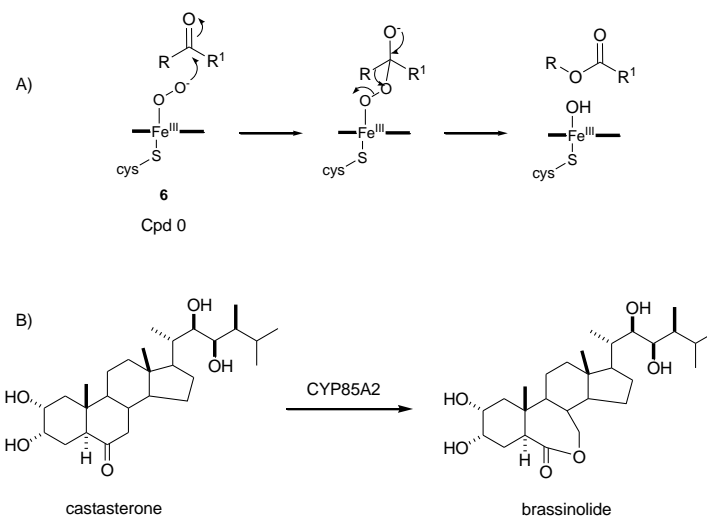


Figure 1.5 A) *The general Baeyer-Villiger mechanism for the formation of lactone from a ketone as catalysed by ferric hydroperoxy species.* B) *CYP85A2 catalyses the rate determining Baeyer-Villiger reaction in the brassinolide biosynthesis from castasterone.*

1.2.2.5. P450 as an aromatase

P450_{aromatase} (CYP19) can catalyse the C-C bond cleavage, hydroxylation as well as the oxidation reactions as shown in Fig. 1.6.⁷⁰ The 19-methyl hydroxylation of androst-4-ene-3,17-dione happens with retention of configuration and the methyl group elimination in the third step causes the aromatization of the ring in the given substrate.⁷⁰ Studies on this reaction also showed that the conversion takes place in 3 steps and each step requires one equivalent of both NADPH and O₂⁷⁰ and this reaction is not supported by the artificial oxidants like iodosobenzene or cumene hydroperoxide.⁴⁷

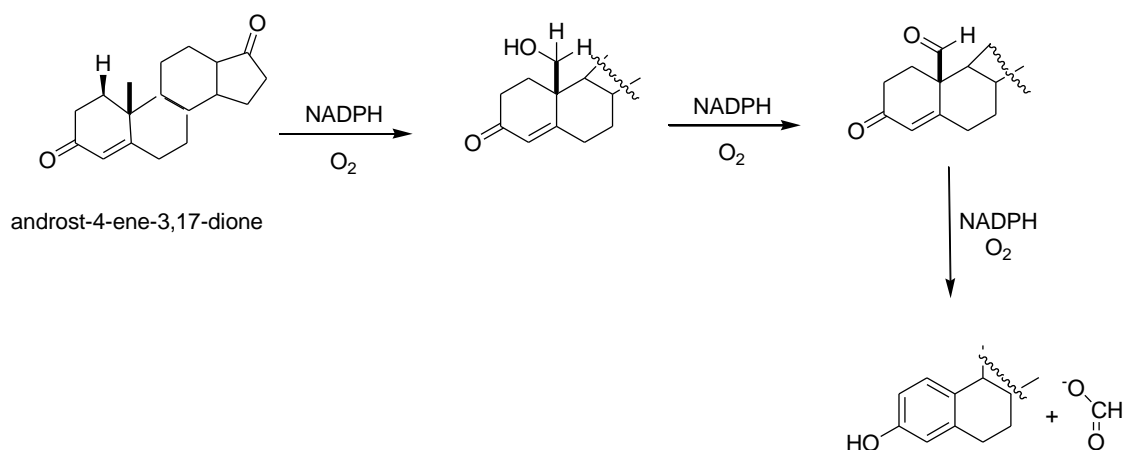


Figure 1.6. The 19-methyl hydroxylation of androst-4-ene-3, 17-dione, formation of diol and the aromatisation of the ring as catalysed by human placenta aromatase.

1.2.2.6. Dehalogenation reactions

CYP101 (cytochrome P450_{cam}), known for the 5-exo-hydroxylation of camphor is also known for the reductive dehalogenation of haloaliphatic compounds.⁷¹ P450 1A2/yeast heterologous system was also shown to dehalogenate hexachloroethane to tetrachloroethylene and pentachloroethane⁷² as shown in Fig. 1.7.

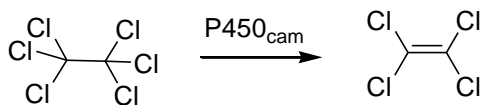


Figure 1.7. P450_{cam} (CYP101) catalyses the reductive dehalogenation of hexachloroethane

1.2.2.7. Oxidative decarbonylation

P450_{hyd} catalyses the conversion of aldehydes to hydrocarbons, with the release of CO₂ but this enzyme was not identified.⁷³ Qiu *et.al.* have identified P450_{hyd} as CYP4G1 in *Drosophila melanogaster* and is fused with NADPH-P450 reductase in oenocytes.⁷⁴ Previously, decarbonylase was reported to be identified only in cyanobacteria that uses a nonheme diiron enzyme.^{75,76,77} The current studies with *Drosophila* and CYP4G2 in housefly proved that the aldehyde decarbonylation occurs by an unique radical mechanism that is different from what occurs in cyanobacteria.⁷⁴

1.2.2.8. Biosynthesis of cyanogenic glucosides

Cyanogenic glucosides (CNGlcs) are amino acid derived natural products that are stored in the plant vacuoles. Dhurrin, the aromatic cyanogenic glucoside is present in millet and its biosynthesis involves the P450s, CYP79A1 and CYP71E1. Jorgenson *et.al.* have identified CYP71E7 in cassava crop that catalyses the conversion of Ile- and Val-derived oximes to their corresponding cyanohydrins. The cyanohydrins in the later steps lead to the formation of the CNGlcs, known as lotaustralin and linamarin. (Fig. 1.8)

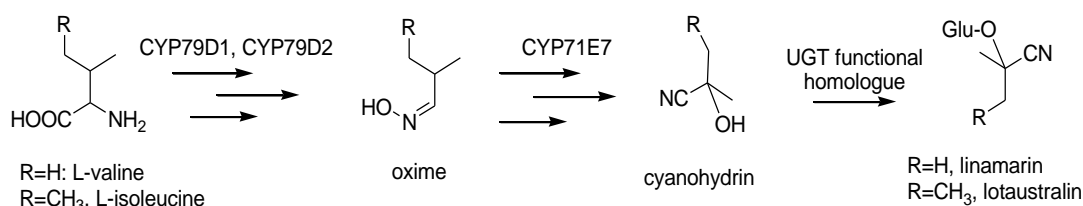


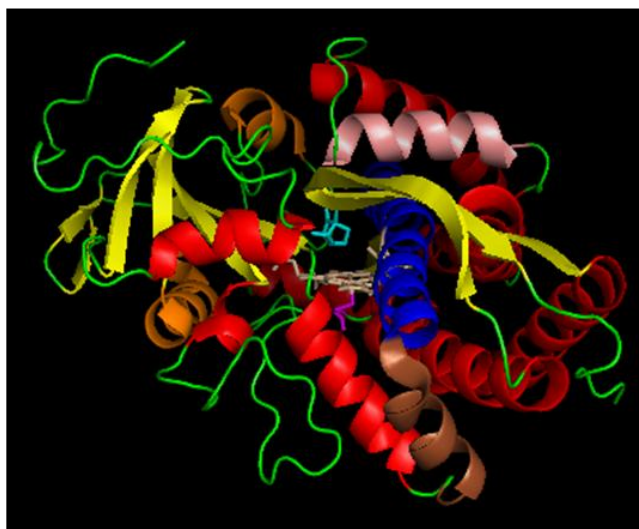
Figure 1.8. Biosynthesis of linomarin and lotanstralin in cassava.

1.3. Structural aspects

The structure and catalytic cycle of CYPs have been studied extensively. The catalytic cycle (Fig. 1.1) was first mapped with P450_{cam}. The cycle begins with the resting state of the enzyme (1, Fig. 1.1), in which a water molecule is believed to be bound to the second axial position on Fe (the first position being occupied by the cysteine thiolate). This state can be detected by UV-visible spectroscopy, because the heme Soret band appears at 392 nm in the resting state of P450_{cam}.⁷⁸ Upon displacement of water by the substrate, the geometry around Fe becomes square pyramidal and the Soret band shifts to 410 nm.⁷⁸ This shift of the Soret band occurs in many other CYPs and has been used to detect the formation of the enzyme-substrate complex. The substrate-bound complex, in the series of steps as shown in Fig. 1.1 forms the iron-oxo species intermediate (7, Fig. 1.1) which has a heme Soret band at 370 nm.⁷⁹

The crystal structure of the P450_{cam} (CYP101A1) monooxygenase¹⁸ isolated from the soil bacterium *Pseudomonas putida* was the first to be solved by T. Poulos in 1987⁸⁰ and became the prototype for several P450 structures. Crystal structures of P450_{BM3}

(CYP102),⁸¹ P450_{terp} (CYP108),⁸² P450_{eryF} (CYP107A)⁸³ CYP17A1,⁸⁴ CYP2C9, CYP3B4 and many others (beyond the scope of this introduction)⁸⁵ have been solved. The structural fold of the P450 superfamily, especially the regions closest to the heme are highly conserved, although the sequence similarity of this region between the different classes is only 20%.¹ The structure of P450 mainly consists of a helical rich region and a beta sheet rich region, with most of the helices and sheets lying in planes perpendicular to the heme.^{17,18,80} The C-terminal residues of the polypeptide cover the inner core of the heme, with the helices I and L fencing the heme core on both sides, whereas the N-terminal helices surround the C-terminus. Helices I and L (Fig 1.9) surrounding the porphyrin fold are highly conserved in all P450s.¹ The heme thiolate ligand, Cys 357 in the case of P450_{cam}, is crucial for regulating the redox potentials in the entire catalytic cycle.⁸⁶



MTTETIQSNANLAPLP_PHPV EHLVFDMDYNPSNLSAGVQEAWA VLQESNVPDLWTRCNGGHW IATRGOLIREAYEDYRHFSSSECPFI **B helix** **B' helix**
 C helix C helix D helix E helix F helix
 PTSMDPPEQRQFRALANOVVG MPV VDK LEN RIOELACSLIE SLRPQGQC NFTE DY AEP **EPI RIFMLLA** GLPEEDIPHLKYLTDQ MTRPDGSMTFAEAKEA 200
G helix **H helix** **I helix** **J helix** **K helix**
 LY **DYLLPIIEQR** RQKPGT **DAISIVAN** GQVNGRPI **TSDEAKRMCGLLLV** GGLDTVNVNLSFSMEFLAK **SPEHROELIER** PERI **PAACE ELLRR FSL** VADGR 300
K' helix **L helix**
 ILTSDYEFHGVQLKKGDQILL **POMLSGL DE RE** NACP MHVDFSRQKVSHHTFGHGSH LCLGOHLARREIIVTLKEWLT **TRIP** DFSIAPGAQIQH KSG IV SGV 400
 QALPLVWDPATTKAV 415

Figure 1.9 Structure of P450_{cam} (PDB code: 2ZWU⁸⁷) with the important helices coloured. Sheets shown in yellow and turns by green. The sequence comprising of 415 amino acids is listed below the structure. Camphor (the natural substrate of P450_{cam}) shown in cyan, heme in beige and Cys357 shown in purple (and by an asterick in the sequence).

Binding of substrates and their orientation relative to key residues around the heme (B' helix)⁸⁸ is important for their regio- or stereoselective hydroxylation.⁸⁹ For example, in P450_{cam}, Y96, present at the C-terminal end of helix B', hydrogen bonds to the keto group of camphor (Fig. 1.10) and coordinates K⁺ via the backbone amide causing stronger binding of camphor to the active site.⁹⁰ The cation bonding enhances the interaction between camphor and P450_{cam}, when compared to the cation-free enzyme. From the early days of P450_{cam} research it has been known that one has to add K⁺ to the buffer to get good camphor binding.¹ The reason the K⁺ helps camphor bind is that it positions Y96 for H-bonding between the Y96 -OH group and the keto group of camphor (Fig. 1.10) The importance of K⁺ in this H-bonding interaction was

further proven in the mutagenesis studies by Di Promo *et.al.*, in which the substrate-induced spin state conversion (which is a consequence of strong substrate binding) was lowered after the conversion of Y96 to Phenylalanine.⁹¹

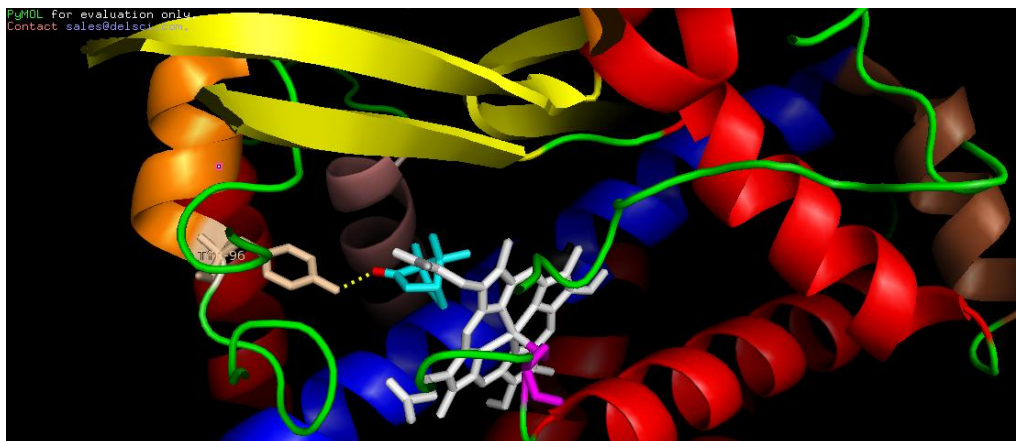


Figure 1.10. *The hydrogen bond co-ordination between Y96 (present on B' helix) and camphor (shown in cyan). PDB code 2ZWU⁸⁷ taken for studies.*

During the formation of compound I (**7**, Fig. 1.1) in the catalytic cycle (Fig. 1.1), the hydroperoxy species (**6**, Fig. 1.1) needs to be protonated distally, to achieve its heterolytic cleavage. The proton for this process comes from a proton shuttle between Thr252 and Glu366 in the case of P450_{cam}.⁹² The two residues hold in place three water molecules that connect the interior of P450_{cam} to the surface of the protein. In P450_{BM3}, the proton shuttle⁹³ is between Thr268 and Glu409 and in peroxidases, the proton shuttle is between His105 and Glu183 residues.^{94 95}

Replacement of T252 with alanine/valine/leucine caused uncoupling of the electrons from redox partners, reducing the hydroxylation efficiency in P450_{cam},^{96,97} whereas the mutation of T252 to serine produced a catalytically active enzyme.⁹⁸ Mutant T252A was found to epoxidise 5-methylenyl camphor, presumably through the formation of the hydroperoxy species (**6**, Fig. 1.1).⁹⁹ This key residue (T252) is absent in P450_{cin} which catalyses the hydroxylation of 1, 8 cineole (Table 1.1, entry 3). In P450_{cin}, N242 in the I-helix acts as a substitute for the proton shuttle T252 of P450_{cam} (Fig. 1.11).¹⁰⁰

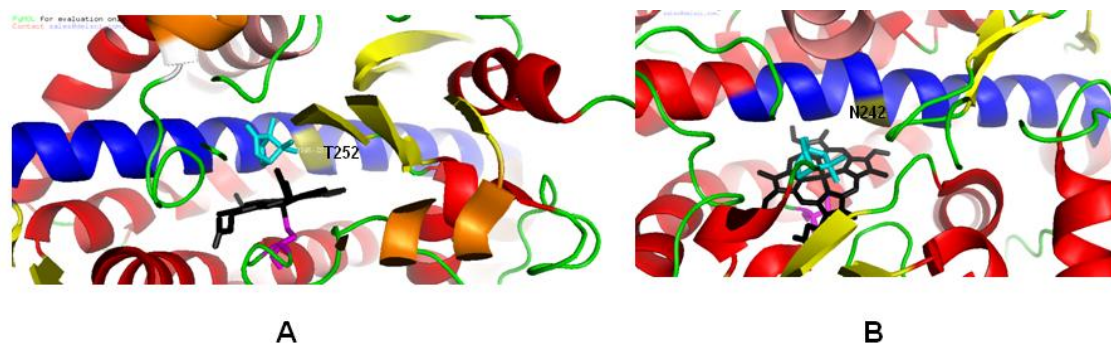


Figure 1.11. *T252 present in the I-helix (coloured by blue) of P450_{cam} (A) helps in the proton shuttle mechanism and is substituted by N242 in P450_{cin} (B). PDB code 2ZWU⁸⁷ taken for studies.*

The axial ligand in P450_{cam}, cysteine 357 is supposed to control the P450 reactivity.⁸⁶ The Cysteine pocket in P450_{cam} encompasses L358, G359, Q360 which stabilise the heme-bound C357 by three hydrogen bonds.¹⁰¹ The Cys pocket is also present in the other P450s (P450_{terp}, P450_{BM3}, etc.) etc suggesting the importance of the hydrogen bonding network close to the active site. These hydrogen bonds control the reduction potential at the iron centre. Galinato *et.al.* have shown that the mutants, L358P and Q360L showed decreased reduction potentials due to the disruption of the H-bonding network.¹⁰¹

In non-P450-type heme proteins, such as peroxidases, globins, histidine is present in the place of Cys and the replacement of C357H deactivates P450s.¹⁰² The mutation from cysteine to selenocysteine in P450_{cam} decreased the catalytic activity by ~ 2 fold. One reason could be that more electron donating nature of the selenocysteine could speed up the formation of compound I but slow its reactivity with the substrate.⁸⁶

The camphor is oriented in the active site of P450_{cam} by a hydrogen bond with the phenolic moiety of tyrosine 96 (Fig. 1.12) and by weak hydrophobic interactions with L244, T101, V247, V253, V295 and F87.¹ Therefore many efforts to engineer P450_{cam}, to accept new substrates, have focused on the residues that line the substrate binding pocket above the heme. (Fig. 1.12)

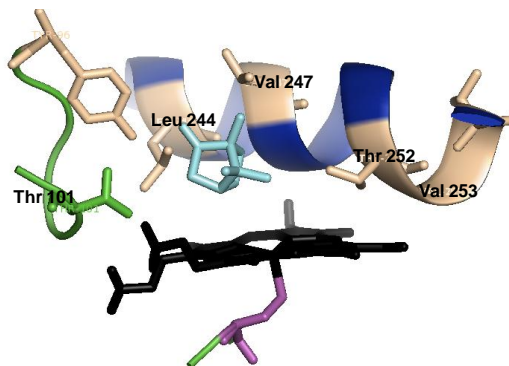


Figure 1.12 The hydrophobic residues present in the substrate binding pocket of P450_{cam}. PDB code 2ZWU⁸⁷ taken for studies.

1.4. Protein Engineering with P450_{cam}

The hydroxylation of D-(+)-camphor, by CYP101A1 and its redox partners, occurs regio- and stereoselectively at the 5-exo position, giving 5-exo-hydroxy camphor on the first round of catalysis (Table 1.1, entry 1) and 5-ketocamphor on the second round of catalysis.¹⁰³ There have been recent advances in altering the active site residues, surrounding the heme, to bind camphor-like analogues, alkanes, and polychlorinated substrates (Tables 1.3 and 1.4)^{39,104,105} Table (1.3) includes some of the mutants of P450_{cam} studied by Wong *et.al.*¹⁰⁶⁻¹⁰⁸ for various substrates.

1.4.1. Alkanes

The wild-type P450_{cam} enzyme does not accept linear alkanes, but the substrate specificity can be changed from camphor to linear alkanes reducing the active site volume with bulky amino acid substitutions (V²⁴⁷ to L²⁴⁷)¹⁰⁹ (Fig. 1.12; Table 1.3 entry 1) Replacement of Y96 by F, W or A disrupts the hydrogen bond between Y96 and camphor, and this decreases the extent of hydroxylation of camphor.¹¹⁰ These replacements also adapted the active site to bind other monoterpenes, alkanes and other substrates (Table 1.3, all entries).^{105,111}

Table 1.3. P450_{cam} mutants and their corresponding substrates (camphor analogues, alkanes)

Mutant	Substrate	Efficiency in mutant
F87W/Y96F/T101L/V247L	Butane	turn-over of 750 min ⁻¹ while the WT enzyme had a turn-over of 0.4 min ⁻¹ ¹⁰⁶ .
Y96F/V247L	Pentane	44.5% NADH coupling compared to WT (1.1%) ^{107,109}
Y96A	Diphenylmethane	turnover of 360 min ⁻¹ while the WT showed no activity ^{112,113}
F87A/Y96F	Phenanthrene	turnover of 374 min ⁻¹ while the WT had low turnover of <0.01 min ⁻¹ . ^{111,114}

1.4.2. Polychlorinated and aromatic pollutants

Polychlorinated compounds have shown to be hazardous to the environment due to their persistence and lack of biodegradation.¹¹⁵ Common problems in degradation of these compounds include their lipid solubility, chemical inertness and the carcinogenic effects.¹¹⁶ Introduction of a hydroxyl group is believed to increase the solubility, which in turn enhances degradability.¹¹⁷ For example, polychlorinated phenol is more degradable by microorganisms than pentachlorobenzene (PeCB).¹¹⁸ The degradation of PeCB, polyaromatic hydrocarbons and other recalcitrant pollutants is a challenge because these compounds are often difficult to oxidise. Therefore, the quest for P450s that can degrade such pollutants has involved active site redesign by directed evolution and other methods.

In general, replacement of F87, Y96 and V247 residues in P450_{cam} (with W, F and L) has been found to be important for the degradation of chlorinated substituents, though the activity decreases with the increasing number of chlorinated substituents. For example, the mutant F87W/Y96F/T101A/L244A/V247L can oxidise PeCB to pentachlorophenol more effectively than the WT.¹¹⁹ More examples of degradation of pollutants, chlorinated compounds by mutant P450_{cam} are listed in Table 1.4.

Table 1.4. P450_{cam} mutants that accept halogenated and polycyclic aromatic mutants

Mutant	Substrate	Efficiency in mutant
Y96A	Phenylcyclohexane	turnover of 5 s ⁻¹ . ¹²⁰
Y96F	Benzocycloarenes	35-70% NADH coupling compared to WT (10-15%) ¹²¹
F87W/Y96F/T101A/ L244A/V247L	Pentachlorobenzene	24.2 ± 0.85% NADH coupling compared to WT (1.1 ± 0.3%) ¹²²
Y96F, Y96F/L244A, Y96F/T101V	1,2,3,4,5,6 hexachloro- cyclohexane (gammmaxene)	NADH coupling of 12-15% while the WT showed no activity. ¹²³
F87W/Y96F/V247L	1,3,5 trichlorobenzene	NADH coupling of 57% ¹²⁴

1.5. Other P450s

Cytochrome P450 (CYPs) have undergone extensive evolutionary diversification and today, CYP proteins are arranged into 10 classes and 267 families. In plants, P450s are responsible for the biosynthesis of alkaloids, terpenoids, lipids, cyanogenic glycosides, plant hormones and ~ 5000 P450 genes have been stored in the database.¹²⁵ CYP51G and CYP710A are responsible for sterol biosynthesis and CYP97 family functions for the biosynthesis of xanthophylls, which are components in photosynthesis.¹²⁶ The catabolism of abscisic acid (ABA), a phytohormone responsible in stomatal closure, to 8-hydroxy abscisic acid is catalysed by CYP707A (Fig. 1.13 (a)).¹²⁷ CYP711A is responsible for the biosynthesis of 5-deoxystrigol from β -carotene (Fig. 1.13 (b)).¹²⁸ Glycyrrhizin, a secondary metabolite in plants that has anti-inflammatory properties and forms from β -amyrin after oxidation by CYP88D6 (Fig. 1.13 (c)).¹²⁹ CYP76B1, a plant P450 from Jerusalem artichoke (*Helianthus tuberosus*) converts herbicides to less lipophilic metabolites, reducing the concentration of the toxic pollutants in soil.¹³⁰

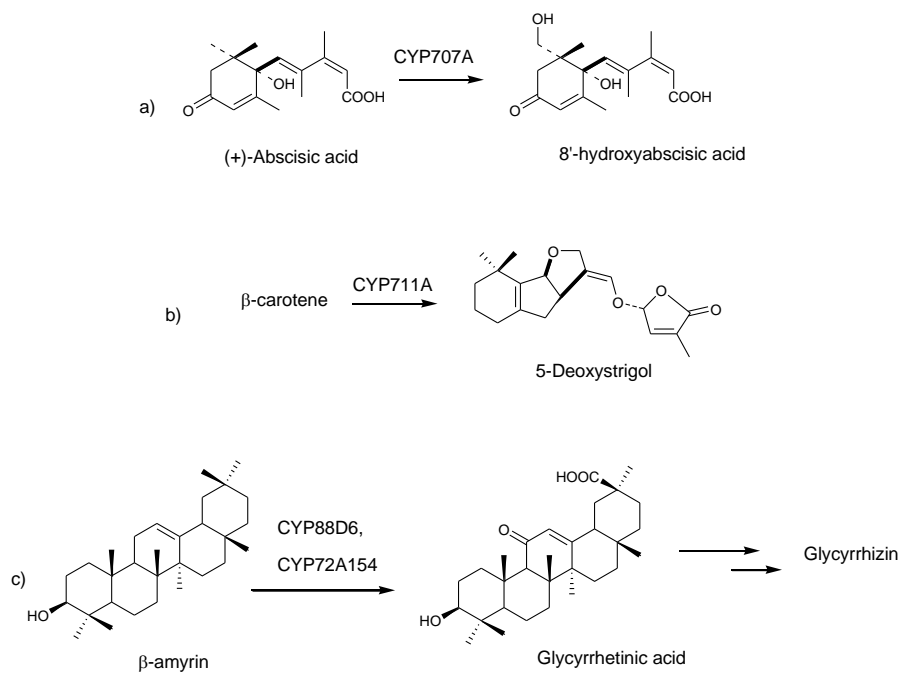


Figure 1.13. The biosynthesis of plant hormones, secondary metabolites (8'-hydroxyabscisic acid, glycyrrhizin) in plants by P450s

The biosynthesis of 20-hydroxyecdysone (20E), an insect hormone responsible for metamorphosis, begins with cholesterol. The conversion of cholesterol to 7-dehydrocholesterol (7-dC) is catalysed by Rieske oxygenase¹³¹ and the conversion of 7-dC to a ketodiol might be performed by a P450, although has not been proved by researchers. The next four hydroxylation steps from the ketodiol to the insect hormone is catalysed by insect P450s (CYP306A1, CYP302A1, CYP315A1 and CYP314A1) (Fig. 1.14).¹³²

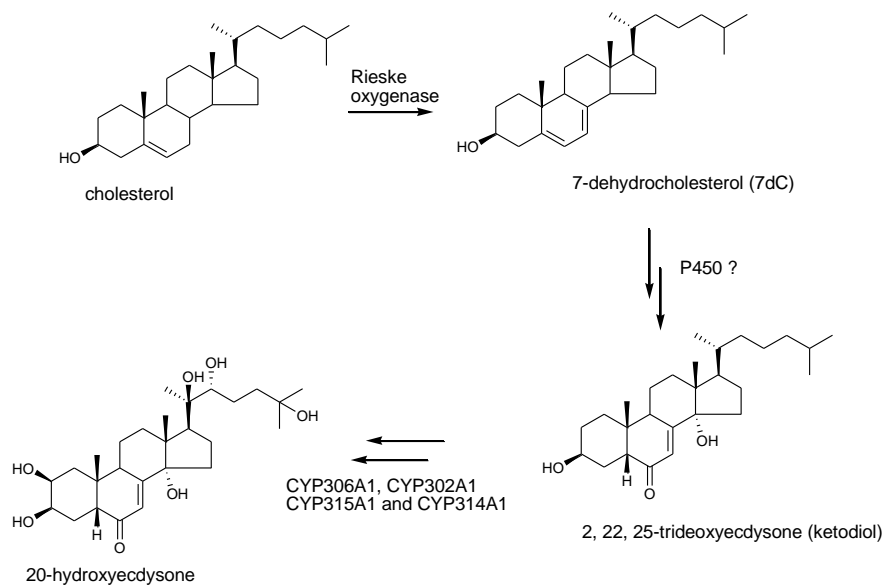


Figure 1.14. The synthesis of 20-hydroxyecdysone from cholesterol.

Some of the human P450s are known for their high substrate promiscuity but have low substrate turn over.⁵⁵ Recent attempts in altering the substrate specificity of the bacterial CYPs to have human P450-like activity was successful for a few researchers. Human P450s have been expressed in *E. coli*, yeast and insects for industrial applications. Propanolol was prepared by engineered P450_{BM3} and chlorzoxazone, a substrate for mammalian P450s was shown to be oxidized by the engineered CYP102 variant (Fig. 1.15)¹³³

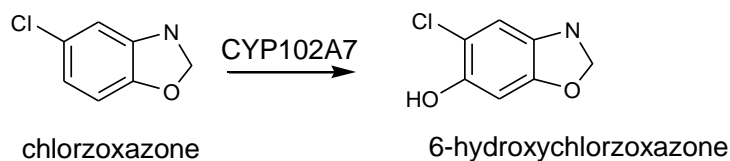


Figure 1.15. Conversion of chlorzoxazone by an engineered CYP102 variant

Kumar *et.al.*¹³⁴ have shown the transformation of progesterone by a CYP2B1 variant and this enzyme was evolved for improved efficiency towards testosterone and 7-benzyloxyresorufin. In contrast to the bacterial enzymes discussed so far, P450s from animals are more difficult to study because of their lower stability *ex vivo*, and this is due to their association with membranes. Nonetheless, they catalyze a similar collection of reactions than the bacterial enzymes. The microsomal class II P450s are poor biocatalysts due to their low stability¹³⁵ and, therefore, P450_{BM3} was engineered to act on human P450 substrates of nutritional or pharmaceutical interest: coumarin, phenacetin and ethoxyresorufin.¹³⁶ Recombinant human P450s CYP1A1, CYP1A2 and CYP1B1 catalyse the hydroxylation of resveratrol, to give piceatannol.⁵⁵

1.6. Recent advances in the use of P450s:

P450s have a wide range of applications in catalysis but the common limitations include the poor stability of the enzyme, poor coupling of the enzyme to the redox partners or the regeneration of the cofactor. Studies on engineering the heme domain by various mutagenesis methods have resulted in improved activity towards various unnatural substrates and improved stability as well. A few recent advances in the application of P450s and the limitations are stated below.

a) Replacement of the nicotinamide cofactor: P450s need a supply of electrons from the cofactor NAD(P)H during the catalytic cycle.¹ The industrial application of the enzyme becomes difficult due to the cost of NADH or NADPH and also, the electron transfer from NAD(P)H to P450 needs the expression of one or more redox partners, which makes these reactions complicated and costly.¹³⁷ Cofactor recycling, the conversion of NAD(P)⁺ to NAD(P)H by a dehydrogenase makes the product isolation difficult.¹³⁸ Surrogate cofactors, like *N*-benzyl-1,4-dihydronicotinamide¹³⁹ and the rhodium complex $[\text{Cp}^*\text{Rh}(\text{bpy})(\text{H}_2\text{O})]^{2+}$ have been employed by researchers, but the process showed gradual loss of activity of the enzyme.¹⁴⁰ In electrochemical methods, cobalt (III) sepulchrate and a platinum electrode were employed for the hydroxylation activity by Estabrook *et.al.* and this method had Co^{III} sepulchrate aggregation as a drawback.¹⁴¹

The peroxide shunt (Fig. 1.2) is a short-cut pathway in the catalytic cycle in which artificial oxidants like cumene-hydroperoxide or *m*-CPBA shunt the P450 directly from the resting state to Cpd I (7, Fig. 1.1). The shunt pathway does not require the reduction of O₂ and therefore, NAD(P)H is not required. Arnold and coworkers employed this pathway for improved activity towards naphthalene and various other substrates using engineered P450_{BM3}.¹⁴²

Jensen *et.al*^{143,144} have reported an entirely different approach of light driven hydroxylation for CYP 79A1, by substituting the cofactor with sunlight. The electron transfer was mediated from the photosystem I to the CYP using the electron acceptors, FdX and FMN-containing flavodoxin (Fld). This approach favoured them two-fold higher turnover rate for CYP79A1.

b) Directed evolution and screening methods. Directed evolution is a well known methodology to engineer enzymes for improved activity towards unnatural substrates.¹⁴⁵ Arnold *et.al.* have reported the improved reactivities of a variety of P450_{BM3} mutants towards alkanes (ranging from propane to decane).^{146,147} The WT P450_{BM3} showed very low activity towards the cycloalkanes, and cyclododecane was not accepted as a substrate at all.¹⁴⁸

P450_{BM3} efficiently catalyses 1^o carbon hydroxylations due to the F87 residue which is positioned just above the porphyrin and helps in substrate positioning relative to the heme.¹⁴⁹ Mutation of these residues has been proven to disrupt the hydrophobic pocket but increases the active site volume, such that the pocket accepts unnatural substrates like naphthalene,¹⁵⁰ terpenes,¹⁵¹ styrene,¹⁵² indole¹⁵³ etc. The F87 residue was used as a template to create two libraries containing 1,500 and 2,500 clones to screen for the hydroxylation of β-ionone using NADPH assay.¹⁵⁴ A combination of the mutants F87A/A328 (F/I/L/V) and F87V/A328 (F/I/L/V) were tested for the activity on cyclooctane, cyclodecane and cyclododecane, and the mutant F87A/A328V was able to oxidise the bulky substrate cyclododecane to 46%.¹⁴⁸ A P450 propane monooxygenase (P450_{PMO} R2) was made from P450_{BM3} by several rounds of directed evolution by Arnold and coworkers. P450_{PMO} R2 oxidised haloalkanes like chloromethane, bromomethane, iodomethane to formaldehyde establishing its activity as a potent dehalogenase.¹⁴⁷ Similarly, the epoxidation of alkenes (styrene) was screened using γ-(4-Nitro-

benzyl)pyridine (NBP) and the product, styrene epoxide formed a purple dye when reacted with NBP.¹⁵⁵

c) Reaction conditions for *in vitro* use of P450s: Hydrophobic substrates sometimes need to be delivered to P450s in organic solvents (such as DMSO) which these enzymes do not tolerate.¹⁵⁶ To overcome this problem, three approaches have been used. First, biphasic solvent systems have been used for CYP102A1 and CYP2D6 catalysis with dextromethorphan as the substrate¹⁵⁷ Second, the Auclair group has reported the use of organic solvents (acetone, acetonitrile, DMSO) with lyophilised CYP3A4 for testosterone hydroxylation.¹⁵⁸ Third, ionic liquids (e.g. 3-ethyl 1-imidazolium chloride) have been found to be good substitutes for organic cosolvents for P450_{BM3} catalysis by Schwaneberg *et.al.*¹⁵⁹

Due to the remarkable catalytic abilities of cytochromes P450, their study and practical development is of interest to many researchers. Aliphatic and aromatic hydroxylation of substrates in chemical synthesis need high temperatures sometimes and P450s show promising abilities in their catalysis with regio- and stereoselectivity. I have discussed barriers to the implementation of cytochromes P450 for practical applications. First, P450s either accept many substrates, with only moderate selectivity or a very narrow range with high selectivity. Both extremes can be problematic in the use of P450s for synthetic or environmental applications. Second, P450s require a nicotinamide cofactor and an electron transfer system under natural conditions. As discussed above, these ancillary factors complicate and increase the cost of P450-based catalytic conditions. Substrate acceptance and specificity has been addressed by mutation of wild-type P450 in the cavity above the heme (Fig. 1.13), whereas the ancillary factors have been replaced by artificial oxidants that bypass the need for O₂ reduction in the catalytic cycle. The problem of substrate promiscuity, improvement in catalysis approached by mutagenesis continues to be a study for many researchers.

1.7. Reactivity of P450_{cam}

The hydroxylation of D(+)-camphor at the 5-exo position,³⁹ is the first reaction of the camphor degradation pathway in strain ATCC 17453 of *Pseudomonas putida*, a

common soil bacterium.¹⁶⁰ The formation of 5-*exo*-hydroxycamphor has been studied in great detail^{4,16,36,38,39} (see section 1.4), but several researchers have noticed that P450_{cam} also produces 5-ketocamphor, presumably by a second hydroxylation of 5-*exo*-hydroxy camphor.¹⁶¹ Such multiple oxidations on a single carbon of the substrate have been documented in other CYPs, most notably steroid-metabolizing CYP51.¹⁶²

In our laboratory, the formation of borneol was observed by both Plettner (unpublished) and later by Rojubally *et al.*¹⁶³ in experiments with recombinant P450_{cam}, PdX and PdR. Even when P450_{cam} was chemically linked to PdX, traces of borneol formed. Experiments with the PdR alone showed that PdR is not responsible for reducing camphor to borneol. PdX, alone did not produce borneol as well. Borneol formed only in the presence of P450_{cam}.¹⁶³ A preliminary experiment by Rojubally, in which crude P450_{cam}/PdX/PdR from *P. putida* was incubated in H₂O with NADD revealed no labelled borneol. In contrast, when the same enzyme preparation was dialyzed against a D₂O buffer, and NADH was used, 2-D borneol formed.¹⁶³ The mechanism of this reaction was not known.

1.8. Objectives of my thesis

A) Redox reactions of P450_{cam} and formation of borneol: The first objective of my thesis was to elucidate the mechanism by which the enzyme P450_{cam} forms the reduction product, borneol.

B) Degradation of endosulfan, by P450_{cam}: The second objective of my thesis was to prepare a mutant library using Sequence Saturation Mutagenesis (SeSaM), and screen the library for mutants that can dehalogenate either 3-chloroindole or endosulfan.

1.9. Thesis layout

This thesis has five chapters. This first chapter introduced CYP chemistry, the catalytic reactions and my objectives. The second chapter describes the early work I did, based on A. Rojubally's results that had not been published in a journal at the time I started. This work was published in *J. Chem. Ecol.*¹⁶⁴ and focused on the conditions under which borneol formed *in vivo* in *P. putida*, as well as on the effect of borneol on the growth of *P. putida*. The third chapter describes my work on the elucidation of the borneol formation mechanism. The fourth chapter describes the SeSaM of P450_{cam} and the identification of a mutant that dehalogenates both 3-chloroindole and endosulfan. The fifth chapter describes the conclusions from this work and some suggestions of future experiments that should be done to further elucidate the borneol formation mechanism and the mechanism of endosulfan dehalogenation.

2. Identification of Camphor Oxidation and Reduction Products in *Pseudomonas Putida*. New Activity of the Cytochrome P450_{cam} System

This chapter is reproduced in part, with editorial changes suggested by the examination committee, from “Identification of camphor oxidation and reduction products in *Pseudomonas putida*. New activity of the cytochrome P450_{cam} system” published in the *Journal of Chemical Ecology*, **2011**, 37(6), 657-667.

Brinda Prasad^a, Adina Rojubally^b and Erika Plettner^a

^a Department of Chemistry, Simon Fraser University, 8888 University Drive, Burnaby, BC, Canada – V5A 1S6.

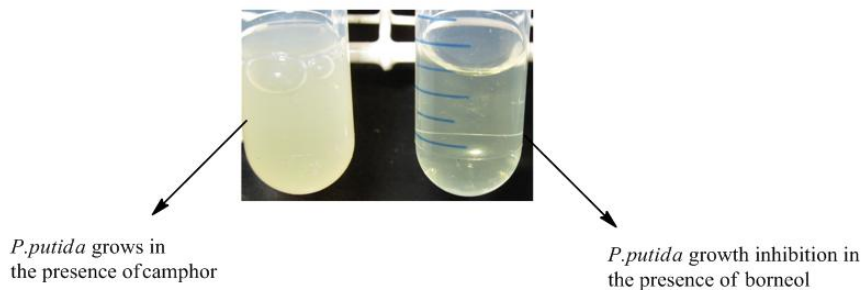
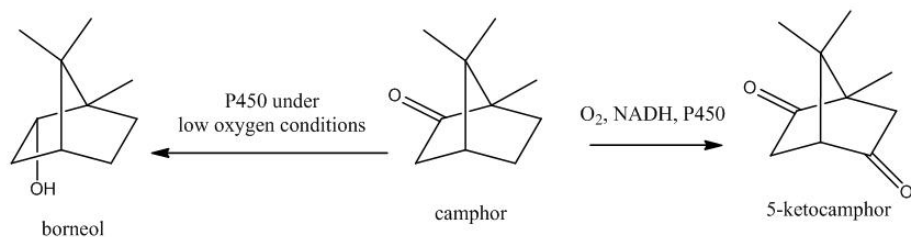
^b Research associate, BC Cancer Agency, Vancouver, BC, Canada

Author Contributions:

B. Prasad performed experiments with the purified P450_{cam} system, with camphor/borneol toxicity and wrote the paper. A. Rojubally performed the standard syntheses and time course experiments with *P. putida*.

2.1. Abstract

P450 enzymes are known for their hydroxylation reactions of non-activated C-H bonds. For example, P450_{cam} from *Pseudomonas putida* oxidizes camphor to 5-exo-hydroxy camphor and further to 5-ketocamphor. This hydroxylation reaction proceeds via a catalytic cycle in which the reduction of dioxygen (O₂) is coupled to the oxidation of the substrate. We have observed that under conditions of low oxygen, *P. putida* and isolated P450_{cam} produce the reduction product of camphor, borneol. In this paper, we outline the formation of borneol, when the catalytic cycle has low oxygen (O₂ ≤ 2 mg/L, ≤ 63 μM) or when the catalytic cycle is shunted by artificial oxidants like *m*-chloro perbenzoic acid, cumene hydroperoxide etc. We also tested the toxicity of camphor and borneol with *P. putida* and *E. coli*. We have found that borneol is less toxic than camphor to *P. putida*, but more toxic to *E. coli*. We discuss a potential ecological advantage of the camphor reduction reaction for *P. putida*.



2.2. Introduction

Cytochrome P450_{cam} isolated from the soil bacterium *Pseudomonas putida*^{165, 166} is a heme monooxygenase^{3,167} which is known to catalyse the hydroxylation of camphor **9** to 5-exo-hydroxycamphor **10**^{168,169} and further to 5-ketocamphor **11**.¹⁷⁰ (Fig. 2.1) The P450_{cam} needs two electron transfer proteins, putidaredoxin (PdX) and putidaredoxin reductase (PdR)²⁵ for its catalytic activity.^{171,172} The catalytic cycle of the enzyme has evolved to couple the highly favourable reduction of O₂ to the unfavourable oxidation of the hydrocarbon substrate. A key intermediate in the catalytic cycle, the iron-oxo species (Fe(IV)=O Por⁺) (**7**, Fig. 1.1) also known as Cpd I, is supposed to be the most reactive species¹⁷³ and is also believed to form via a shunt pathway,^{50,174} when artificial oxidants such as iodosobenzene, cumene hydro-peroxide⁵⁵ or meta chloro perbenzoic acid (*m*-CPBA) are used (Fig. 1.1).¹⁷⁵

We have identified 5-exo-hydroxycamphor **10** and 5-ketocamphor **11** (Figure 2.1) in our enzymatic assays performed with the purified proteins isolated from the soil bacterium *P. putida*. In this paper, we describe the identification of a third product: borneol **12**, using the shunt as well as the regular catalytic conditions. This finding is surprising, because borneol, a reduction product of camphor, formed under conditions that are not considered to be reducing. Also surprisingly, isoborneol (Fig. 2.2) was not detected.

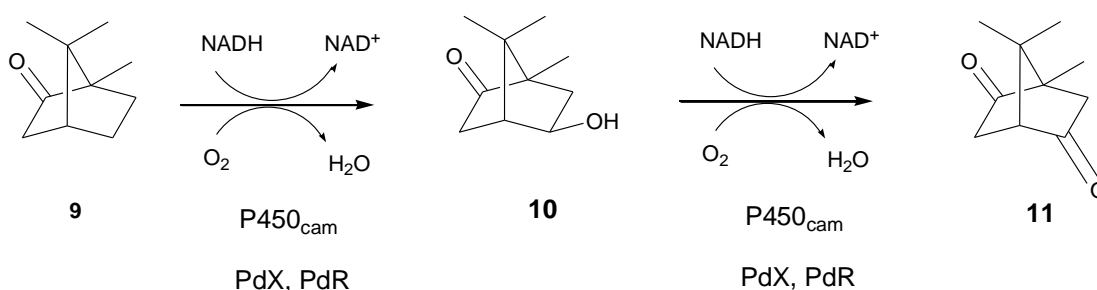


Figure 2.1. *The hydroxylation reaction of camphor: Formation of 5-exo-hydroxycamphor and 5-ketocamphor*

We have found that cytochrome P450_{cam} produces borneol and we describe the conditions under which it forms *in vivo* and *in vitro*. We have compared the toxicity of camphor and borneol against strain ATCC 17453 of *P. putida* (which contains the CAM plasmid) and against *E. coli*, a bacterium that lacks cytochrome P450. The results suggest that the formation of borneol from camphor may confer an advantage to *P. putida*.

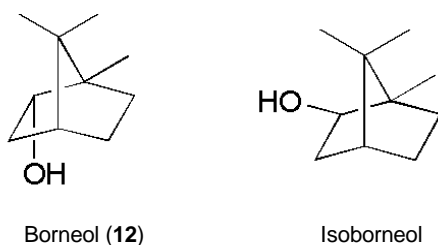


Figure 2.2. *Borneol (12), the reduction product of camphor and isoborneol. Borneol is formed in P. putida but not isoborneol.*

2.3. Materials and Methods

2.3.1. General methods and chemicals.

All solvents were distilled prior to use. Reduced nicotine adenine dinucleotide (NADH), dithiothreitol (DTT), lysozyme, DNase, RNase, Vitamin B₁, riboflavin, δ -aminolevulinic acid, hydrogen peroxide (used for assays), protease inhibitors leupeptin, aprotinin and 4-(2-aminoethyl)-benzenesulfonyl fluoride were purchased from Sigma. *m*-chloro perbenzoic acid was purified by known methods and used for assays.¹⁷⁶ Other shunting agents, cumene hydro-peroxide (CHP), sodium periodate (NaIO₄), calcium hypochlorite (bleach) were used as received. Gas chromatography was performed on a Hewlett Packard 5890 GC, equipped with a flame ionization detector and a 30-m SPB-5 column (Supelco, 0.25 mm ID; 0.25 μ m film thickness).

The instrument was programmed as follows: 80 °C (5 min), 10 °C min⁻¹ to 200 °C (4 min), 50 °C min⁻¹ to 250 °C (20 min); head pressure 15 psi; total flow through the column 1.7 mL min⁻¹. Gas chromatography/mass spectrometry (GC-MS) was carried out on a Varian Saturn 2000 MS equipped with a 30-m SPB-5 column (Supelco, 0.25 mm ID; 0.25 μ m film thickness) and the column was programmed as follows: 45 °C (0.5 min), 7 °C min⁻¹ to 120 °C (1 min), 50 °C min⁻¹ to 260 °C (3 min). Electron impact spectra

were obtained at an emission current of 30 μA , scanning from 50 to 365 amu, with ion storage (SIS mode) 49-375, trap temperature 170 $^{\circ}\text{C}$ and transfer line 250 $^{\circ}\text{C}$. For high sensitivity measurements, electron impact spectra were obtained with ion storage (SIS mode) 90-170. The volume injected into the GC-MS was always 1 μL . Calibration lines were obtained for camphor, borneol, 5-exo-hydroxycamphor and 5-ketocamphor, using standards (borneol and D(+)-camphor, Sigma-Aldrich; 5-exo-hydroxycamphor and 5-ketocamphor were standards prepared by A. Rojubbally). The limits of borneol detection with these two programs were: 1200 $\text{pg}/\mu\text{L}$ (50-365 amu scanning program) and 20 $\text{pg}/\mu\text{L}$ ("high sensitivity" 90-170 amu scanning program).

UV/Vis spectra were obtained on a Cary 300 Bio UV-visible double beam instrument. NADH utilization rates and hydrogen peroxide formation were measured on a thermostatted Hach DR/4000 U spectrophotometer. Activity assays were carried out at 22 $^{\circ}\text{C}$. Electrophoresis was performed on polyacrylamide gels (14%, 29:1) with 0.5% SDS (SDS-PAGE). The samples were reduced by treatment with DTT (31 mg/mL) before loading on gels. Gels were stained with Coomassie Brilliant Blue R (Sigma). Sonication was done on a Branson Ultrasonic sonicator. Centrifugations were carried out with a Beckmann Avanti J-26 XPI centrifuge, equipped with a JLA 8.1000 rotor.

The buffers used were : lysis (20 mM phosphate buffer (K^+), pH 7.4 with 1 mM camphor; T-100 (50 mM Tris, 100 mM KCl, pH 7.4); T-400 (50 mM Tris, 400 mM KCl, pH 7.4); Substrate-free P450 was prepared by passing the substrate bound enzyme over a Sephadex G-10 column equilibrated with 100 mM MOPS (pH 7.0).

2.3.2. *D(+)* camphor purification

D(+) camphor (Sigma) contained ~5% of borneol as confirmed by GC-MS in comparison with borneol standard (Sigma). The camphor was recrystallised from ethanol/water and then purified on silica gel with a hexane: ethyl acetate gradient (from 1:0 (30 fractions, 8 mL) to 99:1 (5 fractions), to 4:1 (8 fractions)). The lowest amounts of borneol that can be detected by GC-MS by the high-sensitivity measurements is 20 pg , as detected from the calibration line. The D(+) camphor was pure as analysed by GC-MS (and had no traces of borneol) as measured from the high sensitivity mass spectral measurements with ion storage (SIS mode) 90-170 (see above). Mass spectrum (EI):

m/z (% of base peak) 153 (M+1, 6), 152 (M⁺, 8), 137(7), 108 (66), 95 (100), 69 (15), 67 (55), 55 (28). MS (CI, isobutene): m/z (% of base peak) 153 (M+1, 100), 137 (2), 135 (6), 108 (10), 95 (3), 81 (10), 69 (12), 67 (20). Other products, 5-ketocamphor and 5-exohydroxy camphor were characterized by NMR and GC-MS in comparison with the prepared standards.

2.3.3. NMR

The proton and the carbon nuclear magnetic resonance spectra were run on a Varian 500 MHz instrument. The chemical shifts (δ) for all compounds are listed in parts per million using NMR solvent as an internal reference. The coupling constants (J) are listed in Hertz (Hz).

2.3.4. Protein production (from *P. putida*)^{160, 177} and the purification steps

P450_{cam}, PdR and PdX were isolated from the *P. putida* ATCC 17453. The *P. putida* were grown in nutrient broth (Gibco) containing 0.5 mg mL⁻¹ of 1-(R)- camphor with shaking (250 rpm) to A₆₀₀ = 0.9 - 1.0. Cells from 2 L of culture were lysed in 50 mL of 20 mM potassium phosphate, pH 7.4, 1 mM camphor. The cell suspension was made 10 mM in EDTA (pH 7.4), lysozyme (100 mg L⁻¹), camphor (1 mM in ethanol) added and stirred for 30 minutes at 4 °C. The suspension was sonicated with 50% duty cycle for 10 minutes, 10 mM with MgSO₄, DNase (2 mg, Sigma), RNase (10 mg, Sigma) were added and stirred for 30 min at 4 °C. The lysate was sonicated for 5 minutes and homogenized in a tissue homogenizer with a Teflon pestle. The homogenized cells were then harvested by centrifugation (7000 × g, 30 min), dialysed with frequent changes of 20 mM potassium phosphate, pH 7.4 containing 1 mM camphor for further purification by ammonium sulphate precipitation. The dialysed lysate of *P. putida* was subjected to a 20% ammonium sulphate cut to remove the cell debris. The 20% supernatant was then carried forward to 55% ammonium sulphate saturation to isolate the proteins. All these three proteins were isolated in the above step and were further purified by DE-52 column using a linear gradient with buffer T-100 to T-400, 1 mM camphor, 1 mM β -mercaptoethanol at 1 mL min⁻¹. The fractions with high absorbances at λ_{392} (in the case of P450), λ_{454} (in the case of PdR), λ_{325} (in the case of PdX) were pooled, checked with

SDS-PAGE (Supplementary Fig. S1) before proceeding with gel-filtration chromatography. The collected fractions were concentrated in an Amicon ultrafiltration cell equipped with a 10kDa membrane (Millipore Corporation, Billerica, MA, USA) and the concentrate (containing P450, PdR and PdX) was loaded onto a S-100 column, eluted with T-100 buffer, 1 mM sucrose, 1 mM camphor at 1 mL min⁻¹. The selected fractions containing $A_{392}/A_{280} \sim 0.14$, $A_{454}/A_{280} \sim 0.11$, $A_{325}/A_{280} \sim 0.25$ were analysed by SDS-PAGE for molecular weight determination. The accurate concentrations of the proteins (PdR and PdX) could not be measured even after further purifications. This partially purified P450_{cam} system was used for the assays (see below).

2.3.5. *In vivo* Assays with *P. putida*

To monitor the conversion of camphor to metabolites by the induction of P450 under aerated and non-aerated conditions, *P. putida* ATCC 17453 strain was grown for 7 generations in two replicates without camphor. Aliquots (20 µl) of the 7th generation cultures (both aerated and non-aerated) were inoculated into 100 ml of nutrient broth medium in a 250 ml flask. This 8th generation of log phase culture was treated with 0.77 g of camphor delivered in DMSO and the absorbances at 280, 392, and 410 nm were recorded at 0 min (immediately after adding camphor), 5 min, 30 min, 60 min, 120 min, 180 min, 240 min, and 8 h under both aerated and non-aerated conditions. At every time point, the sample was centrifuged to collect the pellet and the supernatant. The supernatants from the different time points were extracted with CHCl₃/indanone (7.2 µM) for the extraction of the product(s) and the substrate. Indanone was our internal standard for the quantification of products by GC-MS. A second extraction of the aqueous phase with 0.7 ml of CHCl₃/indanone followed. The combined organic layers were dried over MgSO₄ and analyzed by GC-MS.

2.3.6. *In vitro* Assays with Isolated P450_{cam}, PdR, and PdX Complex

In vitro enzymatic assays were performed in 2 ml of 50 mM phosphate buffer (100 mM K⁺) (pH 7.4). The buffer was sparged with charcoal filtered air/oxygen or argon (both Sigma-Aldrich) prior to use. The proteins could not be separated by the two columns we ran, and the approximate concentrations of the ferric P450 (with camphor), PdR, and PdX were determined by their extinction coefficients $\epsilon_{392} = 104 \text{ mM}^{-1} \text{ cm}^{-1}$, $\epsilon_{454} =$

10.0 mM⁻¹ cm⁻¹, and $\epsilon_{325} = 15.6 \text{ mM}^{-1}\text{cm}^{-1}$.¹⁶⁰ The reaction mixture contained approximately 1.5 μM P450_{cam}, 2.5 μM PdR, 5 μM PdX, and the substrate camphor (2.5 mM). NADH consumption was initiated by the addition of 2.5 μl NADH stock (200 mM) and monitored for 10 min at 340 nm. The experiment was performed in four replicates, and three controls were run in parallel with the treatments: 1) blank: without enzyme but all other reactants added; 2) enzyme and the substrate added to the buffer without NADH; and 3) NADH and the enzyme added without camphor. The reaction was stopped by the addition of 1 ml CHCl₃/indanone (7.2 μM) for the extraction of the product(s) and the substrate. Indanone was our internal standard to quantify products by GC-MS. A second extraction of the aqueous phase with 0.7 ml of CHCl₃/indanone followed. The combined organic layers were dried over MgSO₄ and analyzed by GC-MS.

In assays involving *m*-CPBA as a shunt agent for the catalytic cycle, the reaction mixture contained 1.5 μM P450_{cam}, *m*-CPBA (1 mM), and substrate camphor (1 mM). The experiment was performed in four replicates, and three controls were run in parallel with the treatments: 1) blank: without enzyme but all other reactants added; 2) enzyme and the substrate added to the buffer without *m*-CPBA; and 3) *m*-CPBA and the enzyme added without camphor. The reaction mixture was incubated for 15 min at 22 °C and extracted in the same way as above. The dried organic layers were analyzed by GC-MS.

In assays involving borneol as the substrate and *m*-CPBA as a shunt agent for the catalytic cycle, the reaction mixture contained 2 μM P450_{cam}, *m*-CPBA (1 mM), and substrate (1 mM). The experiment was performed in four replicates, and three controls were run in parallel with the treatments: 1) blank: without enzyme but all other reactants added; 2) enzyme and the substrate added to the buffer without *m*-CPBA; and 3) *m*-CPBA and the enzyme added without borneol. The reaction mixture was incubated for 30 min at 22 °C and extracted in the same way as above. The dried organic layers were analyzed by GC-MS.

2.3.7. Toxicity Assays of Tetracycline, DMSO, Camphor, and Borneol against *P. putida* and *E. coli*

Cultures of the strains ATCC 17453 of *P. putida* and XL-1-blue of *E. coli* were grown overnight, and then were used to inoculate 2x250 ml growing cultures, which were grown at 300 rpm with good aeration until an O.D. of 0.1 was reached. An aliquot

(5 ml) of each of these cultures was transferred separately to Falcon tubes in three replicates, to each of which either camphor, borneol, or tetracycline was added to a final concentration of 1 mM. Dimethyl sulfoxide (DMSO), the solvent used for preparing stocks, was also used as one of the controls. Cultures were grown for 1 h and incubated overnight at 4 °C. They were diluted $10^3\times$, $10^4\times$, $10^5\times$, $10^6\times$, $10^8\times$ in three replicates and then plated on non-antibiotic LB-agar plates in two replicates (20 and 50 μ l) and were incubated overnight at 27 °C. Colonies were counted after overnight incubation. The toxicities of camphor and borneol to the two strains were assessed by measuring the reduction of cell density [colony forming units (CFU)/ml]. To obtain CFU/ml, colonies were grown on agar plates and the numbers of colonies were divided by the volume plated. This, when divided by the dilution factor, gives the CFU/ml in the original sample. We compared *P. putida* with the CAM plasmid to *E. coli*, a species of bacterium known to not contain any P450 genes.¹⁷⁸ A comparison of the relative toxicity between borneol and camphor on *E. coli* was determined by a one-way ANOVA test (Vander Waerden test) with JMP starter software (Cary, NC, USA) with significance determined at $\alpha = 0.05$. The distribution of the data was checked with JMP software and the normal hypothesis was rejected. Therefore, a non-parametric method was used for the analysis. Tukey-Kramer pairwise comparisons were performed to test the effects of camphor and borneol relative to DMSO; Wilcoxon and Vander Waerden comparisons were used to test the effects of camphor and borneol directly.

2.3.8. *IC*₅₀ Experiments with Camphor and Borneol against *E. coli*

Two growing cultures (250 ml each) were inoculated with an overnight grown culture of XL-1-blue of *E. coli* and then grown at 300 rpm with good aeration until a O.D. of 0.1 was reached. An aliquot (5 ml) of this culture was transferred to Falcon tubes to which either borneol or camphor was added in varying concentrations. The final concentrations of these compounds ranged from 0.5 nM to 1 μ M. Dimethyl sulfoxide (DMSO), the solvent used for preparing stocks, was also used as one of the controls. Cultures were grown for 1 h and incubated overnight at 4 °C. They were diluted $10^4\times$ and $10^5\times$ in three replicates and then plated on non-antibiotic LB-agar plates in two replicates (20 and 50 μ l) and incubated overnight at 37°C. The concentration of colony forming units (CFU/ml) was calculated the next day, depending on the number of

colonies. The IC₅₀ was calculated by graphing CFU/ml vs. the logarithm of concentration of compounds.¹⁷⁹

2.4. Results

2.4.1. ***Analysis of Products Formed in *P. putida* Culture with (1*R*)-(+)-Camphor During *in vivo* Assays with Purified P450_{cam} System***

In vivo production of borneol and 5-ketocamphor was monitored under aerated and non-aerated conditions in growing *P. putida* cultures that had been treated with camphor. The quantities of borneol under both aerated and non-aerated conditions increased in the first 180 minutes and later, the rate of borneol formation was higher under non-aerated conditions than under aerated conditions (Fig. 2.3). Borneol detected under poorly aerated conditions was identified by chiral stationary phase GC-FID with a retention time of 29.8 min and compared to the retention times of two products of sodium borohydride reduced (1*R*)-(+)-camphor, borneol (**12**), and isoborneol. Isoborneol, eluted from the cycloSyl B column with a retention time of 25.8 min. This confirms that borneol is the only reduction product detected in the *P. putida* culture.¹⁸⁰

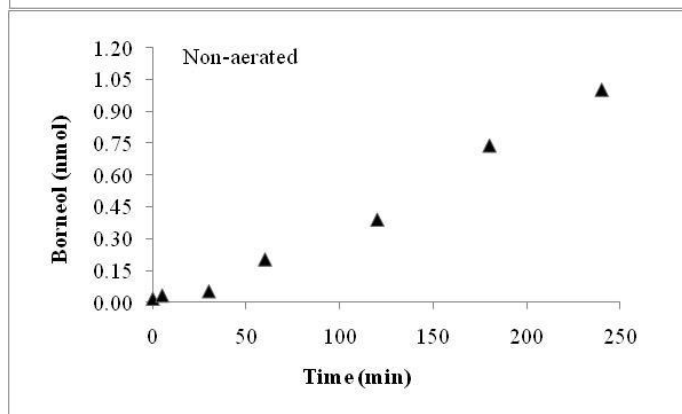
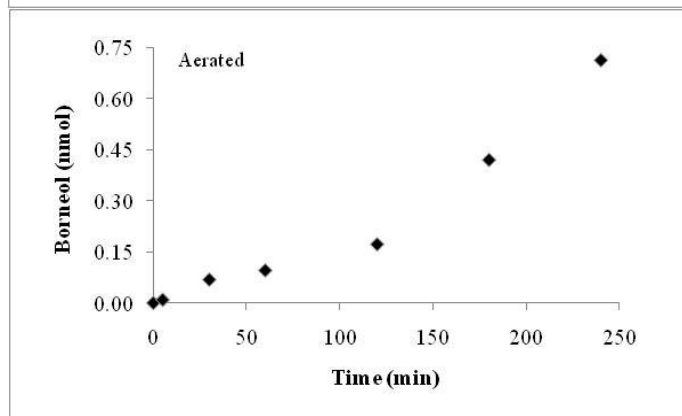
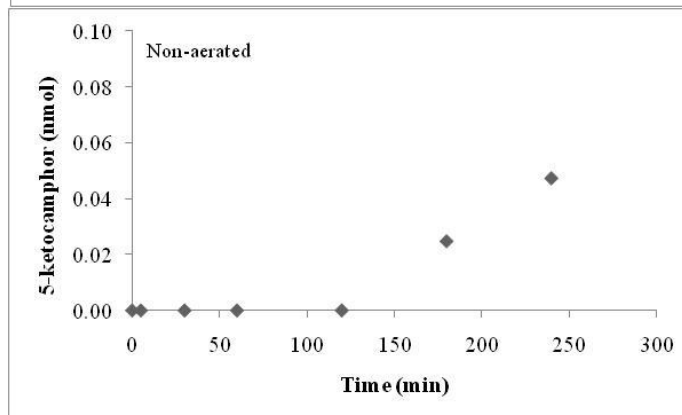
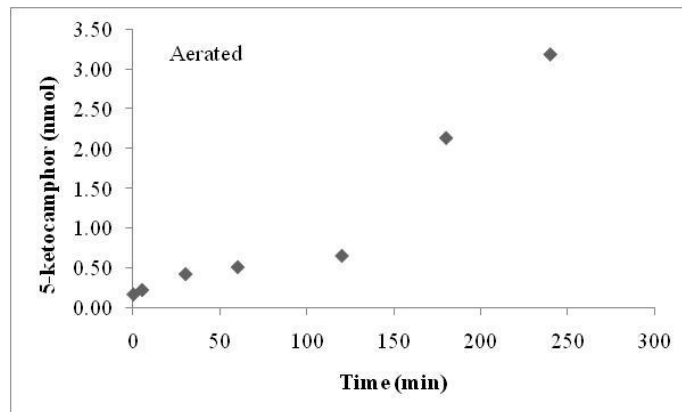


Figure 2.3. Time course quantities of 5-ketocamphor and borneol from an induced culture of *Pseudomonas putida* under aerated and non-aerated conditions.

2.4.2. In vitro assays with the partially purified P450_{cam}, PdR and PdX system:

To determine whether P450_{cam} is involved in the formation of **10**, **11** and **12**, (Figures 2.1 and 2.2) experiments were performed using partially purified P450_{cam} and its redox partners, obtained from *P. putida* induced with camphor.

The reaction mixture contained approximately 1.5 μ M P450_{cam}, 2.5 μ M PdR, 5 μ M PdX, and the substrate camphor (2.5 mM). The first unexpected result was that these proteins cannot be separated during the purification process. We therefore used this partially purified P450_{cam} system in our *in vitro* assays.

Under oxygenated conditions, (when the assay buffer was sparged with oxygen or air), the enzyme complex catalysed the oxidation of camphor to 5-ketocamphor (as the major product) and reduction to borneol (minor product) (Table 2.1). When there was insufficient oxygen for the catalysis, (when the assay buffer was sparged with argon), surprisingly, borneol formed and 5-ketocamphor was not detected. Under these conditions, when the enzymatic pathway was shunted in the presence of *m*-CPBA and cofactor NADH was added, the amount of 5-ketocamphor formed was the same as that of borneol. In this assay, the concentration of 5-ketocamphor formed was less when compared to the oxygenated conditions. When hydrogen peroxide was used in the place of *m*-CPBA under similar conditions, ketocamphor was not detected and less borneol was formed (Table 2.1). In the absence of cofactor in the above mentioned conditions and when *m*-CPBA was used as a shunt agent, 5-ketocamphor was not detected and surprisingly, more borneol was formed than with H₂O₂. This illustrates that the cofactor NADH is not involved in the formation of borneol. Further verification that NADH is not necessary for borneol formation came when NADD was added to the assay reaction mixture containing substrate camphor and the enzyme preparation: deuterated borneol was not detected by GC-MS.¹⁸⁰ Hydrogen peroxide, when added to the system, appears to be inhibitory, giving lower amounts of borneol. Taken together, these observations

suggest that borneol forms under conditions when the bacteria begin to be stressed by low oxygen levels, but are still metabolizing camphor.

Table 2.1. Assays with P450:PdR:PdX complex isolated from *Pseudomonas putida*

Enzymatic assay	Products (nmol min ⁻¹ μmol ⁻¹ P450)		NADH consumed (nmol min ⁻¹ μmol ⁻¹ P450)	H ₂ O ₂ formed (nmol min ⁻¹ μmol ⁻¹ P450)
	Borneol (12)	5-ketocamphor (11)		
O ₂ ^a	2.4 ± 2	207 ± 27	763 ± 181	N/d
Air ^b	65 ± 7	484 ± 121	1303 ± 484	13.6 ± 9
Argon ^c	20 ± 8	N/d	N/d	15.9 ± 8
Argon + <i>m</i> -CPBA + NADH ^d	24 ± 8	32 ± 4	3 ± 1	ND
O ₂ ^a	N/d	272 ± 36	606 ± 10	N/d
Argon+ <i>m</i> -CPBA ^e	71 ± 48	N/d	N/A	ND
Argon + NADH +H ₂ O ₂ ^f	7 ± 5	N/d	ND	ND

Values are average of 4 replicates ± S.E.

N/A = Not Available; ND=Not Determined; N/d = Not detected; The reaction mixture contained approximately 1.5 μM P450_{cam}, 2.5 μM PdR, 5 μM PdX, and the substrate camphor (2.5 mM). NADH consumption was initiated by the addition of 2.5 μl NADH stock (200 mM) and monitored for 10 min at 340 nm.

^a Oxygen was sparged into the buffer for enzymatic assays

^b (Charcoal filtered) air was sparged into the buffer for enzymatic assays

^c The buffer was sparged with argon for the assays

^d The buffer was sparged with argon in the shunt pathway (*m*-CPBA) and the cofactor was added.

^e The buffer was sparged with argon in the shunt pathway. The cofactor NADH was not added to the reaction mixture.

^f The buffer was sparged with argon in the shunt pathway (H₂O₂) and the cofactor NADH was added

2.4.3. Enzymatic assays involving borneol as the substrate

The enzymatic assays involving borneol as the substrate were done under shunt conditions and the products formed were monitored by GC-MS. The conversion of borneol to camphor and further to 5-exo-hydroxycamphor was detected, which shows that this formation of borneol is a reversible reaction. The concentration of camphor was 33 ± 1.6 nmol/min/ μ mol P450 and 5-exo-hydroxycamphor was 50 ± 1.6 nmol/min/ μ mol P450. This illustrates that *P. putida* can convert borneol back to camphor. Borneol was detected as the only reduction product of camphor and therefore, isoborneol was not chosen as a substrate for these enzymatic assays.

2.4.4. Toxicity Assays for Camphor and Borneol

To test for a potential adaptive value for the conversion of camphor to borneol, we compared the relative toxicities of camphor, borneol, and tetracycline on *P. putida* and on *E. coli*. The ANOVA on mean cell densities for each species revealed an effect of treatment (*P. putida*: $P = 0.0056$ and $F = 4.403$; *E. coli*: $P < 0.001$ and $F = 8.632$). Tukey-Kramer pairwise comparisons of the toxicity of the substrates to *P. putida* revealed no significant differences in cell densities following monoterpene treatment relative to DMSO, suggesting that neither camphor nor borneol were toxic to *P. putida* (Fig. 2.4a) (DMSO/camphor pair, $P = 0.3926$; DMSO/borneol pair, $P = 0.9807$; and camphor/borneol pair, $P = 0.6288$). In contrast, treatment with tetracycline did cause a reduction in cell density relative to DMSO (Fig. 2.4a) (DMSO/tetracycline pair, $P = 0.0069$; camphor/tetracycline pair, $P = 0.3196$; and borneol/tetracycline pair, $P = 0.0218$). Wilcoxon and Vander Waerden tests revealed that camphor was more toxic than borneol to *P. putida* (Fig. 2.4a) ($P = 0.025$, $N=3$). Tukey-Kramer pairwise comparisons of the toxicity of the substrates to *E. coli* revealed that camphor, borneol, and tetracycline were all toxic to *E. coli* relative to DMSO (Fig. 2.4b) (DMSO/camphor pair, $P < 0.001$; DMSO/borneol pair, $P < 0.001$; DMSO/tetracycline pair, $P < 0.001$; camphor/borneol pair, $P = 0.9997$; camphor/tetracycline pair, $P = 0.9995$; and borneol/tetracycline pair, $P = 1.0$). Wilcoxon and Vander Waerden comparisons revealed that while both monoterpenes were toxic to *E. coli*, borneol was more toxic than camphor ($P = 0.035$, $N=3$). In addition to this, the IC_{50} of borneol with growing cultures of *E. coli*

ranged from 14.3 nM to 20 nM, whereas the IC_{50} of camphor ranged from 19 nM to 42 nM (Fig. 2.5).

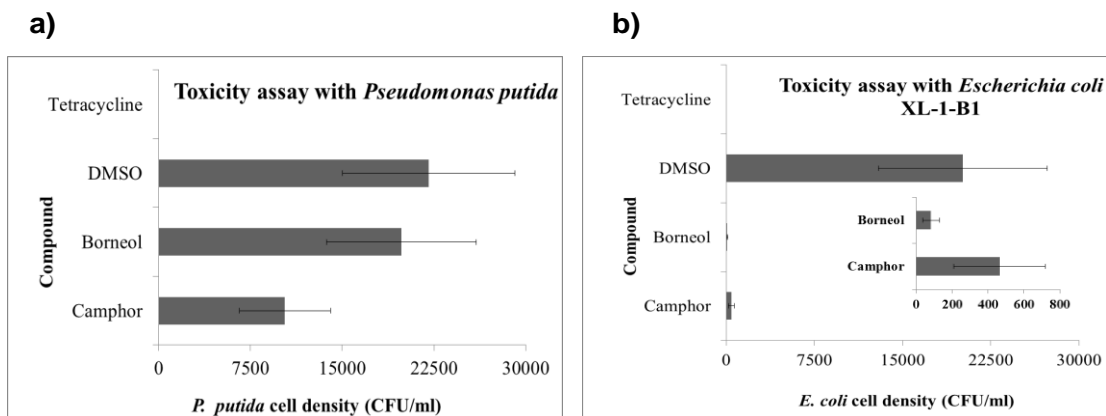


Figure 2.4. Toxicity assays for camphor and borneol in two strains of bacteria: ATCC 17453 of *P. putida* (a) and *E. coli* (b).

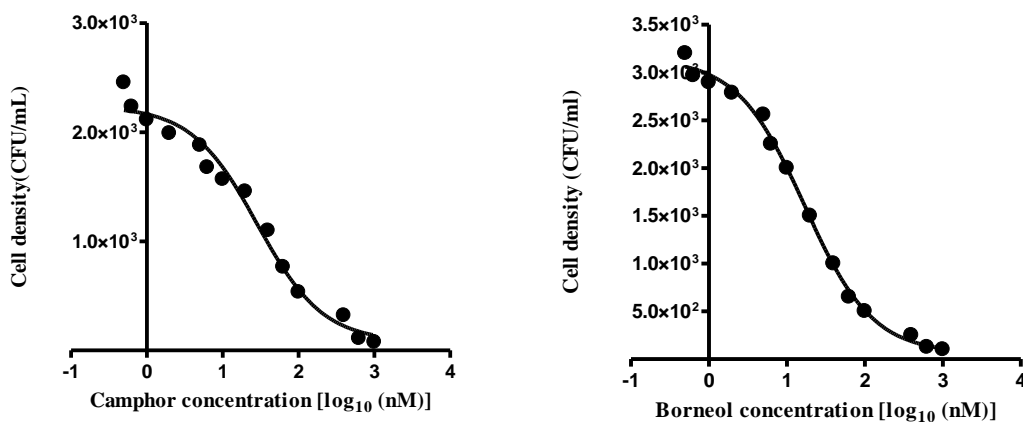


Figure 2.5. IC_{50} experiments on *Escherichia coli* with varying concentrations of camphor and borneol.

2.5. Discussion

Hydroxylation of camphor is catalyzed by the P450_{cam} complex with its redox partners PdR and PdX.^{181,182} The P450 reduces O₂ with electrons from NADH and

incorporates one oxygen atom into product.¹⁸³ Here we have observed that, in addition to the known camphor oxidation products 5-*exo*-hydroxycamphor (**10**) and 5-ketocamphor (**11**), a reduction product, borneol (**12**), forms during P450_{cam} catalysis. The distribution of products appears to be dependent on the reaction conditions. Under well oxygenated conditions, 5-ketocamphor (**11**) is the major product, whereas under poorly aerated conditions, borneol (**12**) is the major product. One way in which borneol could form is via reduction of the 2-keto group of camphor with NADH, but NADH does not react directly with camphor.

Previous studies may have missed the formation of borneol, because various camphor-derived compounds that elute after camphor like borneol, isoborneol (Figure 2.2), and 5-*exo*-hydroxycamphor elute closely on non-polar GC columns typically used for this analysis. Furthermore, the mass spectra of the oxygenated bornyl-based monoterpenes (**9**, **10**, **11**, **12** and isoborneol) are very similar, because of a strong tendency to fragment to ions with *m/z* of 108, 95, 81, and 67. From studies with ¹⁷O-labeled camphor, we know that none of these ions contain oxygen.¹⁸⁴ The products of camphor oxidation and the reduction product, borneol were detected in the early stages of metabolism, up to ~6 h of culture. Further metabolism of borneol to 5-*exo*-hydroxy borneol (**12**) was observed in the non-aerated conditions, which suggests that the reduction to borneol and its further hydroxylation to (**12**) occurs in the intact bacterium. To test for a potential adaptive value for this reaction, we compared the relative toxicity of camphor and borneol on *P. putida* and on *E. coli*. This experiment suggested that camphor is toxic to both *E. coli* and *P. putida*, whereas borneol is more toxic than camphor to *E. coli*. Therefore, formation of borneol may confer an advantage to strains of *P. putida* that metabolize camphor and are competing with other bacteria that do not metabolize camphor. Under conditions of low oxygen, borneol forms from camphor, and this compound is less toxic than camphor itself to *P. putida* but more toxic to P450-free bacteria such as *E. coli*.

We are not aware whether *E. coli* and *P. putida* compete with each other ecologically (Scifinder search for whether the organisms *E. coli* and *P. putida* compete with each another in nature yielded no references). We know that *P. putida*, for example, exists in soil and in sink sludge¹⁸⁵ (from where the camphor metabolizing strain of *P. putida* was originally isolated). *E. coli* is a widespread enteric bacterium, but can also

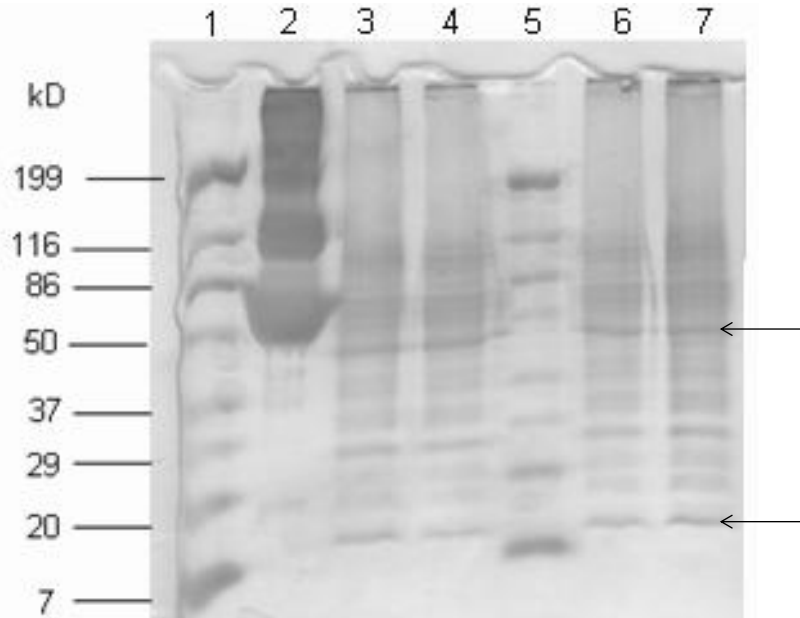
exist outside of vertebrate organisms (in soil or in water), as some past tragic incidents with drinking water in rural areas have demonstrated.¹⁸⁶

Bacterial P450's have been widely studied in the past for their ecological functions in the detoxification of both natural and artificial toxicants. For example, P450 BM3 from *Bacillus megaterium* hydroxylates fatty acids, fatty amides, and alcohols at the ω -1, ω -2, or ω -3 positions, making them less amphiphilic (Narhi and Fulco, 1986). P450 isolated from the actinomycete *Nonomuraea recticatena* IFO 14525, catalyzes the hydroxylation of oleanolic acid, a toxic triterpene.¹⁸⁷ P450s from members of the order *Actinomycetales* catalyze pentachlorophenol dehalogenation and the degradation of sulphonyl-urea herbicides.¹⁸⁸

2.6. Summary

In summary, we have identified the reduction product borneol by using the substrate camphor and purified *P. putida* proteins. The source of electrons for the reduction reaction was not the nicotinamide cofactor. This gave us a thought of exploring the reduction mechanism even further to discover the side product of the reduction reaction in addition to borneol. Although P450_{cam} was a well studied enzyme, the reduction reaction was not reported previously. The source of electrons for this reduction reaction and our proposed mechanism are described in the third chapter.

2.7. Supplementary information



Supplementary figure 2.S1. The SDS-PAGE gel analysis of the proteins ($P450_{cam}$, PdR and PdX) obtained after purification from anion-exchange (DE-52) column. Lanes 1, and 5 are molecular markers; Lane 2 is the BSA standard. Lanes 3, 4, 6, and 7 are the fractions collected from the DE-52 column. The arrows show the approximate positions where we expect $P450_{cam}$ (47 kDa), PdR (46 kDa) and PdX (12 kDa) to appear.

3. The Borneol Cycle of Cytochrome P450_{cam}: Mechanism and Advantages to *Pseudomonas Putida*

This chapter is reproduced in part, with editorial changes suggested by the examination committee, from “Water Oxidation by a Cytochrome P450. Mechanism and function of the reaction” published in PloS One 2013, 8(4): e61897.

Brinda Prasad^a, Derrick J. Mah^a, Andrew R. Lewis^a, Erika Plettner^a

^aDepartment of Chemistry, Simon Fraser University, Burnaby, BC, Canada - V5A 1S6

Author contributions

B. Prasad purified the proteins PdR and PdX, performed all the enzymatic assays, the NMR experiments, and wrote the paper. D. Mah performed experiments in determination of the new extinction coefficient for P450_{cam}. A. Lewis optimised the ¹⁷O NMR conditions and worked together with B. Prasad in designing the ¹⁷O NMR experiments. E. Plettner planned the project and worked on elucidating the reduction mechanism.

3.1. Abstract

P450_{cam} (CYP101A1) is a bacterial monooxygenase that catalyzes the oxidation of camphor, the first committed step in camphor degradation, with simultaneous reduction of oxygen (O₂). We report that P450_{cam} catalysis is controlled by oxygen levels: at high O₂ concentration, P450_{cam} catalyzes the known oxidation reaction, whereas at low O₂ concentration the enzyme catalyzes the reduction of camphor to borneol. We confirmed, using ¹⁷O and ²H NMR, that the hydrogen atom added to camphor comes from water, which is oxidized to hydrogen peroxide (H₂O₂). This is the first time a cytochrome P450 has been observed to catalyze oxidation of water to H₂O₂, a difficult reaction to catalyze due to its high barrier. The reduction of camphor and simultaneous oxidation of water are likely catalyzed by the iron-oxo intermediate of P450_{cam}, and we present a plausible mechanism that accounts for the 1:1 borneol:H₂O₂ stoichiometry we observed. This reaction has an adaptive value to bacteria that express this camphor catabolism pathway, which requires O₂, for two reasons: 1) the borneol and H₂O₂ mixture generated is toxic to other bacteria and 2) borneol down-regulates the expression of P450_{cam} and its electron transfer partners. Since the reaction described here only occurs under low O₂ conditions, the down-regulation only occurs when O₂ is scarce.

3.2. Introduction

P450_{cam} (CYP101A1), enables a strain of *Pseudomonas putida* (a soil bacterium) to use (1R)-(+)-camphor **9** (Fig. 2.1) as a carbon source, and oxidises at the 5th position to give 5-exo-hydroxycamphor **10** and 5-ketocamphor **11** (Fig. 2.1) ¹⁸⁹. Here we describe how P450_{cam} can also reduce camphor to borneol **12** (Fig. 3.1) under low O₂ conditions, and how borneol regulates the expression of the P450_{cam} system. Catalytic water oxidation is difficult to achieve, because the reaction is endothermic and has a large barrier. ¹⁹⁰⁻¹⁹² To our knowledge, this is the first description of a cytochrome P450 oxidizing water.

We have observed that at low oxygen concentration, regardless of whether compound I (**7**, Fig. 1.1) forms *via* reduction of O₂ or by shunting with oxidants, P450_{cam} not only produces the oxidation products 5-exo-hydroxy camphor (**10**) or 5-ketocamphor (**11**), but can also reduce camphor to borneol (**12**) (Fig. 3.1) ¹⁹³. We have interpreted this reaction to give *P. putida* an ecological advantage over other non-camphor metabolising bacteria because borneol is bactericidal to non-P450 containing bacteria, but not to *P. putida* ¹⁹³. In this chapter, the mechanism of the camphor reduction reaction and the regulatory effect of the product, borneol, on the expression of P450_{cam} will be discussed.

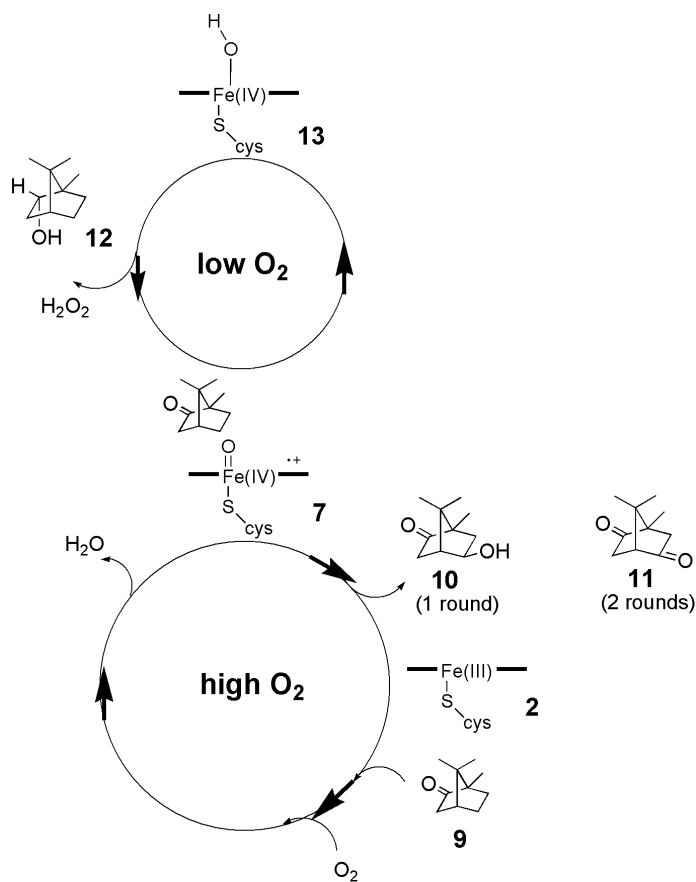


Figure 3.1 Under highly oxygenated conditions, P450_{cam} hydroxylates camphor (9) to 5-exo-hydroxy camphor (10) and further to 5-ketocamphor (11), whereas under low oxygen conditions, P450_{cam} reduces camphor to borneol (12). Details of the high O₂ cycle are shown in Fig. 1.1 and the details of the low O₂ cycle are shown in Fig. 3.6.

3.3. Materials and Methods

3.3.1. General

3.3.1.1. Materials

All solvents were distilled prior to use. Nicotine adenine dinucleotide, reduced (NADH), Dithiothreitol (DTT), lysozyme, DNase, RNase, Vitamin B₁, riboflavin, 5-aminolevulinic acid, hydrogen peroxide (used for assays), protease inhibitors leupeptin, aprotinin, and 4-(2-aminoethyl)-benzenesulfonyl fluoride, butylated hydroxytoluene (BHT), cytochrome P450 CYP3A4 (C-4982), superoxide dismutase (S5639), catalase (C-1345), glucose oxidase (G-2133) were purchased from Sigma.

Ethylenediaminetetraacetic acid (EDTA) was purchased from Fisher Scientific. Ferrous sulphate (FeSO_4) was purchased from Allied Chemical, Canada. Gas chromatography/mass spectrometry (GC-MS) was carried out on a Varian Saturn 2000 MS equipped with a 30-m SPB-5 column (Supelco, 0.25 mm ID; 0.25 μm film thickness) and the column was programmed as follows: 45 °C (0.5 min), 7 °C min^{-1} to 120 °C (1 min), 50 °C min^{-1} to 260 °C (3 min). Electron impact (EI) spectra were obtained at an emission current of 30 μA , scanning from 50 to 365 amu, with ion storage (SIS mode) 49-375, trap temperature 170 °C and transfer line 250 °C. UV/Vis spectra were obtained on a Cary 300 Bio UV-visible double beam instrument. NADH utilization rates and hydrogen peroxide formation were measured on a thermostatted Hach DR/4000 U spectrophotometer. Activity assays were carried out at 22 °C. Electrophoresis was performed on polyacrylamide gels (14%, 29:1) with 0.5% SDS (SDS-PAGE). The samples were reduced by treating with 1 μL of DTT stock (31 mg/mL) before loading on gels. Gels were stained with Coomassie Brilliant Blue R (Sigma). Sonication was done using a Branson Ultrasonic sonicator. Centrifugations were carried out with a Beckmann Avanti J-26 XPI centrifuge, equipped with a JLA 8.1000 rotor.

The buffers used were: lysis (20 mM phosphate buffer (K^+), pH 7.4 with 1 mM camphor; T-100 (50 mM Tris, 100 mM KCl, pH 7.4); T-400 (50 mM Tris, 400 mM KCl, pH 7.4). Buffers for nickel columns were: rinse buffer (20 mM Tris, pH 8.0); low imidazole buffer (5 mM imidazole, 20 mM Tris, 0.5 M NaCl, pH 8.0); strip buffer (0.1 M Ethylenediaminetetraacetic acid (EDTA), 0.5 M NaCl, pH 8.0). For P450_{cam} purifications, all buffers contained 1 mM camphor. Substrate-free P450 was prepared by passing the substrate bound enzyme over a Sephadex G-10 column equilibrated with 100 mM 3-(N-morpholino) propane sulfonic acid (MOPS, pH 7.0).

3.3.1.2. Methods

Deuterium (^2H) NMR spectra were recorded on a Bruker AVANCE II 600 MHz spectrometer (operating at 92.124 MHz). A Bruker 5 mm TCI cryoprobe was used with samples maintained at a temperature of 298 K. ^2H field-locking and field sweep were turned off. Samples were contained in 3 mm diameter MATCH nmr tubes filled to 40 mm (volume ca. 185 μL). Acquisition details: 10,240 transients summed, spectral width 15 ppm, transmitter offset 6.5 ppm, 11054 complex points acquired, 15 degree pulse with

recycle delay of 1 s between transients, no decoupling of ^1H during FID acquisition. Acquisition time was 14.2 h per spectrum.

The ^{17}O NMR spectra were run on a Bruker AVANCE III 500 MHz NMR spectrometer (operating at 67.808 MHz) equipped with a Bruker 5 mm TBO probe and samples were maintained at a temperature of 298 K. Samples were contained in 5 mm diameter nmr tubes filled to 50 mm (volume ca. 600 μL). Acquisition details: 1,000 or 25,000 transients summed, spectral width 503 ppm, ^{17}O transmitter offset 50 ppm, ^1H transmitter offset 4.78 ppm, 32768 complex points acquired, 90 degree pulse with recycle delay of 1 s between transients, and inverse-gated WALTZ-16 composite pulse decoupling of ^1H during FID acquisition. Acquisition time was 12 min per spectrum or 300 min (when catalase was present). The chemical shifts (δ) for all compounds are listed in parts per million using the NMR solvent as an internal reference (H_2^{17}O ($\delta=0$ ppm) or 4.78 ppm for ^2H).

3.3.1.3. Protein expression and purification

E. coli strain BL21 (DE3) (Novagen) containing the appropriate plasmid ¹⁶³ were grown in Luria Broth-ampicillin (LB-amp) medium at 37 °C with shaking (250 rpm) to $A_{600} = 0.9 - 1.0$ ¹⁶³. At this point, cells were harvested by centrifugation, resuspended in fresh LB-ampicillin medium, and after 2 h of growth, IPTG (240 mg L^{-1}) and trace additives were added. The cultures, except for PdR, were grown for 12 h at 27 °C (PdR was grown for 6 h). The cells were harvested by centrifugation (30 min, 7000 \times g) and stored at -85 °C until lysis. Additives were: FeCl_2 (0.1 μM), 5-aminolevulinic acid (1 mM), Vitamin B₁ (10 μM) for P450; FeCl_2 (0.1 μM) and $\text{Na}_2\text{S}\cdot 9\text{H}_2\text{O}$ (0.1 μM) for redoxin; riboflavin (1 mM) for reductase.

The lysis steps of P450 and PdR remained the same as described for *P. putida* ¹⁶⁰ except that 1 mM camphor was added to the buffer in which P450 culture was lysed. The dialysed lysate of P450, or PdR was individually subjected to a 20% ammonium sulphate cut to remove the cell debris. The 20% supernatant was then carried forward to 45% ammonium sulphate saturation to isolate the protein. The 20-45% pellet was resuspended in T-100 buffer (50 mM Tris, 100 mM KCl, pH 7.4), camphor (1 mM) was added in the case of P450 and purified by DE-52 (anion exchange column) using a linear gradient with buffer T-100 to T-400, 1 mM camphor and 1 mM β -mercapto ethanol

(P450 only) at 1 mL min^{-1} . The fractions with high absorbances at λ_{392} (in the case of P450), λ_{454} (in the case of PdR) were checked with SDS-PAGE. The collected fractions were pooled and concentrated using an Amicon ultrafiltration cell equipped with a YM-10 membrane and the concentrated protein was individually loaded onto a S-100 column, eluted with T-100 buffer, 1 mM sucrose, 1 mM camphor (P450 only) at 1 mL min^{-1} . SDS-polyacrylamide gel electrophoresis showed a single band for P450 and PdR.

In the case of PdX, cells from 2 L of culture were lysed in lysis buffer (0.25 M NaCl, 20 mM Tris/HCl, pH 8.0). Lysozyme (10 mg mL^{-1}), DNase (2 mg, Sigma), and RNase (10 mg, Sigma) were added and the solution was stirred for 30 min at $4 \text{ }^\circ\text{C}$. The lysate was sonicated with 50% duty cycle for 10 minutes, stirred for 10 min at $4 \text{ }^\circ\text{C}$, and homogenized with a pestle. The homogenized cells were then harvested by centrifugation ($10500 \times g$, 30 min) and dialysed with frequent changes of lysis buffer followed by further purification by ammonium sulphate precipitation. The dialysed lysate was subjected to a 20% ammonium sulphate cut to remove the cell debris. The 20% supernatant was then carried forward to 90% ammonium sulphate saturation overnight to isolate the protein. The 20-90% pellet was resuspended in 5 mL of rinse buffer (20 mM Tris HCl, pH 8.5), dialysed against this buffer for 3 h and harvested at 5000 rpm for 5 min. The dialysed supernatant was loaded on a $\sim 5 \text{ cm Ni}^{2+}$ -His bind column and eluted with strip buffer (10 mL \times 3), low imidazole buffer (10 mL \times 2), high imidazole buffer (10 mL \times 4). The fractions with $A_{280}/A_{325} < 5.0$ were pooled, dialysed with 100 mM Tris, 100 mM KCl, pH 7.4 and the concentrated PdX protein was frozen to $-85 \text{ }^\circ\text{C}$. The concentrations of ferric P450 (with camphor), PdR and PdX were determined by their extinction coefficients ($\epsilon_{392} = 68.5 \text{ mM}^{-1} \text{ cm}^{-1}$, $\epsilon_{454} = 10 \text{ mM}^{-1} \text{ cm}^{-1}$, $\epsilon_{325} = 15.6 \text{ mM}^{-1} \text{ cm}^{-1}$ respectively).

3.3.1.4. Determination of new P450_{cam} extinction coefficient

The extinction coefficient of $\epsilon_{280\text{nm}}$ can be predicted from specific amino acid residues¹⁹⁴, 5 tryptophan residues¹⁹⁵, 9 tyrosine residues¹⁹⁶ and 8 cysteine residues¹⁹⁷. This value was determined to be $41.91 \text{ mM}^{-1} \text{ cm}^{-1}$ and with the addition of hemin at $\epsilon_{280\text{nm}}$ ($22.5 \text{ mM}^{-1} \text{ cm}^{-1}$)¹⁹⁸, the predicted value was $64.41 \text{ mM}^{-1} \text{ cm}^{-1}$, which is similar to the literature value of P450_{cam}¹⁹⁴. Using the literature value of P450_{cam} at $\epsilon_{280\text{nm}}$, 63.3 mM^{-1}

1cm^{-1} ¹⁹⁴, $\epsilon_{392\text{nm}}$ value was calculated using Beer-Lambert Law and was found to be 68.6 $\text{mM}^{-1}\text{cm}^{-1}$ and $\epsilon_{410\text{nm}}$ value was calculated to be 71.1 $\text{mM}^{-1}\text{cm}^{-1}$.

Table 3.1 *Calculated and literature values of P450_{cam} extinction coefficients at selected wavelengths.*

Wavelength (nm)	Calculated extinction coefficient, ($\text{mM}^{-1}\text{cm}^{-1}$)	Literature extinction coefficient, ($\text{mM}^{-1}\text{cm}^{-1}$) ²
280	64.4	63.3
392	68.6	102
410	71.1	86.5

3.3.2. Description of Enzymatic Assays

3.3.2.1. Assays with recombinant proteins

Enzymatic assays were performed in 1 mL of 50 mM phosphate buffer (100 mM K^+) (pH = 7.4) bubbled with air/oxygen. The reaction mixture contained 200 nM P450_{cam}, 200 nM PdR, 1000 nM PdX and the substrate camphor (1 mM). NADH consumption was initiated by the addition of 0.625 mM NADH and monitored for ten minutes at 340 nm. The reaction was stopped by the addition of 1 mL 7.2 μM indanone in CHCl_3 for the extraction of the product(s) and the substrate. Indanone was the internal standard for the quantitation of products by gas chromatography / mass spectrometry (GC-MS). A second extraction of the aqueous phase with 0.7 mL of CHCl_3 / indanone followed. The combined organic layers were dried over MgSO_4 and analysed by GC-MS.

In assays involving *m*-CPBA as a shunt agent for the catalytic cycle, the reaction mixture contained P450_{cam} (180 nM), *m*-CPBA (1 mM), and the substrate camphor (1 mM). The reaction mixture was incubated for 15 minutes at 22 °C and extracted as described previously. The dried organic layers were analysed by GC-MS.

3.3.2.2. Steady-state kinetics

Enzymatic assays were performed under shunt conditions (as mentioned above) to determine the K_M and k_{cat} for formation of borneol and 5-ketocamphor in normal and

D₂O buffers. 1 mL of 50 mM phosphate buffer (100 mM K⁺, pH = 7.4 or pD 7.4) contained camphor at varied concentrations ranging from 30 μM to 2500 μM, and 180 nM P450_{cam}. 1 mM shunt agent (*m*-CPBA) was added to the reaction mixtures containing camphor concentrations 500 μM to 2500 μM and to the rest of the concentrations, *m*-CPBA was optimised to a 1:1 ratio with the substrate concentration to avoid the destruction of the heme in P450. The reactions for 5-ketocamphor formation were carried out using vials fitted with PTFE septa and pressurized with pure O₂. The reaction mixtures were incubated for 20 minutes at room temperature and extracted with CHCl₃/indanone and analysed by GC-MS. The k_{cat} and K_M were estimated from the non-linear regression using Graph pad Prism 4.

3.3.2.3. Assays in D₂O buffer

Assays were performed in 1 mL 50 mM phosphate buffer (made from D₂O) of pD 7.4. The pH of the buffer was adjusted according to the equation: pD = pH meter reading + 0.4.¹⁹⁹ For assays with the complete P450_{cam} system, the reaction mixture contained: P450_{cam} (180 nM), PdX (900 nM), PdR (180 nM), NADH (0.6 mM), camphor (1.2 mM), and O₂ was bubbled into the mixture. For assays with shunted P450_{cam}, the reaction mixture included camphor (1.25 mM), *m*-CPBA (1 mM), and P450_{cam} (180 nM). Reactions were incubated at 22 °C. The reaction was stopped by the addition of 1 mL 7.2 μM indanone in CHCl₃ for the extraction of the product(s) and the substrate. A second extraction of the aqueous layer was done with 0.7 mL of CHCl₃/indanone. The combined organic layers were dried over MgSO₄ and analysed by GC-MS.

Table 3.3 shows the result of assays with the full system and the shunted P450. For ²H NMR, 34 μg of 12D (2-D-borneol) were collected from pooled extracts of assays that had been run in D₂O. The sample was dissolved in CHCl₃ (300 μL) and 200 μL of the solution was transferred to a 3 mm Bruker MATCH nmr tube.

Assays with shunted P450_{cam} were also performed at 0 °C, 5 °C, 10 °C, 15 °C in 1 mL of Ar-sparged, 50 mM phosphate buffer, in D₂O or H₂O, at pD or pH 7.4. Mixtures contained 200 nM P450_{cam}, camphor (1.25 mM), and *m*-CPBA (1 mM). Samples were collected after 30, 60, 120 and 360 min and checked by GC-MS for the formation of products. Controls contained the reaction mixtures in the absence of the substrate, enzyme or shunt agent.

3.3.2.4. Assays with human P450 (CYP3A4).

To test whether a different camphor-metabolizing P450 is also able to reduce camphor to borneol under low oxygenation, we reacted a human cytochrome P450, (CYP3A4) containing NADPH and the cognate reductase with camphor under shunt conditions. For shunt, the enzymatic assays were performed in 1 mL 50 mM phosphate buffer (150 mM K⁺) of pH 7.4. The reaction mixture included the substrate camphor (1.25 mM), *m*-CPBA (1 mM), and human P450 CYP3A4 (0.5 pmol). The reaction mixture was incubated for 20 min at 22 °C. Controls contained the reaction mixtures in the absence of the substrate, enzyme or shunt agent. The reaction was stopped by the addition of 1 mL 7.2 μM indanone in CHCl₃ for the extraction of the product(s) and the substrate. A second extraction of the aqueous layer was done with 0.7 mL of CHCl₃/indanone. The combined organic layers were dried over MgSO₄ and analysed by GC-MS.

3.3.2.5. Assays with dithionite

To test whether the reduced form of P450_{cam} reduces camphor, P450_{cam} (180 nM) was incubated in 1 ml phosphate buffer (50 mM, 150 mM K⁺) with camphor (1 mM) and dithionite (1 mM). The reaction was stopped, extracted and analyzed as described above in section 3.3.2.1. Reduced P450_{cam}, alone with camphor or with its redox partners and camphor, did not generate borneol in detectable amounts.

3.3.2.6. Alignment of cytochromes P450 and superposition of CYP101A1 (P450_{cam}) and CYP3A4

A search, using the Basic Local Alignment Search Tool (BLAST) on the National Center for Biotechnology (NCBI) web site (<http://www.ncbi.nlm.nih.gov/sutils/blink.cgi?mode=query>) was performed, using the P450_{cam} protein sequence as the reference. The search was done among all non-redundant GenBank CDS translations+PDB+SwissProt+PIR+PRF excluding environmental samples from WGS projects, using BLASTP 2.2.26+.

The BLAST search of the P450_{cam} protein sequence revealed related CYPs (19, with ≥ 40% sequence identity, and 50 with ≥ 30 but < 40% sequence identity), all from soil and marine bacteria. Protein sequences (16 in total) were then chosen, along with P450_{nor}, a distant fungal CYP from *Fusarium oxysporum* (locus1XQD_A), that was not

detected in the BLAST search and that catalyzes the reduction of nitric oxide.²⁰⁰ These protein sequences were then subjected to exhaustive pairwise alignment, using Neighbor-joining phylogeny in SECentral (Align Plus 4.0, Scientific and Educational Software, Durham, NC, USA). The result of this alignment is shown in the upper portion of Fig 3.8.

It is important to note that the DT pair (251 and 252) and E366 in P450_{cam} are highly conserved among these CYPs. These are the residues known to hold the water molecules above the porphyrin. In addition, the O₂ tunnel is conserved, with hydrophobic residues. For example, F (163 in P450_{cam}) is highly conserved, A167 in P450_{cam} is either A, V, I, M or L in the others (19 related CYPs with ≥ 40% sequence identity), I220 in P450_{cam} is I, V, F or M in the others (19 related CYPs with ≥ 40% sequence identity), A219 in P450_{cam} is A, L, V, M or F in the others (19 related CYPs with ≥ 40% sequence identity) and L245 in P450_{cam} is L, V or I in the others (19 related CYPs with ≥ 40% sequence identity). Hydrophobic residues from the crevasse in P450_{cam}, that are also hydrophobic in all the others, include the residues that align with L257, M261, P278, I281, L371 and L375 of P450_{cam}. Thus, it is possible that the water oxidation, coupled to the reduction of an organic substrate, is widespread among bacteria in the environment. A similar exhaustive pairwise alignment was done with eight vertebrate class II P450s and P450_{cam} as the reference and the results are in the lower portion of Fig. 3.8. To superimpose the three dimensional structures of P450_{cam} and CYP3A4, the structures were visualized, superimposed and docked in Molecular Operating Environment (MOE). Briefly, the PDB structures were opened in MOE and prepared by calculating the protonation of each residue at pH 7.0, 300K and 0.1 M salt, and assigning charges according to the default settings under “Compute|Protonate 3D”. For superposition, the two proteins were first aligned, using the “Align” protocol, then they were superimposed, with P450_{cam} as the reference, with “all residues” and “accent secondary structure matches” selected. The results from superposition are discussed in the section 3.4.7.

3.3.2.7. The effect of camphor, borneol and DMSO on the expression of P450_{cam}, PdX, and PdR

To study the effect of borneol on the induction of the P450_{cam} system, we grew *P. putida* for 7 generations at 27 °C without camphor under aerated conditions, and then divided the culture into three equal portions. Camphor (0.03g in 300 μL DMSO), borneol

(0.03g in 300 μ L DMSO) or the control (DMSO), was added to one of the three portions, and the cultures were incubated at 27 $^{\circ}$ C. Samples collected at regular intervals up to 4 h were harvested at 10,000 \times g for 90 seconds at 4 $^{\circ}$ C. The entire experiment was performed in 3 replicates. Cultures induced with camphor were divided into three portions after 60 minutes and borneol (0.015g in 300 μ L DMSO), DMSO, or no compound/solvent was added to one of the three portions (Fig. 3.13a). Lysis of the cultures was performed as described previously¹⁶³. The clarified lysate samples obtained at regular time intervals were scanned from 200-700 nm and the concentrations of P450_{cam}, PdR, and PdX were obtained from the characteristic absorbances. The extinction coefficients we have determined for purified P450_{cam} (Table 3.1) were used to estimate the concentration of P450_{cam} in the lysates. In order to correct for the increase in absorbance due to bacterial growth, the enzyme concentration was divided by the number of colony forming units obtained for that time point.

Using Graphpad prism software, the Kruskal-Wallis test was chosen to compare the effects of 5 groups (camphor, borneol, DMSO, camphor + borneol, camphor + DMSO) and ANOVA (Tukey-Kramer test) was performed within each time series of the three replicates for each treatment.

3.4. Results and Discussion

3.4.1. Reaction conditions leading to formation of borneol

We have observed that borneol forms as a major product of P450_{cam} at low O₂ concentration (O₂ \leq 2 mg/L, \leq 63 μ M, as measured by O₂ meter) (concentration of O₂ in water under normal ambient conditions, 1 atm is ca. 10 mg/L)²⁰¹. *In vivo*, this occurs when cultures are poorly aerated¹⁹³ and, *in vitro*, this occurs when the buffer is sparged with argon in an open vial. In contrast, the known oxidation products **10** and **11** (Fig. 3.1) form at high O₂ concentration (\sim 9 mg/L = 284 μ M). *In vivo*, this occurs when cultures are well aerated and, *in vitro*, this occurs when pure O₂ is bubbled into the buffer (Fig. 3.1). To map the mechanism of the reduction, we have performed experiments with the recombinant proteins (P450_{cam}, PdX, and PdR), isolated from expression in *E. coli* (Table 3.2). Assays were carried out in phosphate buffer (50 mM phosphate, 150 mM

K⁺, pH 7.4), with NADH and camphor. Our extinction coefficient values were used for the calculation of the enzyme concentration (Table 3.1). Under high oxygenation (with pure O₂ bubbled into the buffer), we observed 5-*exo*-hydroxy camphor as a major product (Table 3.2, entry 1). Similar experiments under mid-range oxygenated conditions (O₂ ≤ 5 mg/L) yielded borneol as the only product (Table 3.2 entry 2). The formation of borneol under these conditions was 34-fold less compared to 5-*exo*-hydroxy camphor that formed under high oxygenated conditions and this could be because of the slower formation of iron-oxo species (compound I).

Under poor buffer oxygenation, in the absence of NADH, P450_{cam} shunted with *m*-CPBA (Fig. 1.1, pathway “i”) reduced camphor to borneol (Table 3.2 entries 3 and 4). The observation that borneol formed in the absence of NADH indicates that NADH is not the source of electrons for the reduction reaction. Furthermore, shunted P450_{cam} under high buffer oxygenation gave more 5-ketocamphor than borneol (Table 3.2 entry 5), indicating that O₂ levels are important in the regulation of the reaction platform followed by the enzyme.

Table 3.2. Assays with recombinant proteins. Formation of borneol, 5-exo-hydroxy camphor and 5-ketocamphor under various conditions.

Enzymatic assay	Products (nmol min ⁻¹ nmol ⁻¹ P450)			NADH consumed (nmol min ⁻¹ nmol ⁻¹ P450)	H ₂ O ₂ formed (nmol min ⁻¹ nmol ⁻¹ P450)	4e ⁻ uncoupling (nmol min ⁻¹ nmol ⁻¹ P450)
	Borneol	5-keto camphor	5-exo-hydroxy camphor			
O ₂ ¹	7.5 ± 4	20 ± 5	950 ± 465	1331 ± 270	ND	660 ± 235
air ²	28 ± 9	ND	ND	335 ± 13	297 ± 103	80 ± 10
rP450+ <i>m</i> -CPBA ³	249 ± 28	ND	ND	N/A	291 ± 29	N/A
Ar + rP450+ <i>m</i> -CPBA ^{3,4}	404 ± 19	16 ± 4	ND	N/A	444 ± 16	N/A
O ₂ + rP450+ <i>m</i> -CPBA ^{3,5}	173 ± 39	354 ± 12	ND	N/A	204 ± 17	N/A

Values are the average of 4 replicates ± S.E. 50 mM potassium phosphate buffer (pH 7.4) was used for all the assays. Experimental details are included in the supporting information.

ND = Not Detected; N/A = Not Applicable

¹ The reaction mixture contained recombinant P450_{cam}, PdR and PdX and NADH. Oxygen (99%) was bubbled into the buffer for 60 seconds before the assay. The 4e⁻ uncoupling was calculated by taking the difference between the total NADH required and observed. ² The reaction mixture contained recombinant P450_{cam}, PdR, PdX, and NADH. Air (charcoal filtered) was bubbled into the buffer before the assay. ³ The assay was performed using recombinant P450_{cam} and *m*-CPBA as a shunt agent. ⁴ The buffer was sparged with argon (99%). ⁵ The buffer was treated with oxygen (99% pure, Sigma Aldrich) and assays were performed using camphor.

3.4.2. Source of the 2-H in borneol.

The source of the hydrogen attached to C-2 of borneol was further investigated in assays using deuterated phosphate buffer (50 mM phosphate in D₂O, 150 mM K⁺, pD 7.4). Using recombinant proteins (P450_{cam}, PdR, and PdX), under mid-range oxygenated conditions (with air), we detected the enzymatic conversion of camphor to 2-D-borneol **12D** (Fig. 3.2) using ²H NMR.

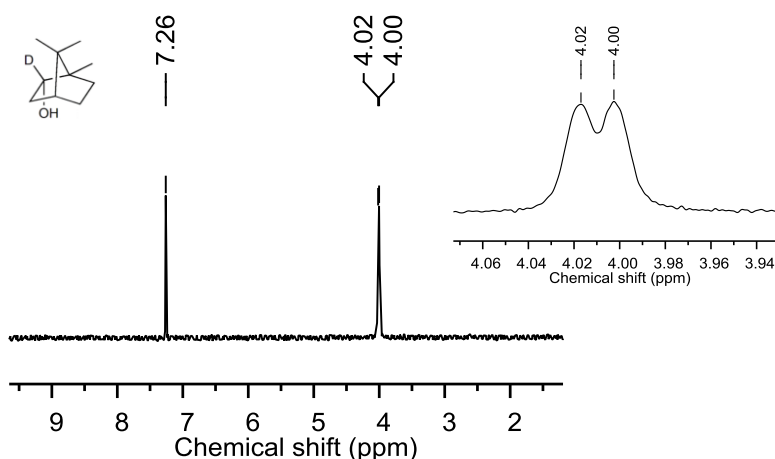


Figure 3.2. ^2H NMR of the 2-D-borneol obtained from the recombinant proteins incubated in 50 mM deuterated phosphate buffer (pD = 7.4) with camphor and *m*-CPBA. The extracted product was backwashed with H_2O .

We also detected 5-ketocamphor, as well as the depletion of NADH (Table 3.3). Similar experiments using NADD (deuterated nicotinamide cofactor) in non-labeled phosphate buffer did not yield 2-D-borneol.¹⁸⁰ All these experiments lead to the conclusion that water is the source of H_{exo} attached to C-2 in borneol formed by P450_{cam}.

When the reaction was performed in H_2O (Table 3.2), for the NADH-catalyzed reaction, the hydrogen peroxide produced was also due to two electron uncoupling.¹⁶³ However, when the reaction was performed in D_2O in the NADH-catalyzed reaction, hydrogen peroxide was not detected. Given that two equivalents of NADH are needed to reach ketocamphor and no NADH is needed to get borneol, I attributed the high amount of NADH consumed to four electron uncoupling. Under shunt conditions in D_2O , part of the hydrogen peroxide was from the borneol cycle (6 nmol/min/nmol P450). The remaining H_2O_2 may have come from the following series of reactions:

- 1) $\text{Cpd I} + \text{D}_2\text{O} \rightarrow \text{Cpd II-H} + \text{OD}^\bullet$
- 2) $\text{Cpd II-H} + \text{OD}^\bullet \rightarrow \text{Fe(III)porphyrin} + \text{D}_2\text{O}_2$

Table 3.3. Formation of 2-D-borneol and 5-ketocamphor in D₂O buffer, with the full P450_{cam} system and with the shunted P450_{cam}.

Assay condition	D-borneol (nmol min ⁻¹ nmol ⁻¹ P450)	5-ketocamphor (nmol min ⁻¹ nmol ⁻¹ P450)	NADH consumed (nmol min ⁻¹ nmol ⁻¹ P450)	H ₂ O ₂ (nmol min ⁻¹ nmol ⁻¹ P450)
rP450 _{cam} + rPdX + rPdR + NADH + camphor (pD=7.4) ^{1, 2}	6 ± 3	53 ± 24	562 ± 230	ND
rP450 _{cam} + <i>m</i> -CPBA + camphor (pD=7.4) ^{1, 3}	6 ± 3	ND	N/A	57.4 ± 10.4

3.4.2.1. Assays with other shunting agents

Enzymatic assays were performed in 50 mM phosphate buffer (150 mM K⁺, pH 7.4), with recombinant P450_{cam} (180 nM), substrate camphor (1.25 mM) and one of the shunt agents (cumene hydroperoxide, sodium periodate, *m*-CPBA or calcium hypochlorite (bleach)) added at a final concentration of 1 mM.

The reaction was stopped by the addition of 1 mL 7.2 μM indanone in CHCl₃ for the extraction of the product(s) and the substrate. A second extraction of the aqueous layer was done with 0.7 mL of CHCl₃/indanone. The combined organic layers were dried over MgSO₄ and analysed by GC-MS (Table 3.4).

The borneol cycle is independent of how Cpd I is generated: through the reduction of O₂ or the shunt pathway (Fig. 1.1). Borneol formation was seen with all the shunt agents tested (*m*-CPBA, cumene hydroperoxide, periodate and bleach; Table 3.4).

Table 3.4. Formation of borneol and hydrogen peroxide from the P450 catalytic cycle using other shunt agents

Shunt agent	Borneol (nmol min ⁻¹ nmol ⁻¹ P450) ¹	Hydrogen Peroxide (nmol min ⁻¹ nmol ⁻¹ P450) ¹	P value ²
Cumene hydroperoxide	428 ± 285	518 ± 105	0.1
Sodium periodate (NaIO ₄)	750 ± 183	697 ± 285	0.9
Calcium hypochlorite (bleach)	775 ± 283	988 ± 122	0.3
r-P450 _{cam} + <i>m</i> -CPBA (table 3.2, entry 3)	249 ± 28	291 ± 29	0.1
Ar + rP450 _{cam} + <i>m</i> -CPBA (table 3.2, entry 4)	404 ± 19	444 ± 16	1.1
O ₂ + rP450 _{cam} + <i>m</i> -CPBA (table 3.2, entry 5)	173 ± 39	204 ± 17	0.87

3.4.2.2. ¹⁷O NMR of H₂O₂

If camphor is reduced to borneol by electrons from water, then water should be oxidized to hydrogen peroxide. We observed H₂O₂ along with borneol, approximately in a 1:1 stoichiometric ratio when P450_{cam} was shunted with *m*-CPBA (Table 3.2, entries 3-5) or with other oxidants (Table 3.4).

We prepared H₂¹⁷O¹⁸⁴ (Supplementary information) and incubated the reaction mixture containing 1 mM camphor, 1 mM *m*-CPBA and recombinant P450_{cam} (0.1 μM) in ¹⁷O phosphate buffer (50 mM, 150 mM K⁺, pH 7.4 made with H₂¹⁷O) for 12 h to detect the formation of H₂¹⁷O₂. To this assay mixture, P450_{cam} (0.02 μM) and *m*-CPBA (0.2 mM) were added at 2 h intervals, to form detectable amounts of H₂¹⁷O₂. A new resonance was observed at 178 ppm in the ¹⁷O NMR spectrum, (Fig. 3.3 (a)) which matched the chemical shift of H₂¹⁷O₂ reported in the literature²⁰² and of our prepared standard¹⁸⁴. Controls (in the absence of *m*-CPBA, enzyme or substrate) were run simultaneously, and this resonance was not detected (Figs. 3.3(b), 3.3(c) and 3.3(d)), which led us to conclude that the new peak could not have come from the hydrolysis of *m*-CPBA.

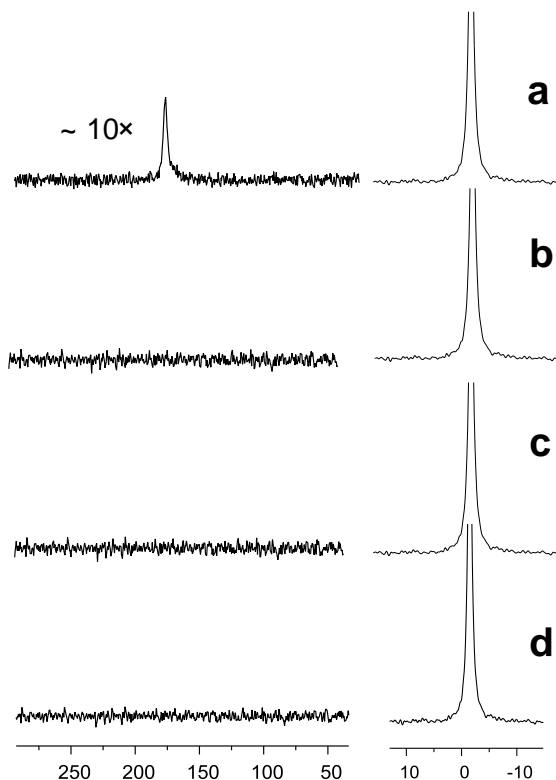


Figure 3.3. ^{17}O NMR spectrum of the incubation mixture in ^{17}O phosphate buffer (pH 6.3) containing: a) camphor, recombinant P450_{cam} and $m\text{-CPBA}$, b) camphor and recombinant P450_{cam} ($m\text{-CPBA}$ absent), c) camphor and $m\text{-CPBA}$ (enzyme absent), and d) $m\text{-CPBA}$ and recombinant P450_{cam} (substrate absent). The peaks at 0 ppm and 178 ppm correspond to H_2^{17}O and $\text{H}_2^{17}\text{O}_2$, respectively.

When catalase (an enzyme that disproportionates H_2O_2 to water and O_2) was added to the reaction mixture, the resonance at 178 ppm disappeared (Figure 3.4), confirming that the 178 ppm resonance is due to $\text{H}_2^{17}\text{O}_2$.

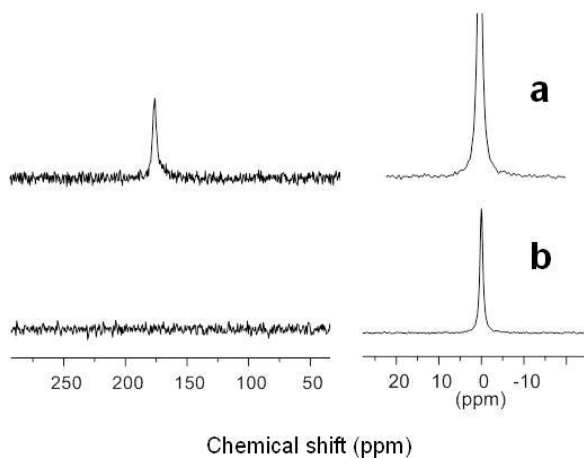


Figure 3.4. ^{17}O NMR spectra of the incubation mixture under shunt conditions using 1 mM *m*-CPBA in ^{17}O phosphate buffer (final pH 6.3) containing 1 mM substrate camphor and recombinant P450_{cam} : a) before and b) after addition of catalase (1 unit). The peak at 178 ppm corresponds to $\text{H}_2^{17}\text{O}_2$ and that at 0 ppm is due to H_2^{17}O .

3.4.3. Dependence of the H_2O_2 (^{17}O) chemical shift on pH

We observed that the pH of the assay mixtures dropped from 7.4 to 6.3 after 30 minutes of incubation. The pK_a of *m*-CPBA is 7.6²⁰³. The drop in pH likely comes from the *meta*-chlorobenzoic acid formed during the shunt reaction. Chemical shifts in ^{17}O NMR are reported to be dependent on pH and temperature²⁰⁴. The chemical shift of the $\text{H}_2^{17}\text{O}_2$ standard prepared by the electrolysis of phosphate buffer (made from H_2^{17}O) was 178 ppm (at a final pH 3.9). The prepared standard was buffered to different pH values ranging from 3-10 and the chemical shift remained constant from pH 3-8 (Figure 3.5). At pH 10, the chemical shift changed to 194 ppm, due to the formation of HO-O^- (Figure 3.5). The hydrogen peroxide formed during the borneol cycle had a chemical shift of 178 ppm, matching the chemical shift of fully protonated $\text{H}_2^{17}\text{O}_2$.

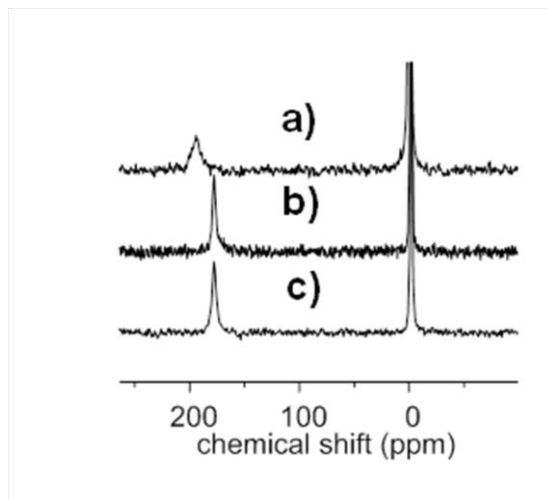


Figure 3.5. ^{17}O NMR spectra of $\text{H}_2^{17}\text{O}_2$ (obtained by electrolysis of H_2^{17}O) buffered at a) pH 10, b) pH 3, and c) pH 9.

3.4.4. Kinetic Isotope Effects (KIE)

The reaction catalyzed by P450_{cam}, shunted with *m*-CPBA in D_2O , gave 2-D-borneol at a much slower rate than the same reaction performed in normal water. A large kinetic isotope effect ($k_{\text{H}}/k_{\text{D}}$) of ~ 50 (Table 3.5) was observed in borneol formation and the ratio of the rates remained the same at all temperatures. The magnitude and temperature independence of the $^1\text{H}/^2\text{H}$ kinetic isotope effect (KIE) suggests that hydrogen transfer through tunnelling could occur at the rate-determining step in the reduction of camphor to borneol²⁰⁵⁻²⁰⁷.

Table 3.5. Assays with recombinant P450_{cam} under selected temperatures. Formation of borneol and D-borneol under shunt conditions with the addition of m-CPBA.

Temperature (°C)	v _H (nmol of borneol/min/nmol P450) ¹	v _D (nmol of D- borneol/min/nmol P450) ¹	v _H /v _D ²
0	148 ± 5	2.5 ± 0.5	59.2 ± 1.9
5	128 ± 18	2.2 ± 0.8	58.2 ± 20.8
10	147 ± 39	2.5 ± 0.8	58.8 ± 20.8
15	166 ± 32	2.8 ± 0.3	59.3 ± 13.6
20	244 ± 33	4.3 ± 0.5	56.7 ± 10.1

¹ Data represent the average ± S.E. of 4 replicates. ² Ratios were calculated from the averages.

The random errors were calculated by the formula ($\frac{\Delta^2(F)}{F^2} = \frac{\Delta^2(x)}{x^2} + \frac{\Delta^2(y)}{y^2}$) wherein F denotes v_H/v_D, x and y denote v_H and v_D. ΔF, Δx and Δy denote their corresponding errors.

In contrast, the KIE (¹H/²H) for hydrogen peroxide formation are much smaller, suggesting that this product does not form at the rate-limiting step (Table 3.6).

Table 3.6. Assays with recombinant P450_{cam}, shunted with m-CPBA in H₂O and D₂O at selected temperatures. Formation of H₂O₂ or D₂O₂.

Temperature (°C)	v _H (nmol of H ₂ O ₂ /min/nmol P450) ¹	v _D (nmol of D ₂ O ₂ /min/nmol P450) ¹	v _H /v _D
0	266 ± 112	138 ± 16	1.9 ± 0.8
5	647 ± 93	106 ± 6	6.1 ± 0.9
10	589 ± 104	178 ± 31	3.3 ± 0.8
15	363 ± 105	178 ± 31	2 ± 0.6
20	183 ± 14	57 ± 10	3.2 ± 0.6

¹ Values are average of 4 replicates ± S.E.

3.4.5. Determination of K_M and k_{cat} for borneol formation

Borneol formation under shunt conditions is saturable, with a K_M = 699 ± 88 μM and k_{cat} = 426 ± 20 min⁻¹ for camphor (Fig. 3.6a). Similarly, ketocamphor formation under

oxygenated shunt conditions is saturable with a $K_M = 83 \pm 10 \mu\text{M}$ and $k_{\text{cat}} = 461 \pm 14 \text{ min}^{-1}$ for camphor (Fig. 3.6b).

In D_2O buffers, the formation of D-borneol was saturable with a $K_M = 802 \pm 107 \mu\text{M}$ and $k_{\text{cat}} = 9 \pm 0.4 \text{ min}^{-1}$ for camphor (Fig. 3.6a). Ketocamphor formation under oxygenated shunt conditions is saturable with $K_M = 118 \pm 6 \mu\text{M}$ and a similar $k_{\text{cat}} = 465 \pm 6 \text{ min}^{-1}$ for camphor. Therefore, borneol formation requires oxidation of P450_{cam} , either through shunting or through intermediates **2** to **7** of the catalytic cycle (Fig. 1.1). Therefore, compound I (Cpd I) must be involved in both borneol and ketocamphor formation (Fig. 3.1). It is interesting to note that the K_M for ketocamphor formation under high O_2 concentration is 9-fold lower (see above) than that for borneol formation under low O_2 concentration. This suggests that camphor binding and possibly positioning might be affected by O_2 concentrations. Surprisingly, the k_{cat} is the same for both reactions, even though there appears to be a larger barrier in the borneol cycle than in the normal oxidation reaction. This larger-than-expected k_{cat} suggests that, consistent with the observed KIE, H-atom tunneling is occurring in the borneol cycle. Under high O_2 concentrations using D_2O as the solvent, 5-ketocamphor (table 3.3) was detected as the only product suggesting that deuterium atoms from the solvent do not participate in the reaction. Steady-state kinetic assays for ketocamphor formation in D_2O buffers resulted in similar k_{cat} as in H_2O buffers. In contrast, a 60-fold decrease in k_{cat} (with a similar K_M) was detected for borneol formation (Fig. 3.6). This illustrates that the solvent molecules participate only in the borneol formation, but not in ketocamphor formation.

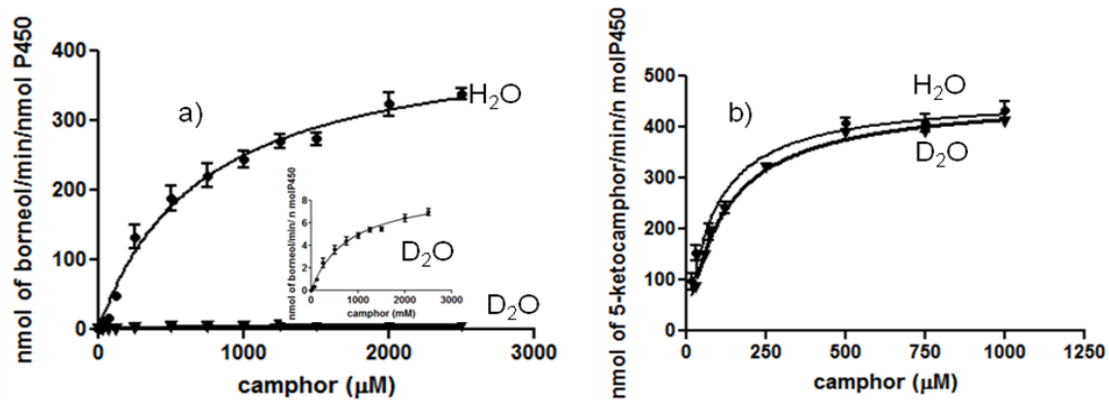


Figure 3.6 a) *Michaelis-Menten kinetics for borneol and b) 5-ketocamphor formation, under shunt conditions (with m-CPBA). To ensure a constant high O_2 concentration for the 5-ketocamphor formation kinetics, reactions were run in vials fitted with septa and pressurized with pure O_2 .*

3.4.6. Reduction Mechanism

We propose that water reduces and protonates Cpd I as a first step in the borneol cycle, giving protonated Cpd II **13** and a hydroxyl radical (OH^\bullet) (Fig. 3.7). The formation of OH^\bullet in water has been estimated from electrochemical data ²⁰⁸, and the formation of species **13** from Cpd I has been estimated at $\Delta G^\circ = -410 \text{ kJ/mol}$ ²⁰⁹. Therefore, the first step of the proposed reduction mechanism (Steps I and II, Fig. 3.7) involves the abstraction of a hydrogen atom from water by Cpd I to form the Fe(IV)-OH complex **13** (Fig. 3.7), which is favourable ($\Delta H \sim -160 \text{ kJ/mol}$) (Fig. 3.7). Three water molecules are known to be poised above the Fe-porphyrin and are held in place by hydrogen bonds to Thr 252, Asp 251 and Glu 366 ²¹⁰, so it is plausible that Cpd I could attack water instead of camphor. Next, we propose that the hydroxyl radical combines with the water molecule to yield hydrogen peroxide and a hydrogen atom (Step III, Fig. 3.7). By our estimate, this step is highly unfavourable ($\Delta H^\circ \cong 570 \text{ kJ/mol}$, section 3.4.7). Simultaneous transfer of the hydrogen atom from step III to the carbonyl group of camphor forms a borneol radical (Step IV, Fig. 3.7). A non-strained ketone such as acetone reacting with a hydrogen atom has a potential of approximately -2 V (ΔG° is +173 kJ/mol) ²¹¹. However, because camphor is quite a strained ketone, and that strain is relieved by the reduction, we have estimated this reaction to be slightly favourable ($\Delta H^\circ \sim -79 \pm 8 \text{ kJ/mol}$, section 3.4.7). Finally, the transfer of a hydrogen atom from protonated Cpd II to the borneol radical forms borneol and Cpd I (Steps V and VI, Fig. 3.7) ($\Delta H^\circ \cong 13 \text{ kJ/mol}$), completing the “borneol cycle”. The net reaction is endothermic, with $\Delta H^\circ \cong 305 \pm 8 \text{ kJ/mol}$ (section 3.4.7, Fig. 3.7).

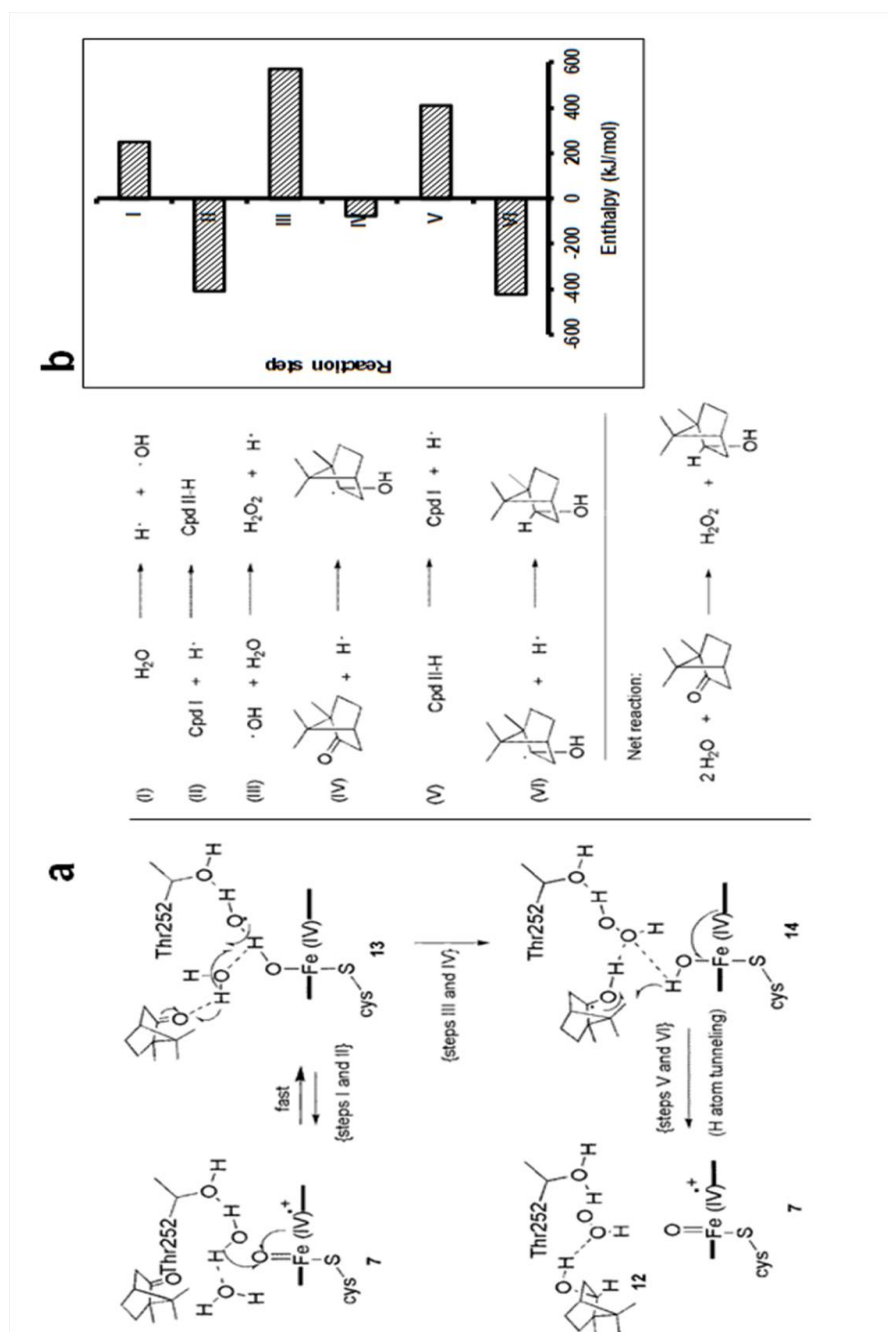
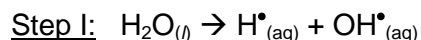


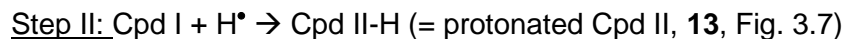
Figure 3.7 *The proposed reduction mechanism and the Born-Haber estimates. a) Proposed reduction mechanism of P450_{cam} that accounts for the simultaneous formation of borneol (12) and H₂O₂ in a 1:1 stoichiometry. b) Born-Haber estimates of the reduction mechanism.*

3.4.7. *Thermodynamic calculations in hydroxylation and the borneol cycle*

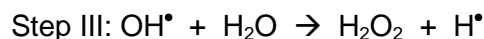
The mechanism presented in Fig. 3.7 was divided into six steps, and the contribution from each step was calculated using literature data, if available (Fig. 3.8). For the estimation of the heat of formation of borneol (see step IV below), calculations were done on the MOPAC interface of Chem 3D (v. 11), using the AM-1 method, the closed shell (restricted) wave function, the optimizer EF and water as solvent. All atoms were allowed to move freely, to a minimum RMS of 0.1. Heats of formation were estimated, using that program, for both camphor in water and borneol in water.



The reduction potential of $\text{OH}^* + \text{H}^+ + \text{e}^- \rightarrow \text{H}_2\text{O}_{(l)}$ has been estimated by Koppenol and Liebman as $\varepsilon_0 = 2.59 \pm 0.04$ V. This yields a ΔG_0 value of -250 ± 4 kJ/mol. Step I is the reverse, or 250 ± 4 kJ/mol²⁰⁸.



The properties of Cpd II-H have been estimated by Green, Dawson and Gray. Based on the one-electron reduction potential of Cpd I ($\varepsilon_0 I = 1.3 \pm 0.1$) and the pK_a of Cpd II-H, they estimated the ΔG_0 dissociation of $\text{Cpd II} \rightarrow \text{Cpd I} + \text{H}^*$ to be 98 ± 4 kcal/mol (= 410 ± 17 kJ/mol). Step II is the reverse, or -410 ± 17 kJ/mol²⁰⁹



We have estimated this as follows: From Koppenol and Liebman we know that Step I is 250 kJ/mol. The heat of formation of $\text{H}_2\text{O}_{(l)}$ is -285.8 kJ/mole.²¹² The heat of formation of H^* is listed as $+218$ kJ/mol.²¹² Therefore, based on the energy of Step I, and assuming that most of this energy comes from enthalpy contributions,⁵ we estimate the heat of formation of $\text{OH}^*_{(aq)}$ as -253.8 kJ/mol.

This value now enables us to estimate the ΔH_0 for Step III, using the listed heat of formation for H_2O_2 of -187.8 kJ/mol²¹² and this works out to be $+569.8$ kJ/mol.



For this step, we first had to estimate the heat of formation of the borneol radical. The heat of formation of camphor has been measured as $-76.3 \pm 0.6 \text{ kcal/mol} = -319 \pm 2 \text{ kJ/mol}$.²¹³ The heat of formation of borneol has not been measured, to our knowledge and, therefore, we estimated it from the heat of formation of camphor combined with semi-empirical calculations. Both, camphor and borneol were energy minimized, and their heats of formation were estimated, as described in the general section above. For camphor, we obtained “ H_f ” = $-47.89 \text{ kcal/mol} (-200.3 \text{ kJ/mol})$ and for borneol we obtained “ H_f ” = $-66.68 \text{ kcal/mol} (-278.9 \text{ kJ/mol})$. These results make sense, since camphor is a strained ketone, and this strain is somewhat relieved in borneol. Also, both compounds were energy-minimized in water, and borneol should be better solvated than camphor. The difference between these two calculated values is: “ ΔH_f ” = -78.6 kJ/mol . In our experience with that software, these estimates have errors of approximately 4 kJ/mol . Therefore, borneol should be 78.6 kJ/mol more stable than camphor, which gives us a $\Delta H_o(\text{borneol}) = \Delta H_o(\text{camphor}) - 78.6 \text{ kJ/mol} \cong -398 \pm 6 \text{ kJ/mol}$.

Now the ΔH_f of the borneol radical can be estimated from the following equation:



which is a C-H bond dissociation reaction. Detailed listings of C-H bond dissociation energies have been compiled by Blanksby and Ellison.⁵ They list primary C-H bond dissociation energies as $423 \pm 2 \text{ kJ/mol}$ and secondary C-H bond dissociation as 392 kJ/mol . We have chosen the higher value to get an upper estimate because the C-H that is α to the OH group in borneol should be more polarized than a hydrocarbon C-H and, therefore, slightly more difficult to break homolytically.

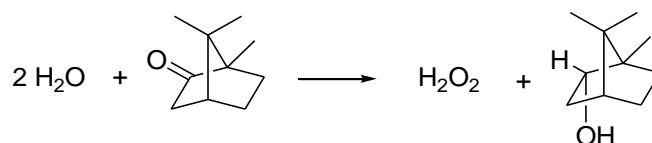
From the values for borneol ($-398 \pm 6 \text{ kJ/mol}$) and H^\bullet (218 kJ/mol) we estimate that the borneol radical has $\Delta H_o \cong -180 \pm 8 \text{ kJ/mol}$.

Now the ΔH_o of Step IV can be estimated from camphor ($-319 \pm 2 \text{ kJ/mol}$), H^\bullet (218 kJ/mol) and borneol radical ($-180 \pm 8 \text{ kJ/mol}$), and this gives $\Delta H_o = -79 \pm 10 \text{ kJ/mol}$.

Step V: is the reverse of Step II and, therefore has a $\Delta H_o \cong 410 \pm 17 \text{ kJ/mol}$, provided entropy contributions are negligible.

Step VI: This step is a C-H bond formation reaction; the C-H bond dissociation in reverse. To be consistent with our previous choice (Step III), we used -423 ± 2 kJ/mol.

Net reaction.



Overall, using all the steps of Born-Haber cycle, we obtain a net $\Delta H_o = 318 \pm 16$ kJ/mol for the borneol cycle.

The value of $\Delta H_o = H_{\text{products}} - H_{\text{reactants}} = (-187.8 + -398) - (-571.6 + -319) = 305 \pm 8$ kJ/mol.

The borneol cycle could end in two ways (Fig. 3.7 b): i) the oxidation of an enzymatic residue by Cpd I or ii) the abstraction of a H-atom from an additional water molecule by the borneol radical and the “rebinding” of the resulting OH^\bullet to the OH^\bullet bound on Cpd II-H. This would result in a second molecule of H_2O_2 . Both proposed termination reactions lead to the ferrous P450.

The involvement of OH-radicals in H₂O₂ formation has been proposed previously for electrolytic catalysts that oxidize water to O₂ (via an intermediate peroxide)¹⁹⁰ and also for a recently discovered water oxidation catalyst that produces H₂O₂ during electrolysis.^{191,192} Interestingly, the latter MnO_x catalyst stops the water oxidation process at H₂O₂, because the peroxide is solvated and stabilized by hydrogen bonding to ethylamine and/or water in the electrolyte.^{191,192} Analogously, here we propose that hydrogen bonding within the water cluster in the hydrophobic P450_{cam} active site is essential for stabilization of the various reactive intermediates and of the H₂O₂ formed. The turnover numbers with regard to H₂O₂ formation we have observed are ~ 7, whereas the electrocatalytic systems give turnover numbers of 20-1500 for complete water oxidation to O₂.¹⁹⁰ This difference arises because P450_{cam} only has access to thermal energy to perform this “uphill” reaction, whereas the electrocatalytic systems are run at overpotentials.¹⁹⁰⁻¹⁹²

The proposed mechanism accounts for our observation that borneol and hydrogen peroxide form in a 1:1 stoichiometric ratio, provided 2-electron uncoupling is negligible (Tables 3.2 and 3.4). Given that Cpd I appears to be involved in the borneol cycle, our previous¹⁹³ and current data also suggest that Cpd I might be regulated by O₂ levels: under high oxygenation, Cpd I sequentially hydroxylates camphor to **10**, or **10** to **11** (Fig. 3.1). Under poor oxygenation, Cpd I enters the borneol cycle that couples the oxidation of water to H₂O₂ to the simultaneous reduction of camphor to borneol (Fig. 3.1).

In assays with CYP3A4 (a human cytochrome P450) (section 3.3.2.4) under shunt conditions, 5-*exo*-hydroxy camphor formed as a major product. There were no detectable amounts of borneol, suggesting that the reduction cycle is specific to bacterial enzymes such as P450_{cam} (section 3.3.2.6). One possible explanation is that CYP3A4 exhibits cooperativity with certain substrates²¹⁴ and is allosterically activated with others²¹⁵. Shunting with *m*-CPBA, the enzyme produced 18.6 ± 0.6 μmol/min/μmol P450 of 5-*exo*-hydroxy camphor, but no detectable borneol. Therefore, the borneol formation reaction is not general to camphor-metabolizing cytochromes P450.

A BLAST search against the P450_{cam} sequence revealed many other bacterial cytochromes P450 that show sequence identities for the three residues that hold a set of

Figure 3.9.

Alignment of microbial cytochromes P450 against P450_{cam} (upper portion) and of vertebrate class II P450s, also against P450_{cam} (lower portion). Microbial sequences used: gamma prot 1 = marine gamma proteobacterium HTCC2207 (ZP_01225512), Novo ar CYP = Novosphingobium aromaticivorans CYP 101D2 (PDB 3NV6), Sphingo echi = Sphingomonas echinoides ATCC14820 (ZP_10341012), Novo CYP 101D1 = a camphor hydroxylase from Novosphingobium aromaticivorans DSM 12444 (PDB 3LXI), Sphing chlor = Sphingomonas chlorophenicum camphor hydroxylase (ZP_10341012), Azospir B510 = Azospirillum sp. B510 (YP_003451823), Azospir = (BAI74843), P450 Burk H160 = Burkholderia sp. H160 (ZP_03264429), P450 Burk MCO-3 Burkholderia cenocepacia MC0-3= (YP_001774494), Sping Witt R = Sphingomonas wittichii RW1 (YP_001262244), Citromicrobi = Citromicrobium bathyomarinum JL354 (ZP_06860768), Novo CYP 101 = Novosphingobium aromaticivorans DSM12444 CYP 101C1 (PDB 3OFT_C), Sping E 14820 = Sphingomonas echinoides ATCC 14820 (ZP_10339023), gamma prot 2 = marine gamma proteobacterium NOR51-B (ZP_04956740), Sphingomonas = Sphingomonas sp. KC8 (ZP_09138048), Sphing chl L = Sphingobium chlorophenicum L-1 (YP_004553185), P450 nor = Cytochrome P450nor from Fusarium oxysporum (BAA03390). Vertebrate P450s: Cyp lan deme = lanosterol 14- α demethylase isoform 1 precursor Homo sapiens (NP_000777), CYP 2C9 = human liver limonene hydroxylase (P11712), CYP 4A11 Homo sapiens (NP_000769), CYP 4F12 = fatty acyl Ω -hydroxylase Homo sapiens (NP_076433), CYP 4F2 = leukotriene-B(4) omega-hydroxylase 1 precursor Homo sapiens (NP_001073), CYP 3A5 form 1 = CYP 3A5 isoform 1 Homo sapiens (NP_000768), CYP 3A4 = CYP 3A4 isoform 1 Homo sapiens (NP_059488), CYP26B1 = retinoic acid hydroxylase Homo sapiens (NP_063938).

Superposition of P450_{cam} (1DZ4,³⁸ on CYP3A4 (1TZN,²¹⁶ reveals that the active site of CYP3A4 is much larger and more polar than that of P450_{cam}. In P450_{cam}, camphor is surrounded by closely packed hydrophobic residues, which could form a cage around the reactive intermediates. (Fig. 3.10) The only water in the active site of the camphor-bound structure is in the water channel between Glu 366 and Thr 252, whereas the CYP3A4 active site can hold numerous water molecules in the absence of a ligand (Fig. 3.10). Docking of camphor into the active site of CYP 3A4 reveals the camphor bound near the porphyrin, capped by five phenylalanine residues and surrounded by Arg 212,

Ser 119, Ile 120, Ile 301 and H-bonded to Arg 105 (Fig. 3.10). This more open arrangement may not provide the necessary stabilization for water oxidation to occur. Furthermore, the different positioning of the camphor within the active site may also preclude its utilization as an electron acceptor during the water oxidation and, therefore, the reaction was not observed in CYP3A4.

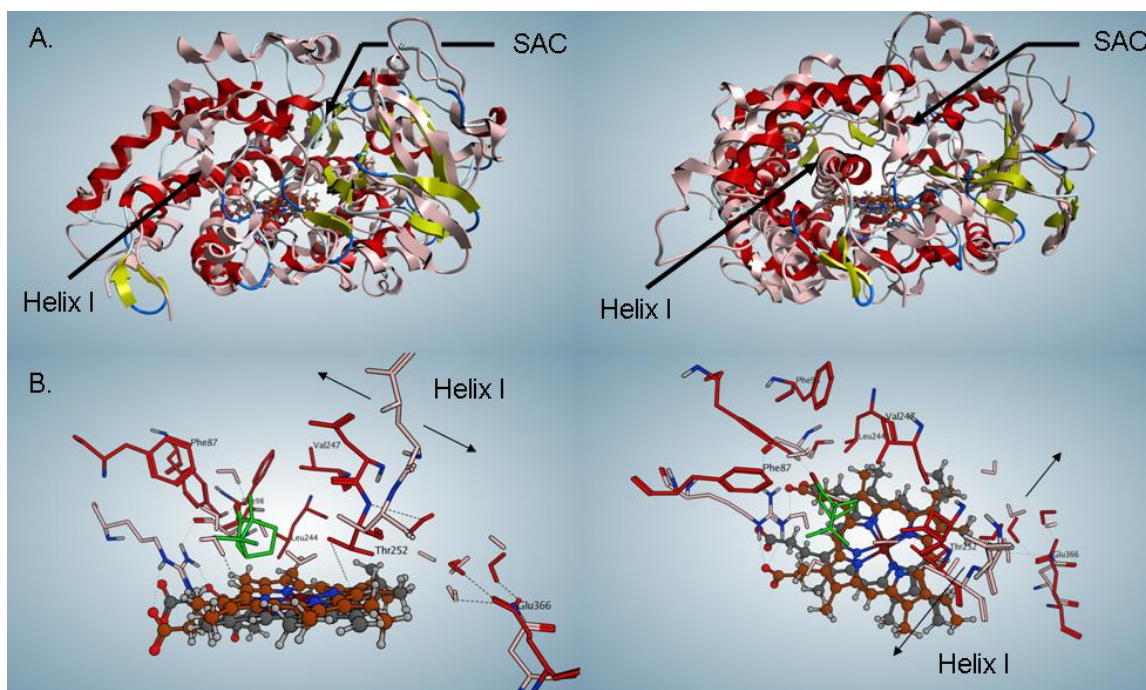


Figure 3.10 Superposition of P450_{cam} and P450 3A4. a) Top row: superimposed ribbon diagrams of P450_{cam} (1DZ4) and CYP3A4 (1TQN). P450_{cam} is shown with red helices and yellow sheets, whereas CYP3A4 is shown all in pink. The porphyrin for P450_{cam} is shown in gray and the one for CYP3A4, in brown. The two views are orthogonal to each other. The substrate access channel (SAC) is marked, as is Helix I, the central pillar of the fold. b) Lower row: superimposed active sites of P450_{cam} and CYP3A4. The porphyrin of P450_{cam} is shown in gray, the one for CYP3A4 in brown. The camphor ligand of P450_{cam} is shown in green. Residues from the two proteins are red (P450_{cam}) and pink (CYP3A4). The two views are orthogonal to each other.

Amunom *et.al.* have stated that mammalian P450s can reduce 4-hydroxynonenal to 1,4-dihydroxynonenal under low oxygen conditions,²¹⁷ similar to our results presented in this paper. However, differences in the reacting mechanisms can be associated to the

different reacting species of the P450. They proposed that the reduction occurs by the ferrous (Fe (II)) species of P450 where the electron source to the P450 is from NADPH through the NADPH-P450 reductase. We propose that the reduction of camphor to borneol involves the iron-oxo species where the source of electrons to the P450 is from a water molecule, and not from NADPH. Kaspera *et. al.* have stated that P450_{BM3} from *Bacillus megaterium* can reduce *p*-methoxy-benzaldehyde to methoxy-benzalcohol ²¹⁸. The source of electrons for this reaction is from a direct hydride transfer from NADPH or NADPH reduces the flavin mononucleotide which reduces the substrate. Studies also observed no deuterium incorporation from D₂O suggesting that there could be domain interactions in P450_{BM3} or proton transfer interactions involved in the reduction of flavins decreased in rate. In comparison to our reduction proposal, we found that our source of electrons is from water, and not from a direct hydride transfer. Lastly, Kaspera *et. al.* determined that the aldehyde reduction reaction was not reversible, whereas in our proposal the camphor reduction reaction is reversible and important to the bacteria.

3.4.8. Control experiments with reactive O₂ species/quenchers:

In vitro assays under shunt conditions were performed with a free radical quencher (BHT), a free metal chelator (EDTA), catalase and superoxide dismutase, to determine whether free reactive oxygen species are involved in borneol formation (Table 3.7). Under shunt conditions using *m*-CPBA, with poor buffer oxygenation, the enzyme formed more borneol than 5-ketocamphor (Table 3.7, entry 1). In the presence of catalase (Table 3.7, entry 2), the borneol formed was ~ 50% lower due to the decomposition of H₂O₂ to O₂. We confirmed that O₂, but not H₂O₂, had an effect in lowering borneol formation by performing experiments with O₂ scavengers (glucose/glucose oxidase) (Table 3.7, entry 3). With catalase alone, the O₂ formed by the catalase-mediated decomposition of H₂O₂ regulated the enzyme such that it produced some ketocamphor. In contrast, in the presence of catalase and glucose oxidase/glucose, the O₂ was destroyed and no ketocamphor formed. To check if superoxide plays a role in borneol formation, we performed experiments with superoxide dismutase and detected no significant effect in borneol formation (Table 3.7, entry 4). To check if the radicals proposed in the mechanism of the reduction (see below, Fig. 3.6) can diffuse out of the P450's active site, we experimented with BHT, and noticed no significant effect (Table 3.7, entry 5). This suggests that any radical species involved in

the borneol cycle do not exist long enough to diffuse out of the active site of P450_{cam}. To test if a metal impurity plays a role in our assays under shunt conditions, experiments were performed with EDTA, and we detected no effect on borneol formation (Table 3.7, entry 6). To check if free iron (outside of active site) plays a role in reduction reaction, experiments were performed with ferrous sulphate and *m*-CPBA, in the absence of P450_{cam} and we did not detect borneol or 5-ketocamphor formation (Table 3.7, entry 7). These experiments suggest that the reduction of camphor to borneol is catalysed by P450_{cam} alone, does not involve any adventitious metal species outside of the P450 active site and does not involve the diffusion of reactive oxygen species, other than the product H₂O₂, out of the active site.

Table 3.7. Tests for involvement of free reactive oxygen species: formation of borneol, 5-ketocamphor and H₂O₂.

Enzymatic assay	Products (nmol min ⁻¹ nmol ⁻¹ P450)		Borneol: 5- ketocamphor	H ₂ O ₂ formed (nmol min ⁻¹ nmol ⁻¹ P450)
	Borneol	5-keto camphor		
Ar + rP450+ <i>m</i> - CPBA ¹	443 ± 41	21 ± 2	23 ± 3	494 ± 16
Ar + rP450+ <i>m</i> - CPBA + catalase ²	246 ± 20	18 ± 1	13 ± 0.6	ND
Ar + rP450+ <i>m</i> - CPBA + glucose/glucose oxidase ³	469 ± 16	ND	N/A	ND
Ar + rP450+ <i>m</i> - CPBA + superoxide dismutase ⁴	398 ± 10	ND	N/A	428 ± 34
Ar + rP450+ <i>m</i> - CPBA + BHT ⁵	454 ± 28	25 ± 6	20 ± 4	478 ± 22
Ar + rP450+ <i>m</i> - CPBA + EDTA ⁶	438 ± 34	19 ± 6	29 ± 8	412 ± 33
Ar + FeSO ₄ + <i>m</i> - CPBA ⁷	ND	ND	N/A	ND

Values are the average of 4 replicates ± S.E. 50 mM potassium phosphate buffer (pH 7.4) was used for all the assays and was sparged with argon (99%). Camphor was the substrate in all assays. Experimental details are included in the supporting information.

ND = Not Detected; N/A = Not Applicable

¹ The assay was performed using recombinant P450_{cam} and *m*-CPBA as a shunt agent. ² The assay was performed using recombinant P450_{cam}, *m*-CPBA and catalase. ³ The assay was performed using recombinant P450_{cam}, *m*-CPBA and glucose/glucose oxidase. ⁴ The assay was performed using recombinant P450_{cam}, *m*-CPBA and superoxide dismutase. ⁵ The assay was performed using recombinant P450_{cam}, *m*-CPBA and butylated hydroxytoluene. ⁶ The assay was performed using recombinant P450_{cam}, *m*-CPBA and EDTA. ⁷ The assay was performed using *m*-CPBA and ferrous sulphate.

3.4.9. Role of oxygen in the borneol cycle

The reaction path taken by P450_{cam} (camphor oxidation vs. borneol cycle, Fig. 1b) is controlled by oxygen concentration. Oxygen could exert its effect in two ways: 1) by affecting the interaction of P450 with its redox partners, or 2) by directly interacting with P450. Our results demonstrate that the former cannot be the case, because the effect was seen in the absence of PdX and PdR (Table 3.2). Therefore, P450_{cam} must bind O₂ not only for catalysis, but also for allosteric regulation.

Recently, cytochrome P450 2E1 has been shown to form endoperoxide rearrangement products when reacted with 1,1,2,2-tetramethylcyclopropane²¹⁹. This suggests that there must be O₂ bound in that enzyme near the active site, which reacts with the rearranged radical formed by H-atom abstraction from 1,1,2,2-tetramethylcyclopropane. Cytochromes P450 are known to be allosterically regulated by their substrates or co-substrates²²⁰. Studies with other O₂-utilizing enzymes, such as diiron monooxygenases²²¹, laccase²²² and amine oxidase²²³ have revealed that O₂ can be bound in hydrophobic tunnels that are separated from the access channel for the other substrates of these enzymes. In P450_{cam}, a hydrophobic O₂ entry channel and two O₂ binding cavities have been identified in Xe-treated crystals⁸⁸. Two Xe atoms are bound near the porphyrin edge in a hydrophobic pocket lined by F163, A167, heme allyl, I220, A219, C242 and L245. The other two Xe atoms appear bound in a crevasse lined by L371, T370, L257, M261, water and S260 (first Xe) and I275, K372, T376, L375, L371, P278 and I281 (second Xe). The putative O₂ binding site in P450_{cam} is located near the edge of the porphyrin, near the water channel (Fig. 3.11).

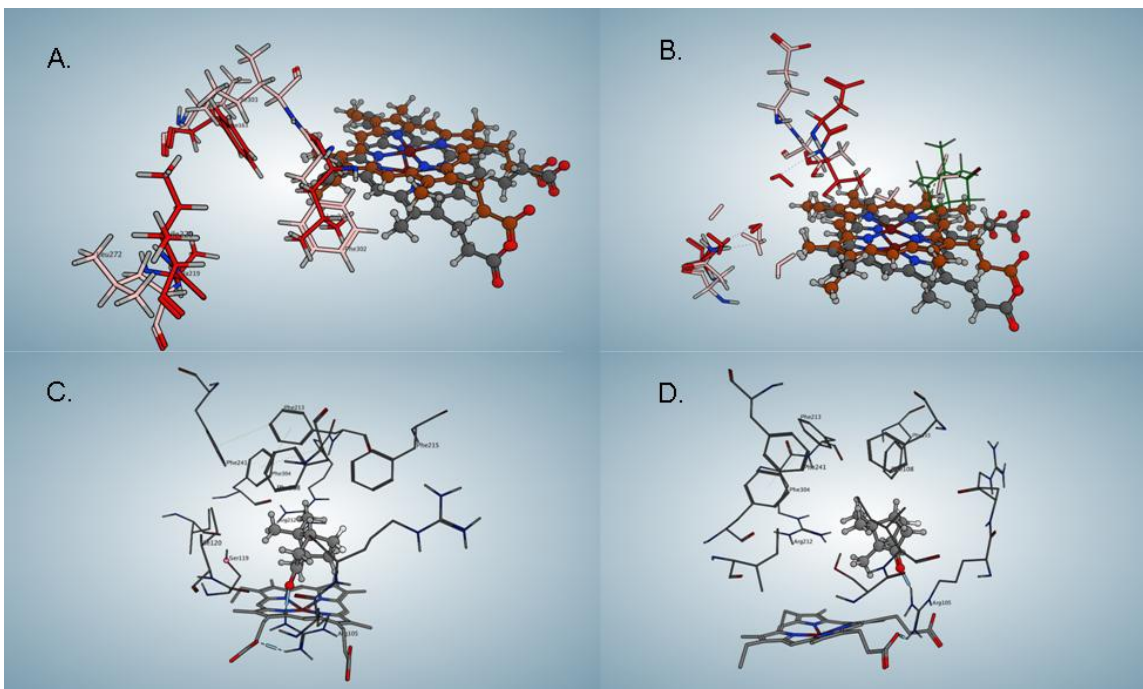


Figure 3.11. Sites in P450_{cam} and in CYP3A4 with camphor docked. A) Oxygen binding site in P450_{cam} (residues shown in red), with superimposed residues in CYP3A4 shown in pink. The porphyrin of P450_{cam} is gray, and the one for CYP3A4 is brown. B) Water channel in P450_{cam} (residues shown in red), with superimposed residues in CYP 3A4 shown in pink. The view in a) and b) are from a similar angle, to emphasize the closeness of the O₂ binding site and the water channel in P450_{cam}. C) and D) Camphor docked into the active site of CYP3A4 (orthogonal views). The H-bond from Arg 105 to the camphor ketone can be seen in the lower right portion of D).

We have found a hydrophobic tunnel in P450_{cam} that includes the Xe binding sites, using MOLEonline 2.0²²⁴ on the structure believed to represent the P450_{cam} oxo complex (1DZ9). The binding sites are good candidates for O₂ binding because they are hydrophobic and distinct from the substrate access route.^{80,88} Also, the sites are good candidates for allosteric regulation of P450 because they are near the plane of the porphyrin. It is plausible that an O₂ molecule bound near the heme could affect the reactivity of Cpd I.

The O₂ binding site in P450_{cam} is closer to the porphyrin than the equivalent site in CYP3A4, and the O₂ binding site is lined by different residues (Fig. 3.11). Furthermore, the O₂ binding site in P450_{cam} is close to the water channel, the only

source of water in the camphor-filled active site of P450_{cam}. It is reasonable to hypothesize that the O₂ site, the porphyrin, the water channel and the tightly held camphor, all of which are near each other, could affect each other by allosteric effects in P450_{cam}.

There are two ways the cycle could end. Cpd I might oxidize a nearby enzymatic residue or, alternatively, the borneol radical might abstract a H-atom from water, giving borneol and OH[•], and the hydroxyl radical could rebind with the OH[•] bound in Cpd II-H, to give a second H₂O₂ and the ferric enzyme (Fig. 3.8b).

3.4.10. Toxicity assays of borneol, hydrogen peroxide with *E. coli* and *P. putida*

Previously we have determined the effect of borneol and camphor on the growth of *P. putida* and *E. coli*.¹⁹³ To determine the effects of hydrogen peroxide, we have tested the toxicity of H₂O₂ and a 1:1 stoichiometric mixture of borneol and H₂O₂ on both *P. putida* and *E. coli*, a bacterium that lacks cytochrome P450¹⁷⁸ (Figs. 3.12 and 3.13). The borneol/H₂O₂ mixture was lethal to *E. coli* and slightly toxic to *P. putida* (Figs. 3.12 and 3.13). The latter observation prompted us to explore whether borneol affects the expression of the P450_{cam} system. The IC₅₀ of hydrogen peroxide and of a 1:1 mixture of borneol and hydrogen peroxide were determined for *E. coli* as described in chapter 2 by graphing CFU/ml vs. the logarithm of concentration of compounds (section 2.3.8) and found to be 7 nM and 17 nM, respectively whereas H₂O₂ was found to be less toxic to *P. putida* (IC₅₀ was found to be 48 nM (Fig. 3.12)). In comparison, the IC₅₀ of borneol alone was 19.3 nM for *E. coli*.¹⁹³

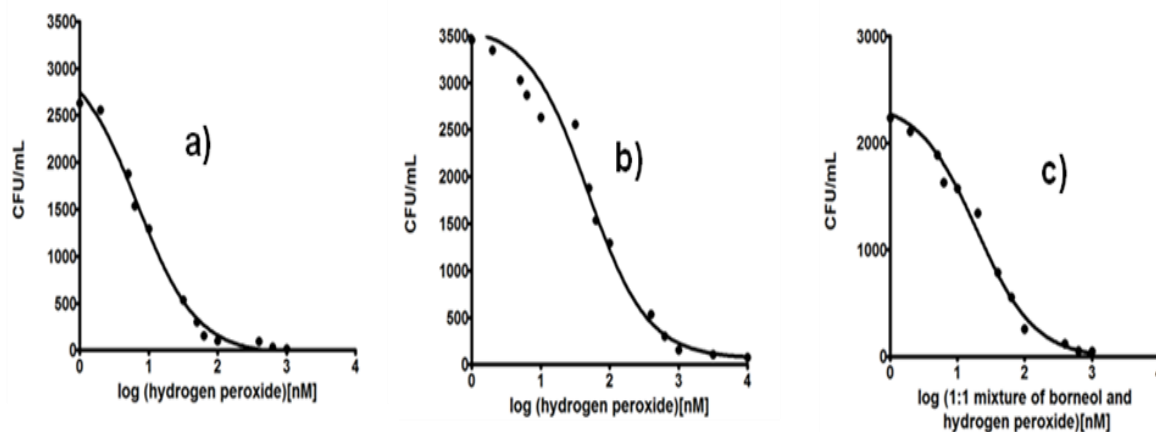


Figure 3.12. IC₅₀ determination of a) H₂O₂ and b) of a 1:1 (molar) mixture of borneol and H₂O₂ against *E. coli*, a species of bacterium that lacks cytochrome P450.

The effect of borneol:H₂O₂ (1:1 molar ratio), borneol, or H₂O₂ on the survival of *P. putida* (strain ATCC 17453) and *E. coli* (strain XL-1 BL) with the stationary cultures of these two strains was performed in the same way as described previously¹⁹³.

The mean cell densities of *E. coli* and *P. putida* stationary cultures that had been incubated with borneol, H₂O₂ or a 1:1 mixture of borneol and H₂O₂ for 16 h, revealed a significant effect of treatment (ANOVA for *P. putida*, $P < 0.0001$; $F = 8.93$ and for *E. coli*, $P < 0.0001$; $F = 12.07$). Turkey-Kramer pairwise comparisons of borneol, hydrogen peroxide, 1:1 mixture of borneol + hydrogen peroxide, and the control (dimethyl sulphoxide, DMSO) for each bacterial species revealed that hydrogen peroxide or the 1:1 mixture of borneol + hydrogen peroxide are bacteriostatic to *P. putida* (DMSO/hydrogen peroxide: $P < 0.01$; DMSO/borneol: $P < 0.01$; DMSO/borneol + hydrogen peroxide: $P < 0.01$). In contrast, borneol, hydrogen peroxide and the 1:1 mixture were highly toxic (DMSO/hydrogen peroxide: $P < 0.01$; DMSO/borneol: $P < 0.01$; DMSO/borneol + hydrogen peroxide: $P < 0.01$) to *E. coli* (no colonies were observed, Fig. 3.13). This difference in the toxicity of the borneol cycle products on the producer, compared to a bacterial species that lacks P450, may be an adaptive advantage for *P. putida* during times of low aeration, when camphor resources cannot be metabolized but borneol has been produced.

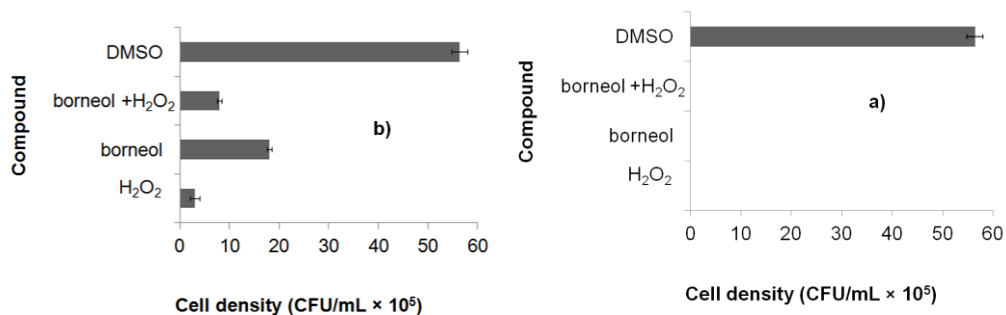


Figure 3.13. Effect of 16 h incubation of stationary *E. coli* (a) and *P. putida* (b) cultures with borneol: H₂O₂ (1:1), borneol, or H₂O₂ (1 mM).

3.4.11. Adaptive advantage of the borneol cycle to *P. putida*

The camphor metabolism pathway, of which P450_{cam} catalyzes the first step, is encoded on the CAM plasmid under the control of the Cam repressor. This repressor dissociates from the upstream control region of the Cam operon upon binding of camphor, ensuring that the entire operon is expressed when camphor is present.¹⁸²

We detected a steep increase in the characteristic absorption bands of P450_{cam}, PdR, and PdX only in the culture induced with camphor, about 80 min after initial induction with camphor. Absorptions plummeted approximately 60 min after the addition of borneol to camphor-induced culture(s) (Fig. 3.14). This decrease in P450, PdR, and PdX expression must be due to the borneol addition, because the camphor-induced cultures that did not receive borneol expressed significantly higher levels of P450, PdR and PdX/CFU/mL than the borneol-treated cultures (Figs. 3.14, 3.15 and 3.16)

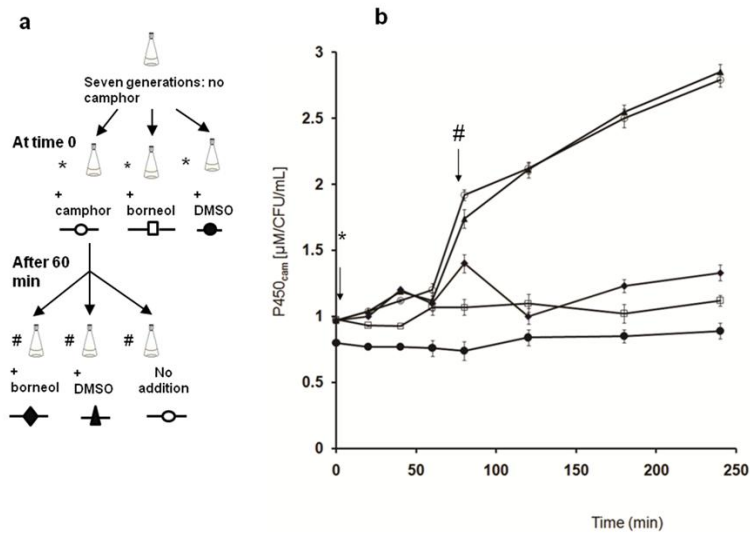


Figure 3.14. a) Outline of the experiment used to determine the effect of camphor and borneol on P450_{cam}, PdX and PdR expression. b) The effect of camphor, borneol and DMSO on the P450 expression by *P. putida* (ATCC 17453). The concentration of P450_{cam} was obtained from the Soret peak absorbances and was normalized against the number of colony forming units/mL. The absorbances at 392 nm and 410 nm correspond to the substrate containing and free P450_{cam} Soret band. Points represent the average \pm S. E. of three replicates.

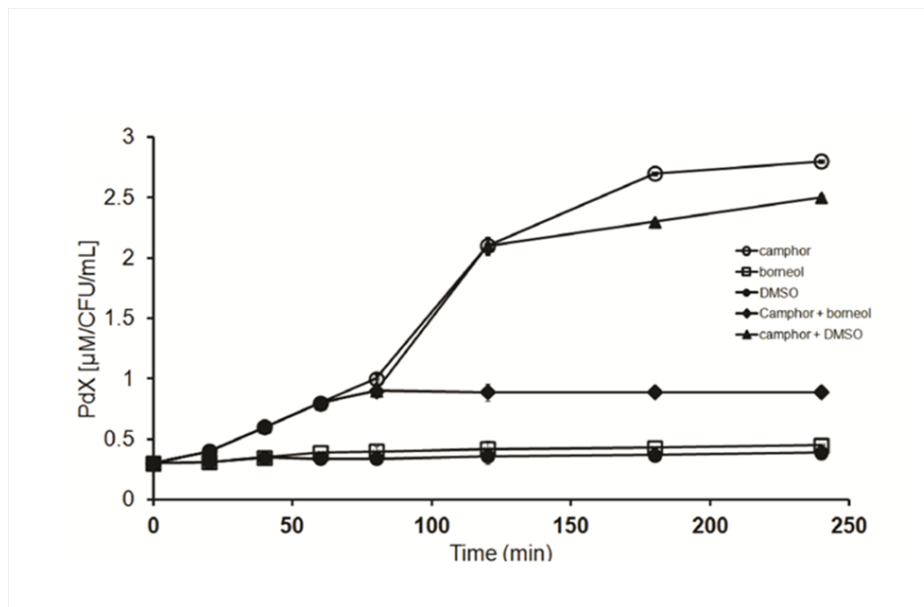


Figure 3.15. *The effect of camphor, borneol and DMSO on the PdX expression by Pseudomonas putida (ATCC 17453). The concentration of PdX was obtained from the absorbance at 325 nm that corresponds to the Fe₂S₂ cluster of PdX and was normalized against the number of colony forming units/mL. Points represent the average ± S. E. of three replicates.*

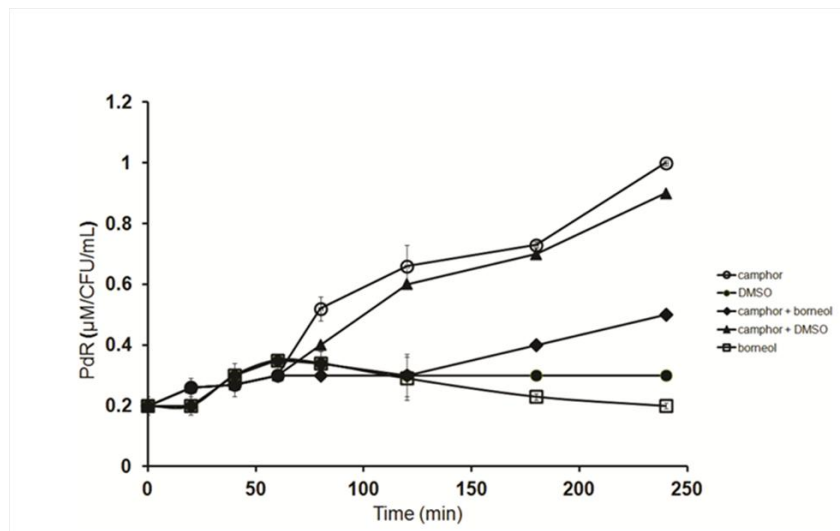


Figure 3.16. The effect of camphor, borneol and DMSO on the PdR expression by *Pseudomonas putida* (ATCC 17453). The concentration of PdR was obtained from the absorbance at 454 nm that corresponds to the flavin moiety of PdR and was normalized against the number of colony forming units/mL. Points represent the average \pm S. E. of three replicates.

Using Graphpad prism software, the Kruskal-Wallis test was chosen to compare the effects of 5 groups (camphor, borneol, DMSO, camphor + borneol, camphor + DMSO). The effect of camphor was significant on the expression of P450_{cam} after 80 minutes ($P < 0.01$). The DMSO treatments differed significantly at each time point after induction from the camphor-induced treatments ($P < 0.01$).

ANOVA (Tukey-Kramer test) was performed within each time series of the three replicates for each treatment. Camphor showed a significant effect of increasing the P450 expression ($P < 0.01$), 80 min after its addition to the culture (marked * in Fig. 3.14). The addition of DMSO to the camphor-induced cultures did not have any effect ($P > 0.01$ within the DMSO series). The addition of borneol to the camphor-induced culture showed a significant decrease in expression 80 minutes after its addition to the camphor-induced culture (marked # in Fig. 3.13) ($P < 0.01$). In the borneol and camphor-treated cultures, the normalized P450_{cam} levels 120 min. after borneol addition were

close to the background expression at 0 minutes (Fig. 3.14). The results for PdX and PdR are shown below in Figures 3.15 and 3.16.

The borneol down-regulation of P450_{cam}, PdX, and PdR might be advantageous to *P. putida* during periods of low soil aeration. Because the camphor degradation pathway requires four O₂/camphor (to reach 5-hydroxy-3,4,4-trimethyl-2-heptenedioic acid- δ -lactone), and the P450_{cam}-catalyzed oxidation is the first committed step²²⁵, it is advantageous to regulate camphor metabolism at the first step. When aeration increases, low levels of P450_{cam} convert borneol back to camphor¹⁹³, and this frees the Cam operon from borneol down-regulation.

3.5. Conclusions of this chapter

We describe the borneol cycle of P450_{cam}, a cycle that occurs at low O₂ concentration. The cycle connects to the known catalytic cycle *via* Cpd I which is regulated by O₂ levels: at low O₂ concentration, Cpd I oxidises water, whereas at high O₂ concentration, Cpd I oxidises camphor.

The Cpd I-catalyzed reaction of P450_{cam} proposed here (Fig. 3.6) is independent of the redox partner proteins (PdX and PdR) and of how Cpd I forms (O₂ reduction or shunt). The reaction occurs both *in vitro* (this paper) and *in vivo*¹⁹³. We show here that P450_{cam} couples the oxidation of water to H₂O₂ and the reduction of camphor to borneol. We have presented evidence that: i) water is the source of the 2-H in the borneol; ii) water is oxidized to form H₂O₂ when camphor is reduced; and iii) the transfer of an H atom from water to C-2 of camphor occurs at a rate-limiting step in the borneol cycle and involves tunneling. We propose that the reactivity of Cpd I is regulated by O₂ concentration, and we have located a potential access channel where O₂ might bind to P450_{cam} to exert its allosteric control.

The borneol and H₂O₂ formed serve several ecological functions. First, borneol and H₂O₂ are not very toxic to *P. putida*, whereas the combination is lethal to bacteria such as *E. coli* which do not contain any P450¹⁹³, and this may give *P. putida* an advantage in bacterial communities. Secondly camphor induces the expression of P450, PdX, and PdR, whereas borneol decreases the expression of these gene products in *P.*

putida. These features of the P450_{cam} may protect the bacteria from excessive exposure to borneol and reactive oxygen species during prolonged periods of low oxygen concentration.

4. Screening of Cytochrome P450_{cam} SeSaM library with 3-chloroindole as the substrate to identify the dehalogenated metabolites of Endosulfan

4.1. Introduction

Endosulfan is a hexachlorinated cyclodiene pesticide used extensively in horticulture.²²⁶ Due to its high toxicity, it has been banned in most countries around the world.²²⁷ Nonetheless, it is still being used in India on rice, oilseeds and pulses as of 2013.²²⁸ Endosulfan exists as a pair of isomers, α and β , in the ratio of 7:3.²²⁹ (1, Fig. 4.1) It has been termed a “priority pollutant,” because its half-life in the soil is 4-6 months.^{230,231} in comparison to low-persistent pollutants, malathion and carbaryl, with half-lives of 5-8 days.^{232,233} The reason endosulfan is so persistent is that it is difficult to biodegrade.²³⁴

Biodegradation of endosulfan begins with the oxidation of the sulfite to the sulfate (Fig. 4.1, 2). The sulfate can be either singly or doubly hydrolyzed, yielding endosulfan diol (3) or the monosulfate (4). The monosulfate can cyclise to give ether (5). The diol (3) can be either singly or doubly oxidized to yield the mono- or dialdehyde (6 and 7, respectively). Monoaldehyde (6) can form hemiacetal (8), and this can be oxidized further to lactone (9). The diol, dialdehyde and lactone are less toxic to aquatic organisms²³⁵ than endosulfan. However, the sulfate is more toxic than endosulfan in all toxicity studies.^{235, 236} The biodegradation process has been studied with fungi (*Asperigillus niger*, *Cladosporium oxysporum*),²³⁷ enriched microorganisms (*Ochrobacterum sp.*, *Arthrobacter sp.*, *Bulkholderia sp.*),²³⁸ soil bacteria, mixed microbial cultures,²³⁹ enzymes (e.g. *Mycobacterium tuberculosis* ESD)²⁴⁰ by using endosulfan as an only sulfur source or carbon source for microbes, and endosulfan diol was detected as the major product.^{241,242}

It is important to note that all of the metabolites reported so far (1-9, Fig. 4.1) still have the hexachlorinated bicyclic nucleus of the original pesticide intact. The degradation of endosulfan with less than normal or no accumulation of the toxic sulfate,

has been targeted before,²⁴³ but the enzymatic degradation of the chlorinated end of endosulfan has not been accomplished according to our knowledge. Cytochrome P450s catalyse the oxidation of hydrocarbons, among many other reactions.²⁴⁴ The wild-type P450_{cam} (CYP101A1) hydroxylates camphor at the 5th position to form 5-exo-hydroxy camphor and 5-ketocamphor.¹⁶⁴ The crystal structure of P450_{cam} with camphor bound has revealed that camphor is bound with the 5-exo C-H bond poised very precisely above the iron porphyrin.^{80,1,38} We tested wild type P450_{cam} with endosulfan, because of the structural resemblance, but found that only compounds (**2**, **3**, **6**, **7** and **9**) were formed (see below), suggesting that P450_{cam} can accommodate endosulfan in its active site but does not position the polychlorinated end above the porphyrin, which is a necessary requisite for oxidation. We therefore hypothesized that mutating the active site of P450_{cam} could lead to correct positioning of endosulfan for oxidation at the chlorinated end.

Mutagenesis studies of P450_{cam} have been reported for various substrates (section 1.6). For example, mutating Y96, a residue that hydrogen bonds to camphor and thereby positions it, resulted in mutants that accept substrates such as alkanes,^{106,107} α -pinene,²⁴⁵ polychlorinated benzenes,¹²⁴ diphenylmethane.¹⁰⁵ In general, replacement of F87, Y96 and V247 residues in P450_{cam} (with W, F and L) has been found to be important for the degradation of chlorinated substrates, though the activity decreases with the number of chlorinated substituents. For example, the mutant F87W/Y96F/T101A/L244A/V247L can oxidise pentachlorobenzene to pentachlorophenol more effectively than the WT.¹¹⁹ Chlorinated cyclodienes are not among the substrates oxidized by cytochrome P450_{cam} mutants that have been reported.

We targeted to mutate the active site of P450_{cam} to dehalogenate the hexachlorinated end of endosulfan, the diol or the dialdehyde. There are two approaches to altering the substrate selectivity of an enzyme: 1) targeted alteration based on structural models of the enzyme¹⁰⁷ or 2) directed evolution.²⁴⁶ Directed evolution is a strategy to alter the properties of a protein by multiple random mutation of the corresponding gene, followed by a selection. In general, a directed evolution approach is comprised of three steps:²⁴⁷ a) random mutagenesis of the gene,²⁴⁸ b) amplification of the mutated library and c) screening for the variants.

For random mutagenesis of the gene, there are 3 options: 1) error-prone PCR,²⁴⁹ 2) multi-template PCR²⁵⁰ and 3) Sequence Saturation Mutagenesis (SeSaM).^{251,252,253,254} We chose SeSaM because it can achieve up to 16.7% of consecutive nucleotide exchanges which is remarkable (as opposed to recurring isolated mutations (hot-spots) obtained with the first two methods).²⁵⁵ The challenge with large libraries of mutants is the identification of mutants with the desired activity. Various selection/screening methods have been reported for large libraries of mutants. The colorimetric/fluorimetric assays, in which the product, styrene oxide is converted to a colored or a fluorescent dye, by reaction with gamma-(4-nitrobenzyl)pyridine (NBP), is an easy method of detection, reported with cytochrome P450 BM-3 variant 139-3.²⁵⁶ One limitation of this assay is that the colorimetric agent (for e. g., hydrazines used for ketone detection) may be inhibitory to P450 reactivity. In a different selection method (survival screen), bacteria that are expressing the enzyme are selected on media that contains the substrate of interest. The selection process can be improved in this case if the given substrate is toxic to bacteria and the metabolites of the substrate are less toxic than the substrate itself. But this process is not useful if the substrate is bactericidal to bacteria or the product(s) formed is (are) more toxic than the substrate itself, which can result in no growth of bacteria.

In this work, we used two approaches to screen the SeSaM library for endosulfan dehalogenation: 1) a combination of both pre-selection and colorimetric assays to find P450 mutants from the SeSaM library that can dechlorinate 3-chloroindole and 2) a survival screen with endosulfan itself. We chose 3-chloroindole because indole has been reported to be hydroxylated by P450s at the 3rd position to form the colored dyes, isatin and indigo.²⁵⁷ In our case, formation of isatin and indigo from 3-chloroindole was evidence of dehalogenation of substrate. We hypothesized that some active clones from the 3-chloroindole screen would also dehalogenate endosulfan. In addition to this, the library was also screened on minimal media with endosulfan as the only carbon source. In this case, the transformants that harboured an endosulfan-degrading P450_{cam} mutant grew. The library preparation, screening and identification of the active variants for endosulfan degradation are described in the following sections of this chapter.

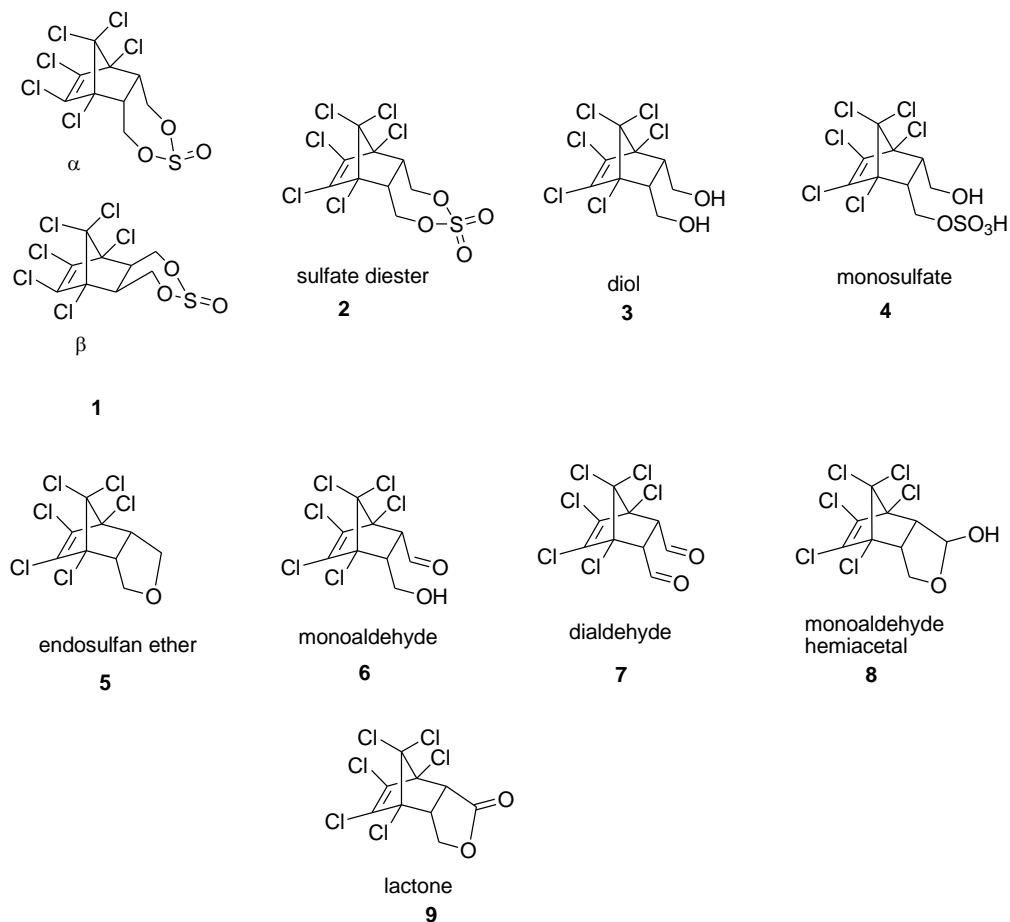


Figure 4.1. Endosulfan and its metabolites reported in the literature.

4.2. Materials and Methods

4.2.1. Experimental

The chemicals were of analytical grade and purchased from Sigma-Aldrich Chemie (Taufkirchen Germany), Applichem (Darmstadt, Germany) or Carl Roth (Karlsruhe, Germany). The nucleotide analog dPTP was purchased from Jena Biosciences (Jena, Germany) and dPTP α S and dGTP α S were generously provided by

Biolog Life Science Institute (Bremen, Germany). All other nucleotides were purchased from Fermentas (St. Leon-Rot, Germany). Taq DNA-Polymerase was obtained from Qiagen (Hilden, Germany). All other DNA-polymerases, the terminal deoxynucleotidyltransferase (TdT) were obtained from New England Biolabs (Frankfurt, Germany). DNA was quantified using a NanoDrop photometer (NanoDrop Technologies, Wilmington, DE, USA). The PCR reactions were performed in 0.2 ml thin-walled PCR tubes from Sarstedt (Nuembrecht, Germany) using a Mastercycler gradient PCR-machine from Eppendorf (Hamburg, Germany). Volumes higher than 50 μ l were distributed in multiple tubes. *m*-Chloro perbenzoic acid (*m*-CPBA) was purchased from Sigma-Aldrich and purified by reported methods.¹⁷⁶ Centrifugations were carried out with a Beckmann Avanti J-26 XPI centrifuge (Mississauga, ON, Canada), equipped with a JLA 8.1000 rotor.

The ³⁵Cl NMR spectra were run on a Bruker AVANCE III 500 MHz NMR spectrometer (operating at 67.808 MHz) equipped with a Bruker 5 mm TBO probe and samples were maintained at a temperature of 298 K. Samples were contained in 5 mm diameter nmr tubes filled to 50 mm (volume ca. 600 μ L). Acquisition time was 12 min per spectrum or 300 min (when catalase was present). The chemical shifts (δ) for all compounds are listed in parts per million using 10 mM NaCl in D₂O as an internal reference. The ¹⁷O NMR spectra were run in the same way as described in the section 3.3.1.2

4.2.2. SeSaM methodology

To explore the complete protein sequence, Schwaneberg *et.al.* have developed a novel technique called Sequence Saturation Mutagenesis (SeSaM). SeSaM is an economical random mutagenesis method which can be accomplished in 2-3 days to generate a mutant library. SeSaM is comprised of 4 steps (Supplementary figure S1). 1) a pool of DNA fragments with random lengths is generated, 2) a universal base is added at the 3' termini of the DNA fragments, using Deoxynucleotidyl terminal transferase (TdT). 3) Elongation of the DNA fragments to the full length genes and, finally, 4) Replacement of the universal bases by the standard nucleotides (Details are in the Supporting information and SeSaM library validation shown in table S1).

4.2.3. Cloning of SeSaM libraries

Restriction sites (*EcoR1* and *Hind III*) were incorporated in the mutant libraries of the step 4 reactions by PCR, for cloning the libraries into the pALXtreme-1a vector (an inhouse pET (+28a) vector) (Supplementary figure S2). The ligation mix was transformed in chemically competent DH5 α cells and plated on LB-agar/kanamycin plates.²⁵⁸ Thirty colonies from the transformation reaction were picked randomly and checked by high-throughput PCR. The PCR products were run on 0.8% agarose gel to check the presence of inserts, and it was observed that only one clone contained the insert (1.5 kb), prompting us to use a different library cloning strategy. The culture of the positive clone (1 μ l) was inoculated into 2 mL of TYM 505/Kan medium, grown overnight at 37 °C and the plasmid was isolated using the Nucleospin plasmid kit (Macherey-Nagel, Dueren, Germany). Taking this whole plasmid as a template, the P450_{cam} SeSaM library acted as a megaprimer in a PCR, described as MEGAWHOP.²⁵⁹ The PCR products were digested by *DpnI*, to eliminate the methylated template plasmid. To check *DpnI* digestion efficiency, a 50 μ l PCR reaction mixture (containing the megaprimer, template plasmid, dNTPS, PfuI enzyme and buffer) was taken as a control and digested with 10U of *DpnI* overnight. Colonies were not observed on this control plate which suggested that the MEGAWHOP and the *DpnI* digestion processes worked efficiently. Twelve clones each from the library were checked (Supplementary figure S3) for the presence of the insert (by culture and PCR), and the positive clones were grown in LB/kan medium overnight. The isolated plasmids from these clones were sequenced at Eurofins MWG Operon, Germany. The SeSaM library was checked with the sequenced clones (table S1) and glycerol stocks of the library were made for further experiments with endosulfan.

4.2.4. Preparation of 3-chloroindole

The 3-chloroindole was prepared from indole (Sigma Aldrich, CAS # 120-72-9) in two steps as reported previously.²⁶⁰

N-chloro indole. To 0.585 g (1 mmol) of indole, 500 mL of *n*-pentane, 125 mL of sodium hypochlorite and 125 mL of water were added and stirred at 0 °C for 3 h. The organic layer was separated and the aqueous layer was extracted with an additional 100

mL of *n*-pentane. The combined organic layer(s) were dried over K₂CO₃. Pentane was distilled under vacuum and the oily residue was stored at 4 °C.

3-chloro indole. To the oily residue in a 2 L flask, 500 mL of *n*-butanol and 7.5 g of K₂CO₃ were added, and the reaction was refluxed for 2 h. The alcohol was removed under reduced pressure and to this, 200 mL of water and 200 mL of CHCl₃ were added. The layers were separated and the chloroform layer was dried over K₂CO₃ and distilled under vacuum. The oily residue was purified by column chromatography using chloroform as the solvent and the isolated product (70.1 mg, yield 70%) was characterized by NMR. ¹H NMR analysis (chemical shift in δ): 8.08 (NH proton), 7.03-7.73 (m, 5H, C(2)H and aromatic H). Alternatively, ~ 50 mg of the oily residue was purified by preparative TLC using chloroform as the developing solvent and monitored under U.V. The 3-chloroindole band was cut out and dissolved in ethyl acetate for ~45 minutes. Silica was filtered under gravity and the solvent was evaporated under vacuum to give 3-chloroindole (5 mg).

4.2.5. IC₅₀ experiments with 3-chloroindole and endosulfan

Overnight grown culture of BL21 cells acted as an inoculum for 20 mL of LB medium (with no antibiotics). The culture was grown at 37 °C for an hour until the O.D. was 0.1. The culture was then diluted 1000x and to 3 mL of this diluted culture, 3-chloroindole or endosulfan was added in varying concentrations (from 5 μM to 300 μM for 3-chloroindole and from 70 nM to 300 μM for endosulfan). This step was performed in 3 replicates. The cultures with the mentioned compounds were grown at 37 °C for an hour and kept at 4 °C overnight. An aliquot (20 μL) of each replicate was plated on LB-agar/non-antibiotic plates the next day and incubated overnight at 37 °C. The next day, colonies were counted, and IC₅₀ values were obtained using Graphpad prism software. Subsequent screening protocols were conducted at 2x IC₅₀ values for 3-chloroindole and IC₉₀ values for endosulfan.

4.2.6. Screening of 3-chloroindole with the SeSaM library using additives

The MEGAWHOP products (libraries and the wild type P450_{cam}) and the empty vector (pALXtreme-1a) (2 μl) were transformed in BL21-(DE3), plated on LB-agar

(kanamycin) plates supplemented with IPTG (80 μ M), 3-chloroindole (12 μ M), δ -amino levulinic acid (1 mM), vitamin B₁ (10 μ M), FeCl₂ (0.1 μ M) and *m*-chloro perbenzoic acid (*m*-CPBA, 0.3 μ M). The *m*-CPBA allows the cytochrome to form the Fe-oxo form (Compound I), without reducing O₂. This is known as the peroxide shunt.¹³⁷ Plates were incubated overnight at 37 °C. The active clones were identified by the blue colour (indigo) or orange colour (isatin) and the plasmids were isolated from colored colonies, to check for the presence of the inserts. Sequencing of the isolated plasmids was performed at Macrogen, Korea.

4.2.7. Protein expression with the selected clone(s):

The clone(s) with the P450_{cam} insert was/were grown individually in 2 mL LB/Kan at 37 °C overnight with good aeration and the culture(s) were harvested at 10,000 rpm for a minute at RT the next day. To the pellet, 2 mL of fresh LB/Kan medium was added and grown for 2-3 h at 37 °C. Supplements, IPTG (80 μ M), 5-amino levulinic acid (1 mM), vitamin B₁ (10 μ M), FeCl₂ (0.1 μ M) were added and the protein expression was carried forward at 27 °C for 16h. The lysis and the protein purification steps were performed as described in section 3.3.1.3.

In addition, a 12 L culture of the desired clone was grown and the protein expression, lysis and the purification steps were performed as described in section 3.3.1.3 and the purified protein was used for the *in vitro* assays and steady-state kinetics.

4.2.8. In vitro assays with the mutated and the wild type P450_{cam} proteins

Enzymatic assays were performed with the P450_{cam} mutant(s) (180 nM), 1 mM endosulfan/3-chloroindole, 1 mM *m*-CPBA in 1 mL phosphate buffer (K⁺) (pH 7.4) and three controls (in the absence of the substrate, shunt agent or the enzyme) were run in parallel and the reaction mixtures incubated for 15 minutes at RT. Extraction was performed with CHCl₃/indanone (7.2 μ M, internal standard),¹⁶⁴ the extract was dried with MgSO₄ and the presence of the metabolites was checked by GC-MS. Metabolites formed were compared to their respective standards.

4.2.9. Determination of Cl and H₂O₂ in the enzymatic assays by ³⁵Cl and ¹⁷O NMR:

Enzymatic assays were performed in 1 mL 50 mM phosphate buffer (made from D₂O) of pD 7.4. The pH of the buffer was adjusted according to the equation: pD = pH meter reading + 0.4.¹⁹⁹ The reaction mixture contained endosulfan diol (200 μM), P450_{cam} (180 nM) and *m*-CPBA (200 nM). Reactions were incubated at 22 °C for 15 minutes. Controls (in the absence of shunt or the enzyme or the substrate) were run simultaneously and the ³⁵Cl spectra were run as mentioned in the methods section. For ¹⁷O NMR studies, the reaction mixture was prepared as described in section 3.4.2.2.

4.2.10. Steady-state kinetic assays for indole and 3-chloroindole hydroxylation with the P450_{cam} mutant(s):

Steady state kinetic assays were performed in 1 mL phosphate buffer (50 mM, 150 mM K⁺), pH 7.4 with varying amounts of 3-chloroindole (substrate concentrations varied from 20 μM to 1 mM), 1 mM *m*-CPBA, 180 nM mutant P450_{cam} and the reaction mixtures were monitored for 15 minutes at 246 nm for the formation of isatin. The concentrations of the product, isatin were estimated using the extinction coefficient (2.3 mM⁻¹ cm⁻¹) as reported previously.²⁶¹ The determinations of V_{max}, K_M were done using nonlinear regression with Graphpad Prism software. HPLC analysis was performed by a reversed-phase C₁₈ HPLC column using an isocratic solution of ACN:H₂O (70:30). The flow rate was 1 mL/min and λ_{max} was set to 247 nm for the separation of isatin and 3-chloroindole.

4.2.11. Determination of Fe-CO absorbance at 450 nm

To 1 mL phosphate buffer (50 mM, 150 mM K⁺, pH 7.4), mutant P450_{cam} (180 nM), dithionite (1 mM) added, and to this reduced enzyme, carbon monoxide (99% pure, SIGMA) was bubbled for 2 minutes (Supplementary figure S4).

4.2.12. MOE simulations

Docking simulations were performed using Molecular Operating Environment (MOE, Chemical Computing Group, Montreal, Canada). Crystal structure information of P450_{cam} (CYP101A1) was obtained from Protein Data Bank and substrate bound

P450_{cam} with PDB code 2ZWU⁸⁷ was used for the docking studies [with the ferric form of the enzyme]. The protein was imported into MOE as a PDB structure, each residue protonated at pH 7, 300 K and 0.1 M salt and the charges were assigned according to the default settings under “Compute|Protonate 3D”. Ligands (3-chloroindole and endosulfan) were constructed in MOE using “builder” and imported into the MOE database as “.mdb” files. Prior to docking, camphor was deleted and potential docking sites were identified on the protein (by setting “all atoms” (protein + heme) as the receptor) using the option “site finder”. Dummy atoms were placed at each site targeted for docking and these dummy atoms were markers used by the docking algorithm. Ligands were docked using an induced fit protocol and all atoms of the P450 polypeptide and the porphyrin chosen as the receptor. Triangle matcher was used for placement, rescored by London dG, forcefield for refinement, rescored using GBVI/WSA dG; a maximum of 30 poses were retained. Of the retained poses, the one with the reactive centre (the 2-3 bond in 3-chloroindole and C=C bond in endosulfan) closest to Fe (an arbitrary distance of 5 Å fixed) was selected for further studies.

4.2.13. Screening of the SeSaM library with endosulfan as the substrate

The SeSaM library glycerol stock (10 µL) was inoculated into 3 mL LB/kan medium and grown overnight at 37 °C. The culture was diluted 10⁶ × with LB medium and 20 µL was plated on minimal media plates/kanamycin (with no carbon source). To the treatment plates, the measured IC₉₀ concentration of endosulfan (250 µM), *m*-CPBA (0.3 µM), δ-amino-levulinic acid (1 mM), FeCl₂ (0.1 µM), Vitamin B₁ (10 µM), IPTG (100 µM) were added and three controls (in the absence of substrate/IPTG/shunt (*m*-CPBA)) were maintained for the experiment. The experiment was performed in 3 replicates and the plates were incubated at 27 °C overnight. Plasmids isolated from the clones were checked for the presence of P450_{cam} insert using PCR (Terra PCR direct polymerase mix, Clontech laboratories, CA). Sequencing was performed at Macrogen, Korea.

4.2.14. Transformation of the selected mutant in *P. putida* (ATCC 17453)²⁶²

The mutant that most actively catalyzed 3-chloroindole oxidation was transformed into *P. putida* (ATCC 17453), the strain that harbors the CAM plasmid. This

CAM plasmid encodes the early steps of the camphor degradation pathway, and includes the two redox partners of the wild-type P450_{cam}.^{4,38,103} As a control, wild-type P450_{cam} in the same *pET* vector was also transformed into *P. putida*. The ATCC 17453 strain was grown overnight in LB medium at 27 °C at 250 rpm. 500 µL of this culture acted as an inoculum for 10 mL fresh broth and grown for 3-4 h until the cell density was 10⁹/mL. The cells were kept on ice for 20 minutes, harvested and resuspended in 1/10 volume of CaCl₂. Plasmid DNA (3 µL) isolated from the previous step was added and the cell/DNA mixture was incubated at 4 °C for 60 minutes and subjected to a heat pulse at 42 °C for 2 min, diluted 10x with LB medium and incubated at 30 °C for an hour. The culture was harvested and the pellet was resuspended in 50 µL LB medium, plated on LB/kan plates and grown overnight at 30 °C. The clones obtained were checked for the presence of P450 insert using PCR (Terra PCR direct polymerase mix, Clontech laboratories, CA).

4.2.15. Biodegradation of endosulfan using P450_{cam} SeSaM library

The transformed *P. putida* (ATCC 17453) from the previous step was inoculated in regular broth (Difco nutrient broth) and incubated overnight at 30 °C. The bacteria acted as an inoculum for 1 L of fresh nutrient broth until the O.D. was 0.7-0.9. The culture was harvested at 7000xg at RT for 30 minutes and the pellet was suspended in 60 mL M9 minimal medium (Na₂HPO₄·7H₂O, KH₂PO₄, NaCl, MgSO₄, CaCl₂, and NH₄Cl) and 10 mL of the suspended pellet was distributed equally in the treatment and the control flasks. Controls (in the absence of the substrate, boiled bacteria, and transformed wild-type *P. putida*) were run in parallel. Cultures were treated with: endosulfan (100 µM, 1 mL), supplements needed for the protein expression (IPTG (100 mM, 80 µL), FeCl₂ (2g/mL, 10 µL), 5-aminolevulinic acid (500 mM, 180 µL), vitamin B₁ (10 µM) and camphor (0.8 M, 600 µL)) for induction of the CAM pathway.^{160,263}

The flasks were covered by a cork that held a Porapak (Waters Corporation, MA, USA) column in the middle. The cultures were incubated for a week, and culture samples were collected every 24h. Porapak columns were exchanged every 24h, rinsed with 500 µL CHCl₃ twice and the eluents were checked for the presence of endosulfan and its volatile metabolites by GC-MS. Culture samples (1 mL) collected every 24h were harvested at 10,000xg for a minute and the supernatants were extracted with CHCl₃ (1

mL). The aqueous layers were back-extracted with CHCl_3 and the organic layers were dried over Na_2SO_4 and analyzed by GC-MS.

4.2.16. *In vitro* assays with endosulfan as the substrate

In vitro enzymatic assays were performed with 1 mL phosphate buffer (50 mM 150 mM K^+ , pH 7.4) that contained P450_{cam} (1.5 μM), *m*-CPBA (1 mM), substrate endosulfan (1 mM) in four replicates. The buffer was sparged with O_2 or argon prior to the assay. Three controls (without enzyme, without substrate and without shunt) were run in parallel with the treatments. The reaction mixture was incubated for 15 minutes at 22 °C and extracted in the same way as above. The dried organic layers were analysed by GC-MS.

4.2.17. Biodegradation of endosulfan diol using P450_{cam} mutant (E156G/V247F/V253G/F256S)

The active mutant from 3-chloroindole epoxidation (E156G/V247F/V253G/F256S) was transformed in *P. putida* (ATCC 17453), inoculated in regular broth (Difco nutrient broth) and incubated overnight at 30 °C. The bacteria acted as an inoculum for 1 L fresh nutrient broth medium until the O.D. was 0.7-0.9. The culture was harvested at 6000 rpm (Beckmann Avanti centrifuge, JLA 8.1 rotor) at RT for 30 minutes and the pellet was suspended in 60 mL M9 minimal medium ($\text{Na}_2\text{HPO}_4 \cdot 7\text{H}_2\text{O}$, KH_2PO_4 , NaCl , MgSO_4 , CaCl_2 , and NH_4Cl) and 10 mL of the suspended pellet was distributed equally in the treatment and the control flasks. In addition to this, the wild-type *P. putida* gene was cloned in *pET* vector and transformed in *P. putida* (ATCC 17453). The transformed WT bacteria were grown in the same fashion as above and acted as a control to check the background activity of enzymes from P450_{cam} operon. In addition, two more controls were performed: a) the transformed *P. putida* culture (with the mutant) was boiled and treated with camphor b) *P. putida* was not transformed with either mutant or WT P450_{cam} and checked for degradation with endosulfan.

Endosulfan diol was added at IC_{90} concentration to the growing *P. putida* cultures (1 mM, 100 μL), supplements needed for the protein expression (IPTG (100 mM, 80 μL), FeCl_2 (2g/mL, 10 μL), 5-aminolevulinic acid (500 mM, 180 μL), vitamin B_1 (10 μM) and

camphor (0.8 M, 600 μ L)) for induction of the CAM pathway. The cultures were incubated for 3 days and samples collected every 24h. The culture flasks were fitted with a Porapak column to trap any volatile compounds that form from the diol metabolism. Porapak columns were exchanged every 24h and rinsed with 500 μ L CHCl_3 twice and the eluents were checked for the presence of endosulfan diol and its metabolites by GC-MS. Samples (1 mL) collected every 12 h were harvested at 10,000 \times g for a minute and the supernatants were extracted with CHCl_3 (1 mL). The aqueous layers were back-extracted with CHCl_3 and the organic layers were dried over Na_2SO_4 and analysed by GC-MS.

4.2.18. *In vitro* assays with endosulfan diol as the substrate

In vitro enzymatic assays were performed in 1 mL phosphate buffer (50 mM 150 mM K^+ , pH 7.4) that contained P450_{cam} (1.5 μ M), *m*-CPBA (1 mM), substrate endosulfan diol (1 mM) in four replicates. Endosulfan diol was detected as the major product in the degradation of endosulfan and was reported to be less toxic. To avoid the toxic effects of endosulfan at its higher concentrations, the diol was used for further studies. The buffer was sparged with O_2 or argon prior to the assay. Three controls (without enzyme, without substrate and without shunt) were run in parallel with the treatments. The reaction mixture was incubated for 15 minutes at 22 $^\circ\text{C}$ and extracted in the same way as above. The organic extracts were silylated using BSTFA to check for the presence of volatile intermediates and analysed by GC-MS. The dried organic layers were analysed by GC-MS.

4.3. Results

4.3.1. *Identification of active mutants for the hydroxylation of 3-chloroindole*

The mutant P450_{cam} library ($\sim 10^6$ variants)²⁴⁶ with a mutation frequency (substitution/base: 3×10^{-3}) was screened with 3-chloroindole (**10**), as described in section (4.2.6) of the experimental section (Supplementary Fig. S5). We have found that 3-chloroindole was toxic to bacteria (IC_{50} 6 μ M) (Supplementary Fig. S6), and the corresponding “indigo-assay” products (isatin and indigo) were less toxic to the bacteria.

To estimate the number of hits obtained in this selection process, I also plated the cells transformed with the library onto LB-agar/kanamycin control plates that did not have 3-chloroindole or any other additives (section 4.2.6). The transformation and selection process was performed twice and the results are shown in Table 4.1.

Table 4.1. Active mutants isolated by screening the P450_{cam} SeSaM library with 3-chloroindole.

Transformation	Control plates (CFU/mL)	Treatment (CFU/mL)	Survival rate (%)	Pink colonies	# of clones taken for sequencing
1	$(7.6 \pm 1.0) \times 10^5$	1200 ± 120	0.15	8	8
2	$(7.2 \pm 0.6) \times 10^5$	1000 ± 100	0.13	4	4

Screening of the mutant library (with approximately 3 mutations/clone, based on the sequencing results of 12 clones) with 12 μ M 3-chloroindole (2 \times the IC₅₀ concentration) under shunt conditions, using *m*-CPBA resulted in ~30 colonies per plate out of which at least 15 were pink or blue colored, due to the formation of isatin (**11**) or indigo, respectively. In the absence of shunt or the expression additives, and with the wild-type control, the colonies formed (~ 5-7) were only white. Plasmids isolated from the 12 pink and two white colonies were sequenced. I was looking for mutants that formed isatin (pink colored colonies) and the sequencing results of those mutants are listed in Table 4.1.

In vitro assays were performed with all the sequenced mutants, and isatin was detected as a major product with a few mutants (Table 4.2). The colonies that showed white colour on the plates during the screening process did not show enzymatic activity in these assays. Isatin from these reactions was isolated by reverse-phase HPLC and analyzed by GC-MS (Fig. 4.2), ¹H and ¹³C NMR (Supporting Fig. S7 and S8). The compound matched an authentic isatin standard (Fig. 4.2).

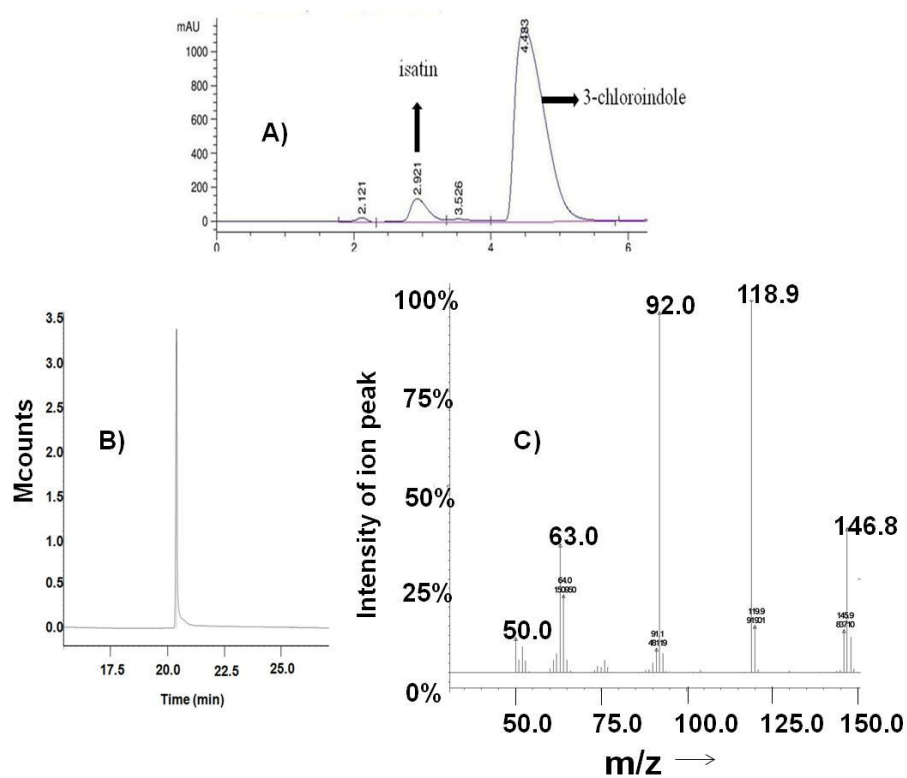


Figure 4.2. *A) HPLC of isatin produced in the in vitro assays with P450_{cam} mutant IND1 (Table 4.2), 3-chloroindole under shunt conditions B) Gas chromatogram and C) Mass spectrum of enzyme-produced isatin purified by HPLC*

Table 4.2. Active mutants isolated by screening the P450_{cam} SeSaM library with 3-chloroindole.

Clone Name	P450 _{cam} Mutant	Rate of isatin production (nmol/min/nmol of P450 _{cam}) ^a
IND1	E156G/V247F/V253G/F256S	156 ± 2
IND2	G60S/Y75H	132 ± 1
IND3	D97F/P122L/Q183L/L244Q/	114 ± 5
IND4	G120A/G248S/D297H/Y179H	97 ± 7
IND5	Y179H	72 ± 10
IND6	G93C/K314R/L319M	69 ± 8
WT	Wild type	ND ^b

^a Mean ± S. E. of 4 technical replicates. ^b Not detected.

4.3.2. Steady-state kinetic analysis of the isolated mutants:

The amounts of isatin formed were highest for the mutants IND1, IND2 and IND3. The rates of 3-chloroindole hydroxylation were measured with the selected mutants and normalized for the nmol of P450_{cam} taken in the reaction (Table 4.3, Supplementary Fig. S9). The IND1 mutant had a lower K_M , but similar k_{cat}/K_M compared to the other mutants.

Table 4.3. Steady-state kinetic assays with the three most active mutants towards 3-chloroindole oxidation.

Clone Name	Mutations	K_M (μM)	k_{cat} (min^{-1})	k_{cat} / K_M ($\text{min}^{-1}\text{M}^{-1}$) $\times 10^6$
IND1	E156G, V247F, V253G, F256S	260 ± 50	480 ± 30	1.8 ± 0.6
IND2	G60S, Y75H	510 ± 90	1100 ± 100	2.1 ± 1.2
IND3	D97F, P122L, Q183L, L244Q	470 ± 90	1100 ± 100	2.3 ± 1.2

4.3.3. Proposed hypothesis for the formation of isatin:

The proposed hypothesis for the hydroxylation of 3-chloroindole (**10**) by P450_{cam} mutant(s) to generate isatin (**11**) is shown in Figure 4.3. I propose that the substrate forms an epoxide which ring-opens to the chlorohydrin. The chlorohydrin loses HCl to give 3-chloroindoxyl, that undergoes further oxidation to form isatin. Attempts to characterize 3-chloroindoxyl were unsuccessful as it was a transient species. The reaction of 3-chloroindole with *m*-CPBA alone, did not form isatin, demonstrating that P450_{cam} was necessary for 3-chloroindole oxidation. One of the three mutants that were able to dehalogenate 3-chloroindole to form isatin (IND1, Table 4.3) was further tested for the degradation of endosulfan.

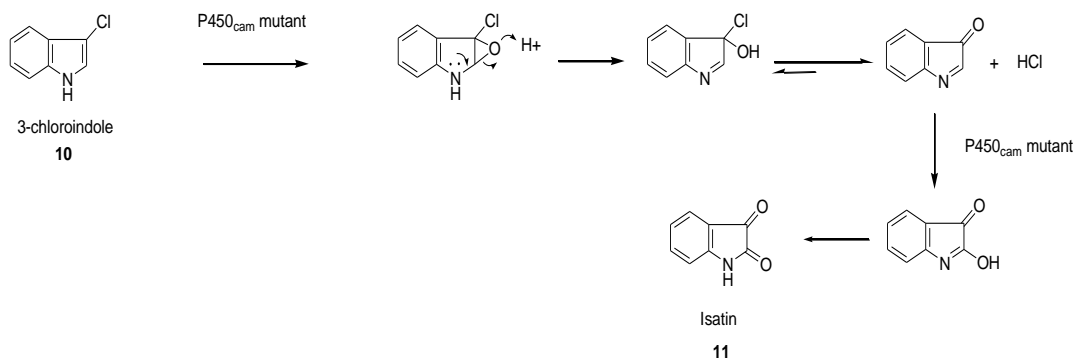


Figure 4.3. Proposed mechanism for the formation of isatin from 3-chloroindole, catalysed by P450 compound I

4.3.4. Screening of SeSaM library with endosulfan as the substrate:

As an alternate screen, the SeSaM library was grown with endosulfan at IC₉₀ concentration and the mutants that survived were able to metabolise endosulfan. Seven mutants survived in each of the treatment plates, and 2 mutants survived in each of the control plates that lacked either the shunt or the expression additives. In the control plates with no substrate/shunt or additives, $(9.2 \pm 0.2) \times 10^5$ CFU/mL were obtained whereas, in the treatment plates, 300 ± 10 CFU/mL were obtained. Seven mutants that survived were randomly picked for sequencing and the mutant, K314E/V247F/D297N (ES7) that produced higher amounts of endosulfan dialdehyde in the *in vitro* assays was carried forward for the biodegradation studies (see below) (table S2).

4.3.5. Biodegradation of endosulfan diol using the P450_{cam} mutant (IND1) isolated from 3-chloroindole screen:

To test if the mutant IND1 (Table 4.3) dehalogenates endosulfan, two sets of assays were performed: 1) *in vitro* with the purified recombinant mutant P450_{cam}, and 2) *in vivo* with transformed *P. putida*.

1) The *in vitro* assays were performed with the purified recombinant mutant P450_{cam}, endosulfan diol as a substrate under the shunt conditions. When the buffer was sparged with oxygen, endosulfan dialdehyde was detected as a major product (Supplementary Fig. S10) in the treatments. In the silylated organic extracts, a new metabolite with a M⁺ 224 was detected after 30 minutes of incubation exclusively in the

treatments. When the buffer was sparged with argon, endosulfan dialdehyde was detected and in addition to this, a new metabolite with a M+1 135 (Supplementary Fig. S10), and in the trimethylsilylated organic extracts, a new metabolite with a M⁺ 224 were detected after 30 minutes of incubation exclusively in the treatments, prompting us to characterize the metabolite and study the involvement of P450_{cam} in its formation (see below, section 4.3.7).

2) For the *in vivo* biodegradation studies with endosulfan diol, the mutant IND1 (Table 4.3) isolated from 3-chloroindole screen was transformed into *P. putida* by the reported protocol (Supplementary Fig. S11) (section 4.2.14). The soil bacterium *P. putida* utilizes camphor as a carbon source and the genetic information for camphor degradation is encoded on a CAM plasmid, which is controlled by the Cam repressor. Camphor induces the production of P450_{cam} and its redox partners (PdX, PdR), when the repressor dissociates from the upstream region of the CAM operon. P450_{cam} needs these redox partners (in the absence of shunt agent) for its catalytic activity. The reason for transforming the mutant IND1 (Table 4.3) into *P. putida* was to check if endosulfan can be degraded by P450 in the presence of its redox partners.

Endosulfan dialdehyde was identified as the major metabolite in the treatments and in addition, endosulfan monoaldehyde, endosulfan lactone were also detected as minor metabolites. The metabolites were identified in comparison to the retention times of synthetic standards. Endosulfan monoaldehyde and dialdehyde were also detected in the controls (non-transformed and transformed *P. putida* cultures). In addition, a new metabolite with a M+1 135, described above (Fig. S10) was detected exclusively in the treatments, within 12h of incubation, exclusively in the treatments, and the titer of this compound increased with time. The diol titer decreased by 70% in 3 days of incubation in the treatments and only by 30 % in the controls. The 30% decrease in diol titer in the WT-transformed control bacteria was due to formation of endosulfan monoaldehyde, dialdehyde and lactone (Fig. 4.4).

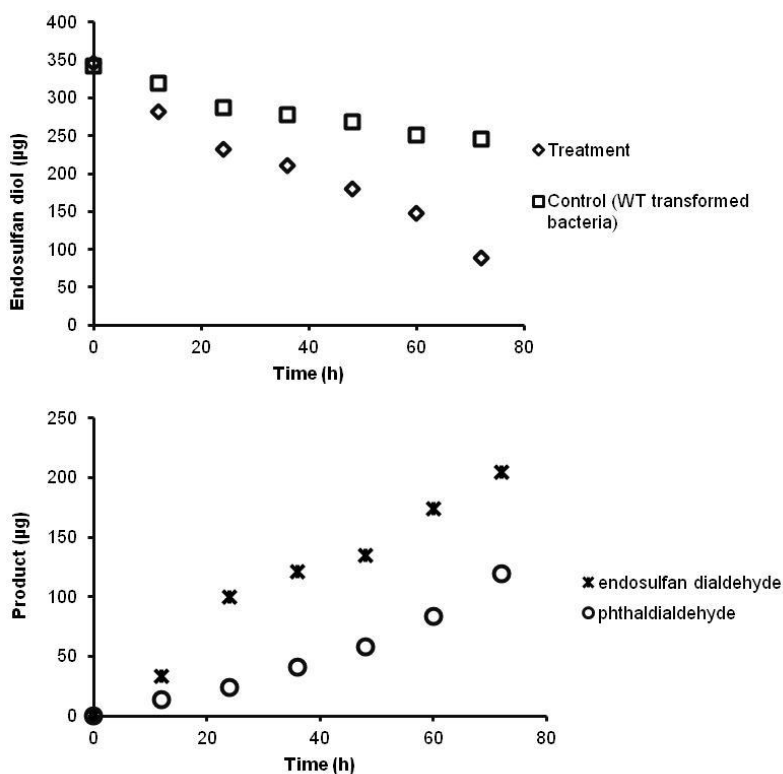


Figure 4.4. Biodegradation of endosulfan diol by the $P450_{cam}$ mutant IND1 and the formation of metabolites endosulfan dialdehyde and the $M+1 = 135$ compound in the treatments. Treatment: $P450_{cam}$ mutant IND1 in plasmid pALXtreme-1a transformed in *P. putida* ATCC 17453. Control: Wild-type $P450_{cam}$ in plasmid pALXtreme-1a transformed in *P. putida* ATCC 17453.

4.3.6. Biodegradation of endosulfan using the $P450_{cam}$ mutant V247F/D297N/K314E (ES7) isolated from endosulfan screen:

In the previous section, I have described how the $P450_{cam}$ mutant IND1 also accepts endosulfan diol as a substrate. In this section, I describe how the most active mutant from the endosulfan screen (see section 4.3.4, Table S2) was tested *in vivo* in the same manner. Briefly, the mutant ES7 isolated from endosulfan screen was transformed in *P. putida* and the biodegradation studies were carried out in the same way as described in the previous section with endosulfan as a substrate. Endosulfan diol was detected as the main product, along with endosulfan dialdehyde. After 3 days of incubation, the new metabolite with $M+1$ 135 formed, and the progress was monitored for 7 days of incubation (Figure 4.5). The formation of the new metabolite was 2x slower

with this mutant than with mutant IND1. After 7 days, the cultures were harvested and the extraction, purification of the oily residue by column chromatography to isolate the M+1 = 135 compound were performed as described below.

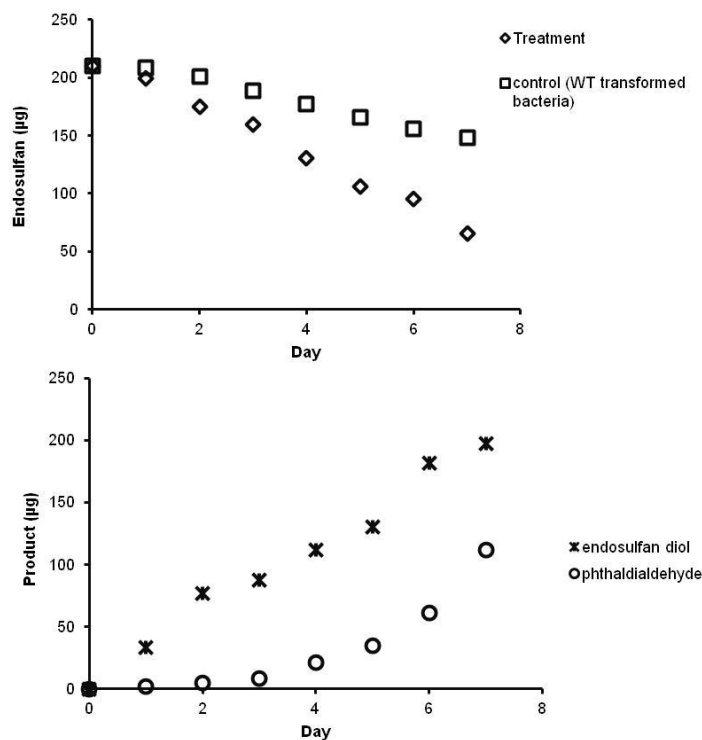


Figure 4.5. *Biodegradation of endosulfan by the isolated mutant ES7 and the formation of metabolites endosulfan diol and the M+1 = 135 compound in the treatments. Treatment: P450_{cam} mutant ES7 in plasmid pALXtreme-1a transformed in P. putida ATCC 17453. Control: Wild-type P450_{cam} in plasmid pALXtreme-1a transformed in P. putida ATCC 17453.*

4.3.7. Isolation and identification of metabolites obtained from the *in vivo* and *in vitro* assays of endosulfan diol biodegradation:

The cultures (from sections 4.3.5 and 4.3.6) were harvested and the supernatants were extracted with chloroform. The organic extracts were dried over sodium sulfate and concentrated under vacuum. The oily residue (~ 100 mg) was purified by column chromatography using hexane: EtOAc (3:1) and the fractions (30-72) monitored by TLC were concentrated to give a yellow solid.

The mass spectrum of the yellow solid showed the fragmentation peaks 134.8, 117.8, 105 and 76 (Fig. 4.6). The ^1H NMR showed a signal at 10.5 ppm (2H) corresponding to aldehyde protons, two signals at 7.99 ppm (2H) and 7.78 ppm (2H) corresponding to aromatic protons (Supplementary Fig. S13). The ^{13}C NMR showed a signal at 192.3 ppm (aldehyde carbons), 136.2 ppm, 133.2 and 131 corresponding to aromatic carbons (Supplementary Fig. S14). By elemental analysis, this solid was shown to have 71.3% carbon, 4.47% hydrogen and 23% oxygen proving the molecular formula to be $\text{C}_8\text{H}_6\text{O}_2$. These data are consistent with phthaldialdehyde.

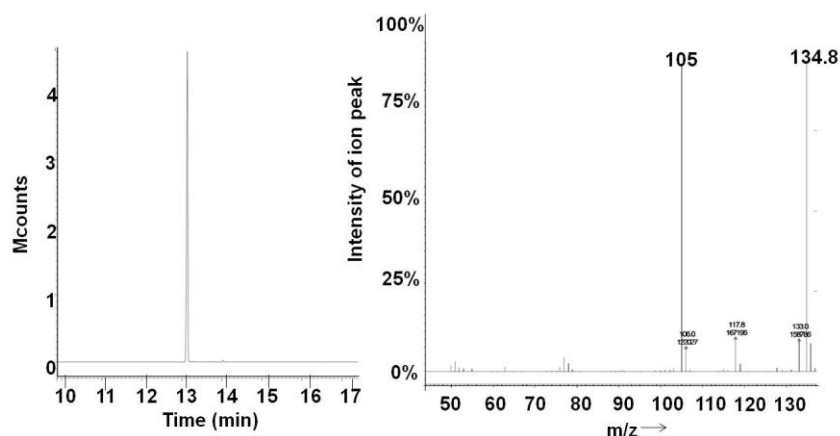


Figure 4.6. *Gas chromatogram and mass spectrum of phthaldialdehyde isolated from the *in vitro* and *in vivo* assays with $P450_{cam}$ mutants (see above) and endosulfan diol as the substrate*

In addition to phthaldialdehyde, the TLC analysis of the oily residue also showed a red-colored spot that was initially predicted to be a phenolic intermediate. This metabolite was isolated by the preparative TLC using the solvent system, hexane:acetone (2:1) and trimethylsilylated by BSTFA for GC-MS analysis. The non-derivatized phenol is not volatile enough for gas chromatographic analysis, but the trimethylsilyl ether is. The mass spectrum of this trimethylsilylated intermediate showed the fragmentation peaks 224.5, 209.5, 153 and 75.2 (Fig. 4.7). NMR showed a signal at

9.6 ppm (2H), 7.42 (d, 1H), 6.37 (dd, 1H) and 6.20 (d, 1H). (Supplementary Fig. S15).

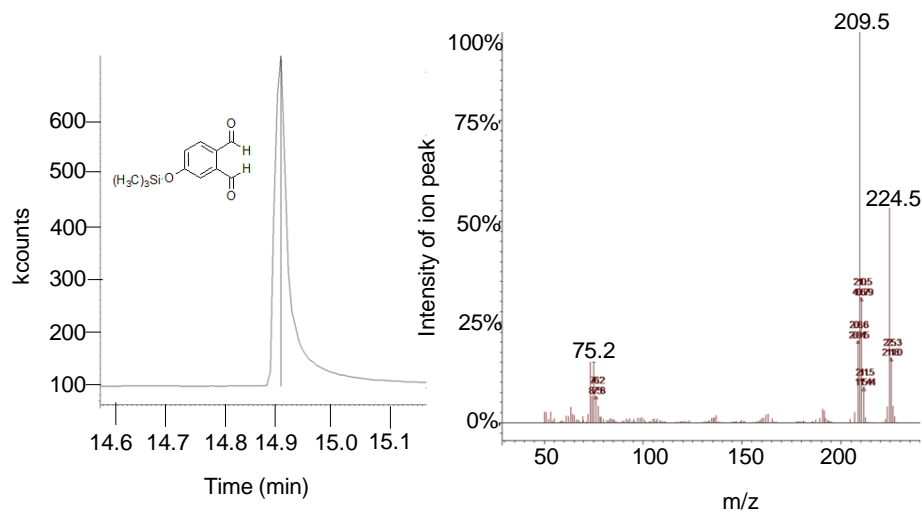


Figure 4.7 *Gas chromatogram and mass spectrum of silylated 3-hydroxy phthalaldehyde isolated from the in vitro and in vivo assays with P450_{cam} mutants (see above) and endosulfan diol as the substrate*

4.3.8. Proposed mechanism in the biodegradation of endosulfan and the formation of phthalaldehyde:

The proposed mechanism for the formation of phthalaldehyde from endosulfan is shown in Figs. 4.8, 4.9 and 4.10. We propose that endosulfan forms sulphate (**2**) by P450 oxidation, which is hydrolysed to endosulfan diol (**3**). Endosulfan dialdehyde (**7**) forms after the double oxidation of the diol by P450_{cam} (Stage 1, Fig. 4.8).

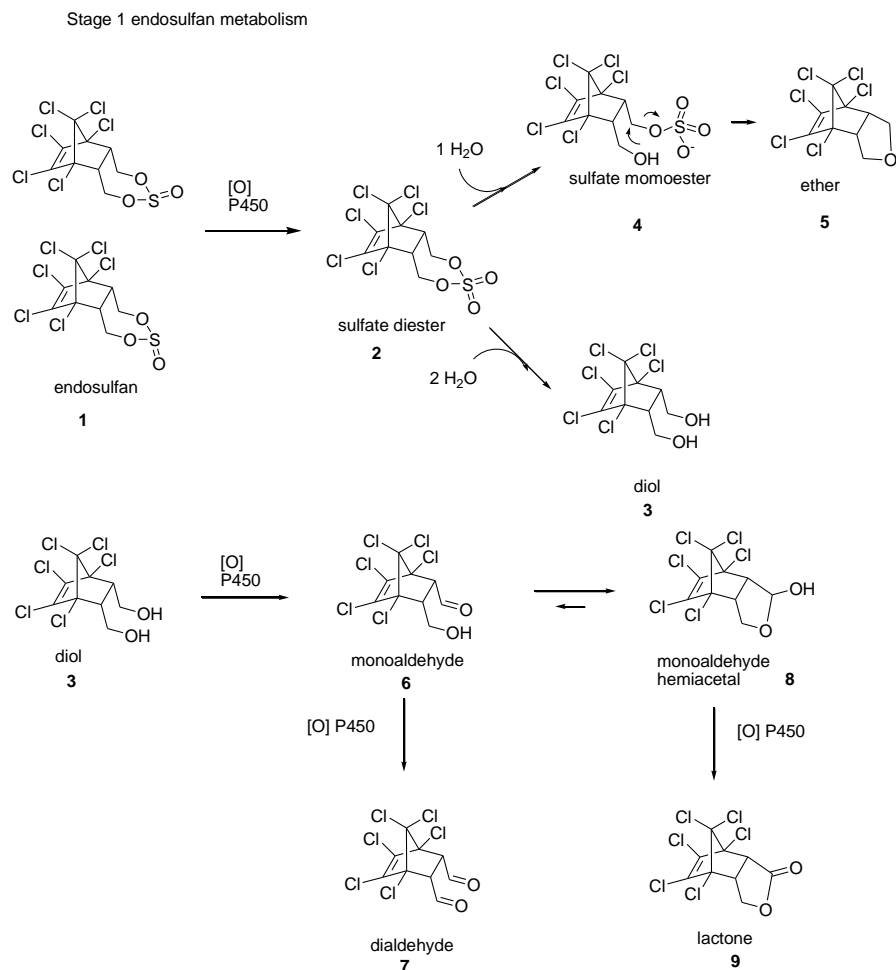


Figure 4.8. Stage 1 in the metabolism of endosulfan. Formation of metabolites 3-9.

Epoxidation of dialdehyde (7) at the chlorinated end generates (12), which immediately gets protonated to generate (13). Attack of water on (13) and simultaneous release of HCl generates the strained, probably unstable species (14), that rearranges to the more stable intermediate (15). Intermediate (16), that forms from (15) after further hydrolysis and release of HCl, undergoes decarboxylation, to form (17) that releases a molecule of HCl to form (18) (Stage 2, Fig. 4.9).

Stage 2 endosulfan metabolism

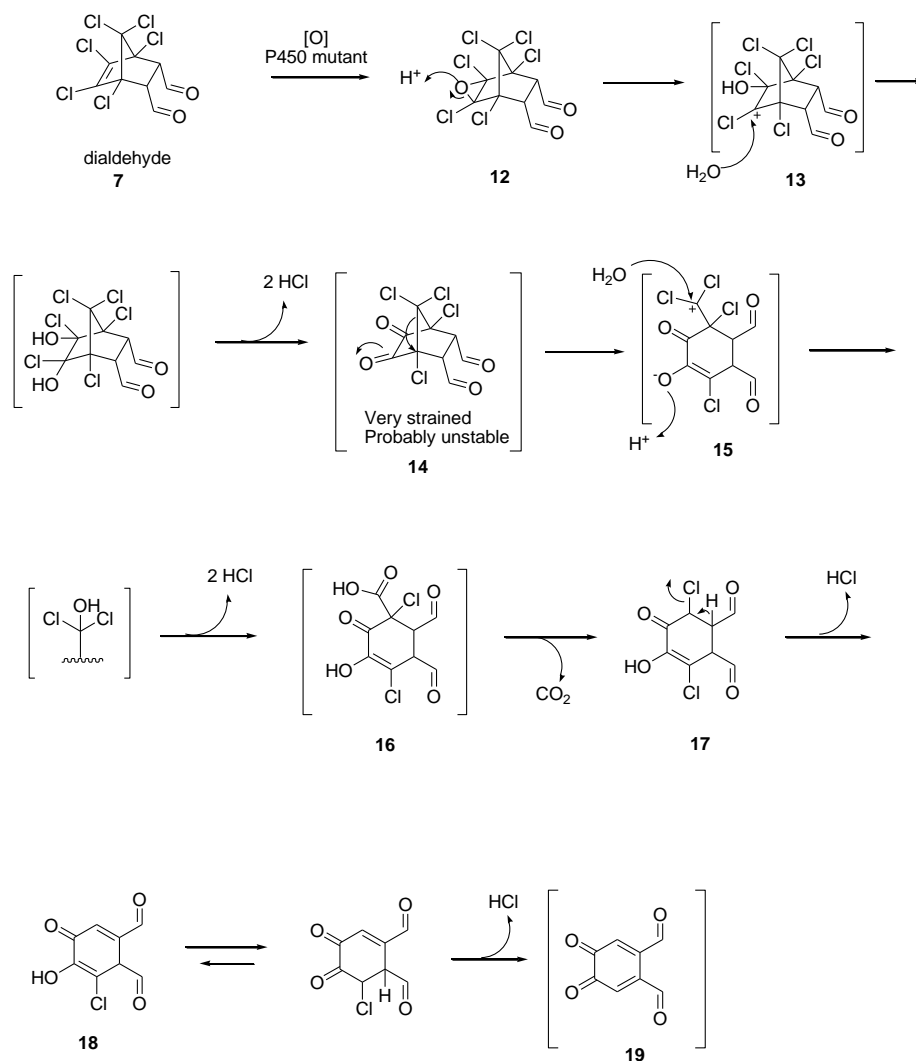


Figure 4.9. Stage 2 in endosulfan metabolism: Biodegradation of endosulfan dialdehyde.

Intermediate **18** can eliminate an additional HCl, to give diketone **19**, which would need to be reduced. We have recently reported that P450_{cam} oxidizes two molecules of water to hydrogen peroxide, with the simultaneous reduction of camphor to borneol (Prasad *et. al.* PLoS One, in press). We propose that (**19**) can be reduced by three rounds of reduction, each with concomitant oxidation of two molecules of water to H₂O₂, to form phthaldialdehyde (**25**). I hypothesize that this process of ketone to alcohol reduction with simultaneous formation of hydrogen peroxide (Stage 3, Fig. 4.10) is similar to the borneol cycle described in chapter 3 of this thesis. Consistent with this

hypothesis, phenolic intermediates (**22**) and (**23**), which are tautomers of (**20**) and (**21**), respectively, have recently been isolated together (data not shown). The phenolic intermediate, (**23**) has been purified and characterised by GC-MS (Fig. 4.7) and ^1H NMR (Supplementary Fig. S15). If the pathway shown in Figs. 4.8, 4.9 and 4.10 is correct, then endosulfan diol degradation should give two inorganic products: Cl^- (6 equivalents per endosulfan diol converted to either **22**, **23** or **25**) and H_2O_2 .

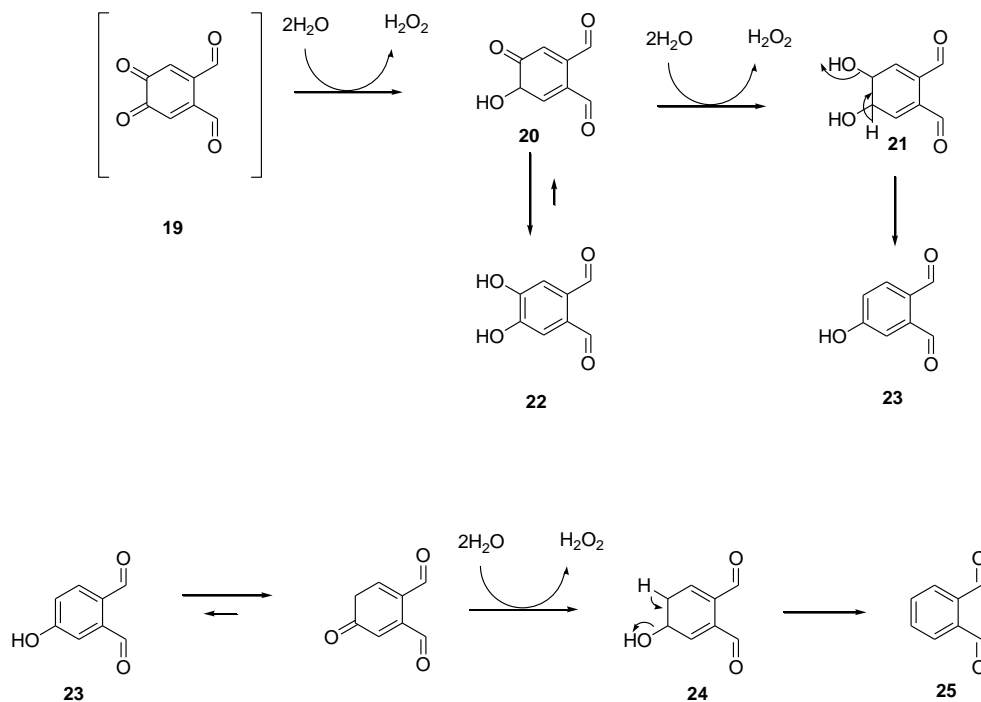


Figure 4.10. Stage 3 in endosulfan metabolism. Formation of phthalaldehyde.

The release of chloride ions during the biodegradation of endosulfan diol was monitored by ^{35}Cl , and the results suggested that a signal for Cl^- (0 ppm) was observed in the treatments, but missing in all controls (Fig. 4.11 A). The formation of H_2O_2 , in the conversion of (**19**) to (**25**) was detected in the treatments and missing in the controls (Fig. 4.11 B).

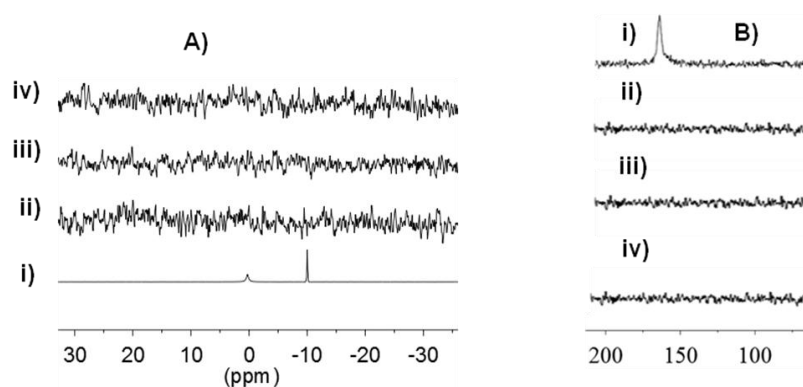


Figure 4.11. A) The ^{35}Cl NMR spectrum of the incubation mixture containing i) endosulfan diol, mutant IND1, and *m*-CPBA. ii) mutant IND1 and *m*-CPBA (diol absent). iii) diol and *m*-CPBA (mutant IND1 absent). iv) diol and IND1 (*m*-CPBA absent). The peak at 0 ppm corresponds to aq. Cl⁻, and the peak at -10 ppm is a synthetic peak (ERETIC2) with an area equal to that observed for an external sample of 10 mM NaCl in D₂O. B) ^{17}O NMR spectrum of the incubation mixture in ^{17}O phosphate buffer containing: i) endosulfan diol, mutant IND1, and *m*-CPBA. ii) mutant IND1 and *m*-CPBA (diol absent). iii) diol and *m*-CPBA (mutant IND1 absent). iv) diol and IND1 (*m*-CPBA absent). The peak at 175 ppm corresponds to H₂¹⁷O₂.

4.3.9. Docking of 3-chloroindole in the active site of P450_{cam}:

To verify whether 3-chloroindole fits into the active sites of the mutants better than wild-type P450_{cam}, *in silico* docking calculations were performed. First, 3-chloroindole was docked in the active site of P450_{cam} (WT as well as the mutant IND1). V247, V253 and F256 can be seen close to the active site heme (Fig. 4.13) (section 1.4). The WT enzyme showed no activity with 3-chloroindole hydroxylation in the *in vitro* assays (Table 4.1), and the docking suggests that 3-chloro indole is wedged in between F256 and L244. The 'NH' of 3-chloroindole is poised exactly above the Fe, which may cause it to coordinate and inhibit catalytic turnover. Even during the screening, some colonies remained colourless, which suggests that WT or the mutations present farther from the active site of the enzyme had low activity with 3-chloroindole hydroxylation (Table 4.1).

The proposed mechanism for the formation of isatin (Fig. 4.3) suggested that the C-2 or C-3 of 3-chloroindole should be close to Fe for getting oxidised. The poses obtained after docking 3-chloroindole in the active site of IND1 suggested that at least 5

of them had the C-2 close to Fe and 6 poses had the C-3 close to Fe (the distance from C-2 to Fe and C-3 to Fe was around 5 Å). We hypothesise that compound I is responsible for the epoxidation of 3-chloroindole (Fig. 4.3) and the docking results suggested that both C-2 or C-3 have a chance to get attacked for the formation of 3-indoxyl (Fig. 4.3), that further results in the formation of isatin. The poses obtained after docking 3-chloroindole in the active site of WT suggested that only one of them had the C-2 close to Fe and the rest of poses were much farther, giving less chance for the compound I to attack the substrate at the C2-C3 bond (Fig. 4.12).

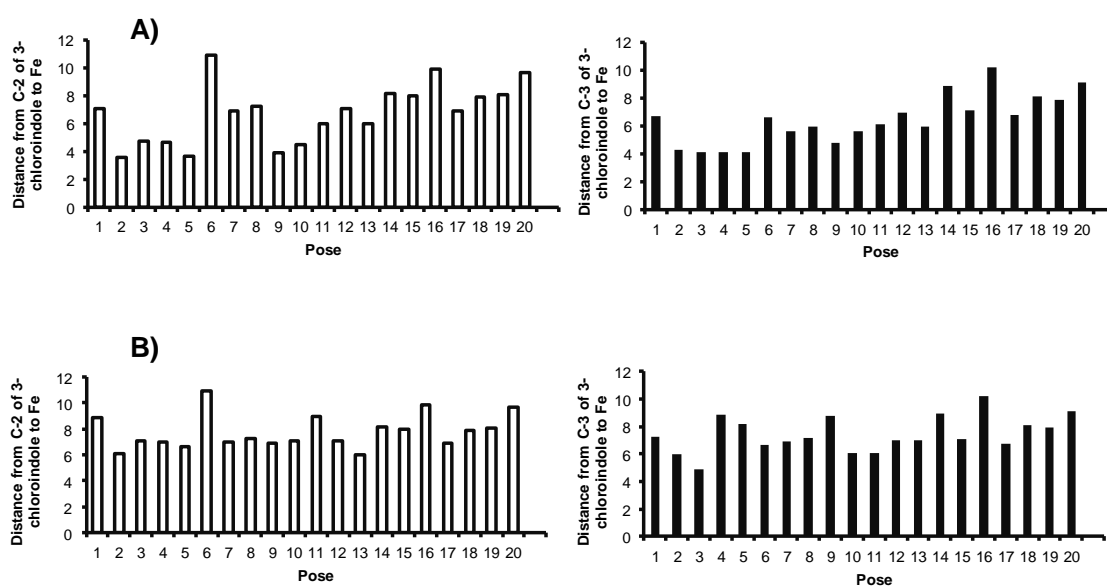


Figure 4.12. A) Graphical representation of the distances from C-2 and C-3 to Fe in the poses of 3-chloroindole obtained after docking 3-chloroindole in the active site of IND1. B) Graphical representation of the distances from C-2 and C-3 to Fe and the poses of 3-chloroindole obtained after docking 3-chloroindole in the active site of WT P450_{cam}.

The mutations V247F, F256S and V253G in IND1 create a more open cavity above the porphyrin in the active site than the cavity seen in WT P450_{cam}. For example, it is interesting to note that in the model of the mutant, F247 and the 3-chloroindole are exactly orthogonal (Fig. 4.13), suggesting that a sp²C-H/π interaction now plays a role in positioning 3-chloroindole above the porphyrin.

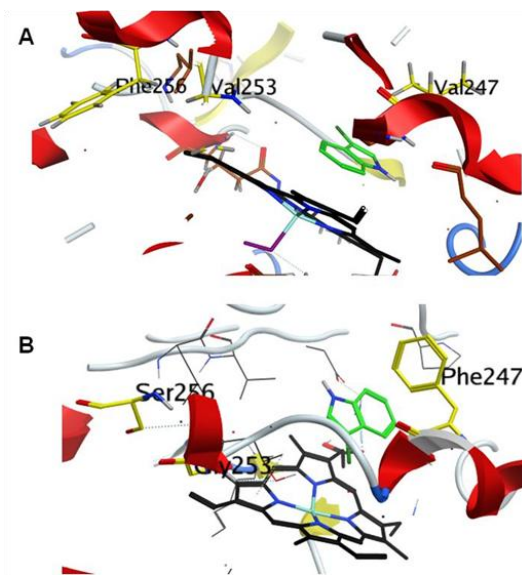


Figure 4.13 A) 3-chloroindole docked in the wild-type P450_{cam} (pose 3 from the Fig. 4.10 B selected). B) 3-chloroindole docked in the mutant IND1 (pose 5 from the Fig. 4.10 A selected). The porphyrin is shown in black, 3-chloroindole in green and the amino acid residues in yellow.

4.3.10. Docking of endosulfan diol in the active site of P450_{cam}:

Endosulfan diol was docked into the WT and the mutant, IND1 (isolated from 3-chloroindole screen). The poses obtained after docking endosulfan diol in the active site of IND1 suggested that at least 12 of them had the C-2 close to Fe and 3 poses had the C-3 close to Fe (the distance from C-2 to Fe and C-3 to Fe was around 5 Å) (Fig. 4.14 A). The poses obtained after docking the diol in the active site of WT suggested that only 5 of them had the C-2 close to Fe and 14-15 poses had the C-8 and C-9 close to Fe. (Fig. 4.14 B). In the proposed biodegradation mechanism (Figs. 4.8, 4.9 and 4.10), the epoxidation of endosulfan dialdehyde (7, stage 2, Fig. 4.9) is necessary for the further dechlorination steps. With the docking results, we hypothesise that the mutant IND1 can position the endosulfan diol with the chlorinated end sufficiently close to Fe for epoxidation, the first step in the proposed biodegradation. In contrast, the WT enzyme appears to position endosulfan diol such that only the hydroxyl groups are close enough to Fe for oxidation (Figs. 4.14 and Fig. 4.15).

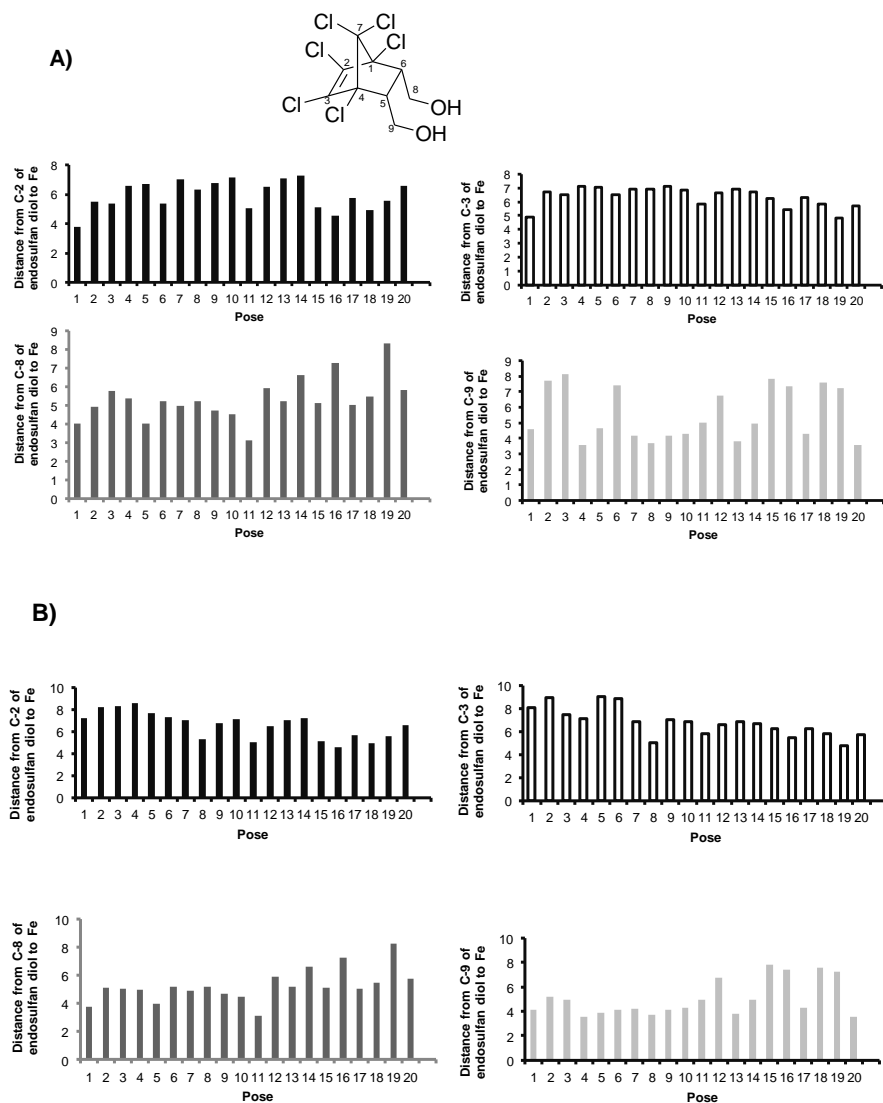


Figure 4.14. A) Graphical representation of the distances of C-2, C-3, C-8 and C-9 to Fe in the poses of endosulfan diol obtained after docking it in the active site of IND1. B) Graphical representation of the distances of C-2, C-3, C-8 and C-9 to Fe in the poses of endosulfan diol obtained after docking it in the active site of WT P450_{cam}.

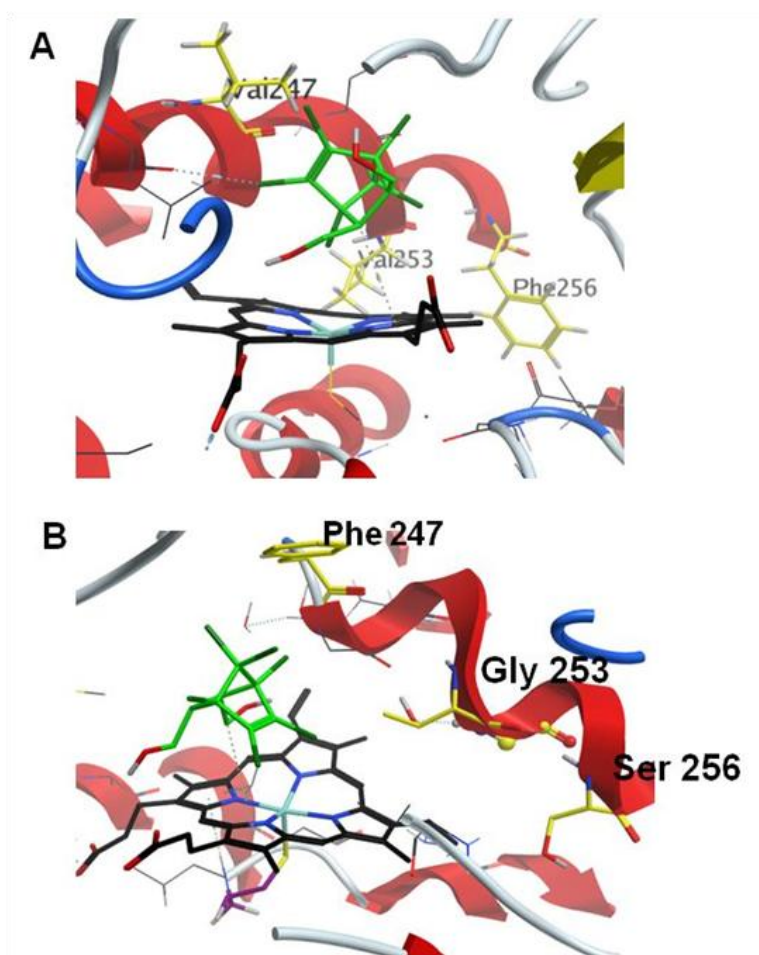


Figure 4.15 A) Endosulfan diol docked in the wild-type P450_{cam}. B) Endosulfan diol docked in the mutant IND 1 (pose 19 selected from 4.11 B). The porphyrin is shown in black, 3-chloroindole in green and the amino acid residues in yellow.

4.3.11. Docking of endosulfan dialdehyde in the active site of P450_{cam}:

Endosulfan dialdehyde was also docked into the WT and the mutant, IND1 (isolated from 3-chloroindole screen). The poses obtained after docking endosulfan dialdehyde in the active site of IND1 suggested that at least 9 of them had the C-2 close to Fe and 10 poses had the C-3 close to Fe (the distance from C-2 to Fe and C-3 to Fe was around 5 Å) (Fig. 4.16 A). The poses obtained after docking the dialdehyde in the active site of WT suggested that only 1 of them had the C-2 close to Fe and 3 poses had the C-8 and C-9 close to Fe (Fig. 4.16 B). The docking results from dialdehyde clearly

suggest that the mutant IND1 can position the dialdehyde sufficiently close to Fe for epoxidation. The C-8 and C-9 of endosulfan dialdehyde in IND1 mutant are farther from Fe, than the C-8 and C-9 of the diol, which suggests a reason why endosulfan diacid is not formed by this mutant.

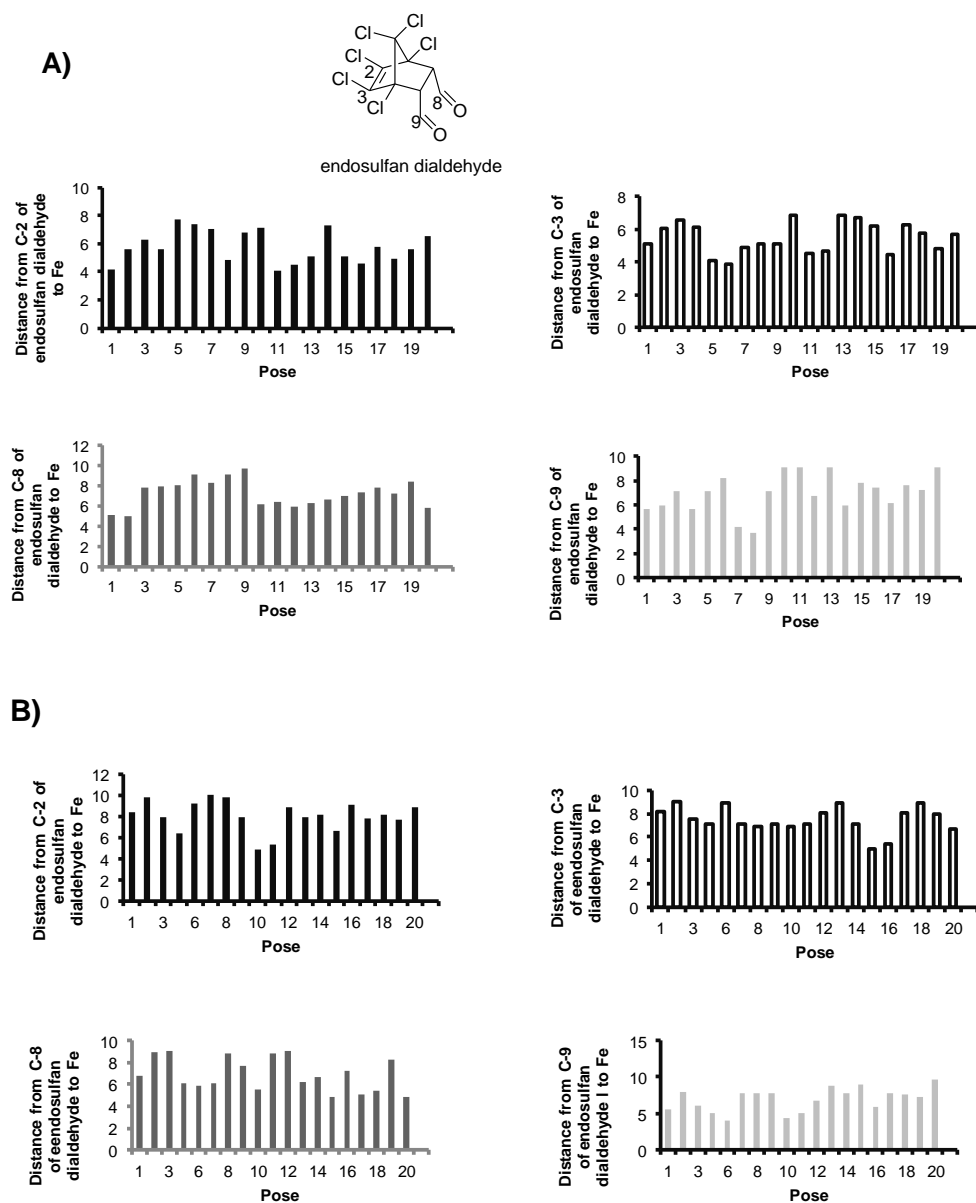


Figure 4.16 A) Graphical representation of the distances of C-2, C-3, C-8 and C-9 to Fe in the poses of endosulfan dialdehyde obtained after docking it in the active site of IND1. B) Graphical representation of the distances of C-2, C-3, C-8 and C-9 to Fe in the poses of endosulfan dialdehyde obtained after docking it in the active site of WT P450_{cam}.

The consecutive deprotonations after epoxidation and rearrangement, may occur in co-operation with Gln 322, His 355 and Lys 344, present close to the active site. Similar docking results were observed for the mutant, ES7 and the lower catalytic turn-

over observed in this case may be due to D297N mutation, that disrupts the hydrogen bond between the carboxylate group of D297 to one of the heme propionate groups.²⁶⁴

4.4. Discussion

One of the main difficulties in the applications of P450_{cam} remains its poor affinity for unnatural substrates.²⁶⁵ The catalytic cycle involves the expulsion of the axially coordinated water molecule from the heme iron upon substrate binding.¹⁶ Poor substrate binding causes an incomplete spin transition of the heme in the active site, which decreases the catalytic efficiency of the enzyme.²⁶⁶ Therefore, there is a need for engineering the active site of the enzyme to enhance the substrate binding affinity, which then enhances the catalytic turn-over of the enzyme. Researchers have attempted to design P450_{cam} variants by either increasing the active site volume for larger substrate molecules,²⁶⁷ or enhancing the substrate binding affinity by complementary non-covalent interactions between the substrate and the suitable amino acid side-chains in the active site.²⁶⁶ It has been reported before that the substrates that do not fit well into the P450_{cam} active site, either because they are too small and do not fill the cavity or because they are too large and cannot position above the Fe, are not turned over¹⁰⁶ (section 1.4)

Previous literature suggests that the wild-type P450_{cam} has no activity towards indole.²⁶⁸ Site-directed mutagenesis of P450_{cam} active site was attempted before by researchers to obtain activity towards indole.²⁵⁷ The amino acids, F87, Y96, T101 and L244 in the active site of the enzyme were mutated, and the mutants were assayed with indole and various substituted indoles,^{257,269} (section 1.4) but not 3-chloroindole. The hydrophobic residue V247, present above heme (section 1.4), was mutated to leucine, to change the shape of the cavity above heme and detect oxidation of a variety of unnatural substrates that include α -pinene, aromatic halides, short-chain alkanes.^{107,109,147,270} Here, we report a novel mutation (V247F) that can alter the activity of P450_{cam} towards dehalogenation of endosulfan. This mutation was also observed in the mutant isolated from endosulfan screen which prompted us to use IND1 for further *in vivo* studies with endosulfan diol. The additional mutations in IND1, V253 to a smaller glycine and F256S create space in the active site and a different positioning of

endosulfan diol above the porphyrin. The results of the activity assays and *in silico* docking experiments are consistent with the interpretation that both 3-chloroindole and endosulfan were well positioned in the mutant active site for turn-over.

The mutant (ES7) isolated from the endosulfan screen had 2x lower activity with the diol (section 4.3.6). The carboxylate group of D297 side chain is reported to have specific interactions with one of the heme propionate groups and the mutation, D297M is reported to have reduced oxidation activity with butane and propane.¹⁰⁷ The residue K314 is not present in the substrate binding cavity and this mutation, K314E has not been reported before. However, it is of interest to note that I found K314 mutations in two of the mutants I isolated (ES7 from the endosulfan screen and G93C/K314R/L319M from the 3-chloroindole screen) Further studies are necessary to verify if these mutations play a role in the dehalogenation.

The reductive dehalogenation of haloalkanes was reported for P450_{cam}.²⁷¹ Here, I have reported a series of new mutants, two of which were very active in the dehalogenation of the pesticide endosulfan or its main halogenated metabolites, endosulfan diol and endosulfan dialdehyde. The products I identified, phthaldialdehyde and 3-hydroxyphthaldialdehyde indicate that dehalogenation of the endosulfan halogenated core is complete. The two mutants of P450_{cam} described here may one day be helpful in the bioremediation of endosulfan or its halogenated metabolites, which are toxic and reaclitrant pollutants.^{226,272-274}

4.5. Conclusions:

In conclusion, we have generated a SeSaM library for P450_{cam} and generated variants that can dehalogenate 3-chloroindole, giving isatin as the major initial product and indigo after overnight oxidation. Indirubin was not detected in our assays. Kinetic assays were performed with the selected mutants that showed the highest hydroxylation activity with 3-chloroindole. SeSaM library preparation for P450_{cam} and screening studies with 3-chloroindole are novel.

Selected mutants from 3-chloroindole screening were tested for endosulfan degradation. Alternatively, the mutant library was also screened with endosulfan at its

IC₉₀ concentration to generate variants that can metabolize it. Our results suggested that the mutants ES7 and IND1 formed endosulfan diol first, then endosulfan dialdehyde, and this was further degraded to phthaldialdehyde under low oxygenation and 3-hydroxyphthaldialdehyde under high oxygenation. Importantly, the full degradation, from endosulfan diol to the phthalaldehydes was observed *in vivo* and also *in vitro* with the purified and shunted mutants. We propose that the initial step of dehalogenation is the epoxidation of the alkene moiety in the halogenated portion of endosulfan dialdehyde. Opening of the epoxide results in a series of chloride eliminations and rearrangements that eventually leave the six carbons of the endosulfan bicycle as the six carbons of 4,5-dioxocyclohexa-2,6-diene-1,2-dicarbaldehyde (*o*-quinone **19**). This compound, we propose, is reduced and dehydrated stepwise, to give the phthaldialdehyde metabolites observed. The latter steps provide two interesting links to chapter 3 of this thesis. First, the proposed reduction reactions, from *o*-quinone **19** to the phthaldialdehydes, do not require any addition of a nicotinamide cofactor. Consistent with proposed borneol cycle in chapter 3, when endosulfan diol was reacted *in vitro* with the mutant and a shunting agent in H₂¹⁷O, labelled H₂O₂ was formed. Second, the O₂ control of the reduction reaction was preserved: the fully reduced and dehydrated product, phthaldialdehyde, formed preferentially under low oxygenation, whereas the phenolic products formed preferentially under high oxygenation.

4.6. Supplementary information

Screening of Cytochrome P450_{cam} SeSaM library with 3-chloroindole as the substrate to identify the dehalogenated metabolites of Endosulfan

4.6.1. Sequence Saturation Mutagenesis (SeSaM)

SeSaM is a simple and economical random mutagenesis method which can be accomplished in 2-3 days to generate a mutant library.²⁵³ SeSaM is comprised of 4 steps: 1) generation of a pool of DNA fragments with random length, 2) addition of a universal base using Deoxynucleotidyl terminal transferase (TdT) at the 3' termini of the DNA fragments, 3) elongation of the DNA fragments to the full-length genes, and 4) replacement of the universal bases by the standard nucleotides.

4.6.1.1. Step 1 of SeSaM:

a) Generation of templates for SeSaM (preliminary step):

Before fragment generation, two templates (forward and reverse), to which bio-SeSaM primers would bind, was generated. (Supplementary Fig. S1) A 50 µl PCR-mixture for the forward template (F_T) reaction contained: 1x Phusion HF Buffer; (New England Biolabs); 0.2 mM of each dNTP; 12.5 pmol of each primer (SeSaM F_{cam}, P450_{cam} R), 2.5 U of Phusion polymerase (New England Biolabs) and 50 ng of wild-type CAM plasmid isolated from *Pseudomonas putida* ATCC 17453 (which contains the P450_{cam} gene) as a template. A 50 µl PCR-mixture for the reverse template (R_T) reaction contained 12.5 pmol of the primers (SeSaM R_{cam} and P450_{cam} F) and the rest same as stated above: PCR program: 98 °C, 30 sec (1 cycle); 98 °C, 10 sec; 60°C, 30 sec; 72 °C, 45 sec (25 cycles); 72 °C, 5 min (1 cycle).

b) Generating a fragment pool with random length distribution:

To generate a homogenous distribution of DNA fragments, the templates (F_T and F_R) were linearly amplified individually with the appropriate forward and reverse primers (as stated above) and with varying percentages of both standard (dATP, dGTP) and α -phosphorothioate nucleotides (dATP α S and dGTP α S), SeSaM Taq polymerase (2 U) and SeSaM Taq buffer (10x). The phosphorothioate bond is susceptible to iodine cleavage in alkaline solution and the cleavage of the PCR products generated a library of fragments upstream of the α -phosphorothioate nucleotides. The fragment library is denoted with the appropriate 'S' analogue of the nucleotide. If dATP α S is used, it generates a 'A' library. Furthermore, if forward template with dATP α S is used, it generated a F_T A library. Similarly, F_T G, R_T A and R_T G libraries were also generated. Homogenous distribution of fragments and absence of uncleaved PCR products in the libraries (after iodine cleavage) was necessary to proceed with the further steps. The distribution of fragments in the libraries was checked on a 0.8% agarose gel (40 min, 96 V) to establish the appropriate percentages of dATP α S and dGTP α S.

c) Generating a fragment pool with random length distribution using bioSeSaM primers:

A second PCR reaction was performed with a biotinylated forward primer and non-biotinylated reverse primer in the presence of standard nucleotides, appropriate percentages of α -phosphorothioate nucleotides, SeSaM Taq buffer (10X) and SeSaM Taq polymerase (2U) with both forward and reverse templates individually (When forward template was used, bioSeSaM F and P450_{cam} R were used as primers and when reverse template was used, bioSeSaM R and P450_{cam} F were used as primers) (Supplementary Fig. S1). The PCR products from the libraries were column purified using the Nucleospin kit to remove the unelongated primers (elution with 80 μ l elution buffer). 10 μ l of 10x Qiagen Taq buffer was added to provide alkaline conditions, followed by addition of 10 μ l of cleavage solution (20 mM iodine in 99 % ethanol). The cleavage reaction was vortexed immediately after setup, and incubated (at 70 °C for 1 h). Biotinylated-DNA fragments were subsequently isolated using magnetic streptavidin beads (M-PVA SAV1, Chemagen, Baesweiler, Germany). For a better yield of single

stranded DNA templates, NTC buffer (Macherey-Nagel, Dueren, Germany) was used for binding on Nucleospin columns.

4.6.1.2. Step 2 of SeSaM: Universal base addition

Universal bases are purine or pyrimidine analogues used in SeSaM to achieve tunable mutational bias with their base pairing abilities. Deoxy 6-(2-deoxy- β -D-ribofuranosyl)-3,4-dihydro-8H-pyrimido-[4,5-C][1,2]oxazin-7-one-triphosphate (dPTP), a pyrimidine analogue which can pair with 'A' and 'G' libraries was used as a universal base in our case (Supplementary Fig. S1). The universal base was enzymatically attached by TdT to the 3' ends of the fragment libraries. The reaction mixture contained 200 ng of step 1 fragments, 1x TdT buffer, 60 pmol dPTP α S, 0.05 mM CoCl₂ and 40 U TdT. The reaction mixtures were heated for 2h at 37 °C and inactivated at 75 °C for 15 min and purified.

4.6.1.3. Step 3 of SeSaM: Full length gene synthesis

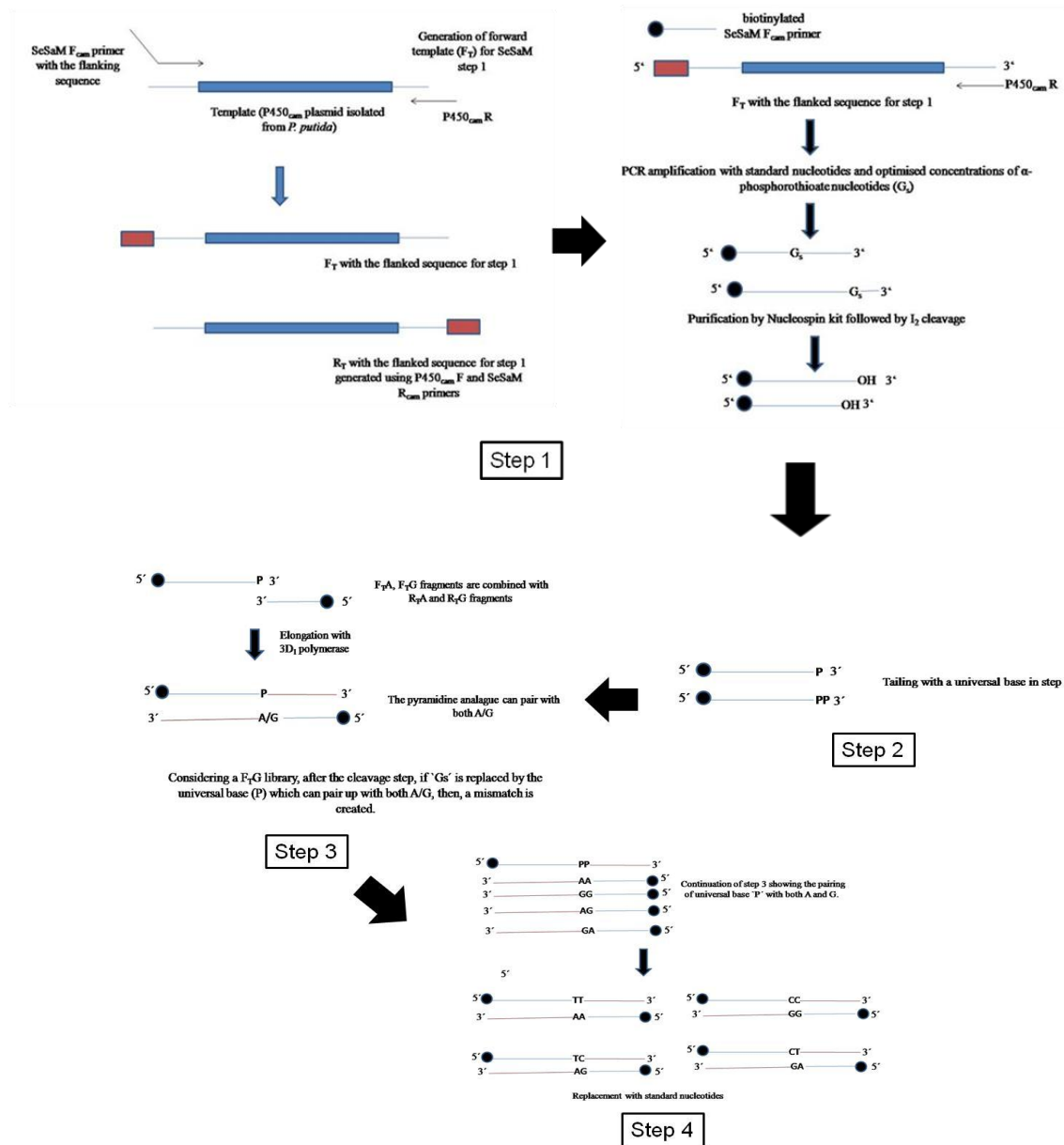
Full length genes can be obtained by the combination of tagged 'forward' and 'reverse' step 2 library fragments. To target all possible transversions, 50 ng 'tailed' fragments from every step 2 fragment library ('G' 'Forward', 'G' 'Reverse', 'A' 'Forward', 'A' 'Reverse') were added to the 100 μ l reaction mixture containing 0.25 mM of each dNTP, 1x Super Taq buffer and 10U 3D₁ polymerase. PCR protocol: 94 °C for 2 min (1 cycle); 94 °C for 30 sec; 51.5 °C for 1 min; 72 °C for 45 sec (20 cycles) or (40 cycles); 72 °C for 5 min (1cycle) was used to generate full length genes by giving 20 cycles or 40 cycles for recombination (Supplementary Fig. S1). Fragments were subsequently purified with the Nucleospin kit.

4.6.1.4. Step 4: Replacement of degenerate base

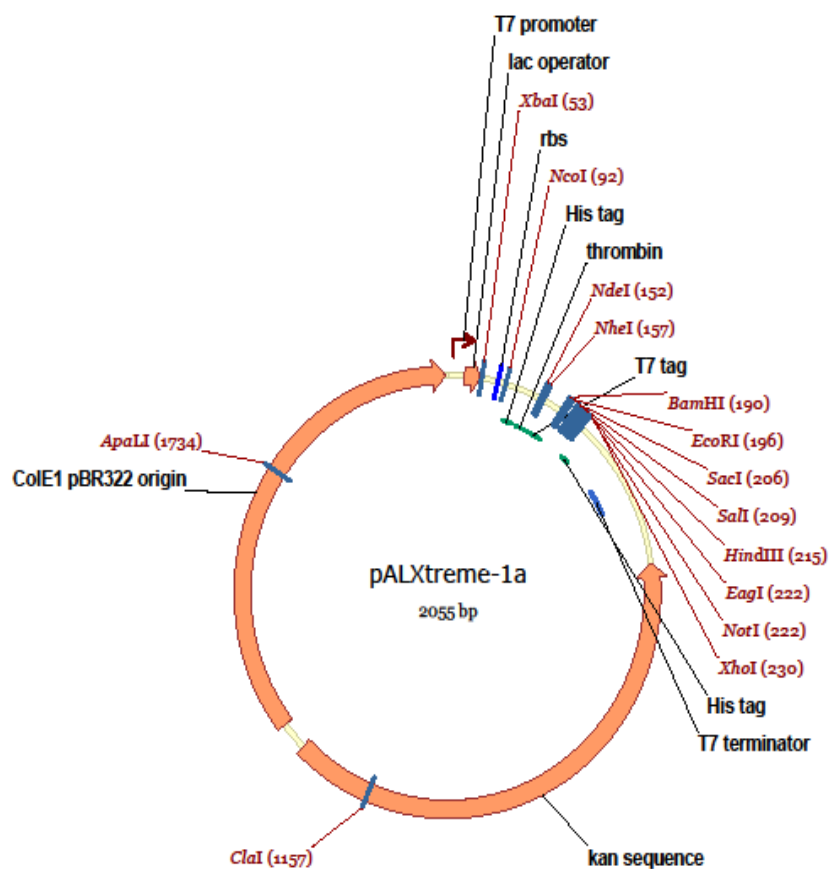
Replacement of the degenerate base by the standard nucleotides was done by a PCR amplification program. PCR reaction mixture (200 μ l) contained 25 pmol of primers SeSaM forward and SeSaM reverse; 2x QiagenTaq buffer; 10U Taq polymerase (Qiagen), 0.4 mM of each dNTP (Supplementary Fig. S1). This mixture was equally divided to which, 20 ng of purified step 3 PCR product (the step 3 amplified product obtained with either with 20 cycles or with 40 cycles) was added individually to check the mutational loads in the step 4 amplification. PCR program: 94 °C for 2 min (1 cycle); 94

°C for 30 sec; 59.5 °C for 30 sec; 72 °C for 30 sec (20 cycles); 72 °C for 5 min (1 cycle).
The resulting PCR products representing the final mutant library was gel extracted for cloning.

4.7. Supplementary Tables and Figures

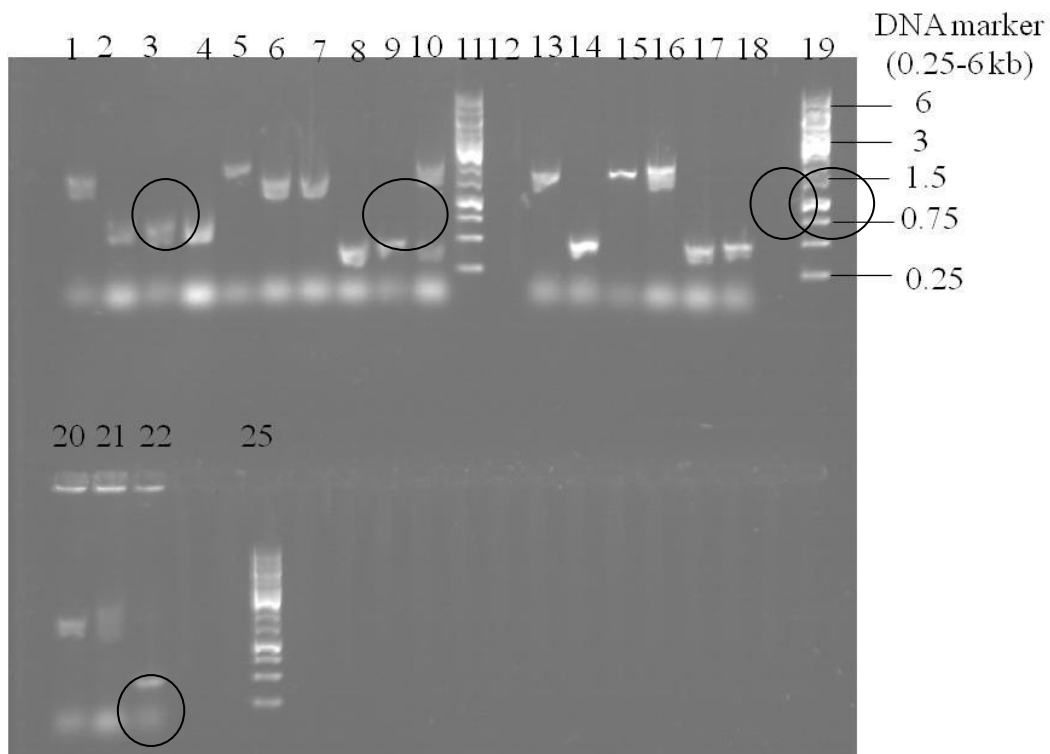


Supplementary figure 4.S1. Steps involved in SeSaM library preparation.

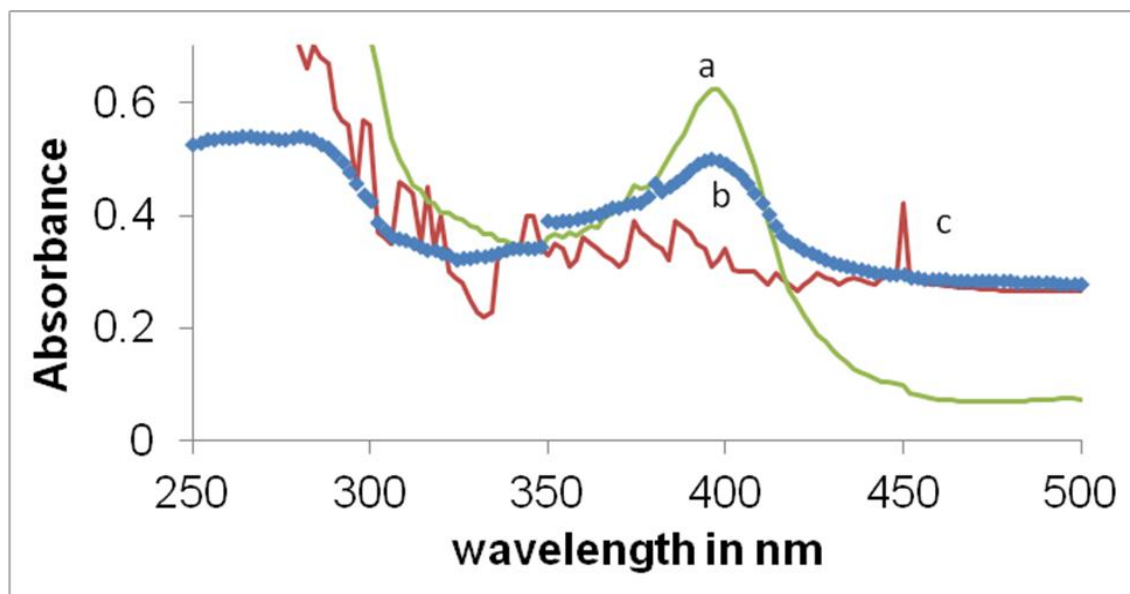


Supplementary figure 4.S2.
pET(+28a) vector

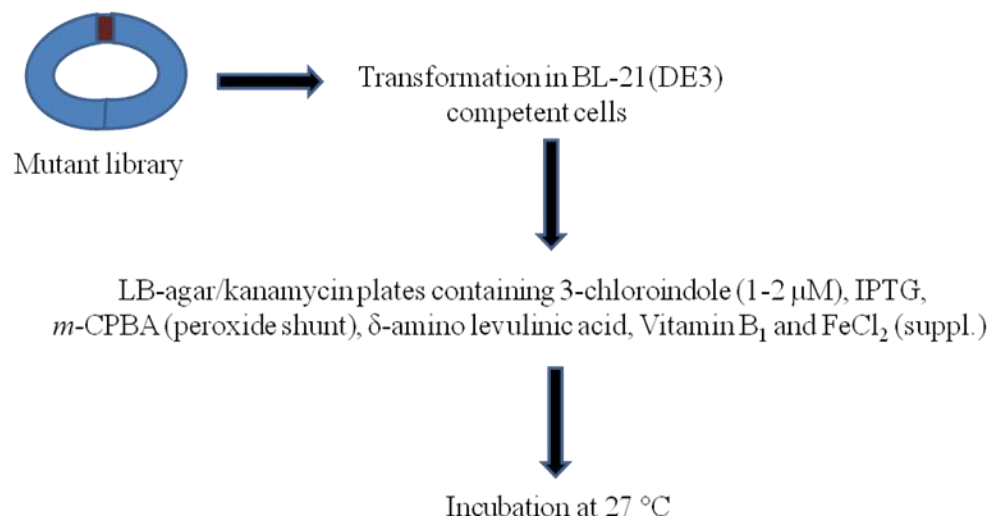
The vector map of pALXtreme-1a, an inhouse



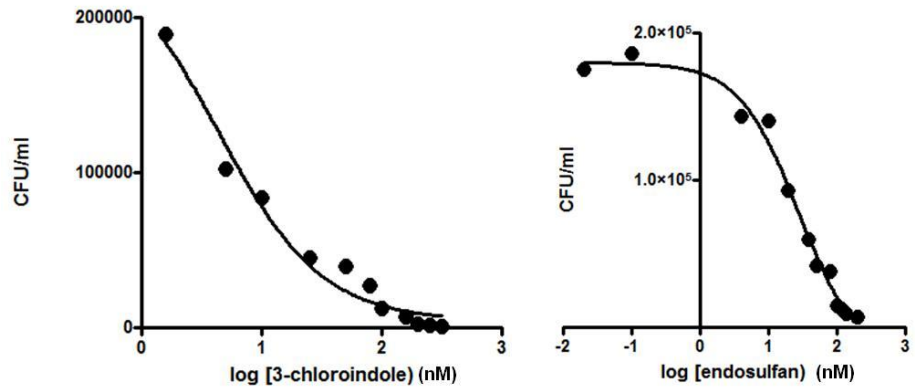
Supplementary figure 4.S3. 0.8% agarose gel analysis of culture PCR for the randomly picked clones from MEGAWHOP step 2 reaction. The positive clones are shown by circles. Lanes 11, 19 and 25 represent the DNA marker with molecular weights ranging from 0.25-6 kbp.



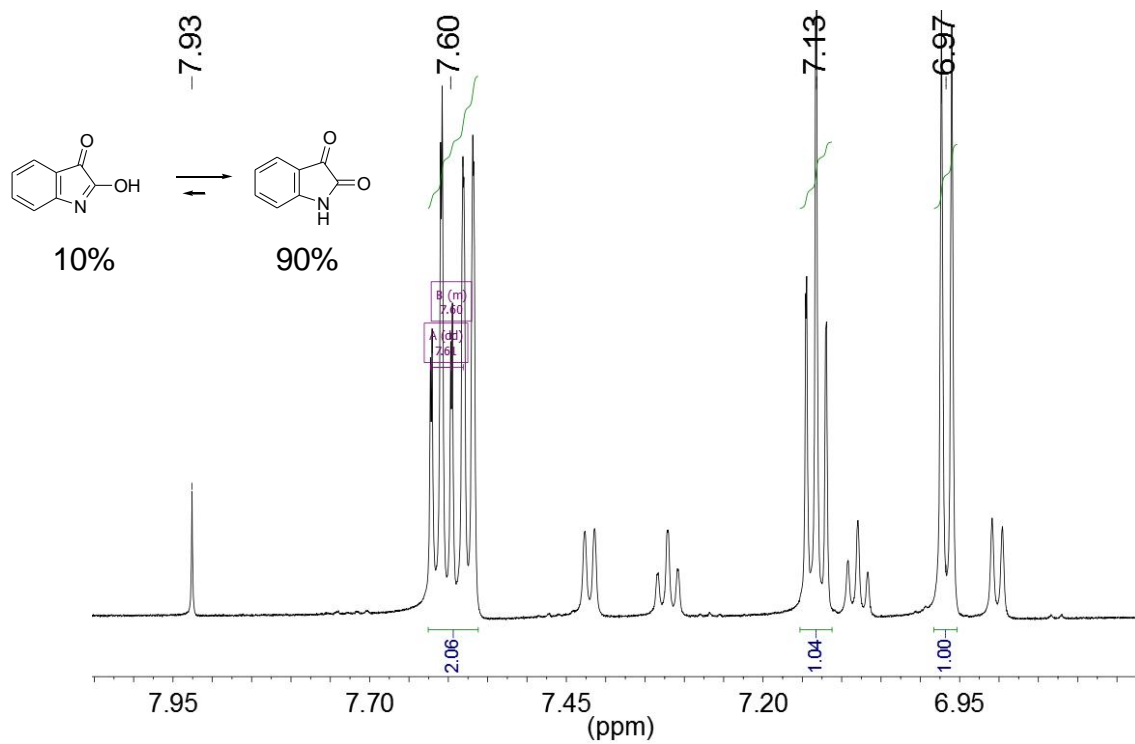
Supplementary figure 4.S4. Determination of Fe-CO absorbance at 450 nm a) The Soret peak of P450_{cam} was detected at 410 nm b) P450_{cam} was reduced by Na₂S₂O₄ and the intensity of Soret peak was reduced. c) CO was bubbled in the reduced protein for ~ 2 min and the absorption of Fe(II)-CO was recorded.



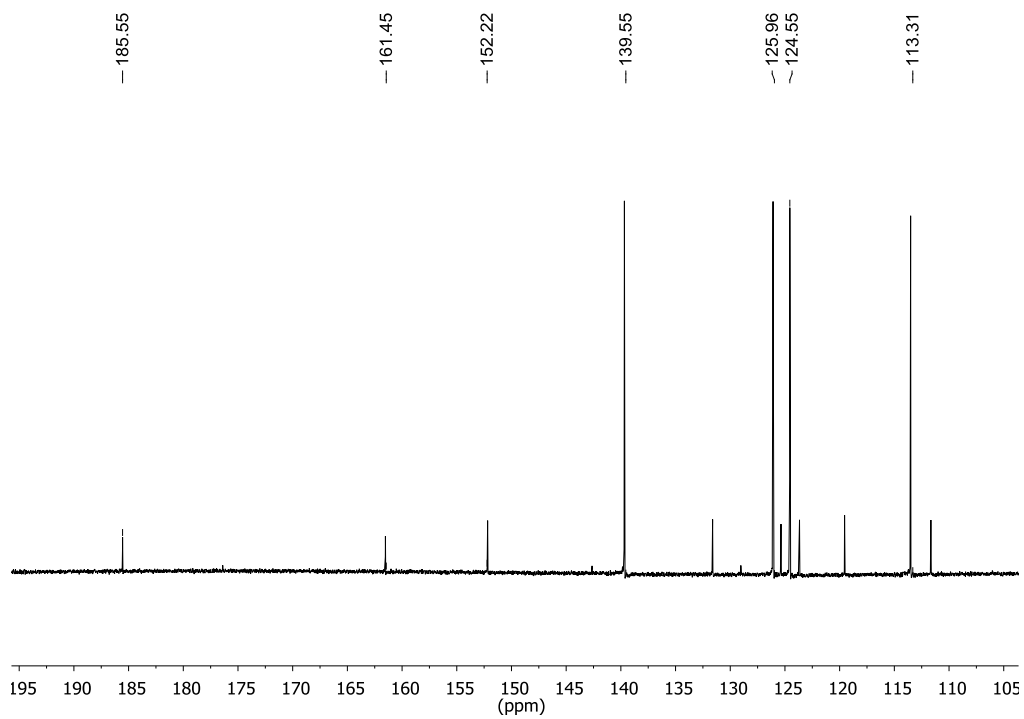
Supplementary figure 4.S5. Transformation of SeSaM P450_{cam} mutant library in BL21(DE3) cells and further screening with 3-chloroindole.



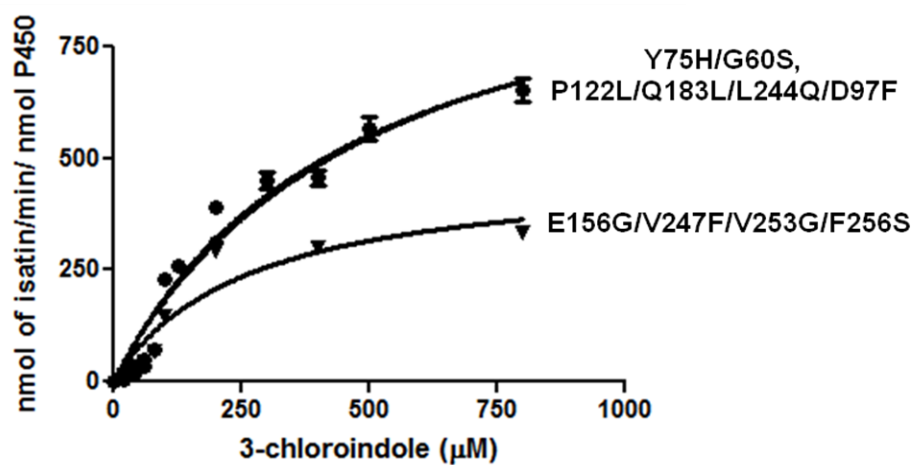
Supplementary figure 4.S6. IC_{50} experiments on *Escherichia coli* using varying concentrations of 3-chloroindole and endosulfan



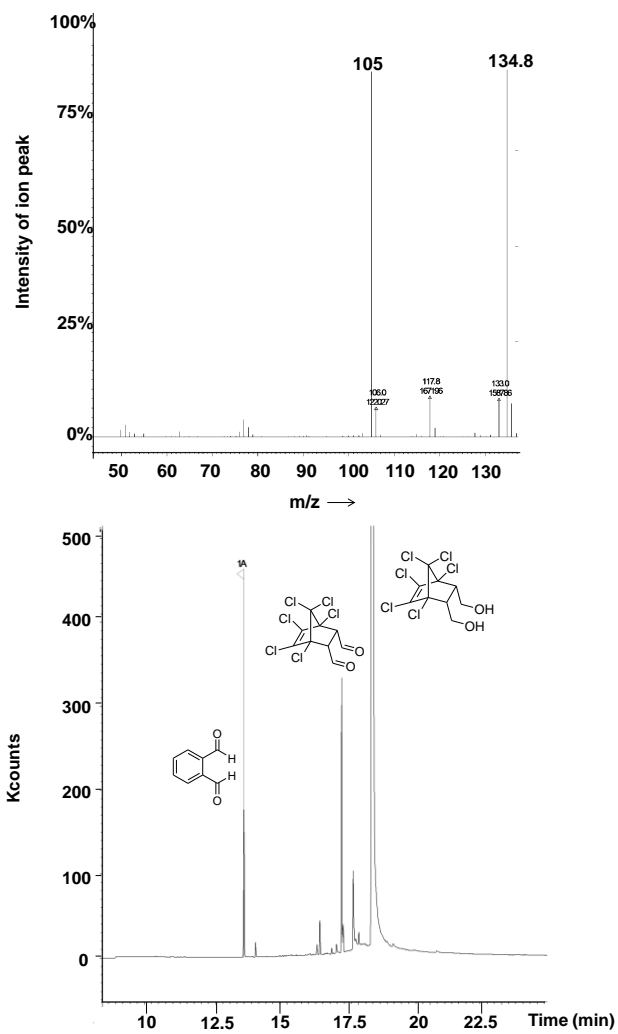
Supplementary figure 4.S7. ^1H NMR of isatin



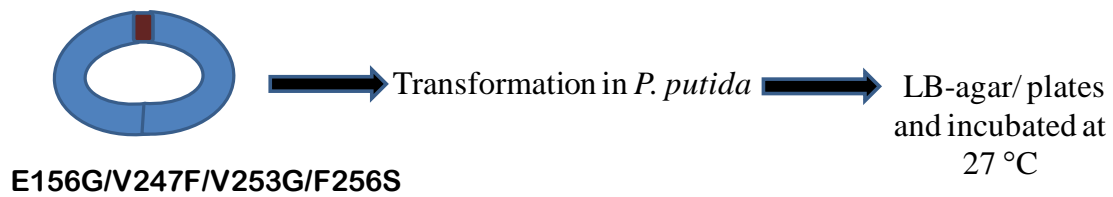
Supplementary figure 4.S8. ^{13}C NMR of isatin



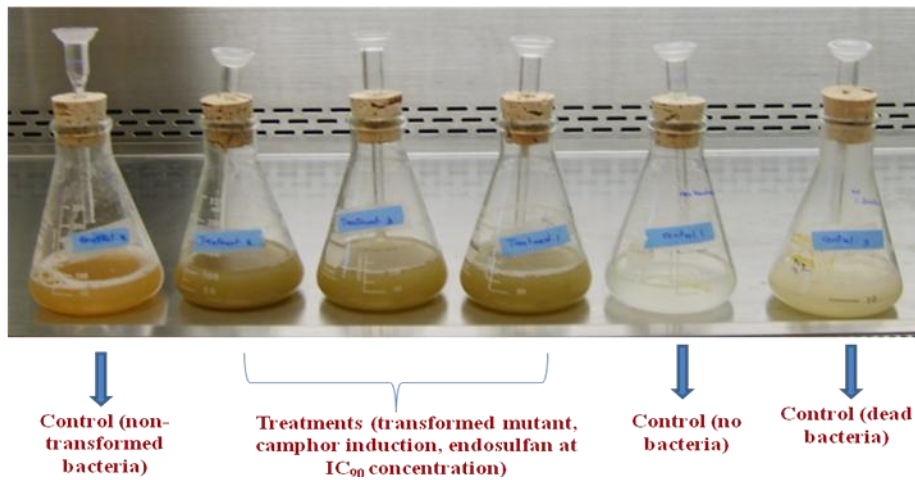
Supplementary figure 4.S9. Steady state kinetic analysis for 3-chloroindole oxidation and formation of isatin



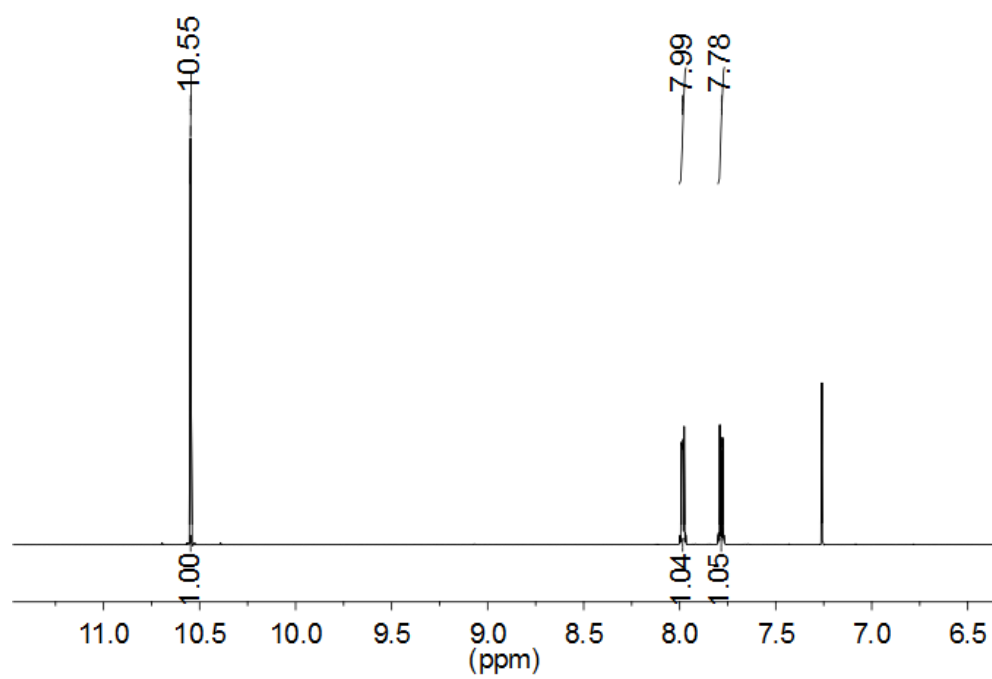
Supplementary figure 4.S10. *In vitro* assay results with endosulfan diol as the substrate under shunt conditions using *m*-CPBA and detection of metabolites by GC-MS. Endosulfan dialdehyde was detected as a major product.



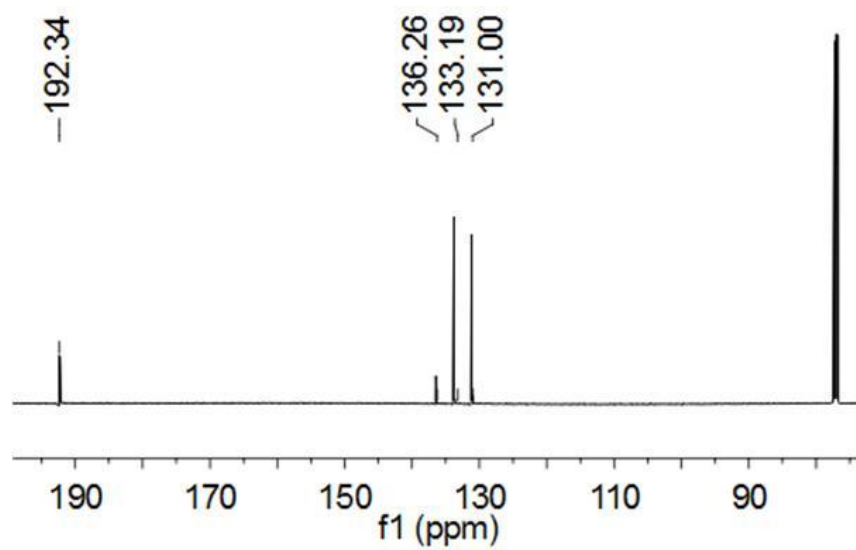
Supplementary figure 4.S11. Transformation of the mutant P450_{CAM} plasmid isolated from 3-chloroindole screen in *P. putida*. The cytochrome P450_{cam} hydroxylase operon present on the CAM plasmid of *P. putida* is responsible for the camphor degradation pathway



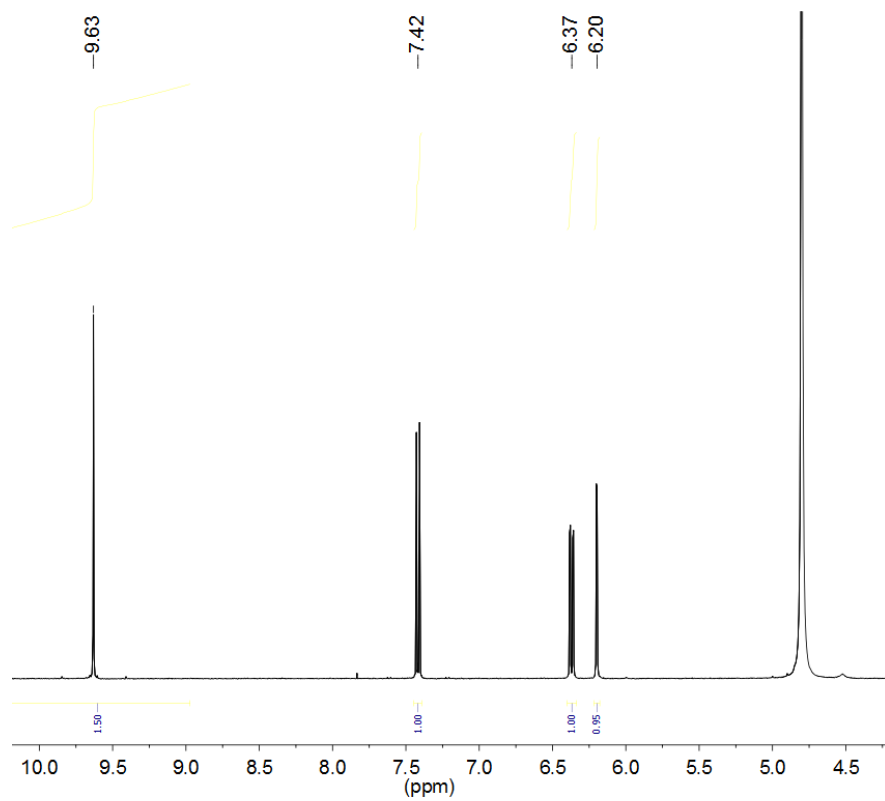
Supplementary figure 4.S12. Experimental design and apparatus for the endosulfan biodegradation experiment with mutant-transformed *P. putida*.



Supplementary figure 4.S13. ^1H NMR of pure phthalaldehyde obtained from *in vitro* assays and the biodegradation studies.



Supplementary figure 4.S14. ^{13}C NMR of pure phthalaldehyde obtained from *in vitro* assays and the biodegradation studies.



Supplementary figure 4.S15. ^1H NMR of 3-hydroxy phthalaldehyde obtained from *in vitro* assays and the biodegradation studies.

Table 4.S1. The results from SeSaM library validation

Aspect	Value
Mutation frequency (substitution/base)	2.7×10^{-3}
Ts/Tv (Transition/transversion)	0.6
% consecutive mutations in the sequenced clones	25
Fraction of stop codons	0.08
Fraction of Gly/Pro	0.16
% WT	0

^a 12 clones were randomly sequenced from both ends using T7 promoter and T7 terminator as primers.

Table 4.S2. List of mutants obtained from the endosulfan screen with their sequences

Screen	Clone	Sequence	Endosulfan dialdehyde (nmol/min/nmol P450)
	ES1	T56A/ N116H/D297N	22 ± 4
	ES2	F292S/A296V/K314E/P321T	25 ± 3
	ES3	Q108R/R290Q/I318N	11 ± 4
	ES4	S221R/I281N	15 ± 3
Endosulfan	ES5	A296P	12 ± 4
	ES6	G120S	12 ± 1
	ES7	V247F/D297N/K314E	52 ± 3

5. Future work

A) Experiments to prove the proposed reduction mechanism for the formation of borneol (borneol cycle):

The proposed reduction mechanism (Fig. 3.7) suggests that water present in the active site of the enzyme is responsible for formation of borneol and H₂O₂. The isotope labeled experiments (Fig. 3.2) and the steady-state kinetics (Fig. 3.6) in H₂O and D₂O were performed to verify borneol formation. The formation of hydrogen peroxide was verified by ¹⁷O NMR. The hypothesis shown in Fig. 3.7 involves compound I as an important intermediate in the borneol cycle. Although this mechanism is supported by NMR and kinetics experiments, a few more experiments can be planned for future studies.

i) Characterisation of compounds I and II, that form in the borneol cycle:

The first question that needs to be addressed is how one could verify if borneol cycle occurs in the active site of the enzyme. This question can't be answered by just the formation of products: borneol and H₂O₂. The involvement of compound I and compound II-H in the mechanism has not been shown experimentally, and observing these reactive intermediates would provide more evidence for the proposed mechanism.

The initial attempts to verify the shunt pathway was performed by Egawa et.al.²⁷⁵ in which the substrate free P450_{cam} and *m*-CPBA were mixed and rapid-scan stopped-flow studies were performed. The weak band at 694 nm and a blue-shifted Soret peak at 367 nm were assigned to a porphyrin π-cation radical. Recent attempts to characterize compound I by stopped-flow kinetics were performed by Green et.al.⁴⁶ In their experiments, the compound I was characterized 35 ms after mixing the ferric CYP119 (a P450 isolated from *Sulfolobus solfataricus*) and *m*-CPBA at 4 °C.

The important question that could be addressed with similar stopped-flow kinetics is how the presence or absence of O₂ affects the formation of compounds I or II. Recall that at high O₂ concentrations in the buffer, more hydroxylation products form (Fig. 3.1), whereas under anoxic conditions, the borneol cycle takes place (Figs. 3.1, 3.7). The two

reactions differ in the reaction of compound I: for hydroxylation compound I abstracts a H atom from the substrate, giving an alkyl radical and compound II-H. The hydroxylation product then forms by a rebound mechanism, in which the OH radical (effectively coordinated to Fe in compound II-H) joins with the carbon radical to furnish the alcohol. In the borneol cycle, compound I abstracts a H atom from water and then proceeds through the cycle as described in Chapter 3 (Fig. 3.7). The hydroxylation reaction was monitored by stopped-flow kinetics.^{79,276} Similar experiments can also be performed for borneol cycle to characterize the compound I and compound II by UV-Visible spectroscopy (stopped flow kinetics) and elucidate the low O₂ cycle mechanism. The main difficulty for this experiment includes the capturing of compound I and II-H intermediates as the lifespan of compound I is expected to be 35-100 ms.

ii) EPR experiments to identify the radical intermediates that form in borneol cycle:

The EPR characterization of compound-ES (Fig. 1.2) was performed by Schünemann et.al.²⁷⁷ In their experiment, the reaction mixture containing the substrate-free P450_{cam} and *m*-CPBA were freeze-quenched at -110 °C after a reaction time of 8 ms. Green et.al. have also reported the EPR measurements of compound I for CYP119 (a P450 isolated from *Sulfolobus solfataricus*).^{278,46} For this, the reaction mixture containing CYP119 and *m*-CPBA were freeze-quenched <25K and the formation of a new paramagnetic radical was assigned to compound I.

Similar experiments can also be planned with freeze-quenched P450_{cam}, *m*-CPBA and camphor to check for the formation of compounds I and II. One difficulty could be the overlapping signals between protein radical, compound I and *m*-chlorobenzoic radical and their assignments.

iii) Monitoring of borneol cycle by UV-Visible spectroscopy:

The reaction between *m*-CPBA and the resting P450 forms compound I, and its formation can be monitored by UV-Visible spectroscopy or by extraction and derivatization with BSTFA, followed by GC-MS quantitation to check for the formation of *meta*-chloro benzoic acid. If the borneol cycle occurs by the proposed mechanism (Fig. 3.7), very little *m*-CPBA will be used for the reaction as the compound I is regenerated. In that case, the excess *m*-CPBA may overlap signals with *m*-chloro benzoic acid, which

may cause difficulty in monitoring the reaction by UV spectroscopy. Monitoring by BSTFA derivatization and GC-MS will show the presence or absence of *m*-chlorobenzoic acid, provided the acid can be extracted quantitatively from the aqueous buffer.

iv) Energy-calculations of the intermediates of borneol cycle:

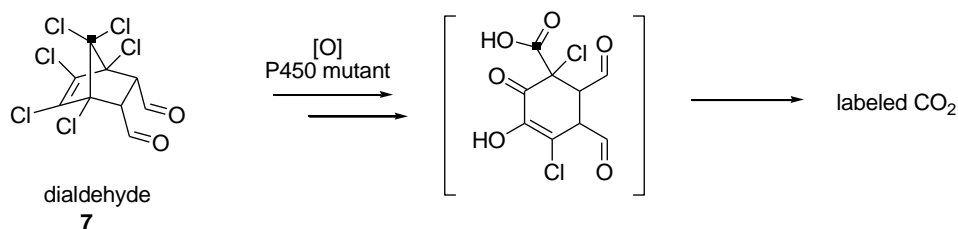
The thermodynamical calculations of the intermediates of borneol cycle (shown in Fig. 3.8) are estimates only. The energy estimates can be known better if the intermediates of the borneol cycle (Fig. 3.7) are simulated, using validated *ab initio* protocols. For now, only rough estimates were provided from the electrochemical data²⁷⁹ and Gaussian calculations.

B) Endosulfan dehalogenation:

Phthaldialdehyde, formed in the biodegradation process, was characterized by ¹H and ¹³C NMR. The phenolic intermediate (**23**) was also characterized recently. Still, additional experiments need to be performed to confirm that the phthaldialdehyde formed was indeed derived from endsulfan diol.

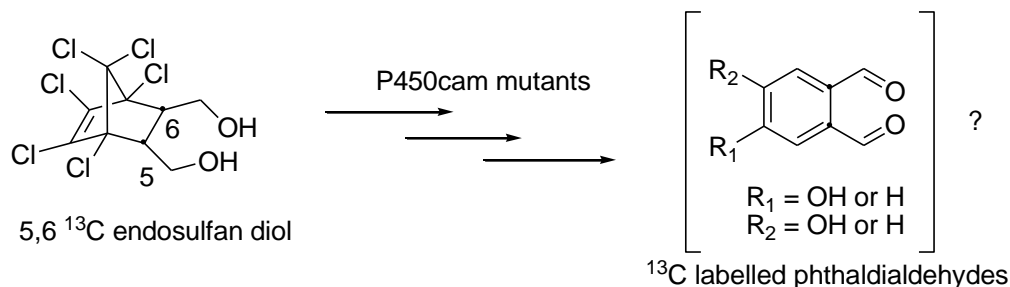
i) If the phenolic intermediate (**23**) is indeed an intermediate during the biodegradation process, enzymatic assays can be performed with the mutant IND1 under shunt conditions to verify if it and phthaldialdehyde form (also see v below). If the experiment is run in D₂O, and **23** forms from **19** (Figs. 4.9 and 4.10) and phthaldialdehyde (**25**) forms from **23** by a reduction akin to the borneol cycle described in Chapter 3, then compound **23** should be deuterated at the 4-position and phthaldialdehyde should be dideuterated at the 4 and 5 positions (see v below).

ii) The release of CO₂ in the biodegradation can be verified by ¹³C studies by labeling endsulfan dialdehyde. The Schematic representation of the reaction is shown below.



The 5-¹³C labeled hexachlorocyclopentadiene, which would be required to synthesize 7-¹³C endosulfan dialdehyde, is not available commercially. Therefore, this approach may not work due to practical difficulties.

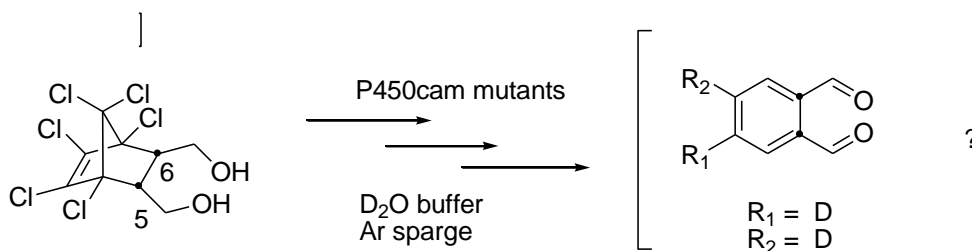
iii) To check the formation of phthaldialdehydes from endosulfan diol, an experiment with ¹³C labelled endosulfan diol can be planned. The (4+2) cyclization reaction of hexachlorocyclopentadiene and 2,3-¹³C maleic acid should give endosulfan diacid. Reduction of endosulfan diacid with LiAlH₄ can furnish the desired diol.



iv) To verify that all the chlorines are indeed eliminated as Cl⁻, detailed mass distribution experiments need to be done. In ³⁵Cl NMR, it is possible to quantify the amount of chloride present in the solution. Therefore, it should be possible to verify that 6 Cl⁻ are released from every endosulfan diol used and/or for every phthaldialdehyde produced. For such an assay to work, however, it is essential that all three phthaldialdehydes (**22**, **23** and **25**) be quantitatively extracted from the aqueous assay mixture.

v) To verify that water is indeed the source of H-atoms added to *o*-quinone **19**, the endosulfan diol dehalogenation reaction needs to be done in D₂O, under Ar sparge (to obtain the phthaldialdehyde preferentially). If the “borneol cycle” is responsible for the reduction, then we expect 2,3-dideuteriophthaldialdehyde to form. A control experiment

could be done with the P450 mutant, PdX, PdR and NADD. If the “borneol cycle” is active, then we do not expect to see deuteriated phthalaldehyde in these controls.



vi) Monitoring of the biodegradation reaction: If the UV/visible peak absorbances of the intermediates (**23** and **25**) are known and if distinct, then this reaction can also be studied by stopped-flow kinetics.

vii) To further verify the mechanism of endosulfan dehalogenation, steady-state kinetics need to be done in normal and D_2O buffers, under O_2 pressure and under Ar pressure, just as was done in Chapter 3. This will help us check for O_2 dependence of the reduction steps and provide indirect evidence that a process similar to the borneol cycle occurs in the dehalogenation mutants as well.

6. References

- (1) De Montellano, P. R. O. *Structural studies on prokaryotic P450s* **1995**, Second edition.
- (2) White, R. E.; Coon, M. J. *Annu Rev Biochem* **1980**, *49*, 315-56.
- (3) Sligar, S. G.; Lipscomb, J. D.; Debrunner, P. G.; Gunsalus, I. C. *Biochem. Biophys. Res. Commun* **1974**, *61*, 290-6.
- (4) Sligar, S. G.; Makris, T. M.; Denisov, I. G. *Biochem. Biophys. Res. Commun* **2005**, *338*, 346-354.
- (5) Blanksby, S. J.; Ellison, G. B. *Acc Chem Res* **2003**, *36*, 255-63.
- (6) Bathelt, C. M.; Ridder, L.; Mulholland, A. J.; Harvey, J. N. *Org Biomol Chem* **2004**, *2*, 2998-3005.
- (7) Groves, J. T.; Vanderpuy, M. *J. Am. Chem. Soc.* **1976**, *98*, 5290-5297.
- (8) Lonsdale, R.; Harvey, J. N.; Mulholland, A. J. *J Phys Chem B*, **2010**, *114*, 1156-62.
- (9) Yoshioka, S.; Takahashi, S.; Ishimori, K.; Morishima, I. *J Inorg Biochem* **2000**, *81*, 141-51.
- (10) Riley, P.; Hanzlik, R. P. *Xenobiotica* **1994**, *24*, 1-16.
- (11) Sono, M.; Roach, M. P.; Coulter, E. D.; Dawson, J. H. *Chem Rev* **1996**, *96*, 2841-2888.
- (12) Ryan, K. J. *Biochim Biophys Acta* **1958**, *27*, 658-9.
- (13) Smith, J. R. L.; Sleath, P. R. *J. Chem. Soc.-Perkin Transac* **1983**, *2*, 1165-1169.
- (14) Smith, J. R. L.; Piggott, R. E.; Sleath, P. R. *Journal of the Chemical Society-Chemical Communications* **1982**, 55-56.
- (15) Smith, J. R. L.; Mortimer, D. N. *Journal of the Chemical Society-Chemical Communications* **1985**, 64-65.
- (16) Schlichting, I.; Berendzen, J.; Chu, K.; Stock, A. M.; Maves, S. A.; Benson, D. E.; Sweet, R. M.; Ringe, D.; Petsko, G. A.; Sligar, S. G. *Science* **2000**, *287*, 1615-22.
- (17) Poulos, T. L.; Finzel, B. C.; Gunsalus, I. C.; Wagner, G. C.; Kraut, J. *J Biol Chem* **1985**, *260*, 16122-30.

- (18) Poulos, T. L.; Finzel, B. C.; Howard, A. J. *Biochemistry* **1986**, *25*, 5314-22.
- (19) Lewis, D. F.; Hlavica, P. *Biochim Biophys Acta* **2000**, *1460*, 353-74.
- (20) Nelson, D. R. *Hum Genomics* **2009**, *4*, 59-65.
- (21) Holden, M.; Mayhew, M.; Bunk, D.; Roitberg, A.; Vilker, V. *J Biol Chem* **1997**, *272*, 21720-5.
- (22) Roome, P. W., Jr.; Philley, J. C.; Peterson, J. A. *J Biol Chem* **1983**, *258*, 2593-8.
- (23) Roome, P. W.; Peterson, J. A. *Arch Biochem Biophys* **1988**, *266*, 41-50.
- (24) Tyson, C. A.; Lipscomb, J. D.; Gunsalus, I. C. *J Biol Chem* **1972**, *247*, 5777-84.
- (25) Katagiri, M.; Ganguli, B. N.; Gunsalus, I. C. *J. Biol. Chem* **1968**, *243*, 3543-6.
- (26) Fruetel, J. A.; Mackman, R. L.; Peterson, J. A.; Ortiz de Montellano, P. R. *J Biol Chem* **1994**, *269*, 28815-21.
- (27) Adamovich, T. B.; Pikuleva, I. A.; Chashchin, V. L.; Usanov, S. A. *Biochim Biophys Acta* **1989**, *996*, 247-53.
- (28) Matson, R. S.; Hare, R. S.; Fulco, A. J. *Biochim Biophys Acta* **1977**, *487*, 487-94.
- (29) Narhi, L. O.; Fulco, A. J. *J Biol Chem* **1986**, *261*, 7160-9.
- (30) Cho, K. B.; Lai, W.; Hamberg, M.; Raman, C. S.; Shaik, S. *Arch Biochem Biophys*, **2011**, *507*, 14-25.
- (31) Haurand, M.; Ullrich, V. *J Biol Chem* **1985**, *260*, 15059-67.
- (32) Miyata, A.; Hara, S.; Yokoyama, C.; Inoue, H.; Ullrich, V.; Tanabe, T. *Biochem Biophys Res Commun* **1994**, *200*, 1728-34.
- (33) Nebert, D. W.; Adesnik, M.; Coon, M. J.; Estabrook, R. W.; Gonzalez, F. J.; Guengerich, F. P.; Gunsalus, I. C.; Johnson, E. F.; Kemper, B.; Levin, W.; et al. *DNA* **1987**, *6*, 1-11.
- (34) Nelson, D. R. *Methods Mol Biol* **1998**, *107*, 15-24.
- (35) Gotoh, O. *Biol Pharm Bull*, **2012**, *35*, 812-7.
- (36) Sligar, S. G.; Gunsalus, I. C. *Proc Natl Acad Sci U S A* **1976**, *73*, 1078-82.
- (37) Guallar, V.; Friesner, R. A. *J Am Chem Soc* **2004**, *126*, 8501-8.
- (38) Schlichting, I.; Berendzen, J.; Chu, K.; Stock, A. M.; Maves, S. A.; Benson, D. E.; Sweet, B. M.; Ringe, D.; Petsko, G. A.; Sligar, S. G. *Science* **2000**, *287*, 1615-1622.
- (39) Davydov, R.; Makris, T. M.; Kofman, V.; Werst, D. E.; Sligar, S. G.; Hoffman, B. M. *J Am Chem Soc* **2001**, *123*, 1403-15.

- (40) Sligar, S. G. *Science*, **2010**, 330, 924-5.
- (41) Luthra, A.; Denisov, I. G.; Sligar, S. G. *Arch Biochem Biophys*, **2011**, 507, 26-35.
- (42) Guengerich, F. P.; Isin, E. M. *Acta Chimica Slovenica* **2008**, 55, 7-19.
- (43) Shaik, S.; Cohen, S.; Wang, Y.; Chen, H.; Kumar, D.; Thiel, W. *Chem Rev*, **2010**, 110, 949-1017.
- (44) Newcomb, M.; Toy, P. H. *Acc Chem Res* **2000**, 33, 449-55.
- (45) Altun, A.; Shaik, S.; Thiel, W. *J. Am. Chem. Soc.* **2007**, 129, 8978-8987.
- (46) Rittle, J.; Green, M. T. *Science*, **2010**, 330, 933-7.
- (47) Akhtar, M.; Wright, J. N. *Nat Prod Rep* **1991**, 8, 527-51.
- (48) Cryle, M. J.; De Voss, J. J. *Angew Chem Int Ed Engl* **2006**, 45, 8221-3.
- (49) Ortiz de Montellano, P. R.; Nelson, S. D. *Arch Biochem Biophys*, **2011**, 507, 95-110.
- (50) Newcomb, M.; Zhang, R.; Chandrasena, R. E.; Halgrimson, J. A.; Horner, J. H.; Makris, T. M.; Sligar, S. G. *J Am Chem Soc* **2006**, 128, 4580-1.
- (51) Newcomb, M.; Halgrimson, J. A.; Horner, J. H.; Wasinger, E. C.; Chen, L. X.; Sligar, S. G. *Proc Natl Acad Sci U S A* **2008**, 105, 8179-84.
- (52) Chefson, A.; Zhao, J.; Auclair, K. *Chembiochem* **2006**, 7, 916-9.
- (53) Kim, S. J.; Latifi, R.; Kang, H. Y.; Nam, W.; de Visser, S. P. *Chem Commun (Camb)* **2009**, 1562-4.
- (54) Pratt, J. M.; Ridd, T. I.; King, L. J. *Journal of the Chemical Society-Chemical Communications* **1995**, 2297-2298.
- (55) Chefson, A.; Auclair, K. *Mol Biosyst* **2006**, 2, 462-9.
- (56) Spolitak, T.; Dawson, J. H.; Ballou, D. P. *J Biol Chem* **2005**, 280, 20300-9.
- (57) Miller, R. E.; Guengerich, F. P. *Biochemistry* **1982**, 21, 1090-1097.
- (58) Meesters, R. J.; Duisken, M.; Hollender, J. *Xenobiotica* **2009**, 39, 663-71.
- (59) Chowdhury, G.; Calcutt, M. W.; Guengerich, F. P. *J Biol Chem*, **2010**, 285, 8031-44.
- (60) Smith, J. R. L.; Sleath, P. R. *J. Chem. Soc.-Perkin Transac* **1983**, 2, 621-628.
- (61) Rettie, A. E.; Rettenmeier, A. W.; Howald, W. N.; Baillie, T. A. *Science* **1987**, 235, 890-893.

- (62) Chadwick, R. W.; Chuang, L. T.; Williams, K. *Pesticide Biochemistry and Physiology* **1975**, *5*, 575-586.
- (63) Hata, S.; Nishino, T.; Katsuki, H.; Aoyama, Y.; Yoshida, Y. *Biochem. Biophys. Res. Commun* **1983**, *116*, 162-166.
- (64) Boyd, D. R.; Sharma, N. D.; Agarwal, R.; McMordie, R. A. S.; Bessems, J. G. M.; Vanommen, B.; Vanbladeren, P. J. *Chemical Research in Toxicology* **1993**, *6*, 808-812.
- (65) Bigi, M. A.; Reed, S. A.; White, M. C. *Nat Chem*, **2011**, *3*, 216-22.
- (66) Behrouzian, B.; Buist, P. H. *Prostaglandins Leukot Essent Fatty Acids* **2003**, *68*, 107-12.
- (67) Kim, T. W.; Hwang, J. Y.; Kim, Y. S.; Joo, S. H.; Chang, S. C.; Lee, J. S.; Takatsuto, S.; Kim, S. K. *Plant Cell* **2005**, *17*, 2397-2412.
- (68) Roberts, S. M.; Wan, P. W. H. *Journal of Molecular Catalysis B-Enzymatic* **1998**, *4*, 111-136.
- (69) Fraaije, M. W.; Kamerbeek, N. M.; van Berkel, W. J.; Janssen, D. B. *FEBS Lett* **2002**, *518*, 43-7.
- (70) Tan, L.; Muto, N. *Eur J Biochem* **1986**, *156*, 243-50.
- (71) Walsh, M. E.; Kyritsis, P.; Eady, N. A. J.; Hill, H. A. O.; Wong, L. L. *European Journal of Biochemistry* **2000**, *267*, 5815-5820.
- (72) Yanagita, K.; Sagami, I.; Shimizu, T. *Archives of Biochemistry and Biophysics* **1997**, *346*, 269-276.
- (73) Reed, J. R.; Vanderwel, D.; Choi, S.; Pomonis, J. G.; Reitz, R. C.; Blomquist, G. J. *Proc Natl Acad Sci U S A* **1994**, *91*, 10000-4.
- (74) Qiu, Y.; Tittiger, C.; Wicker-Thomas, C.; Le Goff, G.; Young, S.; Wajnberg, E.; Fricaux, T.; Taquet, N.; Blomquist, G. J.; Feyereisen, R. *Proc Natl Acad Sci U S A*, *109*, 14858-63.
- (75) Schirmer, A.; Rude, M. A.; Li, X.; Popova, E.; del Cardayre, S. B. *Science* **2010**, *329*, 559-62.
- (76) Warui, D. M.; Li, N.; Norgaard, H.; Krebs, C.; Bollinger, J. M., Jr.; Booker, S. J. *J Am Chem Soc*, **2011**, *133*, 3316-9.
- (77) Das, D.; Eser, B. E.; Han, J.; Sciore, A.; Marsh, E. N. *Angew Chem Int Ed Engl*, **2011**, *50*, 7148-52.
- (78) Ahmet Altun, S. S. a. W. T. *J.A.C.S.* **2007**, *129*, 8978-8987.
- (79) Davydov, R.; Macdonald, I. D. G.; Makris, T. M.; Sligar, S. G.; Hoffman, B. M. *J. Am. Chem. Soc.* **1999**, *121*, 10654-10655.

- (80) Poulos, T. L.; Finzel, B. C.; Howard, A. J. *J Mol Biol* **1987**, *195*, 687-700.
- (81) Ravichandran, K. G.; Boddupalli, S. S.; Hasemann, C. A.; Peterson, J. A.; Deisenhofer, J. *Science* **1993**, *261*, 731-6.
- (82) Hasemann, C. A.; Ravichandran, K. G.; Peterson, J. A.; Deisenhofer, J. *J Mol Biol* **1994**, *236*, 1169-85.
- (83) Cupp-Vickery, J. R.; Li, H.; Poulos, T. L. *Proteins* **1994**, *20*, 197-201.
- (84) DeVore, N. M.; Scott, E. E. *Nature*, **2012**, *482*, 116-9.
- (85) Wester, M. R.; Yano, J. K.; Schoch, G. A.; Yang, C.; Griffin, K. J.; Stout, C. D.; Johnson, E. F. *J Biol Chem* **2004**, *279*, 35630-7.
- (86) Aldag, C.; Gromov, I. A.; Garcia-Rubio, I.; von Koenig, K.; Schlichting, I.; Jaun, B.; Hilvert, D. *Proc Natl Acad Sci U S A* **2009**, *106*, 5481-6.
- (87) Sakurai, K.; Shimada, H.; Hayashi, T.; Tsukihara, T. *Acta Crystallogr Sect F Struct Biol Cryst Commun* **2009**, *65*, 80-3.
- (88) Wade, R. C.; Winn, P. J.; Schlichting, I.; Sudarko *J Inorg Biochem* **2004**, *98*, 1175-82.
- (89) Raag, R.; Poulos, T. L. *Biochemistry* **1989**, *28*, 917-22.
- (90) Di Primo, C.; Hui Bon Hoa, G.; Douzou, P.; Sligar, S. *Eur J Biochem* **1990**, *193*, 383-6.
- (91) Di Primo, C.; Hui Bon Hoa, G.; Douzou, P.; Sligar, S. *J Biol Chem* **1990**, *265*, 5361-3.
- (92) Harris, D. L.; Loew, G. H. *J Am Chem Soc* **1994**, *116*, 11671-4.
- (93) Munro, A. W.; Leys, D. G.; McLean, K. J.; Marshall, K. R.; Ost, T. W.; Daff, S.; Miles, C. S.; Chapman, S. K.; Lysek, D. A.; Moser, C. C.; Page, C. C.; Dutton, P. L. *Trends Biochem Sci* **2002**, *27*, 250-7.
- (94) Efimov, I.; Badyal, S. K.; Metcalfe, C. L.; Macdonald, I.; Gumiero, A.; Raven, E. L.; Moody, P. C. *J Am Chem Soc*, **2011**, *133*, 15376-83.
- (95) Morozov, A. N.; D'Cunha, C.; Alvarez, C. A.; Chatfield, D. C. *Biophys J*, **2011**, *100*, 1066-75.
- (96) Raag, R.; Poulos, T. L. *Biochemistry* **1989**, *28*, 7586-92.
- (97) Raag, R.; Martinis, S. A.; Sligar, S. G.; Poulos, T. L. *Biochemistry* **1991**, *30*, 11420-9.
- (98) Imai, M.; Shimada, H.; Watanabe, Y.; Matsushima-Hibiya, Y.; Makino, R.; Koga, H.; Horiuchi, T.; Ishimura, Y. *Proc Natl Acad Sci U S A* **1989**, *86*, 7823-7.

- (99) Jin, S.; Makris, T. M.; Bryson, T. A.; Sligar, S. G.; Dawson, J. H. *J Am Chem Soc* **2003**, *125*, 3406-7.
- (100) Mehareenna, Y. T.; Li, H.; Hawkes, D. B.; Pearson, A. G.; De Voss, J.; Poulos, T. L. *Biochemistry* **2004**, *43*, 9487-94.
- (101) Galinato, M. G.; Spolitak, T.; Ballou, D. P.; Lehnert, N. *Biochemistry*, **2011**, *50*, 1053-69.
- (102) Yoshioka, S.; Takahashi, S.; Hori, H.; Ishimori, K.; Morishima, I. *Eur J Biochem* **2001**, *268*, 252-9.
- (103) Davydov, R.; Makris, T. M.; Kofman, V.; Werst, D. E.; Sligar, S. G.; Hoffman, B. M. *J. Am. Chem. Soc.* **2001**, *123*, 1403-1415.
- (104) Dietrich, M.; Do, T. A.; Schmid, R. D.; Pleiss, J.; Urlacher, V. B. *J Biotechnol* **2009**, *139*, 115-7.
- (105) Speight, R. E.; Hancock, F. E.; Winkel, C.; Bevinakatti, H. S.; Sarkar, M.; Flitsch, S. L.; Turner, N. J. *Tetrahedron-Asymmetry* **2004**, *15*, 2829-2831.
- (106) Bell, S. G.; Stevenson, J. A.; Boyd, H. D.; Campbell, S.; Riddle, A. D.; Orton, E. L.; Wong, L. L. *Chemical Communications* **2002**, 490-491.
- (107) Bell, S. G.; Orton, E.; Boyd, H.; Stevenson, J. A.; Riddle, A.; Campbell, S.; Wong, L. L. *Dalton Transactions* **2003**, 2133-2140.
- (108) Wong, T. S.; Wu, N.; Roccatano, D.; Zacharias, M.; Schwaneberg, U. *Journal of Biomolecular Screening* **2005**, *10*, 246-252.
- (109) Stevenson, J. A.; Bearpark, J. K.; Wong, L. L. *New Journal of Chemistry* **1998**, *22*, 551-552.
- (110) Dunn, A. R.; Dmochowski, I. J.; Bilwes, A. M.; Gray, H. B.; Crane, B. R. *Proc Natl Acad Sci U S A* **2001**, *98*, 12420-5.
- (111) Harford-Cross, C. F.; Carmichael, A. B.; Allan, F. K.; England, P. A.; Rouch, D. A.; Wong, L. L. *Protein Eng* **2000**, *13*, 121-8.
- (112) Fowler, S. M.; England, P. A.; Westlake, A. C. G.; Rouch, D. R.; Nickerson, D. P.; Blunt, C.; Braybrook, D.; West, S.; Wong, L. L.; Flitsch, S. L. *Journal of the Chemical Society-Chemical Communications* **1994**, 2761-2762.
- (113) Hoffmann, G.; Bonsch, K.; Greiner-Stoffele, T.; Ballschmiter, M. *Protein Engineering Design & Selection* **2011**, *24*, 439-446.
- (114) Sowden, R. J.; Yasmin, S.; Rees, N. H.; Bell, S. G.; Wong, L. L. *Org Biomol Chem* **2005**, *3*, 57-64.
- (115) Carpenter, D. O. *Int J Occup Med Environ Health* **1998**, *11*, 291-303.
- (116) Fetzner, S.; Lingens, F. *Microbiol Rev* **1994**, *58*, 641-85.

- (117) Lee, P. H.; Ong, S. K.; Golchin, J.; Nelson, G. L. *Water Res* **2001**, *35*, 3941-9.
- (118) Radehaus, P. M.; Schmidt, S. K. *Appl Environ Microbiol* **1992**, *58*, 2879-85.
- (119) Xu, F.; Bell, S. G.; Rao, Z.; Wong, L. L. *Protein Engineering Design & Selection* **2007**, *20*, 473-480.
- (120) England, P. A.; Rouch, D. A.; Westlake, A. C. G.; Bell, S. G.; Nickerson, D. P.; Webberley, M.; Flitsch, S. L.; Wong, L. L. *Chemical Communications* **1996**, 357-358.
- (121) Mayhew, M. P.; Roitberg, A. E.; Tewari, Y.; Holden, M. J.; Vanderah, D. J.; Vilker, V. L. *New Journal of Chemistry* **2002**, *26*, 35-42.
- (122) Xu, F.; Bell, S. G.; Rao, Z.; Wong, L. L. *Protein Eng Des Sel* **2007**, *20*, 473-80.
- (123) Sen, S.; Manna, S. K.; Mazumdar, S. *Indian Journal of Chemistry Section a-Inorganic Bio-Inorganic Physical Theoretical & Analytical Chemistry* **2011**, *50*, 438-446.
- (124) Jones, J. P.; O'Hare, E. J.; Wong, L. L. *Chemical Communications* **2000**, 247-248.
- (125) Nelson, D.; Werck-Reichhart, D. *Plant J*, **2011**, *66*, 194-211.
- (126) Mizutani, M.; Ohta, D. *Annu Rev Plant Biol*, **2010**, *61*, 291-315.
- (127) Saito, S.; Hirai, N.; Matsumoto, C.; Ohigashi, H.; Ohta, D.; Sakata, K.; Mizutani, M. *Plant Physiol* **2004**, *134*, 1439-49.
- (128) Booker, J.; Sieberer, T.; Wright, W.; Williamson, L.; Willett, B.; Stirnberg, P.; Turnbull, C.; Srinivasan, M.; Goddard, P.; Leyser, O. *Dev Cell* **2005**, *8*, 443-9.
- (129) Seki, H.; Ohyama, K.; Sawai, S.; Mizutani, M.; Ohnishi, T.; Sudo, H.; Akashi, T.; Aoki, T.; Saito, K.; Muranaka, T. *Proc Natl Acad Sci U S A* **2008**, *105*, 14204-9.
- (130) Morant, M.; Bak, S.; Moller, B. L.; Werck-Reichhart, D. *Curr Opin Biotechnol* **2003**, *14*, 151-62.
- (131) Yoshiyama, T.; Namiki, T.; Mita, K.; Kataoka, H.; Niwa, R. *Development* **2006**, *133*, 2565-74.
- (132) Gilbert, L. I.; Warren, J. T. *Vitam Horm* **2005**, *73*, 31-57.
- (133) Otey, C. R.; Bandara, G.; Lalonde, J.; Takahashi, K.; Arnold, F. H. *Biotechnol Bioeng* **2006**, *93*, 494-9.
- (134) Kumar, S.; Scott, E. E.; Liu, H.; Halpert, J. R. *J Biol Chem* **2003**, *278*, 17178-84.
- (135) Yun, C. H.; Kim, K. H.; Kim, D. H.; Jung, H. C.; Pan, J. G. *Trends Biotechnol* **2007**, *25*, 289-98.
- (136) Park, S. H.; Kim, D. H.; Kim, D.; Jung, H. C.; Pan, J. G.; Ahn, T.; Yun, C. H. *Drug Metab Dispos*, *38*, 732-9.

- (137) Chefson, A.; Zhao, J.; Auclair, K. *Chembiochem* **2006**, *7*, 916-919.
- (138) van der Donk, W. A.; Zhao, H. *Curr Opin Biotechnol* **2003**, *14*, 421-6.
- (139) Ryan, J. D.; Fish, R. H.; Clark, D. S. *Chembiochem* **2008**, *9*, 2579-82.
- (140) O'Reilly, E.; Kohler, V.; Flitsch, S. L.; Turner, N. J. *Chem Commun (Camb)*, **2011**, *47*, 2490-501.
- (141) Faulkner, K. M.; Shet, M. S.; Fisher, C. W.; Estabrook, R. W. *Proc Natl Acad Sci U S A* **1995**, *92*, 7705-9.
- (142) Cirino, P. C.; Arnold, F. H. *Angew Chem Int Ed Engl* **2003**, *42*, 3299-301.
- (143) Jensen, K.; Johnston, J. B.; de Montellano, P. R. O.; Moller, B. L. *Biotechnology Letters* **2012**, *34*, 239-245.
- (144) Jensen, K.; Jensen, P. E.; Moller, B. L. *Acs Chemical Biology* **2011**, *6*, 533-539.
- (145) O'Reilly, E.; Kohler, V.; Flitsch, S. L.; Turner, N. J. *Chemical Communications* **2011**, *47*, 2490-2501.
- (146) Cirino, P. C.; Arnold, F. H. *Curr Opin Chem Biol* **2002**, *6*, 130-5.
- (147) Fasan, R.; Chen, M. M.; Crook, N. C.; Arnold, F. H. *Angew Chem Int Ed Engl* **2007**, *46*, 8414-8.
- (148) Weber, E.; Seifert, A.; Antonovici, M.; Geinitz, C.; Pleiss, J.; Urlacher, V. B. *Chem Commun (Camb)*, **2011**, *47*, 944-6.
- (149) Carmichael, A. B.; Wong, L. L. *Eur J Biochem* **2001**, *268*, 3117-25.
- (150) Misawa, N.; Nodate, M.; Otomatsu, T.; Shimizu, K.; Kaido, C.; Kikuta, M.; Ideno, A.; Ikenaga, H.; Ogawa, J.; Shimizu, S.; Shindo, K. *Appl Microbiol Biotechnol*, **2011**, *90*, 147-57.
- (151) Zhang, K.; El Damaty, S.; Fasan, R. *J Am Chem Soc*, **2011**, *133*, 3242-5.
- (152) Huang, W. C.; Cullis, P. M.; Raven, E. L.; Roberts, G. C. *Metallomics*, **2011**, *3*, 410-6.
- (153) Huang, W. C.; Westlake, A. C.; Marechal, J. D.; Joyce, M. G.; Moody, P. C.; Roberts, G. C. *J Mol Biol* **2007**, *373*, 633-51.
- (154) Urlacher, V. B.; Makhsumkhanov, A.; Schmid, R. D. *Appl Microbiol Biotechnol* **2006**, *70*, 53-9.
- (155) Alcalde, M.; Farinas, E. T.; Arnold, F. H. *J Biomol Screen* **2004**, *9*, 141-6.
- (156) Kumar, S.; Sun, L.; Liu, H.; Muralidhara, B. K.; Halpert, J. R. *Protein Eng Des Sel* **2006**, *19*, 547-54.
- (157) Zhao, J.; Tan, E.; Ferras, J.; Auclair, K. *Biotechnol Bioeng* **2007**, *98*, 508-13.

- (158) Chefson, A.; Auclair, K. *Chembiochem* **2007**, *8*, 1189-97.
- (159) Tee, K. L.; Roccatano, D.; Stolte, S.; Arning, J.; Bernd, J.; Schwaneberg, U. *Green Chemistry* **2008**, *10*, 117-123.
- (160) Gunsalus, I. C.; Wagner, G. C. *Methods Enzymol* **1978**, *52*, 166-88.
- (161) Kim, D.; Heo, Y. S.; de Montellano, P. R. O. *Archives of Biochemistry and Biophysics* **2008**, *474*, 150-156.
- (162) Hata, S.; Oda, Y.; Nishino, T.; Katsuki, H.; Aoyama, Y.; Yoshida, Y.; Nagai, J. *Journal of Biochemistry* **1983**, *94*, 501-510.
- (163) Rojubbally, A., Hua Cheng, S., Foreman, C., Huang, J., Agnes, G., Plettner, E. *Biocatalysis and Biotransformation* **2007**, *25*, 301-317.
- (164) Prasad, B.; Rojubbally, A.; Plettner, E. *Journal of Chemical Ecology* **2011**, *37*, 657-667.
- (165) Davydov, R.; Makris, T. M.; Kofman, V.; Werst, D. E.; Sligar, S. G.; Hoffman, B. M. *J. Am. Chem. Soc* **2001**, *123*, 1403-15.
- (166) Sligar, S. G.; Gunsalus, I. C. *Proc. Natl. Acad. Sci. U S A* **1976**, *73*, 1078-82.
- (167) Sono, M.; Roach, M. P.; Coulter, E. D.; Dawson, J. H. *Chem. Rev* **1996**, *96*, 2841-2888.
- (168) Altun, A.; Shaik, S.; Thiel, W. *J. Am. Chem. Soc* **2007**, *129*, 8978-87.
- (169) Sibbesen, O.; De Voss, J. J.; Montellano, P. R. *J. Biol. Chem* **1996**, *271*, 22462-9.
- (170) Auclair, K.; Moenne-Loccoz, P.; Ortiz de Montellano, P. R. *J. Am. Chem. Soc* **2001**, *123*, 4877-85.
- (171) Lipscomb, J. D.; Sligar, S. G.; Namtvedt, M. J.; Gunsalus, I. C. *J. Biol. Chem* **1976**, *251*, 1116-24.
- (172) Pochapsky, S. S.; Pochapsky, T. C.; Wei, J. W. *Biochemistry* **2003**, *42*, 5649-56.
- (173) Makris, T. M.; von Koenig, K.; Schlichting, I.; Sligar, S. G. *J Inorg Biochem* **2006**, *100*, 507-18.
- (174) Schunemann, V.; Lenzian, F.; Jung, C.; Contzen, J.; Barra, A. L.; Sligar, S. G.; Trautwein, A. X. *J. Biol. Chem.* **2004**, *279*, 10919-10930.
- (175) Egawa, T.; Shimada, H.; Ishimura, Y. *Biochem. Biophys. Res. Commun* **1994**, *201*, 1464-9.
- (176) Aggarwal, V. K.; Gultekin, Z.; Grainger, R. S.; Adams, H.; Spargo, P. L. *J. Chem. Soc.-Perkin Transac 1* **1998**, 2771-2781.
- (177) O'Keefe, D. H.; Ebel, R. E.; Peterson, J. A. *Methods Enzymol* **1978**, *52*, 151-6.

- (178) Cryle, M. J.; Stok, J. E.; De Voss, J. J. *Aus. J. Chem.* **2003**, *56*, 749-762.
2. (179) Vrzal, R.; Starha, P.; Dvorak, Z.; Travnicek, Z. *J Inorg Biochem* **2010**, *104*, 1130-1137.
- (180) A.Rojubally *Ph.D. Thesis, Simon Fraser University* **2007**.
260. (181) Shimada, H.; Nagano, S.; Hori, H.; Ishimura, Y. *J. Inorg. Biochem.* **2001**, *83*, 255-260.
- (182) Gunsalus, I. C.; Sligar, S. G. *Biochimie* **1976**, *58*, 143-7.
- (183) Guengerich, F. P.; MacDonald, T. L. *FASEB J* **1990**, *4*, 2453-9.
- (184) Prasad, B.; Lewis, A. R.; Plettner, E. *Anal Chem* **2011**, *83*, 231-9.
- (185) Shen, H.; Wang, Y. T. *Appl. Environ. Microbiol.* **1995**, *61*, 2754-8.
- (186) Winfield, M. D.; Groisman, E. A. *Appl. Environ. Microbiol.* **2003**, *69*, 3687-94.
- (187) Kinoshita, K.; Yang, Y.; Koyama, K.; Takahashi, K.; Nishino, H. *Phytomedicine* **1999**, *6*, 73-7.
- (188) Munro, A. W.; Lindsay, J. G. *Mol Microbiol* **1996**, *20*, 1115-25.
- (189) Harada, K.; Sakurai, K.; Ikemura, K.; Ogura, T.; Hirota, S.; Shimada, H.; Hayashi, T. *J Am Chem Soc* **2008**, *130*, 432-3.
- (190) Dau, H.; Limberg, C.; Reier, T.; Risch, M.; Roggan, S.; Strasser, P. *Chemcatchem* **2010**, *2*, 724-761.
- (191) Izgorodin, A.; Winther-Jensen, O.; MacFarlane, D. R. *Aust. J. Chem.* **2012**, *65*, 638-642.
- (192) Zhou, F. L.; Izgorodin, A.; Hocking, R. K.; Spiccia, L.; MacFarlane, D. R. *Advanced Energy Materials* **2012**, *2*, 1013-1021.
- (193) Prasad, B.; Rojubally, A.; Plettner, E. *J Chem Ecol*, **2011**, *37*, 657-67.
23. (194) Pace, C. N.; Vajdos, F.; Fee, L.; Grimsley, G.; Gray, T. *Protein Sci* **1995**, *4*, 2411-2420.
- (195) Prasad, S.; Mazumdar, S.; Mitra, S. *FEBS Lett* **2000**, *477*, 157-60.
- (196) Janig, G. R.; Makower, A.; Rabe, H.; Friedrich, J.; Ruckpaul, K. *Biomed Biochim Acta* **1984**, *43*, K17-24.
- (197) Nickerson, D. P.; Wong, L. L. *Protein Eng* **1997**, *10*, 1357-61.
- (198) Thompson, A. M.; Reddi, A. R.; Shi, X.; Goldbeck, R. A.; Moenne-Loccoz, P.; Gibney, B. R.; Holman, T. R. *Biochemistry* **2007**, *46*, 14629-37.

- (199) Chaen, S.; Yamamoto, N.; Shirakawa, I.; Sugi, H. *Biochim Biophys Acta* **2001**, *1506*, 218-23.
- (200) Oshima, R.; Fushinobu, S.; Su, F.; Zhang, L.; Takaya, N.; Shoun, H. *J Mol Biol* **2004**, *342*, 207-17.
- (201) Truesdale, G. A.; Downing, A. L. *Nature* **1954**, *173*, 1236-1236.
- (202) Casny, M.; Rehder, D.; Schmidt, H.; Vilter, H.; Conte, V. *J Inorg Biochem* **2000**, *80*, 157-60.
- (203) Wolak, M.; van Eldik, R. *Chemistry* **2007**, *13*, 4873-83.
- (204) Boykin, D. W.; Baumstark, A. L. *Abstracts of Papers of the American Chemical Society* **1991**, *201*, 172-ORGN.
- (205) Cha, Y.; Murray, C. J.; Klinman, J. P. *Science* **1989**, *243*, 1325-30.
- (206) Huskey, W. P.; Schowen, R. L. *J. Am. Chem. Soc.* **1983**, *105*, 5704-5706.
- (207) Nagel, Z. D.; Klinman, J. P. *Chemical Reviews* **2006**, *106*, 3095-3118.
- (208) Koppenol, W. H.; Liebman, J. F. *J. Phys. Chem.* **1984**, *88*, 99-101.
- (209) Green, M. T.; Dawson, J. H.; Gray, H. B. *Science* **2004**, *304*, 1653-6.
- (210) Hishiki, T.; Shimada, H.; Nagano, S.; Egawa, T.; Kanamori, Y.; Makino, R.; Park, S. Y.; Adachi, S.; Shiro, Y.; Ishimura, Y. *J Biochem* **2000**, *128*, 965-74.
- (211) Wardman, P. *J. Phys. Chem. Ref. Data* **1989**, *18*, 1637-1755.
- (212) Castellan, G. W. *Physical Chemistry* **1983**, *3rd Ed.*, p381.
- (213) Steele, W. V. *J. Chem. thermodyn* **1977**, *9*, 311-314.
- (214) Denisov, I. G.; Baas, B. J.; Grinkova, Y. V.; Sligar, S. G. *J Biol Chem* **2007**, *282*, 7066-76.
- (215) Woods, C. M.; Fernandez, C.; Kunze, K. L.; Atkins, W. M. *Biochemistry*, **2011**, *50*, 10041-51.
- (216) Yano, J. K.; Wester, M. R.; Schoch, G. A.; Griffin, K. J.; Stout, C. D.; Johnson, E. F. *J Biol Chem* **2004**, *279*, 38091-4.
- (217) Amunom, I.; Dieter, L. J.; Tamasi, V.; Cai, J.; Conklin, D. J.; Srivastava, S.; Martin, M. V.; Guengerich, F. P.; Prough, R. A. *Chem Res Toxicol*, **2011**, *24*, 1223-30.
- (218) Kaspera, R.; Sahele, T.; Lakatos, K.; Totah, R. A. *Biochem Biophys Res Commun*, **2012**, *418*, 464-8.
- (219) Cooper, H. L.; Groves, J. T. *Arch Biochem Biophys*, **2011**, *507*, 111-8.
- (220) Hlavica, P.; Lewis, D. F. *Eur J Biochem* **2001**, *268*, 4817-32.

- (221) Song, W. J.; Gucinski, G.; Sazinsky, M. H.; Lippard, S. J. *Proc Natl Acad Sci U S A*, **2011**, *108*, 14795-800.
- (222) Kallio, J. P.; Rouvinen, J.; Kruus, K.; Hakulinen, N. *Biochemistry*, **2011**, *50*, 4396-8.
- (223) Johnson, B. J.; Cohen, J.; Welford, R. W.; Pearson, A. R.; Schulten, K.; Klinman, J. P.; Wilmot, C. M. *J Biol Chem* **2007**, *282*, 17767-76.
- (224) Petrek, M.; Kosinova, P.; Koca, J.; Otyepka, M. *Structure* **2007**, *15*, 1357-63.
- (225) Taylor, D. G.; Trudgill, P. W. *J Bacteriol* **1986**, *165*, 489-97.
- (226) Balayiannis, G. P.; Anastassiadis, M.; Anagnostopoulos, H. *Bull Environ Contam Toxicol* **2009**, *83*(6), 780-782.
- (227) Bajaj, A.; Pathak, A.; Mudiam, M. R.; Mayilraj, S.; Manickam, N. *J Appl Microbiol* **2010**, *109*, 2135-43.
- (228) Sutherland, T. D.; Weir, K. M.; Lacey, M. J.; Horne, I.; Russell, R. J.; Oakeshott, J. G. *J Appl Microbiol* **2002**, *92*, 541-8.
- (229) Shivaramaiah, H. M.; Sanchez-Bayo, F.; Al-Rifai, J.; Kennedy, I. R. *J Environ Sci Health B* **2005**, *40*, 711-20.
- (230) Paul, V.; Balasubramaniam, E.; Kazi, M. *Eur J Pharmacol* **1994**, *270*, 1-7.
- (231) Palma, P.; Palma, V. L.; Matos, C.; Fernandes, R. M.; Bohn, A.; Soares, A. M.; Barbosa, I. R. *Chemosphere* **2009**, *74*, 676-81.
- (232) Liu, D.; Thomson, K.; Strachan, W. M. *Bull Environ Contam Toxicol* **1981**, *27*, 412-7.
- (233) Nigg, H. N.; Reinert, J. A.; Stamper, J. H.; Fitzpatrick, G. E. *Bull Environ Contam Toxicol* **1981**, *26*, 267-72.
- (234) Palma, P.; Palma, V. L.; Fernandes, R. M.; Soares, A. M.; Barbosa, I. R. *Ecotoxicol Environ Saf* **2009**, *72*, 344-50.
- (235) Kwon, G. S.; Sohn, H. Y.; Shin, K. S.; Kim, E.; Seo, B. I. *Appl Microbiol Biotechnol* **2005**, *67*, 845-50.
- (236) Stanley, K. A.; Curtis, L. R.; Simonich, S. L.; Tanguay, R. L. *Aquat Toxicol* **2009**, *95*, 355-61.
- (237) Mukherjee, I.; Mittal, A. *Bull Environ Contam Toxicol* **2005**, *75*, 1034-40.
- (238) Siddique, T.; Okeke, B. C.; Arshad, M.; Frankenberger, W. T., Jr. *J Environ Qual* **2003**, *32*, 47-54.
- (239) Kumar, M.; Philip, L. *J Environ Sci Health B* **2006**, *41*, 81-96.

- (240) Sutherland, T. D.; Horne, I.; Russell, R. J.; Oakeshott, J. G. *Appl Environ Microbiol* **2002**, *68*, 6237-45.
- (241) Awasthi, N.; Manickam, N.; Kumar, A. *Bull Environ Contam Toxicol* **1997**, *59*, 928-34.
- (242) Kullman, S. W.; Matsumura, F. *Appl Environ Microbiol* **1996**, *62*, 593-600.
- (243) Weber, J.; Halsall, C. J.; Muir, D.; Teixeira, C.; Small, J.; Solomon, K.; Hermanson, M.; Hung, H.; Bidleman, T. *Sci Total Environ* **2010**, *408*(15), 2966-84
- (244) Chefson, A.; Auclair, K. *Molecular Biosystems* **2006**, *2*, 462-469.
- (245) Bell, S. G.; Chen, X.; Sowden, R. J.; Xu, F.; Williams, J. N.; Wong, L. L.; Rao, Z. *J Am Chem Soc* **2003**, *125*, 705-14.
- (246) Wong, T. S.; Roccatano, D.; Zacharias, M.; Schwaneberg, U. *J Mol Biol* **2006**, *355*, 858-71.
- (247) Arnold, F. H.; Wintrode, P. L.; Miyazaki, K.; Gershenson, A. *Trends Biochem Sci* **2001**, *26*, 100-6.
- (248) Wong, T. S.; Zhurina, D.; Schwaneberg, U. *Comb Chem High Throughput Screen* **2006**, *9*, 271-88.
- (249) Cirino, P. C.; Mayer, K. M.; Umeno, D. *Methods Mol Biol* **2003**, *231*, 3-9.
- (250) Kanagawa, T. *J Biosci Bioeng* **2003**, *96*, 317-23.
- (251) Wong, T. S.; Roccatano, D.; Loakes, D.; Tee, K. L.; Schenk, A.; Hauer, B.; Schwaneberg, U. *Biotechnol J* **2008**, *3*, 74-82.
- (252) Wong, T. S.; Tee, K. L.; Hauer, B.; Schwaneberg, U. *Nucleic Acids Res* **2004**, *32*, e26.
- (253) Wong, T. S.; Tee, K. L.; Hauer, B.; Schwaneberg, U. *Anal Biochem* **2005**, *341*, 187-9.
- (254) Mundhada, H. *Ph. D. dissertation, Jacobs University, Bremen* **2011**.
- (255) Mundhada, H.; Marienhagen, J.; Scacioc, A.; Schenk, A.; Roccatano, D.; Schwaneberg, U. *Chembiochem*, **2011**, *12*, 1595-601.
- (256) Alcalde, M.; Farinas, E. T.; Arnold, F. H. *J Biomol Screen* **2004**, *9*, 141-6.
- (257) Gillam, E. M.; Notley, L. M.; Cai, H.; De Voss, J. J.; Guengerich, F. P. *Biochemistry* **2000**, *39*, 13817-24.
- (258) Inoue, H.; Nojima, H.; Okayama, H. *Gene* **1990**, *96*, 23-8.
- (259) Miyazaki, K. *Methods Mol Biol* **2003**, *231*, 23-8.
- (260) Derosa, M.; Alonso, J. L. T. *Journal of Organic Chemistry* **1978**, *43*, 2639-2643.

- (261) Hamaue, N.; Yamazaki, N.; Minami, M.; Endo, T.; Hirahuji, M.; Monma, Y.; Togashi, H. *Gen Pharmacol* **1998**, *30*, 387-91.
- (262) Chakrabarty, A. M.; Mylroie, J. R.; Friello, D. A.; Vacca, J. G. *Proc Natl Acad Sci U S A* **1975**, *72*, 3647-51.
- (263) Yu, C.; Gunsalus, I. C. *Biochem Biophys Res Commun* **1970**, *40*, 1431-6.
- (264) Chen, X.; Christopher, A.; Jones, J. P.; Bell, S. G.; Guo, Q.; Xu, F.; Rao, Z.; Wong, L. L. *J Biol Chem* **2002**, *277*, 37519-26.
- (265) Guengerich, F. P. *Arch Biochem Biophys* **2003**, *409*, 59-71.
- (266) Manna, S. K.; Mazumdar, S. *Dalton Trans*, **2010**, *39*, 3115-23.
- (267) Wu, Z. L.; Podust, L. M.; Guengerich, F. P. *J Biol Chem* **2005**, *280*, 41090-100.
- (268) Chowdhury, G.; Dostalek, M.; Hsu, E. L.; Nguyen, L. P.; Stec, D. F.; Bradfield, C. A.; Guengerich, F. P. *Chem Res Toxicol* **2009**, *22*, 1905-12.
- (269) Nakamura, K.; Martin, M. V.; Guengerich, F. P. *Arch Biochem Biophys* **2001**, *395*, 25-31.
- (270) Lai, W.; Chen, H.; Cohen, S.; Shaik, S. *J. Phys. Chem. Letters* **2011**, *2*, 2229-2235.
- (271) Li, S.; Wackett, L. P. *Biochemistry* **1993**, *32*, 9355-61.
- (272) Amin, A. E.; Abdalla, G. A. *Vet Hum Toxicol* **1995**, *37*, 113-6.
- (273) Arshad, M.; Hussain, S.; Saleem, M. *J Appl Microbiol* **2008**, *104*, 364-70.
- (274) Ballesteros, M. L.; Durando, P. E.; Nores, M. L.; Diaz, M. P.; Bistoni, M. A.; Wunderlin, D. A. *Environ Pollut* **2009**, *157*, 1573-80.
- (275) Egawa, T.; Shimada, H.; Ishimura, Y. *Biochem. Biophys. Res. Commun* **1994**, *201*, 1464-1469.
- (276) Gelb, M. H.; Heimbrook, D. C.; Malkonen, P.; Sligar, S. G. *Biochemistry* **1982**, *21*, 370-377.
- (277) V. Schunemann, F. L., C. Jung, J. Contzen, A. Laure Barra, S.G. Sligar, A. X. Trautwein *J. Biol. Chem.* **2004**, *279*, 10919-10930
- (278) Park, S. Y.; Yamane, K.; Adachi, S.; Shiro, Y.; Weiss, K. E.; Sligar, S. G. *Acta Crystallogr D Biol Crystallogr* **2000**, *56*, 1173-5.
- (279) Koppenol, W. H. *J Am Chem Soc* **2007**, *129*, 9686-90.